INVESTIGATIONS ON THE PROPERTIES AND DRUG RELEASES OF BIODEGRADABLE POLYMER COATINGS ON METAL SUBSTRATES AS DRUG CARRIERS

A THESIS SUBMITTED TO
THE GRADUATE SCHOOL OF NATURAL AND APPLIED SCIENCES
OF
MIDDLE EAST TECHNICAL UNIVERSITY

BY

TUNCAY BAYDEMİR

IN PARTIAL FULFILLMENT OF THE REQUIREMENTS
FOR
THE DEGREE OF DOCTOR OF PHILOSOPHY
IN
POLYMER SCIENCE AND TECHNOLOGY

SEPTEMBER 2009

Approval of the thesis:

INVESTIGATIONS ON THE PROPERTIES AND DRUG RELEASES OF BIODEGRADABLE POLYMER COATINGS ON METAL SUBSTRATES AS DRUG CARRIERS

submitted by **TUNCAY BAYDEMİR** in partial fulfillment of the requirements for the degree of **Doctor of Philosophy in Polymer Science and Technology Department, Middle East Technical University** by,

Prof. Dr. Canan Özgen
Dean, Graduate School of **Natural and Applied Sciences** _____

Prof. Dr. Cevdet Kaynak
Head of the Department, **Polymer Science and Technology** _____

Prof. Dr. Erdal Bayramlı
Supervisor, **Chemistry Department, METU** _____

Examining Committee Members

Prof. Dr. Leyla Aras
Chemistry Dept., METU _____

Prof. Dr. Erdal Bayramlı
Chemistry Dept., METU _____

Prof.Dr. Zuhal Küçükyavuz
Chemistry Dept., METU _____

Prof. Dr. Ş. Serpil Aksoy
Chemistry Dept., Gazi University _____

Prof. Dr. Feza Korkusuz
Physical Education and Sports Dept., METU _____

Date: 11.09.2009

I hereby declare that all information in this document has been obtained and presented in accordance with academic rules and ethical conduct. I also declare that, as required by these rules and conduct, I have fully cited and referenced all material and results that are not original to this work.

Name, Last name: Tuncay Baydemir

Signature:

ABSTRACT

INVESTIGATIONS ON THE PROPERTIES AND DRUG RELEASES OF BIODEGRADABLE POLYMER COATINGS ON METAL SUBSTRATES AS DRUG CARRIERS

Baydemir, Tuncay

Ph.D., Department of Polymer Science and Technology

Supervisor: Prof. Dr. Erdal Bayramlı

September 2009, 278 pages

The use of various biodegradable polymers for the improvement of different controlled and long-lasting drug release systems is an active research area in recent years. The application of different metal prostheses, especially titanium based ones, to the human body is also very common. A most important disadvantage of these prostheses is the risk of infection at the application areas that necessitates the removing of the prosthesis with a second surgical operation and reapplication of it after recovery. One of the best ways to solve this problem is to render metal prostheses infection free with controlled and sustainable drug (antibiotic) release systems.

The long term sustained release of relevant antibiotics from the various biodegradable polymer coated metal implants is studied in this thesis. Virtual fatigue analysis and drug loading capacities of titanium and stainless steel samples with different surface pattern and modifications were studied. Various biodegradable polymer and drug combinations were examined and used for coating of metal prosthesis. The aim is to design polymer-drug coated metal implants that are capable of releasing a feasible amount of drug up to a period of at least 1 month. Various coating techniques and surface modifications were also employed to improve the adhesional properties of the drug containing polymers. Their adhesion abilities on the metal substrates were tested by Lap-shear and T-peel tests. Polymer degradation kinetics was followed by viscosity studies. Calibration lines for different drugs were obtained and drug releases on different systems were followed by using UV spectroscopy and microbial antibiotic sensitivity tests.

Among the techniques applied to prevent fast release of drugs initially, the coatings of Vancomycin absorbed β-TCP (β-tricalcium phosphate) homogeneously distributed in poly(D,L-lactide-co-glycolide) solution in chloroform followed by an inert coating with poly(L-lactide) system proved to be feasible. By this technique, initial burst release was minimized and drug release from implants lasted nearly 2 months. Multiple coatings on polymer plus drug coating layer also gave promising results.

In vivo studies on dorsal muscles of native rabbits with antibiotic loaded implants gave no negative effect on the surrounding tissues with high compatibility free of infection.

Keywords: Implant Based Infections, Poly(D,L-lactide-co-glycolide), Poly(L-lactide), β-tricalcium phosphate, Controlled and Sustainable Drug Delivery Systems

ÖZ

METAL SUBSTRATLAR ÜZERİNDE İLAÇ TAŞIYICI OLARAK KULLANILAN BİYOBOZUNUR POLİMER KAPLAMALARIN ÖZELLİKLERİ VE İLAÇ SALIMLARI HAKKINDA İNCELEMELER

Baydemir, Tuncay

Doktora, Polimer Bilimi ve Teknolojisi Bölümü

Tez Yöneticisi: Prof. Dr. Erdal Bayramlı

Eylül 2009, 278 sayfa

Çeşitli biobozunur polimerlerin kontrollü ve uzun süreli ilaç salım sistemleri geliştirilmesinde kullanılması son yıllarda aktif bir araştırma alanıdır. Farklı metal protezlerin, özellikle titanyum bazlı olanların, insan vücudunda farklı ortopedik amaçlar için uygulanması da çok yaygındır. Kullanılan bu protezlerin en önemli dezavantajı ise uygulandıkları bölgelerde protezin ikinci bir operasyon ile alınıp enfeksiyonlu bölgenin iyileştirilmesinin ardından yeniden uygulanmasını gerektiren enfeksiyon oluşma riskidir. Bu problemi çözmek için en iyi yollardan biri metal protezleri kontrollü ve sürdürülebilir ilaç (antibiyotik) salım sistemleri ile donatarak enfeksiyon riski taşımayan hale getirmektir.

Bu tezde, sözkonusu antibiyotiklerin farklı biyobozunur polimer kaplı metal protezlerden uzun süreli ve devamlı salınımı çalışılmıştır. Farklı yüzey deseni ve modifikasyonuna sahip titanyum ve paslanmaz çelik numunelerinin sanal yorulma analizleri ve ilaç yükleme kapasiteleri çalışılmıştır. Çeşitli biyobozunur polimer ve ilaç kombinasyonları çalışılmış ve bu kombinasyonlar metal protezlerin kaplanmasında kullanılmıştır. Buradaki amaç en az bir ay süresince uygun miktarda ilaç salımı yapabilen polimer-ilaç kaplı metal protezler tasarlamaktır. Ayrıca, ilaç içeren polimerlerin yapışma özelliklerini geliştirmek için farklı kaplama teknikleri ve yüzey modifikasyonları uygulanmıştır. Bunların metal yüzeyler üzerindeki yapışma özellikleri Lap-shear ve T-peel testleri ile çalışılmıştır. Polimer bozunma kinetikleri viskozite çalışmaları ile izlenmiştir. Çeşitli ilaçların kalibrasyon doğruları elde edilmiş ve farklı sistemlerdeki ilaç salımları UV spektrofotometresi ve mikrobiyal antibiyotik duyarlılık testleri kullanılarak izlenmiştir.

Başlangıçta olan hızlı ilaç salımını önlemek için denenen metodlar arasında kloroform içerisinde çözünmüş poli(D,L-laktit-co-glikolit) içerisine homojen olarak dağıtılan vankomisin emdirilmiş β-TCP (β-trikalsiyum fosfat) kaplaması ve bunun üzerine yapılan inert poli(L-laktit) kaplaması sisteminin uygulanabilir olduğu kanıtlanmıştır. Bu teknikle, başlangıçta gerçekleşen patlama salım minimize edilmiş ve protezlerdeki ilaç salımları yaklaşık iki aya kadar sürmüştür. Ayrıca, polimer ve ilaç içeren kaplamaların üzerine uygulanan çok katlı kaplamalar da umut verici sonuçlar vermiştir.

Antibiyotik yüklü protezler ile yerel tavşanların sırt kasında yapılan in vivo çalışmaları, protezlerin çevre dokularla enfeksiyon riski taşımaksızın uyumunun yüksek olup herhangi bir olumsuz etkisinin olmadığını göstermiştir.

Anahtar Kelimeler: Protez Temelli Enfeksiyonlar, Poli(D,L-laktit-co-glikolit), Poli(L-laktit), β-trikalsiyum fosfat, Kontrollü ve Sürdürülebilir İlaç Salım Sistemleri

To My Little Prince, Deniz…

ACKNOWLEDGEMENTS

I would like to express my deepest gratitude to my supervisor Prof. Dr. Erdal Bayramlı, for his continuous support, encouragement and guidance during my research.

I would like to express my sincerely acknowledgements to Prof. Dr. Feza Korkusuz and Prof. Dr. Gürdal Alaeddinoğlu for their guidance, valuable advice and precious discussions during the progress of my research. It was an honor for me to work with them and I will always remember the tasteful meetings we had.

I express my special thanks to Prof. Dr. Muharrem Timuçin and Nurşen Koç for their contribution on surface modification studies. I would like to express my sincere thanks to Assoc. Prof. Dr. Petek Korkusuz for helping me in in-vivo studies. I am also thankful to Emir Birant for his help in metal indentation studies.

I would like to express my sincere thanks to Prof. Dr. Teoman Tinçer and Prof. Dr. Güngör Gündüz for giving me the opportunity of using their laboratories.

Fame-Med and Ortopro Companies are greatly acknowledged for providing materials and for their cooperation. Their contributions were very valuable for me.

Special thanks go to Serdar Tan from Department of Metallurgical and Materials Engineering for SEM analysis. His help and advice were very important for me.

I am also very grateful to Sevil Güçlü, Serpil Ökten, Serpil Selvi and Selda Şeker for their helps during my university period without any expectations.

I would also like to thank to our technicians Cafer Kaya, Zeliha Doğruoğlu, Sevim Ulupınar, Halil Memiş, Osman Yaslıtaş and Salih Sarıkaya for their technical and moral supports.

I also wish to extend my acknowledgements and sincere thanks to my colleagues and technicians of General Chemistry and Physical Chemistry laboratories. I had great lab periods with their presence.

This thesis could not have been finished without supports of my friends. I express my special thanks to Aycan Günay, Pınar Kürkçü, Selahattin Erdoğan, Mehmet Doğan, Ümit Tayfun and Burhan Fuat Çankaya from our research group for their friendly and helpful contributions during my studies. I wish to thank also Elif Vargün, Murat Kaya, Semra Tan, Erkan Biber, Ahmet Göktaş and all of my friends from Chemistry and Polymer Science and Technology Departments. Their friendship and support always encouraged me.

I wish to express my sincere thanks and love to all my family; my father, mother, sister, father in law, mother in law and brother in law. I am grateful to them for their endless support and belief in me.

This thesis could not be written without endless love, patient and understanding of my wife Işıl Baydemir. Her presence and enormous support were encouraged me. My deepest love and thanks belong to her.

Last but not the least; I dedicate this dissertation to my son Deniz Baydemir, alias “Little Prince”, who changed my life profoundly. I am very thankful for your coming into my world and my love for you is endless…

TABLE OF CONTENTS

ABSTRACT iv

ÖZ vi

ACKNOWLEDGEMENTS ix

TABLE OF CONTENTS xi

LIST OF TABLES xix

LIST OF FIGURES xxiii

ABBREVIATIONS xxxiv

CHAPTERS

1. INTRODUCTION 1

1.1 Overview of Biomaterials 1

1.1.1 Definition and Use of Biomaterials 1

1.1.2 History of Biomaterials 3

1.1.3 Biocompatibility 3

1.1.4 Materials Used as Biomaterials 4

1.2 Polymeric Biomaterials 5

1.2.1 Definition and Basic Concepts of Polymers 6

1.2.2 Classification of Polymers 7

1.2.3 Polymers as Biomaterials 10
1.2.3.1 Non-degradable Polymeric Biomaterials 12
1.2.3.2 Biodegradable Polymeric Biomaterials 13
1.2.3.2.1 Lactide-Glycolide Polymers 16
1.2.3.2.2 Lactide-Caprolactone Polymers 18
1.2.3.2.3 Poly(vinyl alcohol) 20
1.2.4 Ceramics as Biomaterials 21
1.2.4.1 Tricalcium Phosphate (TCP) Ceramics 22
1.2.5 Metals and Alloys as Biomaterials 23
1.2.5.1 Stainless Steels 25
1.2.5.2 Titanium and Its Alloys 26
1.3 Implant Related Infections 28
1.3.1 Osteomyelitis 33
1.4 Controlled Drug Release Systems 34
1.4.1 Mechanisms of Drug Release Systems 37
1.4.1.1 Diffusion-controlled systems 38
1.4.1.2 Solvent-activated systems 38
1.4.1.3 Chemically Controlled systems 39
1.4.1.4 Magnetically Controlled systems 40
1.4.2 Implantable Drug Delivery Systems 42
1.5 Scope of the Study 43
1.6 Review of Literature 44

2. EXPERIMENTAL 57

2.1 Materials 57

2.1.1 Polymers 57

2.1.1.1 Poly(vinyl alcohol)s 58

2.1.1.2 Polycaprolactone 58

2.1.1.3 Poly(L-lactide), Poly(D,L-lactide-co-glycolide), and Poly(L-lactide-co-ε-caprolactone) 58

2.1.2 Metals and Alloys 60

2.1.3 Ceramics 60

2.1.4 Drugs 60

2.1.4.1 Vancomycin 60

2.1.4.2 Amoxicillin and Derivatives 61

2.1.4.3 Ceftazidime 63

2.1.4.4 Cefazolin 64

2.1.4.5 Ceftriaxone 65

2.1.4.5 Other Chemicals 65

2.2 Experimental Techniques 66

2.2.1 Mechanical Tests 66

2.2.1.1 Fatigue Tests 66

2.2.1.2 Hardness Tests 67

2.2.1.3 Lap Shear Tests 69

2.2.1.4 T-Peel Tests 70

2.2.1.5 Measuring Adhesion by Tape Test 71

2.2.2 Gloss Tests 72

2.2.3 UV-Visible Absorption Spectroscopy (UV-VIS) 73

2.2.4 Scanning Electron Microscopy (SEM) 75

2.2.5 Viscosity Measurements 76

2.2.6 Kirby-Bauer Disc Diffusion Antibiotic Sensitivity Testing..... 77

2.2.7 Energy Dispersive X-Ray Spectroscopy (EDX) 79

2.3 Experimental Methods..... 80

2.3.1 Studies on Metal Surface Geometry 80

2.3.2 Indent Prototype Studies 81

2.3.3 Determination of Biomechanical Changes Related to the Indentation..... 81

2.3.4 Computer Simulation and Fatigue Tests in Virtual Media 81

2.3.5 Hardness, Gloss and Measuring Adhesion by Tape Tests 82

2.3.6 Coating Thickness and Coating Density Measurements..... 83

2.3.7 Calibration Curves for Different Drugs 83

2.3.8 Preparation of Coating Solutions 83

2.3.9 Coating Procedure..... 83

2.3.10 Surface Modification of Titanium Plates 84

2.3.11 Drug Release Studies 84

2.3.12 Polymer Degradation Studies..... 84

2.3.13 Kirby-Bauer Disc Diffusion Antibiotic Sensitivity Tests 85

2.3.14 SEM Analysis 85

2.3.15 In Vivo Tests 85

3. RESULTS AND DISCUSSION 86

3.1 Investigation of Solubility of Polymers and Drugs 86

3.2 Film Formation and Coating Thickness Studies 86

3.3 Indent Prototype Studies 87

3.3.1 Loading Efficiency on Indentations 88

3.3.2 Biomechanical Changes Related to the Indentation 88

3.4 Surface Treatment Studies on Titanium Plates 95

3.4.1 Surface Treatment 95

3.4.2 SEM Analysis 96

3.4.3 EDX Analysis 100

3.4.4 Surface Cleaning of Titanium Alloys Prior to Coating 103

3.5 Persoz Hardness Tests 103

3.6 Gloss Tests 104

3.7 Measuring Adhesion by Tape Test 105

3.8 Lap Shear Tests 106

3.8.1 Lap Shear Tests for PLGA RG 504 107

3.8.2 Lap Shear Tests for Poly(L-lactide) L 209S 108

3.9 T-Peel Tests 111

3.9.1 T-Peel Tests for PLGA RG 504 112

3.9.2 T-Peel Tests for Poly(L-lactide) L 209S 113

3.10 Polymer Degradation Studies 115

3.10.1 Degradation Profile for PLGA RG 504 116

3.10.2 Degradation Profile for Poly(L-lactide) L 209S 120

3.11 Calibration Curves for Antibiotics Used in Release Studies 124

3.11.1 Calibration Curve for Vancomycin 124

3.11.2 Calibration Curve for Alfoxil (Amoxicillin) 125

3.11.3 Calibration Curve for Augmentin (Amoxicillin) 126

3.11.4 Calibration Curve for Fortum (Ceftazidime) 127

3.11.5 Calibration Curve for Cefamezin (Cefazolin) 128

3.11.6 Calibration Curve for Rocephin (Ceftriaxone) 129

3.12 Drug Release Studies 130

3.12.1 Drug Release Studies from Augmentin (Amoxicillin Derivative) Loaded Implants 130

3.12.2 Drug Release Studies from Alfoxil (Amoxicillin) Loaded Implants 132

3.12.2.1 Effect of Polymer Type on Drug Release 132

3.12.2.2 Drug Release Studies from Inert Coating Applied Implants 142

3.12.3 Drug Release Studies from Fortum (Ceftazidime) Loaded Implants 149

3.12.3.1 Drug Release Studies from Inert Coating Applied Implants 149

3.12.3.2 Drug Loading Control Studies 172

3.12.3.3 Disk Diffusion Antibiotic Sensitivity Tests 173

3.12.3.4 Ceftazidime (Fortum) Activity Control Studies 175

3.12.4 Drug Release Studies from Vancomycin Loaded Implants 177

3.12.4.1 Vancomycin Activity Control Studies 177

3.12.4.2 Drug Release Studies on Vancomycin Impregnated TCP 178

3.12.4.2.1 Packing Density Measurement of TCP 178

3.12.4.2.2 Drug Release Studies 178

3.12.4.2.3 Disk Diffusion Antibiotic Sensitivity Tests 182

3.12.4.3 Further Drug Release Studies on Vancomycin Loaded Implants 185

3.12.4.3.1 Drug Release Studies from Antibiotic-Polymer Coated and Antibiotic-TCP-Polymer Coated Metal Substrates 185

3.12.4.3.2 Disk Diffusion Antibiotic Sensitivity Tests 196

3.12.4.3.3 SEM Analysis 201

3.12.4.3.4 In Vivo Analysis 204

3.12.4.4 Drug Release Kinetics 206

4. CONCLUSIONS 214

5. RECOMMENDATIONS 221

REFERENCES 223

APPENDICES

A. DSC THERMOGRAMS OF POLYMERS USED 247

B. REPRESENTATION OF IMAGES OF VANCOMYCIN ITSELF AND AFTER IMPREGNATION INTO β-TCP 250

C. LAP-SHEAR TESTS 252

D. T-PEEL TESTS 259

E. PREPARATION OF PHOSPHATE BUFFERED SALINE (10 x PBS) 267

F. DEGRADATION STUDIES FOR PLGA RG 504 268

G. DEGRADATION STUDIES FOR PL L209 S 272

CURRICULUM VITAE 276

LIST OF TABLES

TABLES

Table 1.1 Uses of biomaterials [10] 2

Table 1.2 Materials for use in the body [10] 5

Table 1.3 Biomedical applications of polymeric biomaterials [10] 13

Table 1.4 Properties of some biodegradable polymers [25] 14

Table 1.5 Names and structures of some biodegradable (co)polymers 16

Table 1.6 Properties of various metallic materials [71] 25

Table 1.7 Composition of 316L stainless steel (American Society for Testing and Materials, F139-86, p.61, 1992) [10] 26

Table 1.8 Chemical compositions of Ti and its alloy (American Society for Testing and Materials, F67-89, p.39, F136-84, p.55, 1992) [10] 27

Table 1.9 Mechanical properties of Ti and its alloy (ASTM F136 American Society for Testing and Materials, F67-89, p.39, F136-84, p.55, 1992 and Davidson et al., 1994) [10] 27

Table 1.10 Classification of implant-associated infections according to the onset of symptoms after implantation [93] 30

Table 1.11 Clinical and economic consequences of infections associated with surgical implants [3] 31

Table 1.12 Distribution of microorganisms causing implant-associated infections [93] 32

Table 1.13 Advantages of local drug release systems over systemic drug therapy [128] 37

Table 2.1 Structures of the polymers used 57

Table 2.2 Some properties of polycaprolactone [146] 58

Table 2.3 Properties of poly(L-lactide), poly(D,L-lactide-co-glycolide) and poly(L-lactide-co-ε-caprolactone) [147-153] 59

Table 2.4 Properties of Persoz and Konig Methods [170] 68

Table 3.1 Coating thickness and coating density measurements 87

Table 3.2 Polymer loading on different indentations 88

Table 3.3 Solutions used, treatment duration and temperatures for surface treatments 95

Table 3.4 Persoz hardness results of polymer coatings 104

Table 3.5 Gloss measurements of polymer coatings 105

Table 3.6 Adhesion measurements of polymer coatings by Tape Tests 105

Table 3.7 Lap shear test results for RG 504 107

Table 3.8 Lap shear test results for L 209S 109

Table 3.9 Lap shear test results for L 209S + drugs 110

Table 3.10 T-peel test results for RG 504 112

Table 3.11 T-peel test results for L 209S 114

Table 3.12 Intrinsic viscosity values for RG 504 (stock solution) 116

Table 3.13 Intrinsic viscosity values of RG 504 at various degradation times 118

Table 3.14 Intrinsic viscosity values for L 209S (stock solution) 120

Table 3.15 Intrinsic viscosity values of L 209S at various degradation times 122

Table 3.16 Absorbance and drug releases for Augmentin loaded plates 131

Table 3.17 Coating formulations and absorbance measurements on Alfoxil loaded titanium plates 134

Table 3.18 Total released drug concentrations from Alfoxil loaded titanium plates 135

Table 3.19 Absorbance measurements and released drug concentrations for Alfoxil loaded titanium implant samples (inert coating applied)..... 143

Table 3.20 Sample weights for inert coating applications (RG 504+Alfoxil) 145

Table 3.21 Coating weights and theoretical drug weight for inert coating applications (RG 504+Alfoxil) 145

Table 3.22 Absorbance measurements (RG 504+Alfoxil)..... 146

Table 3.23 Released drug concentrations (RG 504+Alfoxil) 146

Table 3.24 Sample weights with coatings for specimen A 151

Table 3.25 Coating weights and theoretical drug weights for specimen A 152

Table 3.26 Sample weights with coatings for specimen S..... 153

Table 3.27 Coating weights and theoretical drug weights for specimen S 154

Table 3.28 Absorbance measurements for specimen A (RG 504+Fortum)..... 155

Table 3.29 Absorbance measurements for specimen S (RG 504+Fortum) 155

Table 3.30 Released drug concentrations for specimen A (RG 504+Fortum)..... 156

Table 3.31 Released drug concentrations for specimen S (RG 504+Fortum) 157

Table 3.32 Samples used for drug loading control studies 172

Table 3.33 Zone diameter data for Fortum 173

Table 3.34 Disk diffusion antibiotic sensitivity test results 175

Table 3.35 Sample weights for inert coating applications for samples L-1 and L-2 179

Table 3.36 Coating weights and theoretical drug weights for samples L-1 and L-2 179

Table 3.37 Absorbance measurements for specimens L-1 and L-2 180

Table 3.38 Released Vancomycin concentrations for specimens L-1 and L-2 180

Table 3.39 Disk diffusion antibiotic sensitivity test results for L-1 and L-2 184

Table 3.40 Coating weights and theoretical drug weights for specimen V 187

Table 3.41 Absorbance measurements (1V to 12V) 188

Table 3.42 Released drug concentrations for specimen V 189

Table 3.43 Disk diffusion antibiotic sensitivity test results for V samples 198

Table 3.44 Drug releases from disk diffusion antibiotic sensitivity tests for V samples 199

Table 3.45 Kinetic parameters for samples L-1 and L-2 210

Table 3.46 Kinetic parameters for V coded samples 212

Table F.1 Intrinsic viscosity calculations for RG 504 (2 days) 268

Table F.2 Intrinsic viscosity calculations for RG 504 (1 week) 269

Table F.3 Intrinsic viscosity calculations for RG 504 (4 weeks) 270

Table F.4 Intrinsic viscosity calculations for RG 504 (6 weeks) 271

Table G.1 Intrinsic viscosity calculations for L 209S (2 days) 272

Table G.2 Intrinsic viscosity calculations for L 209S (1 week) 273

Table G.3 Intrinsic viscosity calculations for L 209S (4 weeks) 274

Table G.4 Intrinsic viscosity calculations for L 209S (6 weeks) 275

LIST OF FIGURES

FIGURES

Figure 1.1 Polymerization reactions of lactide and glycolide 17

Figure 1.2 Polymerization reaction of ε-caprolactone 19

Figure 1.3 Polymerization reaction of L-lactide with ε-caprolactone 20

Figure 1.4 Reaction sequence used in the industrial production of PVA [49] 21

Figure 1.5 Interaction between the microorganism, the implant and the host in the pathogenesis of implant-associated infections [94] 29

Figure 1.6 Plasma drug concentrations resulting from multiple injections and/or oral administrations [141] 35

Figure 1.7 Drug levels in the blood with (a) traditional drug dosing (b) controlled delivery dosing 36

Figure 1.8 Polymer-based delivery systems, adapted from [137] 40

Figure 1.9 Schematic representations of possible drug release mechanisms [11] 41

Figure 1.10 Schematic diagram of a magnetically controlled polymeric drug delivery system (From Danckwerts and Fassihi, 1991) [136] 42

Figure 2.1 Structure of Vancomycin 61

Figure 2.2 Structure of Amoxicillin 62

Figure 2.3 Structure of Clavulanic acid 63

Figure 2.4 Structure of Ceftazidime 64

Figure 2.5 Structure of Cefazolin 64

Figure 2.6 Structure of Ceftriaxone 65

Figure 2.7 Typical S-N curves for A) a material that displays a fatigue limit and B) a material that does not display a fatigue limit [168] 66

Figure 2.8 Persoz & Konig pendulum hardness tester [170] 67

Figure 2.9 Form and dimensions of test specimen used for lap shear tests 69

Figure 2.10 Lloyd Tensile tester, grip and a load cell 70

Figure 2.11 Form and dimensions of test specimen used for T-peel tests 71

Figure 2.12 Classification of adhesion test results by tape test 72

Figure 2.13 Possible electronic transitions of σ, π, and n electrons [177] 74

Figure 2.14 Pictures of UV-VIS Spectrophotometers used 74

Figure 2.15 A picture of Scanning Electron Microscope 76

Figure 2.16 A picture of Sputter Coating Device 76

Figure 2.17 Kirby-Bauer disc diffusion antibiotic sensitivity testing 78

Figure 2.18 Working principle of EDX [179] 79

Figure 2.19 An approach to the hip joint design, Grade 2 titanium sample used for the experiments can be seen at right 80

Figure 2.20 Different indentations applied to implants 81

Figure 2.21 Mash vision for Model 4 and applied force graph 82

Figure 3.1 Indent Prototypes (indent 1 is the upper, indent 5 is the bottom one) 87

Figure 3.2 S-N figures for (a) grade 2 titanium alloy and (b) stainless steel 316L 89

Figure 3.3 Virtual media model, FEA stress distribution and S-N diagrams for Indentation Model 1 90

Figure 3.4 Virtual media model, FEA stress distribution and S-N diagrams for Indentation Model 2 91

Figure 3.5 Virtual media model, FEA stress distribution and S-N diagrams for Indentation Model 3 92

Figure 3.6 Virtual media model, FEA stress distribution and S-N diagrams for Indentation Model 4 93

Figure 3.7 Virtual media model, FEA stress distribution and S-N diagrams for Indentation Model 5 94

Figure 3.8 SEM image for sample 1 (1 day, 60 ^{0}C, 2000X) 96

Figure 3.9 SEM image for sample 1 (1 day, 60 ^{0}C, 5000X) 96

Figure 3.10 SEM image for sample 2 (2 days, 60 ^{0}C, 2000X) 97

Figure 3.11 SEM image for sample 2 (2 days, 60 ^{0}C, 5000X) 97

Figure 3.12 SEM image for sample 3 (3 days, 60 ^{0}C, 2000X) 98

Figure 3.13 SEM image for sample 3 (3 days, 60 ^{0}C, 5000X) 98

Figure 3.14 SEM image for sample 4 (7 days, 48 ^{0}C, 2000X) 99

Figure 3.15 SEM image for sample 4 (7 days, 48 ^{0}C, 5000X) 99

Figure 3.16 EDX graph for sample 1 (1 day, 60 ^{0}C) 100

Figure 3.17 EDX graph for sample 2 (2 days, 60 ^{0}C) 101

Figure 3.18 EDX graph for sample 3 (3 days, 60 ^{0}C) 101

Figure 3.19 EDX graph for sample 4 (7 days, 48 ^{0}C) 102

Figure 3.20 Schematic representation of structural change of Ti metal with alkali treatment (A), heat treatment (B) and apatite formation mechanism in SBF(C) [182] 102

Figure 3.21 Typical load-propagation extension graph for lap shear tests 106

Figure 3.22 Comparisons of RG 504 Lap Shear tests 108

Figure 3.23 Comparisons of L 209S Lap Shear tests 109

Figure 3.24 Typical load-propagation extension graph for T-peel tests 111

Figure 3.25 Comparisons of RG 504 T-peel tests 113

Figure 3.26 Comparisons of L 209S T-peel tests 114

Figure 3.27 Metabolic degradation pathways for polyglycolide and polylactide polymers (Böstman OM) [98] 115

Figure 3.28 η_{inh} // η_{red} vs. Concentration graph for stock solution (RG 504) 117

Figure 3.29 Intrinsic viscosity vs. degradation time graph for RG 504 118

Figure 3.30 Change in $\overline{Mv}$ of RG 504 with degradation time 119

Figure 3.31 η_{inh} // η_{red} vs. Concentration graph for stock solution (L 209S) 121

Figure 3.32 Intrinsic viscosity vs. degradation time graph for L 209S 122

Figure 3.33 Change in $\overline{Mv}$ of L 209S with degradation time 123

Figure 3.34 Calibration curve for Vancomycin (at 281 nm) 125

Figure 3.35 Calibration curve for Alfoxil (at 206 nm) 126

Figure 3.36 Calibration curve for Augmentin (at 289 nm) 127

Figure 3.37 Calibration curves for Fortum a) at 208 nm, b) at 256 nm 128

Figure 3.38 Calibration curve for Cefamezin (289.5 nm) 129

Figure 3.39 Calibration curve for Rocephin (at 290 nm) 130

Figure 3.40 Titanium plates used for the experiments ("A-coded" sample on the left, "number-coded" sample on the right) 133

Figure 3.41 Alfoxil release and % release from PVOH (low molecular weight) 136

Figure 3.42 Alfoxil release and % release from PVOH (high molecular weight) ... 137

Figure 3.43 Alfoxil release and % release from Polycaprolactone 138

Figure 3.44 Alfoxil release and % release from PLGA RG 504 139

Figure 3.45 Alfoxil release and % release from poly(D,L-lactide-co-ε-caprolactone) LC 703 140

Figure 3.46 Alfoxil release and % release from Poly(L-lactide) L 209S 141

Figure 3.47 Effect of inert coatings on Alfoxil release 143

Figure 3.48 Titanium plate used for inert coating applications ("Y-coded" sample) 144

Figure 3.49 Alfoxil release profiles for samples 1Y and 2Y 147

Figure 3.50 Alfoxil release profiles for samples 3Y and 4Y 147

Figure 3.51 Alfoxil release profiles for samples 5Y and 6Y 148

Figure 3.52 Alfoxil release profile for sample 8Y 148

Figure 3.53 Titanium plates used for the experiments ("A-coded" sample on the left, "S-coded" sample on the right) 150

Figure 3.54 Fortum release profiles for samples 3A and 4A (208 nm) 158

Figure 3.55 Fortum release profiles for samples 7A and 8A (208 nm) 158

Figure 3.56 Fortum release profiles for samples 11A and 12A (208 nm) 159

Figure 3.57 Fortum release profile for sample 15A (208 nm) 159

Figure 3.58 Fortum release profiles for samples 3A and 4A (256 nm) 160

Figure 3.59 Fortum release profiles for samples 7A and 8A (256 nm) 160

Figure 3.60 Fortum release profiles for samples 11A and 12A (256 nm) 161

Figure 3.61 Fortum release profile for sample 15A (256 nm) 161

Figure 3.62 Fortum release profiles for samples 3A, 7A, 11A and 15A (208 nm) 162

Figure 3.63 Fortum release profiles for samples 4A, 8A, 12A and 15A (208 nm) 162

Figure 3.64 Fortum release profiles for samples 3A, 7A, 11A and 15A (256 nm) 163

Figure 3.65 Fortum release profiles for samples 4A, 8A, 12A and 15A (256 nm) 163

Figure 3.66 Fortum release profiles for samples 9S and 10S (208 nm)..... 164

Figure 3.67 Fortum release profiles for samples 11S and 12S (208 nm)..... 164

Figure 3.68 Fortum release profiles for samples 13S and 14S (208 nm)..... 165

Figure 3.69 Fortum release profile for sample 15S (208 nm)..... 165

Figure 3.70 Fortum release profiles for samples 9S and 10S (256 nm)..... 166

Figure 3.71 Fortum release profiles for samples 11S and 12S (256 nm)..... 166

Figure 3.72 Fortum release profiles for samples 13S and 14S (256 nm)..... 167

Figure 3.73 Fortum release profile for sample 15S (256 nm)..... 167

Figure 3.74 Fortum release profiles for samples 9S, 11S, 13S and 15S (208 nm) .. 168

Figure 3.75 Fortum release profiles for samples 10S, 12S, 14S and 15S (208 nm) 168

Figure 3.76 Fortum release profiles for samples 9S, 11S, 13S and 15S (256 nm) .. 169

Figure 3.77 Fortum release profiles for samples 10S, 12S, 14S and 15S (256 nm) 169

Figure 3.78 Calibration curve for Fortum in terms of zone diameters..... 174

Figure 3.79 Change in Fortum activity with time (in water) 176

Figure 3.80 Change in Fortum activity with time (in PBS) 176

Figure 3.81 Change in Vancomycin activity with time 177

Figure 3.82 Vancomycin release and % release profiles for samples L-1 and L-2 181

Figure 3.83 Disk diffusion antibiotic sensitivity tests for L-1 and L-2 183

Figure 3.84 Vancomycin release profiles for samples L-1 and L-2 according to disk diffusion antibiotic sensitivity tests 185

Figure 3.85 Vancomycin release and % release profiles for samples 1V to 3V 190

Figure 3.86 Vancomycin release and % release profiles for samples 4V to 6V 191

Figure 3.87 Vancomycin release profiles for samples 7V to 9V 192

Figure 3.88 Vancomycin release profiles for samples 10V to 12V 193

Figure 3.89 Disk diffusion antibiotic sensitivity tests for V samples 196

Figure 3.89 Continued; refer to Figure 3.89 (a) for sample numbers 197

Figure 3.90 Vancomycin release profiles for samples 1V to 3V according to disk diffusion antibiotic sensitivity tests 199

Figure 3.91 Vancomycin release profiles for samples 4V to 6V according to disk diffusion antibiotic sensitivity tests 200

Figure 3.92 Vancomycin release profiles for samples 7V to 9V according to disk diffusion antibiotic sensitivity tests 200

Figure 3.93 Vancomycin release profiles for samples 10V to 12V according to disk diffusion antibiotic sensitivity tests 201

Figure 3.94 Scanning Electron Micrographs: (A) Uncoated macroporous surfaces of titanium implants. (B) Coated titanium implants; first layer with Vancomycin impregnated β-TCP (16.2% (w/w) Vancomycin, 1g) dispersed PLGA RG 504 solution in chloroform (10% w/v) and second layer inert coating with PL L209S solution in chloroform (5% w/v). (C) After 1 week immersion in water at 37^0C. (D) After 2 weeks immersion in water at 37^0C. (E) After 3 weeks immersion in water at 37^0C. (F) After 4 weeks immersion in water at 37^0C. (G) After 6 weeks immersion in water at 37^0C. 202

Figure 3.94 Scanning Electron Micrographs: (Cont'd…) 203

Figure 3.95 6 weeks after implantation (hematoxylin and eosin stain, x 200). No evidence for necrosis and tissue damage was observed. Implant material does not damage muscle structure 205

Figure 3.96 6 weeks after implantation (Masson's Trichrome stain, x 100). Ligament formation was observed in the area between implant and muscle. No macrophage formation was observed in formed ligament 205

Figure 3.97 6 weeks after implantation (Masson's Trichrome stain, x 400). It was observed that implant material allowed new blood vessel formation..... 206

Figure 3.98 Plot of kinetic data in accordance with zero-order release model for samples L-1 and L-2 208

Figure 3.99 Plot of kinetic data in accordance with first-order release model for samples L-1 and L-2 208

Figure 3.100 Plot of kinetic data in accordance with Higuchi release model for samples L-1 and L-2 209

Figure 3.101 Plot of kinetic data in accordance with Korsmeyer-Peppas release model for samples L-1 and L-2..... 209

Figure 3.102 Plot of kinetic data in accordance with zero-order release model for V samples. Each result shows the mean ± SD, (n=3)..... 210

Figure 3.103 Plot of kinetic data in accordance with first-order release model for V samples. Each result shows the mean ± SD, (n=3)..... 211

Figure 3.104 Plot of kinetic data in accordance with Higuchi release model for V samples. Each result shows the mean ± SD, (n=3) 211

Figure 3.105 Plot of kinetic data in accordance with Korsmeyer-Peppas release model for V samples. Each result shows the mean ± SD, (n=3)..... 212

Figure A.1 DSC thermogram of poly(D,L-lactide-co-glycolide) (Resomer RG 504) 247

Figure A.2 DSC thermogram of poly(L-lactide) (Resomer L 209S)..... 247

Figure A.3 DSC thermogram of poly(L-lactide-co-caprolactone) (Resomer LC 703) 248

Figure A.4 DSC thermogram of polycaprolactone 248

Figure A.5 DSC thermogram of poly(vinyl alcohol) ($\overline{Mw}$:13.000-23.000) 248

Figure A.6 DSC thermogram of poly(vinyl alcohol) ($\overline{Mw}$:31.000-50.000) 249

Figure B.1 Images of powder Vancomycin 250

Figure B.2 Images of Vancomycin impregnated β-TCP..... 251

Figure C.1 Lap-shear tests for RG 504 coatings on titanium plates (no surface modification)..... 252

Figure C.2 Lap-shear tests for RG 504 coatings on titanium plates (4 No sandpapered) 253

Figure C.3 Lap-shear tests for RG 504 coatings on titanium plates (wire emery) .. 254

Figure C.4 Lap-shear tests for RG 504 coatings on titanium plates (sandblasted) 255

Figure C.5 Lap-shear tests for L 209S coatings on titanium plates (no surface modification)..... 256

Figure C.6 Lap-shear tests for L 209S coatings on titanium plates (4 No sandpapered) 256

Figure C.7 Lap-shear tests for L 209S coatings on titanium plates (wire emery) ... 257

Figure C.8 Lap-shear tests for L 209S coatings on titanium plates (sandblasted)... 258

Figure D.1 T-peel tests for RG 504 coatings on titanium plates (no surface modification) ... 259

Figure D.2 T-peel tests for RG 504 coatings on titanium plates (4 No sandpapered) ... 260

Figure D.3 T-peel tests for RG 504 coatings on titanium plates (wire emery) ... 261

Figure D.4 T-peel tests for RG 504 coatings on titanium plates (sandblasted) ... 262

Figure D.5 T-peel tests for L 209S coatings on titanium plates (no surface modification) ... 263

Figure D.6 T-peel tests for L 209S coatings on titanium plates (4 No sandpapered) ... 264

Figure D.7 T-peel tests for L 209S coatings on titanium plates (wire emery) ... 265

Figure D.8 T-peel tests for L 209S coatings on titanium plates (sandblasted) ... 266

Figure F.1 η_{inh} // η_{red} vs. Concentration graph for degradation of RG 504 (2 days) ... 268

Figure F.2 η_{inh} // η_{red} vs. Concentration graph for degradation of RG 504 (1 week) ... 269

Figure F.3 η_{inh} // η_{red} vs. Concentration graph for degradation of RG 504 (4 weeks) ... 270

Figure F.4 η_{inh} // η_{red} vs. Concentration graph for degradation of RG 504 (6 weeks) ... 271

Figure G.1 η_{inh} // η_{red} vs. Concentration graph for degradation of L 209S (2 days) ... 272

Figure G.2 η_{inh} // η_{red} vs. Concentration graph for degradation of L 209S (1 week) ... 273

Figure G.3 η_{inh} // η_{red} vs. Concentration graph for degradation of L 209S (4 weeks) 274

Figure G.4 η_{inh} // η_{red} vs. Concentration graph for degradation of L 209S (6 weeks) 275

ABBREVIATIONS

A	absorbance
C	concentration
CF	carbon fiber
CHA	calcium hydroxyapatite
d	day(s)
DI	deionized
DNA	deoxyribonucleic acid
EDX	energy dispersive X-ray spectroscopy
FEA	finite element analysis
h	hour(s)
HA	hydroxyapatite
HB	hydroxybutyrate
HV	hydroxyvalerate
k	release rate constant
K_0	zero order release rate constant
K_1	first order release rate constant
K_H	Higuchi release rate constant
K_{KP}	Korsmeyer-Peppas release rate constant
K’	Huggins constant
K’’	Kraemer constant
MIC	minimum inhibitory concentration
mo	month(s)
MW or Mwt	molecular weight
M_t	amount of drug released at time t
M_∞	amount of drug released at infinite time

$\overline{Mn}$	number average molecular weight
$\overline{Mv}$	viscosity average molecular weight
$\overline{Mw}$	weight average molecular weight
n	diffusional exponent
NA	not applicable
PA	polyacetal
PBS	phosphate buffered saline
PCL	polycaprolactone
PDO	polydioxanone
PE	polyethylene
PEEK	polyetheretherketone
PET	polyethyleneterephthalate
PGA	polyglycolide or polyglycolic acid
PLA	polylactide or polylactic acid
PLLA	poly(L-lactide)
PLGA	poly(lactide-co-glycolide)
PLLA/PCL	poly(L-lactide-co-caprolactone)
PMMA	polymethylmethacrylate
PP	polypropylene
PS	polystyrene
PTFE	polytetrafluoroethylene
PU	polyurethane
PVA, PVOH or PVAl	polyvinyl alcohol
PVC	polyvinylchloride
R^2	correlation coefficient
RNA	ribonucleic acid
SBF	simulated body fluid
SEM	scanning electron microscopy
SiC	silicon carbide
SR	silicone rubber
TCP	tricalcium phosphate

T_g	glass transition temperature
T_m	melting temperature
wk	week(s)
w/v	mass of solute (g)/volume of solution (ml)
$[\eta]$	intrinsic viscosity
η_{rel} or η_r	relative viscosity
η_{sp}	specific viscosity
η_{inh}	inherent viscosity
η_{red}	reduced viscosity

CHAPTER 1

INTRODUCTION

1.1 Overview of Biomaterials

The terms biomaterial and biomaterial science are extensively used for nearly 50 years. The concepts and definitions of this scientific area became much more clear, broader and understandable as the new developments in this area were achieved.

1.1.1 Definition and Use of Biomaterials

"Biomaterials" term has been used to describe both the materials derived from biological sources and materials used in the human body for the treatment [6].

A biomaterial can be defined as any systematically, pharmacologically (living or not living) inert substance or combination of substances utilized for implantation within or incorporation with a living system to supplement or replace functions of living tissues or organs. For this purpose, a biomaterial designated to be put in contact with living tissues and/or body fluids resulting in an interface between living and nonliving substances [7, 9, 10].

Along the history, the use of biomaterials can be seen widely. Starting from

ancient civilizations, with the help of the new technologies developed, the importance of the use of biomaterials in our lives became clearer. Today, many devices and implants can be produced and used in human body. Biomaterials in the form of implants (sutures, bone plates, joint replacements, ligaments, vascular grafts, heart valves, intraocular lenses, dental implants etc.) and medical devices (pacemakers, biosensors, artificial hearts, blood tubes, etc.) are widely used to replace and/or restore the function of traumatized or degenerated tissues or organs, to assist and thus improve the quality of life of the patients [8-10].

"Biomaterials and medical devices find an application as prostheses and implants in nearly any medical discipline. The introduction of an implant into a soft or hard tissue induces in a first time a temporary inflammatory reaction followed by a tissue repair around the implant. A prolonged inflammatory reaction after implantation immediately makes rise questions about the biological and medical advantages. In order to improve the tissue integration and subsequently the long-term maintenance, the implant surface can be modified by mechanical, physical, chemical or biological functionalization. The control of the physical, chemical and biochemical properties of an implant surface is one of the most important issues in the design of biomedical devices since the first interaction between a foreign body (implant) and the biological environment occurs at the interface" [9].

Table 1.1 Uses of biomaterials [10]

Problem Area	**Examples**
Replacement of diseased or damaged part	Artificial hip joint, kidney dialysis machine
Assist in healing	Sutures, bone plates, and screws
Improve function	Cardiac pacemaker, intraocular lens
Correct functional abnormality	Cardiac pacemaker
Correct cosmetic problem	Augmentation mammoplasty, chin augmentation
Aid to diagnosis	Probes and catheters
Aid to treatment	Catheters, drains

1.1.2 History of Biomaterials

The history of biomaterials is more than several thousand years. In ancient cultures (Egypt, Greece, Babylonia, China etc.), the use of gold, silver, cupper, lead, wood, teeth of dogs, bones and many other materials possible have been used as biomaterials. In these days, use of these materials was done without knowing the concept and importance of biocompatibility. This term was introduced nearly 50 years ago [9].

By the development of aseptic surgical technique developed by Dr. J. Lister in 1860s the uses of biomaterials become practical. The problems in the previous surgical attempts were resultant infections. Most successful implants were skeletal ones but their inadequate design and low mechanical strength at stress concentrating corners usually resulted in break of the implant. Also corrosion of implants was another problem related with implants. Following improvements in this field, better materials and designs were applied. In 1930s, with the introduction of stainless steel and cobalt chromium alloys, successful fracture fixations were achieved. Use of synthetic polymers became famous as a result of the understanding that PMMA fragments did not cause adverse effects in the human body during World War II. The blood vessel replacements in 1950s and heart valve replacements and cemented joint replacements in the 1960s were followed these achievements. In recent years, much more developments came true in the biomaterial sciences [10].

1.1.3 Biocompatibility

"Definitions of biomaterials and of biocompatibility have changed with respect to the acquired knowledge and the increasing performance of a material. So a biomaterial must now be understood as a (living or not-living) material destined to be put in contact with living tissues and/or with biological fluids to evaluate, treat, modify forms or replace any tissue, organ or function of the body" [9].

"The definition of biocompatibility has even more been changed with respect to the considered material: First defined for biological inert materials, it has been adapted to biological active and finally functionalized materials for drug binding and drug delivery. It also has to consider biodegradable and natural materials. Its today most objective definition should be the property of a biomaterial that is to generate in the host an appropriate reaction. This means that knowing the multiple transient signals in the organism, it is utopia to want not to generate any unwanted reaction. Thus it is preferable to try to minimize it and to control it" [9].

1.1.4 Materials Used as Biomaterials

Biomaterials are primarily used for medical applications usually as prostheses and implants [9, 11]. For different applications, materials can be chosen and modifications and designs can be adjusted accordingly. "In medical applications, biomaterials are rarely used as simple materials and are more commonly integrated into devices" [11].

The materials used for biomedical applications can be grouped into four categories. These are;

(a) metals

(b) ceramics

(c) polymers

(d) composites made from various combinations of (a), (b) and (c) [8].

Another classification of the materials is done by researchers as bioinert and bioactive, biostable and biodegradable etc. Alumina, titania, zirconia, bioglass (or bioactive glasses), carbon and hydroxyapatite (HA) are widely considered as biocompatible ceramics. Metals and alloys that are successful as biomaterials include: gold, tantalum, stainless steel, Co-Cr, NiTi (shape memory alloy), and Ti alloys. A large number of polymers such as polyethylene (PE), polyurethane (PU), polytetrafluoroethylene (PTFE), polyacetal (PA), polymethylmethacrylate (PMMA),

polyethylene terepthalate (PET), silicone rubber (SR), polysulfone, polyetheretherketone (PEEK), poly(lactic acid) (PLA), and poly(glycolic acid) (PGA) are also used in various biomedical applications. HA/PE, silica/SR, carbon fiber/epoxy (CF/epoxy), and CF/PEEK are few examples of polymer composite biomaterials. Each type of biomaterial has its own positive aspects that are particularly suitable for specific application [8].

Table 1.2 Materials for use in the body [10]

Materials	Advantages	Disadvantages	Examples
Polymers	Resilient Easy to fabricate	Not strong Deforms with time May degrade	Sutures, blood vessels, hip socket, ear, nose, other soft tissues
Metals	Strong Tough Ductile	May corrode Dense Difficult to make	Joint replacements, bone plates and screws, dental root implants, pacer and suture wires
Ceramics	Very biocompatible Inert Strong in compression	Brittle Not resilient Difficult to make	Dental; femoral head of hip replacement, coating of dental and orthopedic implants
Composites	Strong Tailor-made	Difficult to make	Joint implants, heart valves

1.2 Polymeric Biomaterials

All living organisms are made up of polymers. They form the building blocks of life. Their presence has been started from the beginning of time. However, the existence of polymers was not clear until the middle of the twentieth century. Along with the development of synthetic polymers and understanding their nature, the doors of a new world were opened to human being. After new developments in polymer world, manmade polymeric materials were started to penetrate into our lives deeply. Without polymers, life can not be as comfortable as today [12].

The use of polymers is boundless. Their great properties give them a chance to be used in every field of life. One of them is as biomaterials. In the following parts, some basic information about polymers is given.

1.2.1 Definition and Basic Concepts of Polymers

Polymers are large molecules consisting of a large number of small component molecules (repeating units). The word *polymer* is derived from classical Greek ***poly*** meaning "many" and ***meres*** meaning "parts." Thus a polymer is a large molecule (macromolecule) built up by the repetition of small chemical units. Most commercial polymers are based on covalent compounds of carbon, although certain synthetic polymers may also be based on inorganic atoms such as silicon [12-16, 20].

The wide variety of polymers includes such natural materials as cellulose, starches, silk, natural rubber, proteins, polysaccharides, DNA and RNA. While these polymers are interesting and have seen widespread use in numerous applications, they are sometimes eclipsed by the seemingly endless variety of synthetic polymers that are available today. From the earliest times, man has used natural occurring polymers for different purposes [11, 16-18].

At first, man-made polymers were produced empirically without knowing the chemical structure of the product. The only concern was the composition. However, with the developments in science, structural concept of polymers became understandable. After these developments about polymers, high numbers of commercial polymers were produced between 1925 and 1950 [12, 14-17, 19].

In recent years, with better understanding polymer structure-property relationships, discoveries of new polymerization techniques and use of new monomers; synthetic polymers have started to find their place. These developments in polymer science made it possible to create polymers by using various elements and polymerization techniques. By the way, desired properties can be obtained in an end product. Polymer materials can be produced in the form of solid plastics, fibers,

elastomers, or foams. They may be hard or soft or may be films, coatings, or adhesives. They can be made porous or nonporous or can melt with heat or set with heat. The possibilities are almost endless and their applications fascinating. Today, their applications become essential for modern living and these materials are used in all areas of daily life, from engineering to medicine [12-15].

1.2.2 Classification of Polymers

Polymers can be classified in different aspects. These are ranging from the origin of the polymer to the preparation techniques. The more basic classification is according to their origin. That means polymers are either natural or synthetic. Many other classifications can be done according to the structure of polymer, polymerization mechanism, thermal behaviour, preparation technique etc. [12]. Below, some brief explanations about different classifications of polymers are given. This information makes much clearer to understand the importance of polymers as biomaterials.

According to Origin:

Polymers may either be natural or synthetic. Enzymes, proteins, nucleic acids, silk, starch, natural rubber, cellulose, alginates etc. are commonly known natural based polymers. On the other hand, there are lots of synthetic polymers belonging fibers, elastomers, plastics, adhesives etc. families [12, 15, 17, 18, 20].

According to Structure:

The structure of a polymer is basically dependant on the functionality of the relevant monomers. A molecule may be classified as monofunctional, bifunctional, or polyfunctional depending on whether it has one, two, or greater than two sites available for linking with other molecules [12]. Therefore, the resultant polymer may be linear, branched, crosslinked, ladder type etc. according to the monomer structure, functionality and polymerization reaction [12, 14, 16, 17, 20].

"Polymers in the solid state may be amorphous or crystalline. When polymers are cooled from the molten state or concentrated from the solution, molecules are often attracted to each other and tend to aggregate as closely as possible into a solid with the least possible potential energy. For some polymers, in the process of forming a solid, individual chains are folded and packed regularly in an orderly fashion. The resulting solid is a crystalline polymer with a long-range, three-dimensional, ordered arrangement. In contrast to crystallizable polymers, amorphous polymers possess chains that are incapable of ordered arrangement. They are characterized in the solid state by a short-range order of repeating units. These polymers vitrify, forming an amorphous glassy solid in which the molecular chains are arranged at random and even entangled" [12].

Polymers may be either homopolymers or copolymers depending on their composition. Polymers composed of only one repeating unit in the polymer molecules are known as *homopolymers.* Polymers composed of more than one different repeating unit in the polymer molecule are defined as *copolymers* [12-17]. The different kind of copolymers (unspecified, statistical, random, alternating, block and graft) is given elsewhere [13, 15, 16].

"Polymers may also be classified as fibers, plastics, or elastomers. The reason for this is related to how the atoms in a molecule (large or small) are hooked together. The ability for close alignment of molecules depends on the structure of the molecules. Those molecules with regular structure can align themselves very closely for effective utilization of the secondary intermolecular bonding forces. The result is the formation of a *fiber.* Fibers are linear polymers with high symmetry and high intermolecular forces that result usually from the presence of polar groups. They are characterized by high modulus, high tensile strength, and moderate extensibilities (usually less than 20%). At the other end of the spectrum, there are some molecules with irregular structure, weak intermolecular attractive forces, and very flexible polymer chains. These are generally referred to as *elastomers.* Chain segments of elastomers can undergo high local mobility, but the gross mobility of chains is restricted, usually by the introduction of a few cross-links into the structure. In the

absence of applied (tensile) stress, molecules of elastomers usually assume coiled shapes. Consequently, elastomers exhibit high extensibility (up to 1000%) from which they recover rapidly on the removal of the imposed stress. Elastomers generally have low initial modulus in tension, but when stretched they stiffen. *Plastics* fall between the structural extremes represented by fibers and elastomers. However, in spite of the possible differences in chemical structure, the demarcation between fibers and plastics may sometimes be blurred. Polymers such as polypropylene and polyamide can be used as fibers and as plastics by a proper choice of processing conditions" [12].

According to Thermal Behaviour:

According to thermal responses, polymers are classified as *thermoplastics* or *thermosets*. Thermoplastic polymers soften and flow under the action of heat and pressure. Upon cooling, the polymer hardens and assumes the shape of the mold. They can be remolded into any shape using various polymer processing techniques. On the other hand, a thermoset is a polymer that, when heated, undergoes a chemical change to produce a cross-linked, solid polymer and chain motion of them is greatly restricted by a high degree of crosslinking. Thermosets usually exist initially as liquids called prepolymers; they can be shaped into desired forms by the application of heat and pressure, but are incapable of undergoing repeated cycles of softening and hardening. The basic structural difference between thermoplastics and thermosets is that thermoplastic polymers are composed mainly of linear and branched molecules, whereas thermosets are made up of cross-linked systems [12-16, 20].

According to Preparative Technique:

Wallace Carothers classified the polymers according to their polymerization mechanisms as condensation and addition polymerization. However, this classification was found to be unsatisfactory after recognizing some condensation polymerizations have features characteristic to the addition polymerization and some addition polymerizations have features characteristic to the condensation polymerization. Therefore, better classification was done as step-growth

polymerization and chain-growth polymerization [15, 16].

Polymers can be classified according to the preparative techniques used during the polymerization of the monomer. Bulk polymerization, solution polymerization, emulsion polymerization, suspension polymerization, solid state polymerization, gas-phase polymerization and plasma polymerization techniques are the preparative techniques and their definitions are given elsewhere [12, 14, 15].

As it is clear from above brief explanations about the polymer classifications; the properties of polymers can be altered by the application of different polymerization mechanisms and reaction conditions. Produced polymers can be in various structures according to their monomer functionalities and polymerization reaction conditions: Linear, branched, crosslinked, star-like, dendrimer, crosslinked, ladder type etc. Also we may have homopolymers, copolymers, and hydrogels. Polymers can be, crystalline, or amorphous. Molecular weight and its distribution also affect the properties of produced polymer directly. That means mechanical, thermal, and rheological properties of these materials can be modified to make them suitable according to the purpose of usage. As a result, polymers have found various applications as biomaterials as well as for other purposes.

1.2.3 Polymers as Biomaterials

The use of polymers as biomaterials becomes more common with discovering their powerful properties. They can be produced in different forms ranging from nanoparticles to macro product forms according to the purpose of use. Their engineering properties can be adjusted in different ways. They can be used as themselves or modified to resemble for use in human body. Also, their biodegradable and biocompatible properties make them major candidates for biomedical applications.

There are also some disadvantages with the use of polymers as biomaterials.

Their low modulus of elasticity and viscoelastic characteristics make them difficult to use for load bearing applications. Also, purity of polymers is hard to achieve. There are usually additives within the polymers. The leaching of such additives within the body may lead to toxicity or other detrimental effects [21].

The use of natural polymeric materials as biomaterials is also applicable but the usage is limited with respect to limited kind and property of such materials. After the great improvements in polymer sciences, polymers with desired properties can be synthesized and used.

Produced, designed, and modified synthetic polymeric materials have been widely used in sutures, artificial organs such as kidney and heart, medical disposable supplies, prosthetic materials, dental materials, implants, dressings, extracorporeal devices, encapsulants, polymeric drug delivery systems, tissue engineered products, and orthodoses like those of metal and ceramic substituents [10, 13, 15].

The main advantages of the polymeric biomaterials compared to metal and ceramic materials are ease of manufacturability to produce various shapes, ease of secondary processability with desired mechanical and physical properties. The required properties of polymeric biomaterials are similar to other biomaterials that are biocompatibility, sterilizability, adequate mechanical and physical properties, and manufacturability [10]. Also, depending upon the application, polymers used in the biomedical field, must have one or more specific properties such as selective permeability, the ability to biodegrade, and high strength or modulus [15].

Important properties of biodegradable biomaterials are as follows [22, 23]:

- The material should not evoke a sustained inflammatory or toxic response upon implantation in the body.
- The material should have acceptable shelf life.
- The degradation time of the material should match the healing or regeneration

process.

- The material should have appropriate mechanical properties for the indicated application and the variation in mechanical properties with degradation should be compatible with the healing or regeneration process.
- The degradation products should be non-toxic, and able to be metabolized and cleared from the body.
- The material should have appropriate permeability and processability for the intended application.

The polymers that are used in biomedical applications can be either homopolymers or copolymers. However, the basic classification of polymeric biomaterials can be done as *non-degradable* and *biodegradable* polymeric biomaterials.

1.2.3.1 Non-degradable Polymeric Biomaterials

In the non-degradable part of polymeric materials, although we have thousands of different polymers and they could be used as biopolymers, only a small number of polymers are mainly used in medical device fabrications from disposable to long-term implants. Mostly used ones names and general uses are given in the following table:

Table 1.3 Biomedical applications of polymeric biomaterials [10]

Synthetic Polymers	Applications
Polyvinylchloride (PVC)	Blood and solution bag, surgical packaging, IV sets, dialysis devices, catheter bottles, connectors, and cannulae
Polyethylene (PE)	Pharmaceutical bottle, nonwoven fabric, catheter, pouch, flexible container, and orthopedic implants
Polypropylene (PP)	Disposable syringes, blood oxygenator membrane, suture, nonwoven fabric, and artificial vascular grafts
Polymethylmetacrylate (PMMA)	Blood pump and reservoirs, membrane for blood dialyzer, implantable ocular lens, and bone cement
Polystyrene (PS)	Tissue culture flasks, roller bottles, and filterwares
Polyethyleneterephthalate (PET)	Implantable suture, mesh, artificial vascular grafts, and heart valve
Polytetrafluoroethylene (PTFE)	Catheter and artificial vascular grafts
Polyurethane (PU)	Film, tubing, and components
Polyamide (nylon)	Packaging film, catheters, sutures, and mold parts

1.2.3.2 Biodegradable Polymeric Biomaterials

Biodegradable polymers can be either natural or synthetic. Synthetic polymers can be produced with a wide range of desired properties. On the other hand, there is no such chance for natural ones. Therefore, synthetic polymers are preferred usually [24]. "The general criteria for selecting a polymer for use as a degradable biomaterial are to match the mechanical properties and the degradation rate to the needs of the application" [25].

Table 1.4 Properties of some biodegradable polymers [25]

Polymer	T_m (°C)	T_g (°C)	Tensile modulus (MPa)	Degradation time (months)
Polyglycolic acid	225-230	35-40	7	6-12
L-Polylactic acid	173-178	60-65	2.7	>24
D,L-Polylactic acid	Amorphous	55-60	1.9	12-16
Polycaprolactone	58-63	(-65)-(-60)	0.4	>24
85/15 Poly(D,L-lactide-co-glycolide)	Amorphous	50-55	2.0	5-6

Degradable polymeric biomaterials are used to develop devices such as prostheses, porous structures as scaffolds and controlled/sustained drug release agents. Each of these applications demands materials with specific physical, chemical, biological, biomechanical and degradation properties to provide efficient therapy [23].

The application of synthetic biodegradable polymers started only in the later half of 1960's. The past two decades saw the development of a range of new generation synthetic biodegradable polymers and analogous natural polymers specifically developed for biomedical applications [23].

"Current efforts in biodegradable polymer synthesis have been focused on custom designing and synthesizing polymers with tailored properties for specific applications by [23]:
1) developing novel synthetic polymers with unique chemistries to increase the diversity of polymer structure,
2) developing biosynthetic processes to form biomimetic polymer structures and
3) adopting combinatorial and computational approaches in biomaterial design to accelerate the discovery of novel resorbable polymers".

Some of the current biomedical applications of biodegradable polymeric materials include: 1) large implants (bone screws, bone plates, contraceptive

reservoirs etc.) 2) small implants (staples, sutures, nano or micro-sized drug delivery vehicles etc.) 3) plain membranes for guided tissue regeneration and 4) multifilament meshes or porous structures for tissue engineering [23, 26].

The biomaterials are mainly constituted by biodegradable polymers from glycolide, lactide and ε-caprolactone monomers. In addition to these mostly used polymers and copolymers in this area; poly(dioxanone), poly(trimethylene carbonate), poly(carbonate), and poly(vinyl alcohol) are also used in some extent for their good biocompatibility, controllable biodegradability, and relatively good processability. Polymer properties can be tailored from soft elastomerics to rigid engineering plastics. In addition to mechanical properties, degradation rate, hydrophilicity and solubility can be customized for individual applications. A thorough understanding of these properties is critical to designing a quality medical device or controlled-delivery system for use in humans [10, 27].

In Table 1.5, structures and names of some biodegradable polymers and copolymers are given:

Table 1.5 Names and structures of some biodegradable (co)polymers

Structure	**Name**
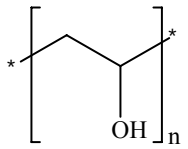	Polyvinyl alcohol (PVA, PVOH or PVAl)
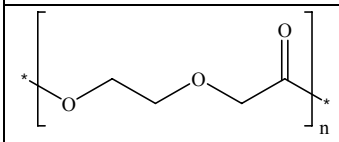	Polydioxanone (PDO)
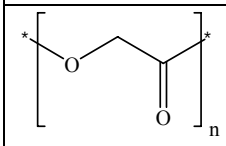	Polyglycolide (PGA)
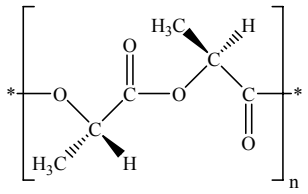	Poly(L-lactide) (PLA or PLLA)
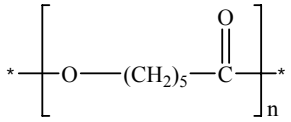	Polycaprolactone (PCL)
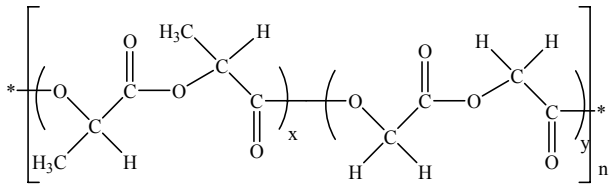	Poly(D,L-lactide-co-glycolide) (PLGA)
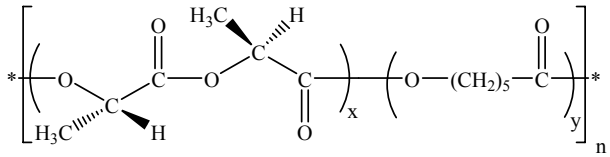	Poly(L-lactide-co-ε-caprolactone) (PLLA/PCL)

1.2.3.2.1 Lactide-Glycolide Polymers

Biodegradable polyesters, especially poly(lactide) (PLA), poly(glycolide)

(PGA) and their copolymers (PLGA) have been extensively studied and used in medicine and surgery for controlled release of drugs, biodegradable sutures and fracture fixation implants. In orthopedic surgery, implants made up of these polymers are absorbed by the body after bone tissue growth in their porous structures. There are some limitations for their use for drug formulations since these polymers are all strongly hydrophobic. On the other hand, they can all be used as controlled drug release agents because of their adjustable biodegradation properties and their high biocompatibilities [2, 6, 28, 29, 30, 31].

PGA is usually obtained by polymerizing diglycolide with a tin catalyst [28]. Similarly, PLA can be obtained from dilactide by stannous octoate catalysed, ring-opening polymerization [28, 32]. These polymers and their copolymers are obtained by liquid-phase polymerization of the cyclic dimers of glycolide, lactide and their mixtures [30].

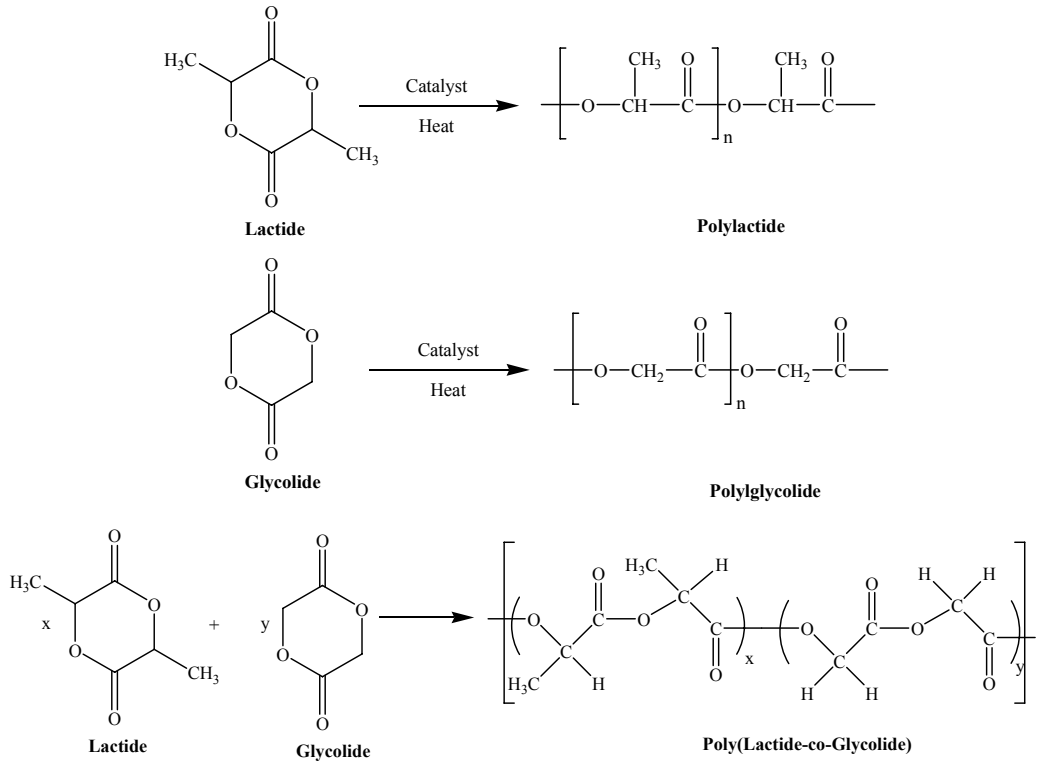

Figure 1.1 Polymerization reactions of lactide and glycolide

PLA, PGA, and PLGA can be degraded into non-toxic substances, and removed from the human body [29]. “An important aspect of the biodegradation of polyesters is the susceptibility of polyesters to hydrolytic degradation. Degradation proceeds by random hydrolytic chain scission of the ester linkages, eventually producing the monomeric hydroxyacid. Two distinct stages in the degradation process have been identified. The first stage, which is nonenzymatic, is restricted to random hydrolytic cleavage of ester linkages. The second stage, which is also nonenzymatic, begins when the molecular weight of the polymer has decreased to the point that chain scission can produce an oligomer small enough to diffuse from the polymer bulk. Catastrophic loss of mechanical strength can occur during this second phase. As the average MW approaches 10.000, microorganisms are able to digest the low MW lactic acid oligomers to produce carbon dioxide and water” [20].

The degradation of PLA, PGA and their copolymers involves random hydrolysis of ester bonds. PLA degrades to form lactic acid monomers which are normally present within the body. Then, enters tricarboxylic acid cycle and is excreted as water and carbondioxide. No significant amounts of accumulation of degradation products have been reported in any of the vital organs [33, 34]. C^{13} labeled PLA has demonstrated little radioactivity in feces or urine. It is also reported that in addition to hydrolysis PGA is also broken down by certain enzymes. Glycolic acid also can be excreted by urine [34, 35].

The rate of degradation is determined by factors such as configurational structure, copolymer ratio, crystallinity, molecular weight, morphology, stresses, amount of residual monomer, porosity and site of implantation [34].

1.2.3.2.2 Lactide-Caprolactone Polymers

PCL is a semicrystalline polymer with a glass transition temperature of about (-60)ºC. The polymer has a low melting temperature (59 to 64ºC) and is compatible with a range of other polymers. PCL degrades at a much lower rate that PLA and is a

useful base polymer for developing long-term, implantable drug delivery systems [34].

Poly(caprolactone) is prepared by the ring-opening polymerization of the cyclic monomer ε-caprolactone. Catalysts such as stannous octoate are used to catalyse the polymerization and low molecular weights alcohols can be used as initiator which also can be used to control the molecular weight of the polymer [28, 34, 36, 37].

The homopolymer has a degradation time of the order of two to three years [34, 38, 39, 40]. PCL with an initial average molecular weight of 50,000 takes about three years for complete degradation in-vitro [34, 41]. Copolymers of ε-caprolactone with D,L-lactide have been synthesized to yield materials with more rapid degradation rates [34, 40]. PCL is considered a non-toxic and a tissue compatible material [34, 38].

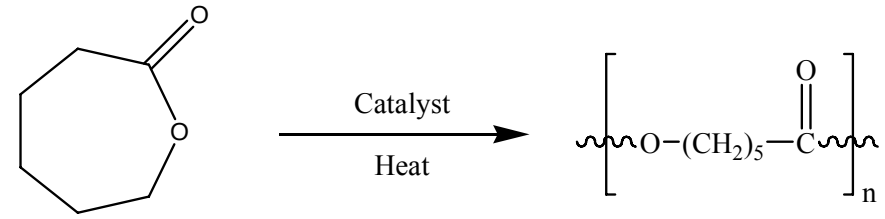

ε-caprolactone Polycaprolactone (PCL)

Figure 1.2 Polymerization reaction of ε-caprolactone

During the past three decades, researches in copolymers of L-lactide and ε-caprolactone have increased steadily as their potential in a wide range of biomedical applications has been realized. These applications have so far included biodegradable controlled-release drug delivery systems [43, 44], monofilament surgical sutures [45, 46], and absorbable nerve guides [47]. Tissue compatibility of these copolymers in

vivo also studied in details [48]. By varying the copolymer composition, monomer sequencing and molecular weight, the copolymer properties can be tailored to meet the specific requirements of each particular application. The copolymers have been shown to be both biocompatible and biodegradable [42].

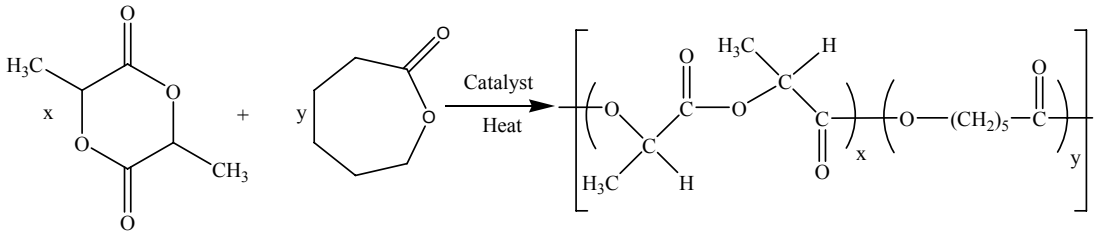

L-lactide ε-caprolactone Poly(L-lactide-co-ε-caprolactone)

Figure 1.3 Polymerization reaction of L-lactide with ε-caprolactone

Biodegradation proceeds via simple hydrolysis (random chain scission) leading to progressively lower molecular weight fragments. In the case of lactide rich fragments, hydrolysis usually continues unabated until L-lactic acid is formed. However, caprolactone rich fragments tend to be taken up in the final stage by macrophages and giant cells and degraded within these cells by enzymes before eventually yielding ε-hydroxycaproic acid. Both L-lactic acid and ε-hydroxycaproic acid are either metabolizable or excretable from the human body without any adverse toxicological effects [42].

1.2.3.2.3 Poly(vinyl alcohol)

Poly(vinyl alcohol) (PVA) production is the largest in volume all over the world among the water soluble polymers [49]. It is not produced by direct polymerization of the corresponding monomer, since vinyl alcohol tends to convert spontaneously into the enol form of acetaldehyde, driven by thermodynamic reasons and with extremely limited kinetic control [49, 50]. Therefore, it is prepared by the

hydrolysis of polyvinyl acetate [28, 49].

The degree of solubility and biodegradability as well as other physical attributes can be controlled by varying the MW and the degree of hydrolysis of the polymer [28, 51]. Polyvinyl acetate, if hydrolyzed to less than 70%, is claimed to be nonbiodegradable under conditions similar to those that biodegrade the fully hydrolyzed polymer [28, 52]. PVA grades with degree of hydrolysis ranging between 70 and 99% are commercially available for applications that are somewhat bound to the degree of polymerization, melting point, and rate of dissolution in water [49]. Biodegradation of PVA and PVA based materials at different conditions is explained in details in elsewhere [49].

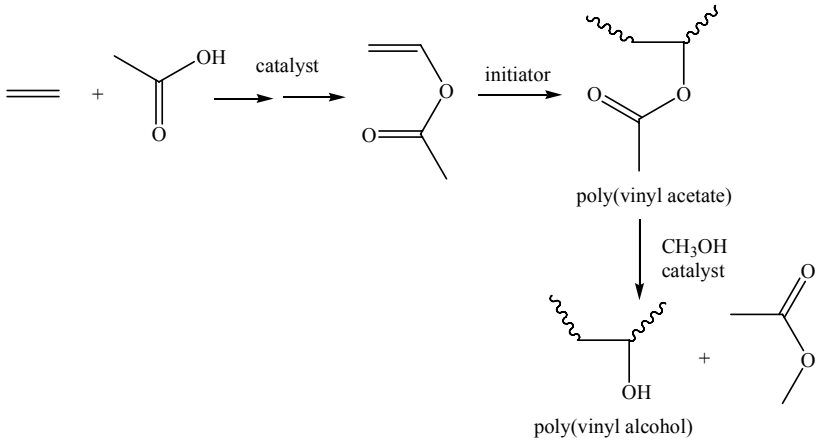

Figure 1.4 Reaction sequence used in the industrial production of PVA [49]

1.2.4 Ceramics as Biomaterials

Ceramics are refractory, polycrystalline compounds, usually inorganic, including silicates, metallic oxides, carbides, and various refractory hydrides, sulfides and selenides. Oxides such as Al_2O_3, MgO, SiO_2, and ZrO_2 contain metallic and nonmetallic elements and ionic salts such as NaCl, CsCl, and ZnS [10, 53]. The

use of ceramic biomaterials was based on the inertness of the materials used and in the following years, bioactive and degradable (partially or fully) ceramics were identified for different clinical purposes [54].

In order to be classified as biomaterial, ceramic material should be nontoxic, nancarcinogenic, nonallergic, noninflammatory, biocompatible and biofunctional for its lifetime in the host [10].

Structural forms of bioceramics have included bulk solids or particulates with and without porosities for tissue ingrowth, and more recently, coatings onto other types of biomaterial substrates. Applications of ceramic biomaterials range from bulk (100%) ceramic structures as joint and bone replacements to fully or partially biodegradable substrates for the controlled delivery of pharmaceutical drugs, growth factors, and morphogenetically inductive substances [54].

Bioceramics can be classified basically as nonabsorbable (relatively inert), bioactive or surface reactive, and biodegradable or resorbable. Aluminum oxide (alumina), zirconia, calcium aluminate, pyrolytic carbon-coated devices and silicone nitrides are examples of nonabsorbable (bioinert) ceramics. They can maintain their properties while in the host. Bioactive or surface reactive ones can form strong bonds with adjacent tissue. Examples of this class are dense nonporous glasses and hydroxyapatites. The last branch of bioceramics is biodegradable or resorbable ceramics. They degrade upon implantation in the host. The rate of degradation depends on the material used. The examples are mainly the variation of calcium phosphate. Aluminum calcium phosphate, coralline, plaster of Paris, hydroxyapatite and tricalcium phosphate can be counted in this class of bioceramics [10].

1.2.4.1 Tricalcium Phosphate (TCP) Ceramics

In general, calcium phosphates have been widely used as biomaterials. In terms of degradability and bioactivity, tricalcium phosphates (TCPs) are preferred

commonly in clinical applications among these bioceramics [55].

The first successful application of calcium phosphate reagent was for the repair of bone defect in human in 1920 [56]. The synthetic scaffolds from calcium phosphates have been employed in orthopedics since 1980's [57].

Calcium phosphate ceramics are biodegradable, biocompatible and osteoconductive materials and have been used widely as bone substitutes in biomedical fields [56-64].

Classification of calcium phosphate ceramics can be done with respect to Ca-P molar ratio and their properties, especially biodegradation, changes accordingly with this ratio [57, 61, 64].

TCP ceramics have general formula $Ca_3(PO_4)_2$. They are also known as calcium orthophosphate, tertiary calcium phosphate or tribasic calcium phosphate. They have α and β forms depending on their crystal structures. Different processing conditions are needed to obtain each one.

Calcium phosphate ceramics, especially β-tricalcium phosphate (β-TCP) and hydroxyapatite (HA) ($Ca_{10}(PO_4)_6(OH)_2$) show excellent bioactivity for bone repair and regeneration because their chemical compositions are very similar to bone [57, 61-64]. Applying different fabrication processes, several forms of calcium phosphates having different density and porosity can be produced [62]. A multicrystalline porous form of β-TCP has been used to correct periodontal defect and augment body contours [10, 65]. X-ray diffraction of β-TCP shows an average interconnected porosity of over 100 μm [10, 66].

1.2.5 Metals and Alloys as Biomaterials

Metallic biomaterials are the dominating group of materials because of their

excellent mechanical properties including high strength, ductility, fracture toughness, wear resistance and electrical and thermal conductivities [10, 67-71].

The most important parameters for metallic biomaterials that they cannot be replaced by polymers or ceramics is their suitability under static, dynamic and impact loads [67, 68, 71].

With having such superior properties, they can be used as total hip and knee joints, artificial joints, dental implants, nails, screws, plates, spinal fixation devices, stents, catheter guide wires, orthodontic archwires etc. [10, 67-71].

Corrosion resistance is one of the most important parameters for metals and alloys to be used as biomaterials [67, 68, 71]. Possible release of toxic metallic ions and particles may cause toxic and allergic reactions. Therefore, metallic biomaterials should have good corrosion resistance [67, 68, 71].

Another important factor for metallic biomaterials is their availability and cost for the production and acceptance as a medical device or implant [67, 70].

As explained properties and studies on metallic materials concerned, stainless steels, CoCr alloys, titanium and alloys, pure niobium and tantalum can be count as metallic biomaterials each one having its own advantages [10, 67-73].

In Table 1.6, some of the physical and mechanical properties of various implant materials are given. Natural bone values are also given for comparison.

Table 1.6 Properties of various metallic materials [71]

Properties	**Natural Bone**	**Ti Alloy**	**Co-Cr Alloy**	**Stainless Steel**
Density (g/cm^3)	1.8-2.1	4.4-4.5	8.3-9.2	7.9-8.1
Elastic modulus (GPa)	3-20	110-117	230	189-205
Compressive yield strength (MPa)	130-180	758-1117	450-1000	170-310
Fracture toughness ($MPam^{1/2}$)	3-6	55-115	N/A	50-200

1.2.5.1 Stainless Steels

The first stainless steel utilized for implant production was the 18-8 (type 302) and is stronger and more corrosion resistant than vanadium steel. Later, known as type 316 stainless steel, having a small percentage of molybdenum to improve the corrosion resistance to salt water, was improved. In 1950s, carbon content of it was reduced to 0.03 weight percent to increase the corrosion resistance and minimize the sensitization. By this way, type 316L stainless steel was produced. Cr, Ni and Mo content of steel is important for having high corrosion resistance and Cr and Ni content of steel determines the austenitic phase formation [10].

The austenitic stainless steels (especially type 316 and 316L) are most widely used for production of implants. Their hardening and strengthening processes can not be achieved by heat treatment but can be done by cold-working. ASTM recommends the use of type 316L rather than type 316 for implant production. The only difference between these two types is their maximum carbon contents [10].

Table 1.7 Composition of 316L stainless steel (American Society for Testing and Materials, F139-86, p.61, 1992) [10]

Element	Composition (w/w %)
Carbon	0.03 max
Manganese	2.00 max
Phosphorus	0.03 max
Sulfur	0.03 max
Silicon	0.75 max
Chromium	17.00-20.00
Nickel	12.00-14.00
Molybdenum	2.00-4.00
Iron	Balance

The compositions of other stainless steel types used for biomedical applications are given in elsewhere [72].

1.2.5.2 Titanium and Its Alloys

Among the metals, titanium and its alloys have an outstanding position due to their excellent balance of mechanical properties, good biocompatibility, good resistance to corrosion and light weight. Therefore, they are the most widely used metals in orthopedic and dental applications [10, 67, 72, 74-77, 79].

The use of titanium for implant fabrication dates back to 1930s. There are four grades of unalloyed commercially pure (cp) titanium and their chemical compositions are given in the following table. For these different grades, oxygen, iron and nitrogen content should be controlled carefully. Especially, oxygen has a great influence on the ductility and strength of the titanium [10].

Table 1.8 Chemical compositions of Ti and its alloy (American Society for Testing and Materials, F67-89, p.39, F136-84, p.55, 1992) [10]

Element	Grade 1	Grade 2	Grade 3	Grade 4	Ti6Al4V*
Nitrogen	0.03	0.03	0.05	0.05	0.05
Carbon	0.10	0.10	0.10	0.10	0.08
Hydrogen	0.015	0.015	0.015	0.015	0.0125
Iron	0.20	0.30	0.30	0.50	0.25
Oxygen	0.18	0.25	0.35	0.40	0.13
Titanium	Balance	Balance	Balance	Balance	Balance

* Maximum allowable weight % of aluminum is 6.00%, Vanadium is 4.00%, and other elements are 0.1% or 0.4% total.

In the following table, some mechanical properties of Ti and its alloy are given.

Table 1.9 Mechanical properties of Ti and its alloy (ASTM F136 American Society for Testing and Materials, F67-89, p.39, F136-84, p.55, 1992 and Davidson et al., 1994) [10]

Property	Grade 1	Grade 2	Grade 3	Grade 4	Ti6Al4V
Tensile strength (MPa)	240	345	450	550	860
Yield Strength (MPa)	170	275	380	485	795
Elongation (%)	24	20	18	15	10
Reduction of area (%)	30	30	30	25	25

Another aspect for preference of titanium and its alloys over other metallic biomaterials is that they have a low solubility and high thermodynamic stability. With these properties, transport and reaction of corrosion products in/with the body elements are prevented [67]. They are also preferable over other metallic biomaterials in terms of occuring allergy problems concerned [72].

Titanium based materials are not bioactive and after implantation they are isolated from bone by surrounding fibrous tissue [74]. Biointegration of them is less when compared to calcium phosphate ceramics [77]. Different functional coating and surface pretreatment techniques can be applied and composite materials can be developed to produce tailored biomaterials [67, 74-84].

Titanium and its alloys find usage in the human body as artificial hip joints, artificial knee joints, bone plates, screws, dental implants etc. for replacing failed hard tissue [72]. In dentistry, they are used for crowns, bridges, partial/complete dentures, metal-ceramic restorations etc. [75].

1.3 Implant Related Infections

Infection is defined as a homeostatic imbalance between the host tissue and the presence of microorganisms. Infection is associated with a large variety of wound occurrences. Usually, sufficient immune response can overcome the microorganism invasion. Otherwise, trials for decreasing bacterial load in the wound should be necessary to maintain wound healing process [85].

Despite the advances in surgical techniques, sterilization and aseptic procedures and newly developed antibiotics and delivery systems, risk of bacterial infection is considerable when facing with musculoskeletal injuries and procedures involving prosthetic implants [5, 83, 85-92].

Implant related infections are typically as a result of growing microorganisms. The consequence is biofilm formation. Pathogenesis of implant related infections involves interaction between the microorganisms (biofilm formation), the implant and the host [93, 94]. Bacteria that have the ability to form biofilms show increased protection from the host defense and high resistance to various antibiotic treatment methods [95].

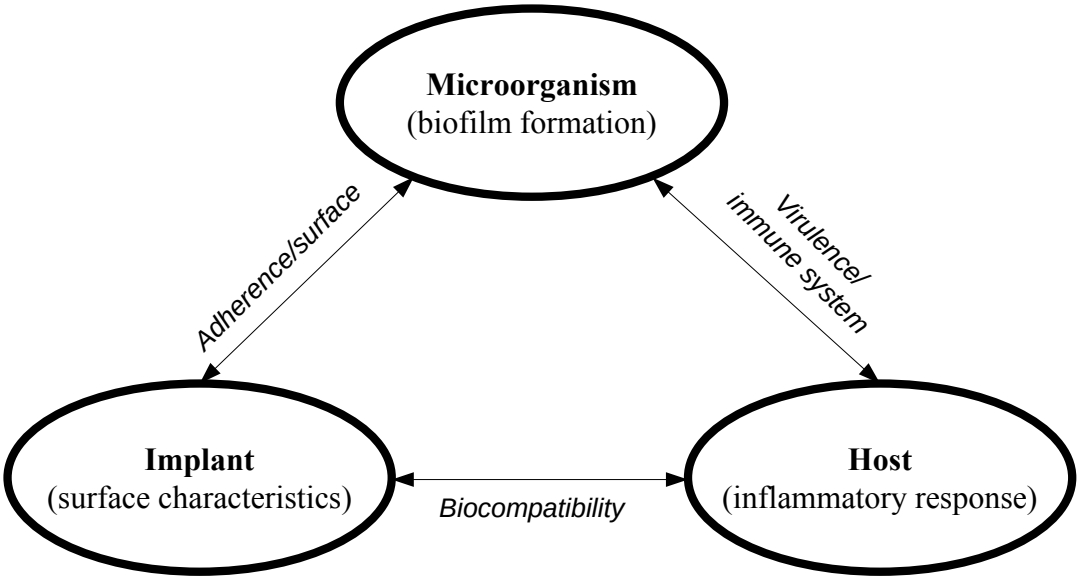

Figure 1.5 Interaction between the microorganism, the implant and the host in the pathogenesis of implant-associated infections [94]

Prosthetic joint infections can be classified as early infection, delayed infection and late infection [93, 94]. The following table gives basic information about these kinds of infections respectively.

Table 1.10 Classification of implant-associated infections according to the onset of symptoms after implantation [93]

Classification	Onset of infection after implantation		Pathogenesis	Typical microorganisms
	Prosthetic joint infections	Infections associated with fracture fixation devices		
Early infection	<3mo	<2wk	During implant surgery or the following 2-4d	Highly virulent organisms such as Staphylococcus aureus or Gram-negative bacilli
Delayed infection	3-24mo	2-10wk	During implant surgery with delayed manifestation	Less virulent organisms such as coagulase-negative staphylococci or Propionibacterium acnes
Late infection	>24mo	>10wk	Predominantly caused by haematogeneous seeding from remote infections	Typically caused by virulent microorganisms such as S. Aureus, β-haemolytic streptococci or gram-negative bacilli

In modern biomaterials science, orthopedic implants gain importance to improve the relevant patients' lives. In USA and United Kingdom, more than 250,000 total hip replacements are performed annually in total. In spite of safety regulations and high biocompatibilities, less than 10% of the patients are at risk to have complications during their lifetime [96].

Nearly, half of the 2 million cases of nosocomial infections that occur each year in USA are as a consequence of indwelling devices applied to patients [3, 93]. The cost of implant related infections are estimated as £ 7-11 million per year [97].

In the range of 3-40% of reported cases about external fixation devices and open fractures can lead to osteomyelitis and septicaemia mainly [97].

The infection rate for primary hip replacement is less than 1% and for knee replacement is less than 2%. [91, 93, 94, 98-100]. Since the infection rates are higher after revision surgery (5-40%), in average, 1-5% of internal fixation devices become infected [85, 90, 92, 94, 95, 101] and this rate decreases to 1-2% in the institutions having highly trained surgeons [95].

Table 1.11 Clinical and economic consequences of infections associated with surgical implants [3]

Implant	Implants inserted in the US annually	Projected infections of implants annually	Average rate of infection (%)	Preferred practice of surgical replacement (no of stages)	Estimated average cost ($)
Cardiovascular					
Mechanical heart valve	85,000	3,400	4	1	50,000
Vascular graft	450,000	16,000	4	1 or 2	40,000
Pacemaker-defibrillator	300,000	12,000	4	2	35,000
Ventricular assist device	700	280	40	1	50,000
Orthopedic					
Joint prosthesis	600,000	12,000	2	2	30,000
Fracture-fixation device	2,000,000	100,000	5	1 or 2	15,000
Neurosurgical-ventricular shunt	40,000	2,400	6	2	50,000
Plastic-mammary implant (pair)	130,000	2,600	2	2	20,000
Urologic-inflatable penile implant	15,000	450	3	2	35,000

Infections related with surgical implants are problematic and more difficult to treat [3, 4, 93, 98, 102-104] since implant surfaces are ideal substrates for bacterial colonization and so for biofilm formation [109]. Treatment usually includes long term systemic antibiotic therapy, repeated surgical procedures, including simple debridement procedures and multiple revisions, and one or two stage removal and replacement of the implant [3, 4, 89, 95, 97-100, 103-108]. These treatments are resulted in considerable morbidity, pain, suffering and higher costs [3, 89, 92, 99, 100, 105, 110]. Also, during the treatment, patients have to stay in hospital for longer periods with having an invalid physical and psychological state [92, 99].

Staphylococcus aureus and coagulase-negative staphylococci are responsible for the majority of implant related infections after surgical procedure [102]. About two thirds of infections are caused by either staphylococcus aureus or coagulase-negative staphylococci [3, 89, 95, 99, 107, 111].

Table 1.12 Distribution of microorganisms causing implant-associated infections [93]

Microorganism	**Frequency (%)**
Staphylococcus aureus	33-43
Coagulase-negative staphylococci	17-21
Streptococci	11-12
Gram-negative bacilli	5-14
Enterococci	3-7
Anaerobes	2-5
Polymicrobial	5-13
Unknown	5-6

(Data are compiled from 40 episodes of infections associated with total knee arthroplasty [112] and 63 episodes with total hip arthroplasty [113])

1.3.1 Osteomyelitis

Osteomyelitis is an inflammatory bone and bone marrow disease caused by microbial infection (gram-positive and gram-negative bacteria) of the bone medullary cavity, cortex and/or periosteum [114-116]. It is a refractory illness and potentially leading to amputation or even death [117].

Two predisposing factors are required for the development of osteomyelitis, which are trauma and introduction of bacteria [114]. The most common cause of osteomyelitis is post-operative sepsis following orthopedic procedures [115].

Osteomyelitis may occur as a result of a bacterial bloodstream infection that spreads to the bone. It can also occur from a nearby infection due to a traumatic injury, frequent medication injections, a surgical procedure, or use of a prosthetic device. Also, individuals with weakened immune systems are more likely to develop osteomyelitis [118].

Osteomyelitis is a disease difficult to treat and eradicate [119]. The treatment of chronic osteomyelitis usually includes removal of infected tissue and foreign bodies by surgical debridement and application of appropriate antibiotic therapy for a period of time usually 4-6 weeks based on bacterial sensitivity [114-116, 120-127, 129-131].

Implant related infections can be caused by all kinds of implanted medical devices and the risk of infection can be either acute or chronic with periods of latency extending the entire life of a patient [128].

Generally, systemic perioperative applications of antibiotics are performed in orthopedic surgery. To prevent deep wound infection caused by inoculated bacteria, high protective tissue levels are achieved [4].

Osteomyelitis and other possible implant related infections are usually treated

by surgical debridement and prophylactic antibiotics [97, 132]. Conventional systemic delivery of antibiotics for prevention and curing of such infections is limited due to systemic toxicity [85, 86, 97, 130, 133], poor penetration into ischemic and necrotic tissue [85, 97, 86, 133] and need for hospitalized monitoring of drug levels and effects [5, 85].

When compared to the conventional antibiotic administration methods, local antibiotic release systems can provide more efficient delivery of higher doses of antibiotics for an extended duration to the site of infection without exceeding the toxic levels [4, 5, 85, 86, 129, 134, 135]. Implant material combined with antimicrobial drugs can serve as a suitable agent for local antibiotic release [90].

Local antibiotic release and further local and controlled antibiotic release systems and devices have been investigated by many researchers. The success rates of treatments are changing according to the efficiency of a system, materials' properties, drug release rates, kind of drugs, kind of bacteria, level of bacterial resistance to antibiotics etc. Optimization for all kinds of implant systems are necessary to minimize the risk of infection and achieve qualified treatments when facing with implant related infections.

1.4 Controlled Drug Release Systems

Drugs were commonly administrated by oral routes as liquids or in powder forms. Later, new routes and dosage forms containing the drug(s) were introduced to avoid the problems occurring through the utilization of the oral route of drug administration. As time progressed, the need for delivery systems that maintain a steady release of drug to the specific area of human body became obvious. Therefore, drug delivery systems were developed to optimize the therapeutic properties of drug products and render them more safe, effective and reliable [136].

From the starting point of pharmacological therapy, the major concern has been

maintaining the steady therapeutic drug levels in vivo. The potential disadvantages of oral and intravenous therapies mainly include;

- high plasma concentrations of drugs that may lead to toxicity
- low drug levels that cause to subtherapeutic blood levels
- having a potential to cause drug resistance in some instances.

To surpass such problems, newly developed controlled release systems were essential [136]. In recent years, studies about targeting drugs to relevant body sites and precise controlling of the drug release rates for prolonged times has shown the possibility of such improvements. Newly developed drug delivery systems have had a great impact on every branch of medicine [137]. Indeed, a large number of new delivery technologies surface each year and every part of the body has been studied as a potential route for administrating both classical and novel drugs. Attractive drug delivery techniques (nanodevices, implants, microfabricated systems, cell encapsulation devices etc.) are currently under intensive study and as a result of these advances; the market for drug delivery is changing drastically [139].

In Figure 1.6 and 1.7, the differences between conventional drug administration and controlled drug release can be seen.

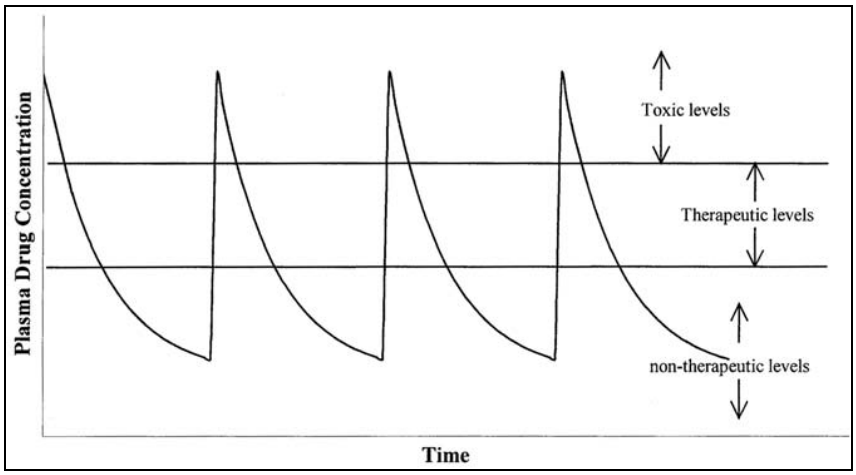

Figure 1.6 Plasma drug concentrations resulting from multiple injections and/or oral administrations [141]

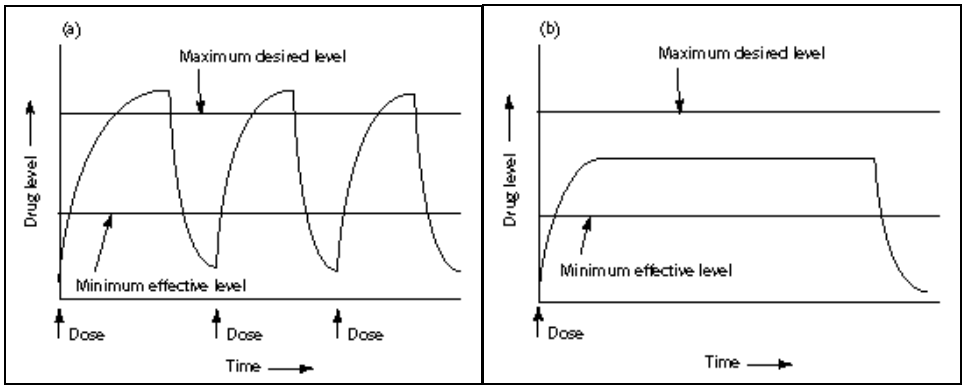

Figure 1.7 Drug levels in the blood with (a) traditional drug dosing (b) controlled delivery dosing

In the early stages, researches were mainly focused on the zero-order release devices that mean maintaining a constant drug concentration in blood for an extended period of time. However, absorption of the drug by the body usually does not follow the zero order kinetics. The main consideration should be to maintain the drug concentration between minimum effective and maximum safe amounts [138].

Local drug release applications are preferred due to the numerous advantages over systemic drug administration methods. These advantages are listed in Table 1.13. The local release applications are considered in the first place to address thrombosis, osteomyelitis, periodontitis, biomedical device related infections and other microbial pathologies or inflammatory complications that are refractory to most conventional methods [128].

Table 1.13 Advantages of local drug release systems over systemic drug therapy [128]

1	Lower doses required
2	Greater control over toxicity and bioavailability of dose
3	Less susceptibility to promoting antibiotic resistance
4	Extended duration of release
5	Possibilities to combine local and systemic drugs with different kinetics
6	Controlled release from surfaces of combination devices directly to site
7	Avoidance of systemic drug exposure
8	Direct mitigation of device-centered infection using combination device release

The above advantages must be weighed against the following concerns in the development of each particular drug-delivery system:

- toxicity of the materials or the degradation products from which the drug is released, or other safety issues such as unwanted rapid release of the drug
- discomfort caused by the system itself or the means of insertion,
- expense of the system due to the drug encapsulation materials or the manufacturing process [137].

1.4.1 Mechanisms of Drug Release Systems

Polymeric drug delivery systems can be classified into four major categories. These are;

- diffusion-controlled systems
- solvent-activated systems
- chemically controlled systems [137, 140] and

- magnetically controlled systems [137].

A combination of these systems is also applicable [137].

1.4.1.1 Diffusion-controlled systems

Diffusion-controlled systems involve two types: reservoir and matrix.

In a reservoir type, powder or liquid form of drug is placed into the various shaped permeable polymer reservoirs. They can be both biodegradable and nonbiodegradable. The important point for biodegradable ones is that their biodegradation rates should be low to release the drug before biodegradation process proceeds. A layer of polymeric material surrounds the core and through which drug slowly diffuses. For the uniform and homogeneous release rates, the thickness of the reservoir should be the same in every point. The major problems arising from reservoir types are the need for removal of the reservoir if it is nonbiodegradable and the ruptures of the reservoir resulting in large amount of drug release called as drug dumping [136, 140].

In the matrix type, the drug is uniformly distributed throughout the polymer matrix and is released at a uniform rate as drug particles dislodge from the polymer network. In such a system, there is no danger of drug dumping [136, 140].

1.4.1.2 Solvent-activated systems

Solvent-activated systems are of two types: osmotically controlled and swelling controlled systems.

In the osmotically controlled system, an external fluid containing a low concentration of a drug moves across a semipermeable membrane to a region inside the device, where the drug is in high concentration. Osmotic pressure tends to

decrease the concentration gradient between one side of the membrane and the other. The inward movement of fluid forces the dissolved drug out of the device through a small orifice [140].

In the swelling controlled systems, the polymer holds a large quantity of water without dissolving. The system consists of hydrophilic macromolecules cross-linked to form a three-dimensional network. A characteristic of such systems is their permeability, for low molecular weight solutes, at a controlled rate as the polymer swells [140].

1.4.1.3 Chemically Controlled systems

Chemically controlled systems also have two classes: the "pendant-chain" system and the biodegradable system.

A "pendant chain system" is one in which the drug molecule is chemically linked to the backbone of the polymer. In the body, in the presence of enzymes and biological fluids, chemical hydrolysis, or enzymatic cleavage, occurs with concomitant release of the drug at a controlled rate [140].

In the bioerodible system, the controlled release of the drug involves polymers that gradually decompose. The drug is dispersed uniformly throughout the polymer and is slowly released as the polymer disintegrates. Two major advantages of erodible systems are polymers do not have to be removed from the body after the drug supply is exhausted, and the drug does not have to be water-soluble. For these advantages, future use of biodegradable polymers is likely to increase more than any other type of polymer in the future [140].

1.4.1.4 Magnetically Controlled systems

Magnetically responsive drug carrier systems, composed of albumin and magnetic microspheres, have been developed for use in cancer chemotherapy. Because of their magnetic characteristics, these microspheres are theoretically capable of enhanced area-specific localization. This carrier system is capable of accommodating a wide variety of drugs. Two major advantages of the magnetically responsive carrier system over other drug delivery systems are its high efficiency for in vivo targeting and its controllable release of a drug at the microvascular level [136, 140].

These different systems can be visualized in Figure 1.8:

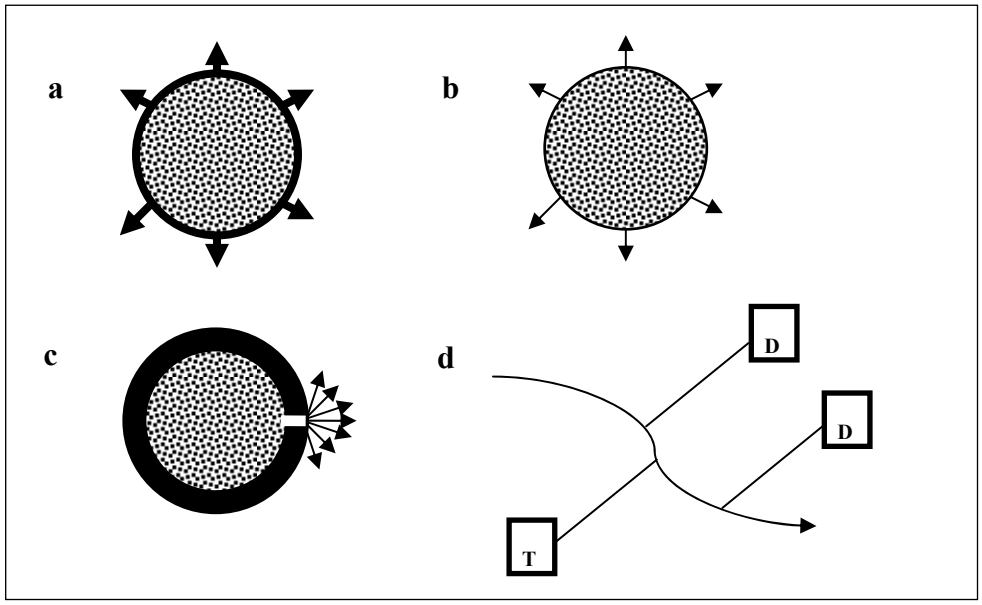

Figure 1.8 Polymer-based delivery systems, adapted from [137]

In **a-c**, small dots represent drug and arrows show the direction in which drug is released. **a.** Reservoir system in which drug diffuses through a polymer membrane. **b.** Matrix system in which the drug is evenly distributed through a polymer system.

c. Osmotic system in which drug is pumped out through a laser-drilled hole. **d.** Polymeric drug conjugates. The curved line represents polymer. The bonds connecting drug (D) and polymer are cleavable inside the body. The targeting moiety (T) is optional [137].

Drug release from biodegradable polymers can occur in the following three mechanisms shown below (Heller, 1985) [11];

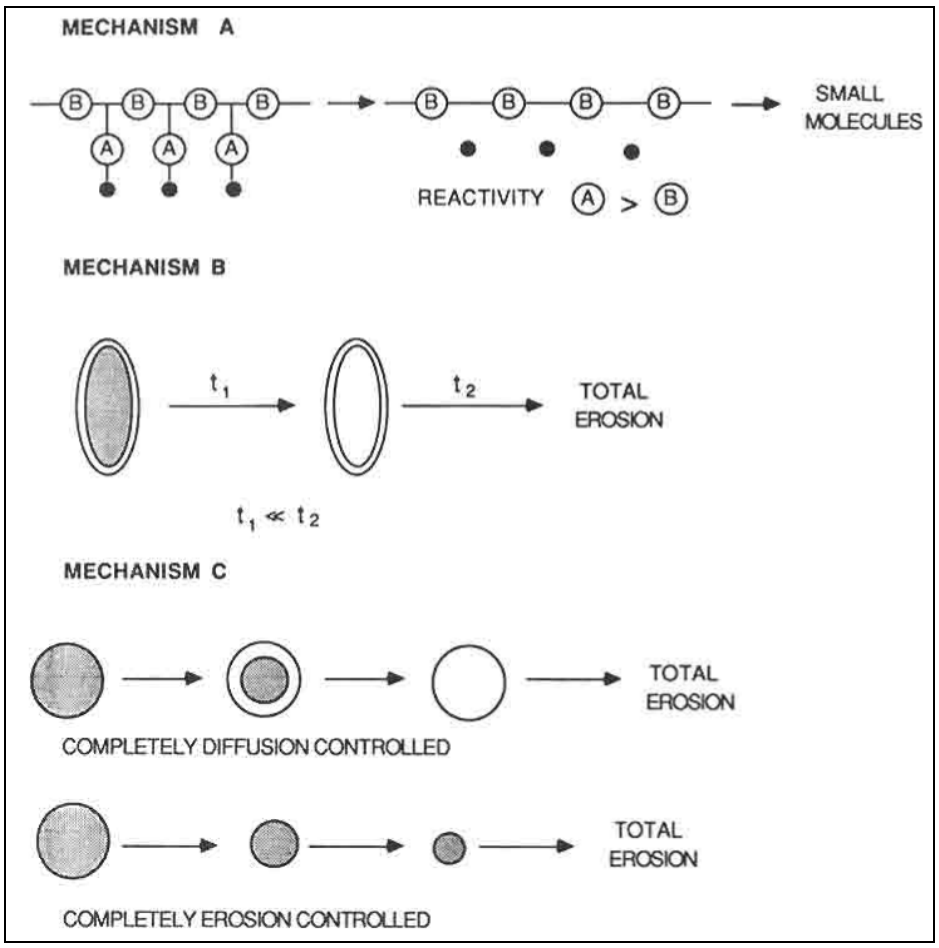

Figure 1.9 Schematic representations of possible drug release mechanisms [11]

In mechanism A, covalently bonded active agent A to the biodegradable polymer backbone composed of B, is released by the hydrolysis of the bond. In

mechanism B, the active agent is contained within a core and is surrounded by a biodegradable and rate controlling polymer membrane. Diffusion controlled release occurs. In mechanism C, the active agent is dispersed in a biodegradable polymer and release of active agent is controlled by diffusion, biodegradation or both [11].

In magnetically controlled systems, small magnetic beads are homogeneously dispersed in a polymer matrix. Diffusion of the drug can be seen through the biological system. When applying external oscillating magnetic field, larger amounts of drug can be released quickly. The following figure represents such system [136]. Magnetically controlled release systems are not limited by such application. Other possible uses of such systems are also possible.

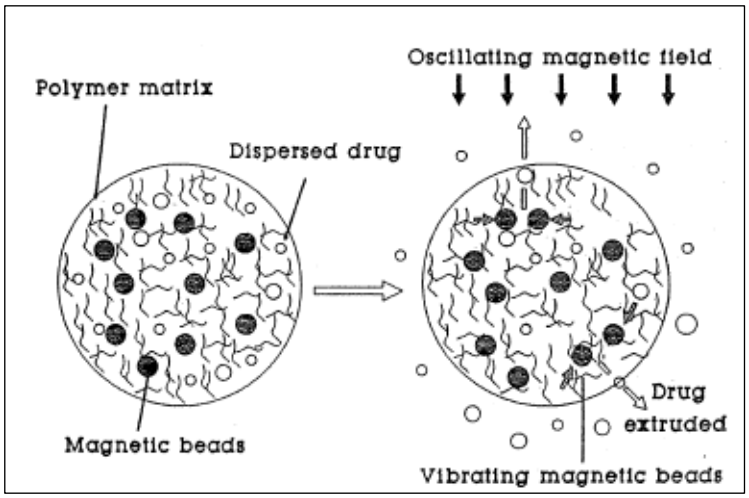

Figure 1.10 Schematic diagram of a magnetically controlled polymeric drug delivery system (From Danckwerts and Fassihi, 1991) [136]

1.4.2 Implantable Drug Delivery Systems

Most extensively studied systems of devices for the release of antibiotics are mainly includes musculoskeletal and orthopedics-related devices, wound dressings,

periodontal devices, and intravascular devices and vascular grafts [85]. According to the purpose; optimization of material selection, material properties, material combinations, coatings, drug properties, body responses, active agent release properties, biodegradation properties etc. are necessary for successful applications. Therefore, the possibility of discovering newly devices seems endless. That is why; the researches on such systems have been increasing as the time proceeds.

1.5 Scope of the Study

The main aim of this study was to develop long-lasting controlled drug release system introduced implant systems. Our idea was to improve such release system introduced implant device to minimize the risk of infections occurring as a result of implant insertions. To achieve this aim, many steps and precautions should be taken. These main steps that were studied can be listed as follows;

- Polymeric film formation and coating thickness studies
- Metal indentation studies
- Surface modification studies
- Studies on the adhesional properties of polymeric films
- Polymer degradation studies
- Studies on antibiotic activities
- Drug release studies (in vivo and in vitro)
- Effect of multilayer coating approach
- Effect of TCP (polymer composite approach)
- Microbial tests
- Antibiotic activity tests
- Antibiotic release kinetics etc.

With the results of these and much more studies, our main aim is to achieve nearly 2 month-lasting controlled drug release system introduced metal implant. Also, other main goals are to reduce the initial fast release of such systems and to improve adhesion for reducing the problems arising from coatings. The uses of such implants are mainly for joint implantations. However, once the system is designed, it can be used in many parts of the human body for different purposes. By the way, getting rid of changing implant material in an infectious situations and providing comfort for patient by reducing the treatment times, pain and expenses for treatments are thought as the final achievements of this study.

1.6 Review of Literature

Schmidmaier et al. [142] studied a controlled, local release of growth factors from a biodegradable polylactide coating of osteosynthetic implants. They investigated the effect of locally applied IGF-1 and TGF-β1 from a biodegradable PDLLA coating of intramedullary implants on fracture healing in a rat model. After 28 and 42 days, respectively, tibiae were dissected for mechanical torsional testing and histomorphometrical analyses. X-rays demonstrated an almost completely consolidated fracture, biomechanical testing showed a significantly higher maximum load and torsional stiffness, and histological and histomorphometric analyses demonstrated progressed remodeling after 28 and 42 days in the group treated with growth factors as compared with controls. They found that PDLLA coating itself revealed a positive effect on fracture healing even without incorporated growth factors. They observed no systemic changes of serum parameters, including IGF-1 and IGF binding proteins, and no differences in body weight and body temperature within and between groups. They conclude that the local application of growth factors from a biodegradable PDLLA coating of osteosynthetic implants accelerates fracture healing significantly without systemic side effects.

Price et al. [5] studied to develop a biodegradable implant coating with

impregnated antibiotics as an adjunct to current therapy of chronic osteomyelitis. They used a polylactic-co-glycolic acid copolymer (PLGA) as the biodegradable carrier and gentamicin as the antibiotic. In the elution study, coated implants were incubated in phosphate buffered saline (PBS) at 37°C and sampled daily for gentamicin levels. The *in vitro* model consisted of test tubes containing Mueller-Hinton culture broth inoculated with $5x10^6$ cfu of *Staphylococcus aureus* and incubated at 37°C. The implants were switched to a new set of inoculated tubes each day. Tubes were sampled for colony counting to determine bactericidal effects. Implant coatings consisted of 40 mg of gentamicin as a 20% mixture with PLGA. The elution curve showed an average level of 138 μg/ml over 15 days. This local concentration would be more than adequate to kill susceptible organisms. The *in vitro* study showed a significant reduction in bacterial growth in the test tubes containing coated implants. This study showed that a thin biodegradable implant coating can be developed with bactericidal activity against the organisms frequently associated with osteomyelitis in cases of open fractures.

Rutledge et al. [86] studied the efficacy and safety of an absorbable polymer (polycaprolactone) as an antibiotic delivery vehicle for treatment of osteomyelitis. They induced an intramedullary osteomyelitis in the femur of adult rabbits by *Staphylococcus aureus* inoculation after use of a sclerosing agent, and then treatment was done with intramedullary irrigation and implantation of a rod made of polycaprolactone, polycaprolactone plus 6% tobramycin, or polymethylmethacrylate plus 6% tobramycin. At defined intervals, the animals were euthanized and culture of the inoculated site was done. Histologic sections of body tissues were made to look for signs of systemic toxicity of the implant. After 4 weeks of treatment, they found a statistically significant difference between the animals that were treated with irrigation alone and the animals that were treated with antibiotic-laden rods of polycaprolactone or polymethylmethacrylate. There was no difference between the antibiotic rod types. No histologic evidence of toxicity was found. From this study, they concluded that bioabsorbable rods of polycaprolactone are a safe and effective means of antibiotic delivery for treatment of osteomyelitis.

Lucke et al. [4] studied to evaluate the efficacy of a new biodegradable, gentamicin-loaded poly(D,L-lactide) (PDLLA) coating of orthopedic devices to prevent implant-related osteomyelitis. The medullary cavities of tibiae in 30 Sprague Dawley rats were contaminated with *Staphylococcus aureus.* Titanium Kirschner wires, uncoated (group II), coated with PDLLA (group III), or coated with PDLLA+ 10% gentamicin (group IV), were implanted. Follow-up was 6 weeks and in weekly intervals X-rays of the tibiae were performed, blood counts were taken, and body temperature and weight were determined. Cultures of implants of group IV showed significantly reduced bacterial growth compared to cultures of groups II and III, and three implants of group IV remained sterile. Further radiological and histological signs of infection were significantly reduced in the gentamicin-coated group compared to groups II and III. No significant differences in body weight, body temperature, and blood parameters between all groups were observed. Thy finally concluded that local application of antibiotic-coated orthopedic devices containing PDLLA and 10% gentamicin significantly reduced implant-related infection in this animal model.

Benoit et al. [129] studied to treat the bone infections with antibiotic loaded plaster of Paris implants coated with poly(lactide-co-glycolide) controlled release system. Implants were loaded with Vancomycin (60 mg/g of carrier). The regulation of the release rate was performed by coating the carrier with a polylactide-co-glycolide polymer composed by 10% (w/w) polyglycolic acid and 90% (w/w) racemic poly(D,L-lactic acid). The release of the antibiotic from the biodegradable matrix was evaluated in vitro. From this investigation, drug elution depends on the coating depth. After a burst effect occurring on the first day of the experiment, therapeutic concentrations were measured during one week when uncoated implants were used. The coating allowed decrease of the burst effect and extended efficient release to more than five weeks when the implants were embedded with six layers (162 mm) of PLA45GA10. This delivery system was implanted into the femoral condyle of rabbits. It was shown that the in vivo release was also closely regulated by the coating depth. In all bone tissues (bone marrow and cortical bone) surrounding the pellets, the drug concentration exceeded the MIC values for the

common causative organisms of bone infections (*Staphylococcus aureus*) for at least four weeks without inducing serum toxic levels. As a result, they concluded that due to its cheapness, facility of use and sterilization, biocompatibility and biodegradability, plaster of Paris coated with PLA45GA10 polymer giving a controlled release of Vancomycin appears to be a promising sustained release delivery system of antibiotics for the treatment of bone and joint infections.

Gürsel et al. [135] studied to treat the implant-related osteomyelitis by using polyhydroxyalkanoate rods. For this purpose, the rods were constructed of poly(3-HB-co-3-HV) and poly(3-HB-co-4-HB), carrying 50% (w/w) Sulperazonet or Duocidt. They were implanted in rabbit tibia in which implant-related osteomyelitis had been induced with *Staphylococcus aureus*. The effectiveness of the antibiotics in the treatment was determined. The establishment of osteomyelitis with bacterial inoculation was complete after 3 weeks with 100% infection rate in all groups. Both antibiotics were found to be highly effective against the bacteria. Following the application of Sulperazone-P(3-HB-co-4-HB) rods, no infective agents could be isolated from the infection site within the 6-week test period, indicating complete treatment of the infection. The overall scores for radiological findings by the end of 6 weeks were 0.8/5 for the antibiotic-loaded rod implanted in the right limb, and 1.1/5 for the antibiotic-free rod implanted in the left limb. There was no statistical difference between the antibiotic-loaded and antibiotic-free polymeric rods. In vivo drug release was almost complete within the first week. The therapy was still very effective even when the release rate was very high. In the SEM of in vitro tested rods, the polymeric component was unchanged in 2 weeks while the drug leached out, leaving voids behind. In vivo, however, the morphology of the implant was significantly modified within 6 weeks post-implantation. They conclude that the dissolution of the drug was the predominant mechanism through which the drug release was controlled since in vivo drug release from implants was completed mostly within one week.

Korkusuz et al. [131] studied the efficacy of locally implanted antibiotic-calcium hydroxyapatite ceramic composites for the treatment of implant-related

osteomyelitis in rats. For this purpose, female Sprague-Dawley rats were anaesthetized with 10 mg/kg intraperitoneal ketamine hydrochloride and their left hind leg was cleaned. The proximal part of the tibia exposed anteriorly and a hole drilled through the cortex into the medullary cavity. A stock strain of *Staphylococcus aureus* was injected through this hole and stainless-steel implants were inserted. The hole was covered with bone wax to prevent bacterial leakage into the soft tissues. After seven weeks, the 150 animals were divided into two groups of 75. The first group was used to compare the effect of antibiotic-CHA composites with that of parenteral antibiotic therapy. In 25 animals, antibiotic-CHA composites, each containing 5 mg of gentamicin sulphate powder were implanted near the site of infection; 25 animals were treated with intraperitoneal injection of gentamicin sulphate for five weeks; and the remaining 25 rats received no treatment. At the end of the study, high concentrations of antibiotics were detected at the site of infection and bacteria were eradicated without removal of the metal implants. Parenteral antibiotics and surgical debridement, alone or in combination with antibiotic-impregnated acrylic bone cement failed to eradicate the infections.

Sasaki et al. [132] studied to produce an implant composed of calcium phosphate cement, gentamicin and poly-L-lactic acid. For this purpose, PLA was liquefied and mixed with gentamicin powder. Then, this mixture was grounded and sieved. Selected ones mixed with calcium phosphate cement and hardening solution. This mixture finally coated with calcium phosphate cement and formed into a cylinder. The results of sustained-release testing in vivo and in vitro demonstrated the effective antibiotic release was achieved over a 2-month period. They reported that they did not only prevent osteomyelitis progression, but also achieve local bond formation.

Stigter et al. [84] studied the carbonated hydroxyapatite (CHA) coatings onto titanium implants by using a biomimetic precipitation method. They applied different antibiotics into the CHA coatings and studied their release and efficacy against bacteria growth in vitro. The used antibiotics were cephalothin, carbenicillin, amoxicillin, cefamandol, tobramycin, gentamicin and Vancomycin. Increased

concentrations of antibiotics in the coating solution led to a higher quantity of antibiotic incorporated into the CHA coating. A bacterial inhibition test on *Staphylococcus aureus* bacteria showed inhibition of growth for all antibiotics that were released from the CHA coating. A release test was conducted in phosphate buffer saline, PBS at pH 7.4 and 37^0C and showed that antibiotics containing carboxylic groups like cephalothin were slower released from the CHA coating than others. At the end of this study, they concluded that certain antibiotics are able to bind/chelate with calcium, resulting in a better incorporation into the CHA coating and a slower release. Therefore, antibiotics incorporated in CHA coatings on titanium implants can be used to prevent post-surgical infections and to promote bone-bonding of orthopedic devices.

Fujimura et al. [102] investigated the in vitro efficacy of clarithromycin (CLA) combined with cefazolin (CFZ) or Vancomycin (VCM) against *Staphylococcus aureus* biofilms formed on titanium devices in order to confirm the efficacy of eradication therapies against device-related infection. The distribution of CLA in muscle tissue surrounding bone was also investigated by liquid chromatography/tandem mass spectrometry in 10 orthopedic patients. Biofilm formation and eradication of *S. aureus* were monitored by scanning electron microscopy and using double-staining dyes. Although *S. aureus* biofilms were not eradicated by CLA, CFZ or VCM alone, CLA combined with CFZ or VCM destroyed biofilms, and *S. aureus* eradication was clearly observed 72 h later. In vitro study showed that treatment with CLA plus CFZ or VCM destroyed staphylococcal biofilms formed on medical devices and eradicated *S. aureus*.

Antoci Jr. et al. [109] examined the effect of covalently bonded Vancomycin on Ti surface on Staphylococci epidermidis, a Gram-positive organism prevalent in orthopedic infections. In this study, *S. epidermidis* colonization was significantly inhibited on Vanc-Ti implants. On the other hand, the gram-negative organism Escherichia coli readily colonized the Vanc-Ti rod, suggesting retention of antibiotic specificity. By histochemical and SEM analysis, Vanc-Ti prevented *S. epidermidis* biofilm formation, even in the presence of serum. Furthermore, when challenged

multiple times with *S. epidermidis*, Vanc-Ti rods resisted bacterial colonization. Finally, when *S. epidermidis* was continuously cultured in the presence of Vanc-Ti, the bacteria maintained a Vancomycin sensitivity equivalent to the parent strain. These findings indicate that antibiotic derivatization of implants can result in a surface that can resist bacterial colonization. They concluded that this method can be used for preventing and treating of periprosthetic infections.

Tunney et al. [105] studied on the susceptibilities of 49 isolates recovered from orthopedic implants to seven antimicrobial agents by the broth microdilution method. Ciprofloxacin and Vancomycin were more active than gentamicin, representing aminoglycosides which are routinely incorporated into bone cement, and also more active than the perioperative antimicrobial agents cefamandole and erythromycin. Therefore, they concluded that the use of ciprofloxacin and Vancomycin in vivo warrants further evaluation.

Radin et al. [83] described the synthesis of thin, resorbable, controlled release bactericidal sol-gel films on a Ti-alloy substrate and determine the effect of processing parameters on its degradation and Vancomycin release. They found that film degradation is the main mechanism underlying the control of release. Using a multi-layer process and various concentrations of Vancomycin, released concentrations exceeded the minimal inhibitory concentration (MIC) of Vancomycin against *Staphylococcus aureus*. As a result of better controlled release from these systems and biocompatible properties, they conclude that these systems can be used to prevent and treat bone infections.

Antoci Jr. et al. [101] proposed a way to prevent bacterial colonization on implants. For this purpose, they covalently attached Vancomycin on titanium surfaces. They found that the Vancomycin-modified surface was stable in aqueous solutions over extended time periods and maintained antibiotic coverage even after insertion of implant. The surface-bound antibiotic prevented bacterial colonization in vitro after exposure to high levels of *S. aureus*, extended incubation in physiological buffers, and repeated bacterial challenges. According to data obtained, they

concluded that they have effectively engineered a stable, bactericidal Ti surface.

Schmidmeier et al. [143] studied on the cold coating of metallic implants with biodegradable thin layer of poly(D,L-lactide) (PDLLA) including growth factors like insulin like growth factor-I (IGF-I) and transforming growth factor-beta 1 (TGF-β1). These implants provided a continuous release of incorporated growth factors. The properties of this bioactive coating were investigated in vitro and in vivo. SEM analysis revealed a coating thickness of in average 14.8 mm on titanium and 10.7 mm on steel wires. Intramedullary implantation and extraction experiments depicted a loss of PDLLA coating from titanium and steel implants of less than 5%. After explantation of the implants, the coating displayed a complete and regular uniformity. Smear tests demonstrated that the coating can be performed under sterile conditions. The PDLLA depicted a reduction of about 8% within 6 weeks in vitro and in vivo. The growth factors were incorporated in a stable form and demonstrated a loss of stability of less than 3% within 42 days and less than 5% within one year. In an elution experiment, 54% IGF-I and 48% TGF-β1 were released within the first 48 h. After 42 days, 76%of IGF-I and 71% of TGF-β1 were detected in the elution fluid by ELISA. Comparable results were obtained in the in vivo experiments after 42 days.

Ramchandani et al. [2] tried to develop and characterize a biodegradable, implantable delivery system containing ciprofloxacin hydrochloride for the localized treatment of osteomyelitis and to study the extent of drug penetration from the site of implantation into the bone. PLGA with lactide to glycolide ratio 50:50 implants were compressed from microcapsules. In vitro dissolution studies were performed to study the effect of manufacturing procedure, drug loading and pH on the release of ciprofloxacin HCl. Rabbit model was used to study the extent of penetration of the drug from the site of implantation The results of in vitro studies illustrated that drug release from implants made by the nonpolar method was more rapid as compared to implants made by the polar method. The release of ciprofloxacin HCl from the implants was biphasic at ≤ 20% w/w drug loading, and monophasic at drug loading levels ≥ 35% w/w. In vivo studies indicated that PLGA 50:50 implants were almost

completely resorbed within five to six weeks. Sustained drug levels, greater than the minimum inhibitory concentration (MIC) of ciprofloxacin, up to 70 mm from the site of implantation, were detected for a period of six weeks.

Wildemann et al. [144] aimed to investigate the potential of IGF-I, TGF-β1 and BMP-2 released from a newly developed application systems of orthopedic implants to induce ectopic bone formation in muscles. For this purpose, titanium discs were coated on one side with the drug carrier poly(D,L-lactide) (PDLLA), with the carrier plus IGF-I and TGF-β1 or with the carrier plus BMP-2. The discs were implanted in the musculus cleidomastoideus of sheep and followed up for 3 months. X-rays were taken after the operation and the day of sacrifice. The muscles plus implant were harvested and prepared for histology. The results of the study showed that the local and controlled release of growth factors from PDLLA coated implants does not induce ectopic bone formation in sheep muscle and could be used in orthopaedic surgery to increase healing without the risk of ectopic bone formation in the surrounding soft tissue.

Ignatius et al. [145] investigated the porous composites made of poly(L, DL-lactide) (PLA) and α-tricalcium phosphate (α-TCP) or the glass ceramic, GB14N, respectively. They applied loaded implant model in sheep. Histological and biomechanical evaluation were performed and compared to autogenous bone transplants at 6, 12 and 24 months after implantation. No significant differences were observed between the composites. After 6 months, the interconnecting pores of the α-TCP-composite and the GB14N-composite were filled with newly formed bone and soft tissue. Only a mild inflammatory response was observed. The reaction was similar after 12 months. However, after 24 months a strong inflammatory reaction was seen. The newly formed bone was partly osteolytic. The adverse reaction occurred simultaneously to a significant reduction of the PLA component. The histological results were reflected by the biomechanical outcomes. Both composites showed compression strengths in the range of the autologous bone graft until 12 months of implantation. The strength of the implants decreased significantly after 2 years. Therefore, they concluded that this study should be improved to use such

implants in clinical applications.

Turner et al. [120] investigated the use of tobramycin-loaded calcium sulfate pellets to maintain high local site antibiotic concentrations for an extended period of time with minimal systemic levels. For this purpose, they loaded calcium sulfate pellets with 10% tobramycin. The number of pellets implanted was calculated to yield an equivalent human maximum prescribed dose and 1.8-fold this dose. These doses converted to approximately 20 mg/kg, and 36 mg/kg, respectively, for the canine. Local and systemic tobramycin levels, pellet resorption, bone response, clinical pathology parameters, and histopathologic responses of potential target organs were analyzed to determine if there was any adverse response for a 28-day period. No adverse effects were detected on any of the organs that were analyzed.

Sampath et al. [115] described the preparation and in vitro evaluation of biodegradable, poly(L-lactic acid), implants for localized delivery of gentamicin sulfate for the treatment of osteomyelitis. For this aim, they prepared cylindrical, poly(L-lactic acid) implants containing gentamicin sulfate by compression of microcapsules prepared by a nonsolvent-induced, coacervation process. Mean particle size distributions of the microcapsules ranged from 278 to 444 μm. The gentamicin sulfate loading of the microcapsules was achieved at least 95% of the theoretical value. In vitro dissolution studies on microcapsules and implants with drug loading vary from 5 to 67% w/w. All batches of microcapsules and implants released greater than 80% gentamicin sulfate within 3 weeks. By comparing with their previous studies, they concluded that PMMA based implants had incomplete and poorly controlled drug release profiles.

Naraharisetti et al. [116] aimed to develop a biodegradable composition that gives sustained release and hence reducing the need for a second surgery to remove the necessity of taking out the nonbiodegradable implant. They produced gentamicin-loaded discs by compressing microparticle-gentamicin mixture obtained by spray drying a mixture of gentamicin in a solution of a biodegradable polymer. Different copolymers of poly(D,L-lactic-*co*-glycolic acid) (PLGA) were used. Different drug

loading levels were studied and it was found that 10% drug loading was optimum for this technique. About 60% of the drug is released in about 5 to 6 days and the remaining drug is released in about 30 days in total. An *in vivo* study was carried on rabbit femur and the local area and systemic concentration of gentamicin was monitored. It was observed that concentration of gentamicin was above MIC values for more than 20 days. It was also shown by computer simulations.

Yamashita et al. [121] treated eighteen patients with chronic osteomyelitis by implanting pieces of antibiotic-impregnated calcium hydroxyapatite ceramic into a cavity produced after thorough surgical excision of necrotic tissue. Within three months the infected sites had all healed. During follow-up ranging from 24 to 75 months there was no recurrence of infection. Infection was controlled and incorporation of the ceramic material into host bone was demonstrated radiographically.

Liu et al. [123] developed novel solvent-free biodegradable capsules for antibiotics and growth factors delivery. To fabricate a biodegradable capsule, they pre-mixed polylactide–polyglycolide copolymers with Vancomycin. The mixture was compression molded and sintered to form a cylinder with a cover of 8 mm in diameter. After the addition of 1 and 10 μg recombinant bone morphogenetic protein (rhBMP-2) into the core, an ultrasonic welder was used to seal the capsules. An elution method was employed to characterize the in vitro release characteristics of the antibiotics and the rhBMP-2 over a 30-day period. The HPLC analysis and the bacterial inhibition test showed that biodegradable capsules released high concentrations and activity of Vancomycin above the MIC values in vitro. The results of ELISA and ALP tests also guaranteed 30 day release of active material. As a result, they concluded that this novel technique can be used for different drugs for long-term releases.

Liu et al. [125] aimed to use biodegradable antibiotic beads for long-term drug release. Different processing factors and effect on release rates were studied. Polylactide-polyglycolide copolymers were mixed with Vancomycin. Different sized

beads were produced by compression and sintering at 55°C. An elution method was employed to characterize the release rate of antibiotic over a 35-day period at 37°C. Drug releases were over the MIC values. A bacterial inhibition test was carried out to determine the relative activity of the released antibiotics. The diameter of the sample inhibition zone ranged from 6.5–10 mm, which is equivalent to 12.5–100% of relative activity. They concluded that by changing processing parameters they could control the release rates of the drugs.

Gitelis et al. [127] studied the biodegradable antibiotic-impregnated implants for treating the chronic osteomyelitis. They used special calcium sulphate kits. Tobramycin and Vancomycin were used as antibiotics. Firstly, antibiotics were mixed with diluent and then this solution mixed onto the calcium sulphate powder. After wetting, this mixture was blended and put into the mold. The final shapes of implants were spheres with 7 mm diameter. These implants were put into the cavities that have osteomyelitis. Classical treatment and the new method studied in parallel on real patients. As a result of their study, they found that their method is advantageous over the intravenous therapy (cost saving, no needed for removal of implant, high doses of antibiotics applicable to the local places and aid in bone repair). They treated different kind of bacteria that causing infection by this implants. They reported that, to date there have been no relapses of infection.

Haris et al. [97] aimed to compare different coating systems on titanium bases with and without an antimicrobial agent and tried to find the most efficient system for resisting *S. aureus* and *S. epidermidis* adhesion and colonization. Also, they tried to find which systems were cytocompatible to fibroblast cells. Five different coatings (PDLLA, PTF, CaP/APC, PU, and PVP) were modified by their impregnation with 10% (w/w) CHA. On the surfaces without CHA, both staphylococcal strains and spread fibroblasts were observed, but on the CHA impregnated surfaces few bacteria and no intact fibroblasts were seen. This study showed that PDLLA and PTF have the best potential as coatings on implants for drug delivery, as they were cytocompatible to hTERT fibroblasts, eluted CHA effectively, and passed mechanical testing.

Ueng et al. [87] investigated poly(DL-lactide-co-glycolide) beads as an antibiotic delivery system in vivo for the treatment of various surgical infections. 50:50 copolymer was mixed with Vancomycin powder and hot compressing molded at 55 ^{0}C to form 8 mm in diameter biodegradable antibiotic beads. The antibiotic beads were implanted in the distal femoral cavities of rabbits for in vivo investigation. MIC values achieved for 56 days. Burst release was reported in the first day. Sample inhibition zone diameters ranged from 8 to 18 mm, and the relative activity of Vancomycin ranged from 9.1% to 100%. Histological observations showed that the materials were biodegradable, resorbed slowly, and did not cause a significant host reaction. This study suggested that this technique for delivery of antibiotics can be used to treat various surgical infections.

Garvin et al. [130] studied the polylactide/polyglycolide antibiotic implants to treat osteomyelitis. In this study, osteomyelitis with *S. aureus* was established in the tibiae of twenty-six adult mongrel dogs and they divided into three groups. Group 1 was treated with parenteral administration of gentamicin every eight hours for four weeks. Group 2 was treated with a polymethylmethacrylate implant containing 100 milligrams of gentamicin that was placed in the tibia for six weeks. Group 3 was treated with a polylactide/polyglycolide implant containing 100 milligrams of gentamicin that was placed in the tibia for six weeks. Specimens of tissue were obtained for quantitative culture and antibiotic immunoassay. The infection was eradicated in ten of the sixteen tibiae in Group 1, in eight of the nine tibiae in Group 2, and in all nine tibiae in Group 3. No significant difference in eradication of the infection reported between the animals that had been treated with a drug releasing implants.

CHAPTER 2

EXPERIMENTAL

2.1 Materials

2.1.1 Polymers

Structures of polymers used for this study are given in Table 2.1.

Table 2.1 Structures of the polymers used

Polymer Name	Structure	Commercial Name
Poly(vinyl alcohol) (PVOH or PVAl)	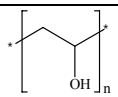	
Polycaprolactone (PCL)	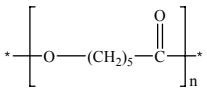	
Poly(L-lactide) (PLA or PLLA)	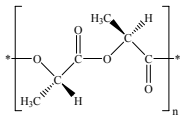	Resomer® L 209S
Poly(D,L-lactide-co-glycolide) (PLGA)	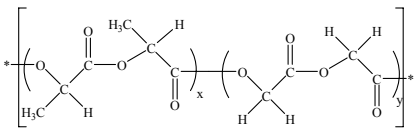	Resomer® RG 504
Poly(L-lactide-co-ε-caprolactone) (PLLA/PCL)	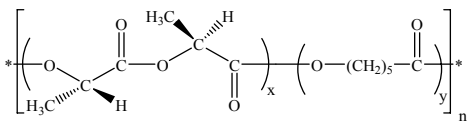	Resomer® LC 703

2.1.1.1 Poly(vinyl alcohol)s

Two kinds of poly(vinyl alcohol)s with different average molecular weights were purchased from Sigma-Aldrich. The average molecular weights of them are 13,000-23,000 and 31,000-50,000 respectively. Degree of hydrolysis of these polymers is 98-99 %.

2.1.1.2 Polycaprolactone

Polycaprolactone was purchased from Sigma-Aldrich, US. The properties of this polymer are given below:

Table 2.2 Some properties of polycaprolactone [146]

Properties	
$\overline{Mw}$	65,000
$\overline{Mn}$	42,500
Appearance	White pellets
Melt Flow Index (MFI) (D1238-73, 80^0C / 0.3MPa)	1.9 g/10 min
Izod Impact (D256-73A, notched)	82 J/m
Hardness (Shore D, D2240-75)	55
Inherent Viscosity	0.55-0.75 dl/g
Elongation (2in/min)	600-1000%
Melting Point	60^0C

2.1.1.3 Poly(L-lactide), Poly(D,L-lactide-co-glycolide), and Poly(L-lactide-co-ε-caprolactone)

These biodegradable polymers were purchased from Boehringer Ingelheim Pharma GmbH & Co. KG, Germany. Basic information and some properties of these polymers are given in Table 2.3:

Table 2.3 Properties of poly(L-lactide), poly(D,L-lactide-co-glycolide) and poly(L-lactide-co-ε-caprolactone) [147-153]

Polymer/Property	**Poly(L-lactide)**	**Poly(D,L-lactide-co-glycolide)**	**Poly(L-lactide-co-ε-caprolactone)**
Code	L 209S	RG 504	LC 703S
Chemical Formula	$-(C_6H_8O_4)_n-$	$-[(C_6H_8O_4)_x(C_4H_4O_4)y]_n-$	$-[(C_6H_8O_4)_x(C_6H_{10}O_2)_y]_n-$
Polymer Composition	NA	48:52 to 52:48 molar ratio D,L-lactide : glycolide	67:33 to 73:27 molar ratio L-lactide : ε-caprolactone
Colour	white or off-white	white to off-white	white to light tan
Shape	irregular granules	powder	irregular granules or flakes
Odour	odourless to almost odourless	almost odourless	odourless to nearly odourless
Inherent viscosity (25^0C; 0,1 % in $CHCl_3$)	2.6-3.2 dl/g	0.45 - 0.60 dl/g	1.3 - 1.8 dl/g
T_g	60 - 65 °C	46 - 50 °C	32 - 42 °C
T_m	180 - 185 °C	amorphous	amorphous
Residual monomer(s)	≤ 0.1%	≤ 0.5%	≤ 2%
Residual solvent(s)	≤ 0.089%	≤ 0.1%	≤ 0.089%
Water	≤ 0.5%	≤ 0.5%	≤ 0.5%
Tin	≤ 60 ppm	≤ 100 ppm	≤ 60 ppm
Heavy metals	≤ 10 ppm	≤ 10 ppm	≤ 10 ppm
Sulphated ash	≤ 0.1%	≤ 0.1%	≤ 0.1%

2.1.2 Metals and Alloys

In this study, medical grade 316L stainless steel and Grade 2 titanium alloy samples were used for various applications. Information about their properties and compositions are given in previous chapter at Table 1.6, Table 1.7, Table 1.8 and Table 1.9.

2.1.3 Ceramics

β-tricalcium phosphate (β-TCP) was used as a ceramic material. It was kindly supplied from Prof. Dr. Muharrem Timuçin's laboratory at METU Metallurgical and Materials Engineering Department. β-TCP is a white amorphous powder with average particle size of 50 μm.

2.1.4 Drugs

2.1.4.1 Vancomycin

Vancomycin is a bactericidial, broad-spectrum glycopeptide antibiotic [126, 154-158] which was isolated by McCormick and coworkers in 1956 [158, 159]. It is highly effective against Gram-positive bacteria including Staphylococcus aureus, Staphylococcus epidermis (and other coagulase-negative staphylococci), streptococci and corynebacterium [126, 129, 154-158] which together constitute about 75% of the bacteria implicated in deep prosthetic infections [129]. It is thermostable at 37°C and readily released in vitro into the surrounding medium [129].

Vancomycin was produced by DBL Mayne Pharma Plc., UK, in powder form for intravenous infusion. The active substance is Vancomycin hydrochloride and the other ingredient is disodium edetate (EDTA disodium) [160]. It has a molecular

weight of 1485.74 g/mol and is a light brownish powder that is readily soluble in water. Molecular formula is $C_{66}H_{75}Cl_2N_9O_{24}$•HCl. The structure of Vancomycin is given in Figure 2.1.

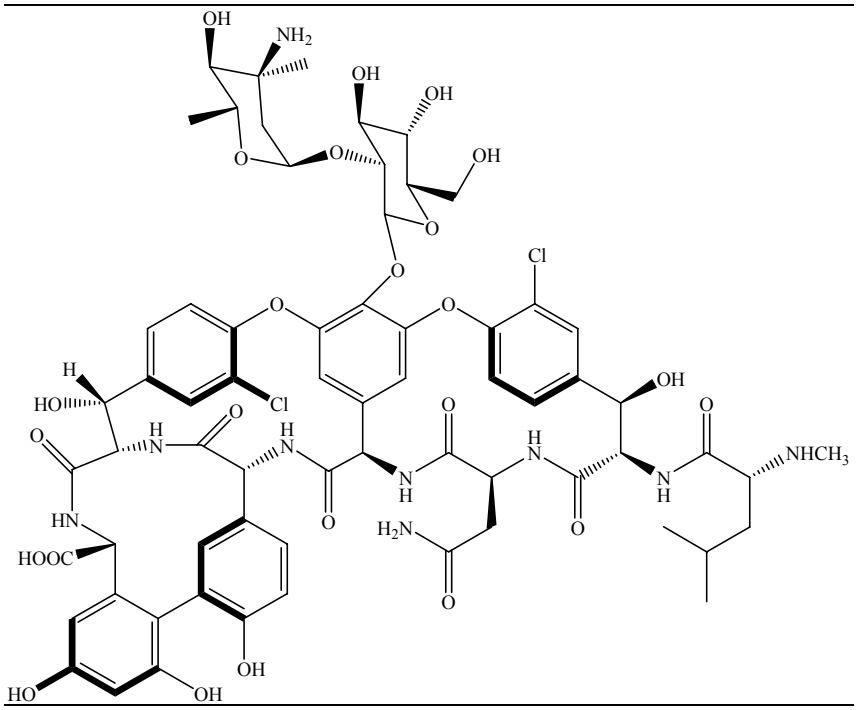

Figure 2.1 Structure of Vancomycin

2.1.4.2 Amoxicillin and Derivatives

Amoxicillin is a β-lactam antibiotic used to treat bacterial infections. Molecular formula of amoxicillin is $C_{16}H_{19}N_3O_5S$ and molecular weight is 365.4 g/mol. It is a semi-synthetic bactericidal broad spectrum penicillin and effective against various bacteria. Bactericidial effect is shown by inhibition of mucopeptid biosynthesis of bacteria cell wall [161].

Amoxicillin was produced by Fako İlaçları AŞ. and Afbar İlaç Sanayi ve

Ticaret AŞ., Turkey, under the name of Alfoxil™ in powder form for injection. It contains sterilized amoxicillin sodium equivalent to 1 g. amoxicillin [161]. The structure of amoxicillin is given in Figure 2.2.

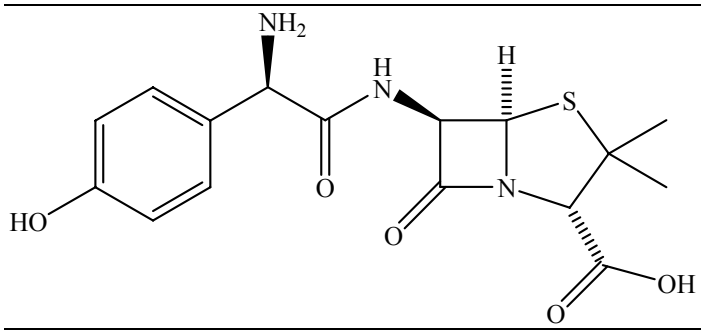

Figure 2.2 Structure of Amoxicillin

Augmentin™ was produced by GlaxoSmithKline, UK, in powder form. It is a combination of amoxicillin sodium (β-lactam) antibiotic and potassium clavulanate (β-lactamase) inhibitor as active materials. Augmentin™ is an antibiotic agent with a notably broad spectrum of activity against the commonly occurring bacterial pathogens. The β-lactamase inhibitory action of clavulanate extends the spectrum of amoxicillin to embrace a wider range of organisms, including many resistant to other β-lactam antibiotics. 1.2 g powder vials for intravenous injection contains amoxicillin sodium equivalent to 1000 mg of amoxicillin and potassium clavulanate equivalent to 200 mg clavulanic acid [165].

The amoxicillin component of the formulations exerts a bactericidal action against many strains of Gram-positive and Gram-negative organisms. The clavulanic acid component has very little bactericidal action. It does however, by inactivation of susceptible β-lactamases, protect amoxicillin from degradation by a large number of β-lactamase enzymes produced by penicillin resistant strains of organisms [165]. Molecular formula for clavulanic acid is $C_8H_9NO_5$ with molecular weight 199.16 g/mol. The structure of clavulanic acid is given in Figure 2.3.

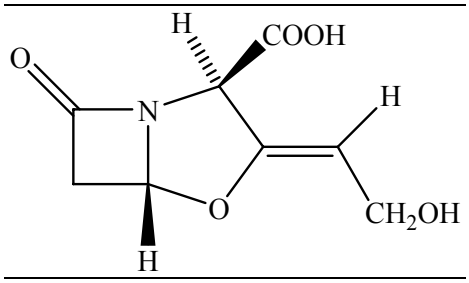

Figure 2.3 Structure of Clavulanic acid

2.1.4.3 Ceftazidime

Ceftazidime is a semi-synthetic β-lactam antibiotic belonging to the third generation cephalosporin. It has a broad spectrum of antimicrobial activity against Gram-positive and Gram-negative bacteria; including Pseudomonas aeruginosa, unlike most third generation drugs [162, 163]. The molecular formula of ceftazidime (as pentahydrate form) is $C_{22}H_{22}N_6O_7S_2.5H_2O$ with a molecular weight 636.65 g/mol.

Ceftazidime was purchased from GlaxoSmithKline, UK, under the trade name of Fortum™. It is in a powder form and suitable for injection. It is light yellowish in color and 1 g injectable powder contains 1 g ceftazidime (in pentahydrate form) and 118 mg sodium carbonate. It shows its bactericidial effect by preventing the synthesis of bacteria cell wall [164]. The structure of ceftazidime is given in Figure 2.4.

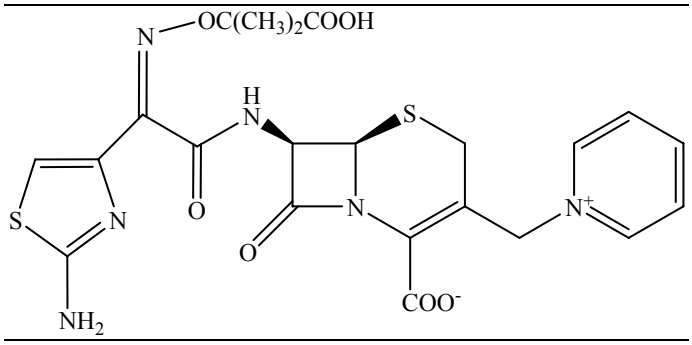

Figure 2.4 Structure of Ceftazidime

2.1.4.4 Cefazolin

Cefazolin is a β-lactam antibiotic belonging to the first generation cephalosporin. It has a broad spectrum of antimicrobial activity against Gram-positive and Gram-negative bacteria. The bactericidial effect is seen as the inhibition of bacteria cell wall synthesis at its last stage [166].

Cefazolin was purchased from Eczacıbaşı, Turkey, under the trade name of Cefamezin®. 500 mg injectable powder contains 500 mg cefazolin (in sodium form) [166]. Cefazolin has a molecular formula $C_{14}H_{13}N_8O_4S_3$ with molecular weight 454.51 g/mol. The structure of cefazolin is given in Figure 2.5.

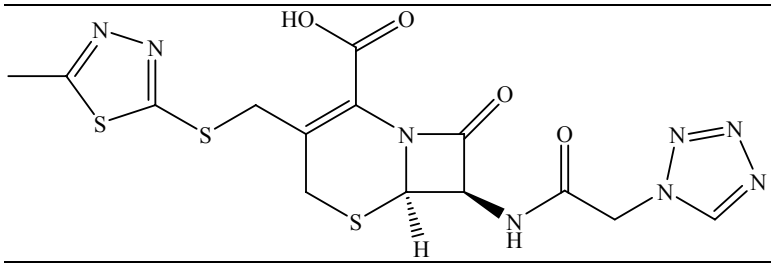

Figure 2.5 Structure of Cefazolin

2.1.4.5 Ceftriaxone

Ceftriaxone is a semi-synthetic β-lactam antibiotic belonging to the third generation cephalosporin. It has a broad spectrum of antimicrobial activity against Gram-positive and Gram-negative bacteria. It is a yellowish-orange crystalline powder which is readily-soluble in water, sparingly soluble in methanol and very slightly soluble in ethanol [167].

Ceftriaxone was purchased from Roche, USA, under the trade name of Rocephin®. 1 g intravenous flacon contains ceftriaxone disodium equivalent to 1 g ceftriaxone [167]. Ceftriaxone has a molecular formula $C_{18}H_{18}N_8O_7S_3$ with molecular weight 554.58 g/mol. The structure of ceftriaxone is given in Figure 2.6.

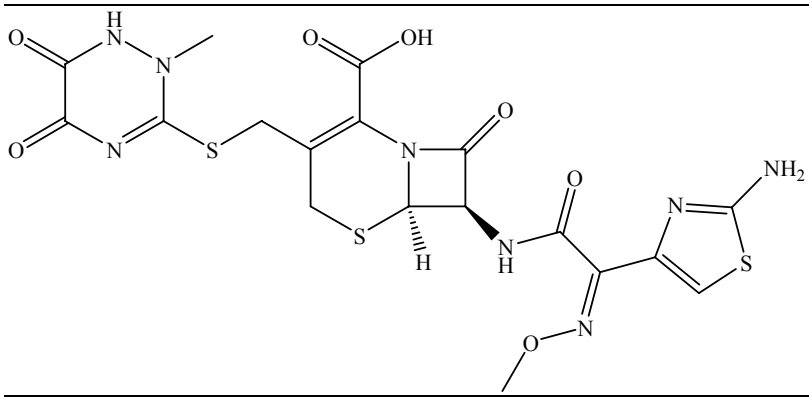

Figure 2.6 Structure of Ceftriaxone

2.1.4.5 Other Chemicals

Chloroform (99%), ethanol (99.5%), and acetone (99.5%) were purchased from J.T.Baker (Holland). NaOH solutions with different concentrations were purchased from Fischer (US).

2.2 Experimental Techniques

The main experimental techniques used for the analyses are discussed in this part.

2.2.1 Mechanical Tests

2.2.1.1 Fatigue Tests

Fatigue tests are used to determine the number of cycles (N) of applied strain at a given level of stress that a sample can sustain before complete failure. This number of cycles is called the "fatigue life". The tests are started by subjecting a sample to cyclic stress at specific maximum stress amplitude and the number of cycles to failure is counted. This procedure is repeated on other samples at decreasing maximum stress amplitudes. The data are plotted as stress (S) versus the logarithm of the number of cycles to failure (N). This curve is known as S-N curve. "Fatigue limit or endurance limit" is the maximum value of applied stress for which failure will not occur no matter for how many cycles the stress is applied [13, 15]. Typical S-N curve is given in Figure 2.7.

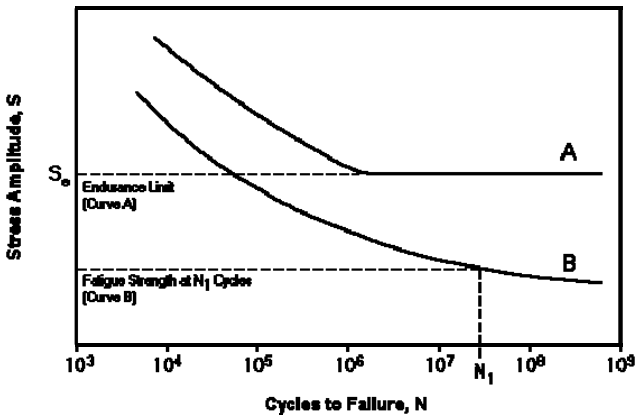

Figure 2.7 Typical S-N curves for A) a material that displays a fatigue limit and B) a material that does not display a fatigue limit [168]

Computer simulations and fatigue tests in virtual media was applied to all indentations (n=5) and materials (n=2). Ansys Workbench 10.0 (ANSYS Inc., USA) program was used for virtual media analysis. The models of titanium and stainless steel samples were graphically drawn in virtual media and 100 N loads were applied by using again with a modeled punch. S-N diagrams and stress distributions of different samples were obtained as a result of these analyses.

2.2.1.2 Hardness Tests

Pendule Persoz & Konig Model 3034 from Braive Instruments, Belgium (Elcometer Instruments GmbH, UK) was used for hardness tests. This equipment can be used in accordance with standards ASTM D4366-92 Standard Test Methods for Hardness of Organic Coatings by Pendulum Damping Tests, BS EN ISO 1522:2001, BS 3900-E5:1998 Paints and varnishes. Pendulum damping test, DIN 53157 Pendelhärte nach König gem, and NFT 30-016 Persoz pendulum [169, 170]. In Figure 2.8, the picture of this instrument can be seen.

Figure 2.8 Persoz & Konig pendulum hardness tester [170]

Persoz hardness instrument consists of a pendulum which is free to swing on two balls resting on a coated test panel. The pendulum hardness test is based on the principle that the amplitude of the pendulum's oscillation will decrease more quickly when supported on a softer surface. The hardness of any given coating is given by the number of oscillations made by the pendulum within the specified limits of amplitude determined by accurately positioned photo sensors. An electronic counter records the number of swings made by the pendulum [169].

The damping time of a pendulum oscillating on a sample indicates its hardness. The amplitude of the oscillations reduces faster when the sample is soft. The Persoz and Konig methods differ by the dimension, period and amplitude of the oscillations. Surface smoothness, film thickness, temperature and relative humidity must all be carefully controlled because these parameters affect the hardness values [170].

The Persoz test measures the time taken for the amplitude of oscillation to decrease from 12° to 4° .The Konig test measures the time taken for the amplitude of oscillation to decrease from 6° to 3° [170]. The major differences of these two methods are given in Table 2.4.

Table 2.4 Properties of Persoz and Konig Methods [170]

	Persoz Method	**Konig Method**
Pendulum	Stainless steel square pendulum, weight 500 g, fitted with 2 balls measuring 8 mm diameter.	Stainless steel triangular pendulum, weight 200 g, fitted with 2 balls measuring 5 mm diameter.
Deflections	From 12° to 4°	From 6° to 3°
Oscillation Period	1 second	1.4 seconds
Damping Time on Glass	Minimum 430 ± 10 seconds	250 ± 4.2 seconds

2.2.1.3 Lap Shear Tests

Lap shear tests were done according to the ASTM D 1002-72 “Standard Test Method for Strength Properties of Adhesives in Shear by Tension Loading (Metal to Metal)” [171]. Lap shear tests determine the shear strength of adhesives for bonding materials. The test method is primarily comparative. The test is applicable for determining adhesive strengths, surface preparation parameters and adhesive environmental durability. The form and dimensions of the specimens are given in Figure 2.9.

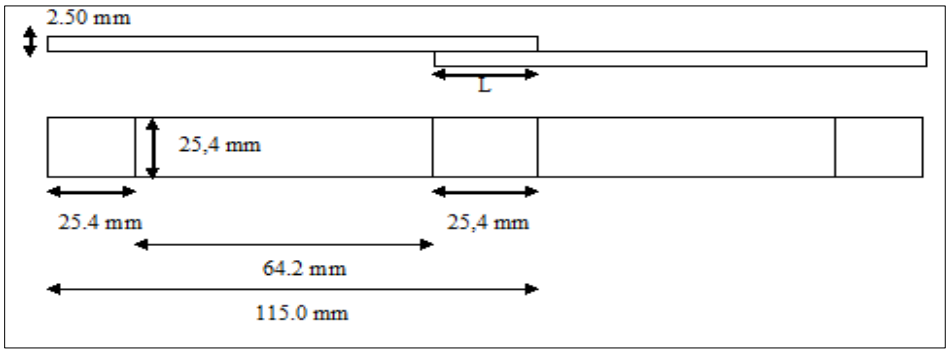

Figure 2.9 Form and dimensions of test specimen used for lap shear tests

The test samples have dimensions of 115 x 25.4 x 2.50 mm. Length “L” describes the area of adhesion occuring between two metal plates. Two ends of test specimen described by marked lines are attached to the tensile tester grips for tests.

Lloyd Instruments, AMETEK (UK), LR5K model tensile tester machine was used for lap shear tests. 5 kN capacity load cell and TG15 model self tightening sliding wedge grip were used for analyses. Preload force was 2 N and crosshead speed was 10 mm/min during the tests. NEXYGEN material test and data analysis software was used for processing the data.

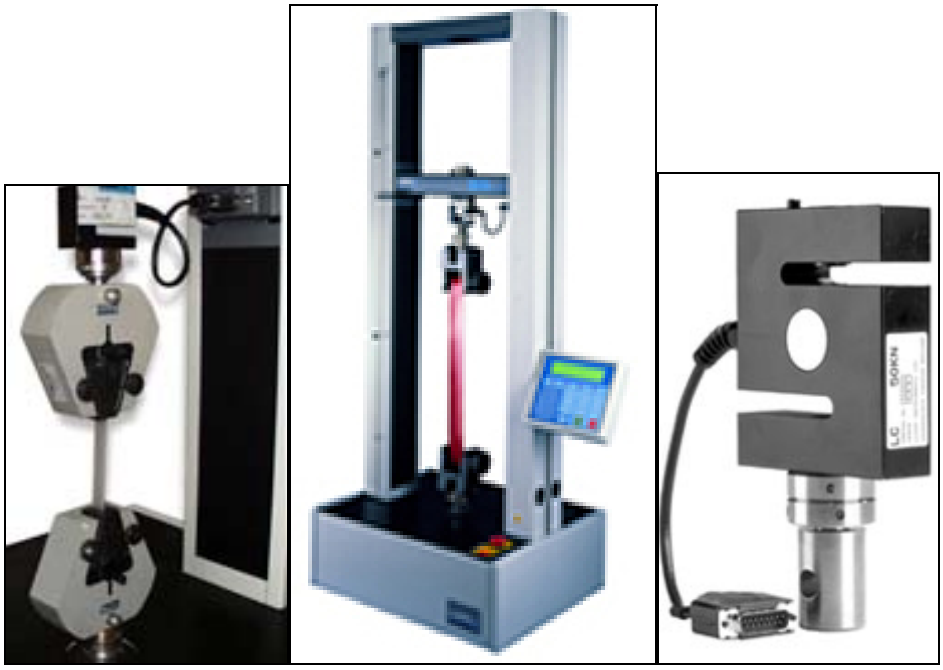

Figure 2.10 Lloyd Tensile tester, grip and a load cell

2.2.1.4 T-Peel Tests

T-peel tests were done according to the ASTM D 1876-93 "Standard Test Method for Peel Resistance of Adhesives (T-Peel Test)" [172]. This test method is used for determination of the relative peel resistance of adhesive bonds between adherents by means of a T-type specimen. The form and dimensions of the specimens are given in Figure 2.11.

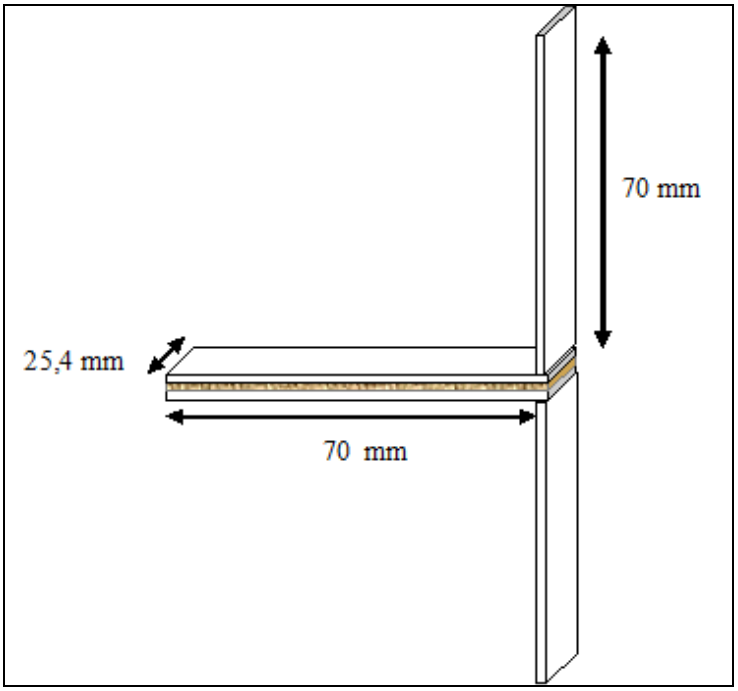

Figure 2.11 Form and dimensions of test specimen used for T-peel tests

The test samples have thickness of 2.50 mm. Textured area between the plates presents the area of adhesion. Two ends of test specimen are attached to the tensile tester grips for tests.

Lloyd Instruments, AMETEK (UK), LR5K model tensile tester machine was used for lap shear tests. 5 kN capacity load cell and TG15 model self tightening sliding wedge grip were used for analyses. Preload force was 2 N and crosshead speed was 10 mm/min during the tests. NEXYGEN material test and data analysis software was used for processing the data.

2.2.1.5 Measuring Adhesion by Tape Test

Measuring adhesion by tape test was done according to the ASTM D 3359-92a "Standard Test Methods for Measuring Adhesion by Tape Test" [173]. These test methods cover procedures for assessing the adhesion of coating films to metallic

substrates by applying and removing pressure-sensitive tape over cuts made in the film. Test Method B is suitable for laboratory use. In this method, a lattice pattern either six or eleven cuts in each direction is made in the film to the substrate. Then, pressure sensitive tape is applied over the lattice and removed. Adhesion is evaluated by comparison with descriptions and illustrations (Figure 2.12) [173].

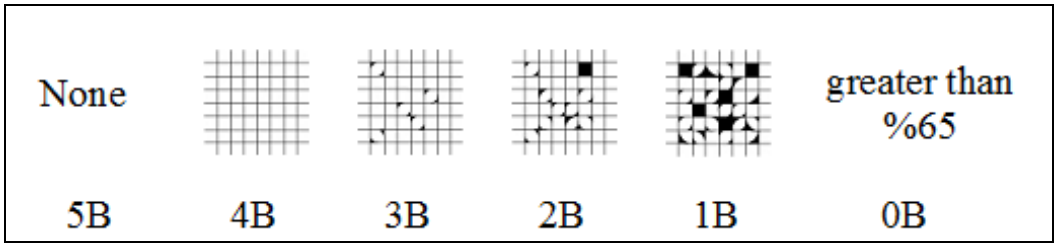

Figure 2.12 Classification of adhesion test results by tape test

2.2.2 Gloss Tests

Gloss is an optical term that describes a surface's ability to reflect light. A high-gloss surface directly reflects light with minimum hazing or diffusion. A glossmeter measures specular reflection, or the capacity of a surface to reflect light. Measurements by this test method correlate with visual observations of surface shininess made at roughly the corresponding angles. A glossmeter comprises an incandescent light source which is directed at the test surface at a specified incidence angle and a receptor which is located at the mirror reflection of the incident beam. A polished black glass with a refractive index of 1.567 is used as a standard and is assigned a gloss of 100 at all geometries. Gloss readings can only be compared between similar materials and test procedures. ASTM D523 covers the measurement of the specular gloss of nonmetallic specimens for glossmeter geometries of 60º, 20º, and 85º [174, 175].

For gloss measurements, BYK-Gardner tri-glossmeter (USA) was used.

2.2.3 UV-Visible Absorption Spectroscopy (UV-VIS)

Molecular absorption in the ultraviolet (UV) and visible (VIS) region of the spectrum is dependent on the electronic structure of the molecules Absorption of energy is quantized, resulting in the elevation of electrons from orbitals in the ground state to higher energy orbitals in an excited state [176]. Absorption of UV-VIS radiation in organic molecules is restricted to certain functional groups (chromophores) that contain valence electrons of low excitation energy. Therefore, many molecules absorb ultraviolet or visible light. Different molecules absorb radiation of different wavelengths. The absorbance of a solution increases as attenuation of the beam increases. The absorption of UV or visible radiation corresponds to the excitation of outer electrons. There are three types of electronic transition which can be considered; (a) transitions involving σ, π, and n electrons, (b) transitions involving charge-transfer electrons and (c) transitions involving d and f electrons [177].

Absorbance (A) is directly proportional to the path length, b, and the concentration, c, of the absorbing species. According to Beer's Law;

$$A = \varepsilon bc \qquad (2.1)$$

where ε is a constant of proportionality, called as absorptivity. By taking advantage of this equation and calibration curves of the relevant drugs, concentrations of them in a solution can be calculated theoretically.

Possible electronic transitions of σ, π, and n electrons are given in Figure 2.13.

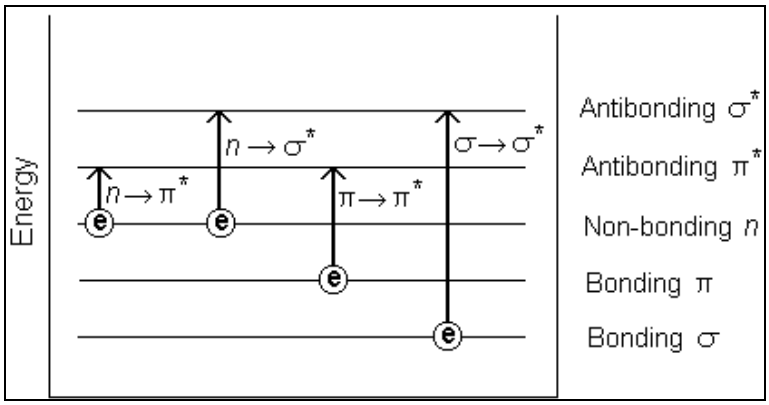

Figure 2.13 Possible electronic transitions of σ, π, and n electrons [177]

In the study, UV spectrophotometer was used to analyze the concentrations of different drugs in solutions. For these analyses, Shimadzu UV-160U and Shimadzu UV-1201 model spectrophotometers and quartz cells were used (Figure 2.14).

Figure 2.14 Pictures of UV-VIS Spectrophotometers used

2.2.4 Scanning Electron Microscopy (SEM)

In SEM, an image of the surface of a polymer can be visualized. In this technique, a fine beam of electrons (5-10 nm in diameter) is scanned across the sample surface of an opaque specimen in synchronization with a beam from a cathode-ray tube [13, 14]. The scattered electrons produced can then result in a signal which modulates this beam. This produces an image with a depth-of-field which is usually 300-600 times better than that of optical microscope. SEM also enables three-dimensional image to be obtained. Scanning electron microscopes in general have magnification ranges from x20 to x100.000 [13]. The surface of a specimen to be analyzed by SEM must be electrically conductive. Therefore, nonconductive materials observed in the SEM are typically coated with a thin, electrically grounded layer of metal to minimize negative charge accumulation from the electron beam [11]. Since polymers tend not to be good conductors, they need to be coated with thin layer of conducting material such as gold [13].

For SEM analyses, JSM-6400 Electron Microscope (JEOL, Japan), equipped with NORAN System-6 X-ray Microanalysis System & Semafore Digitizer (Figure 2.15) at METU Metallurgical & Materials Engineering Department, SEM Laboratory was used. It is equipped with secondary and backscattered electron detectors and an X-ray microanalysis system. It is capable of providing both topographical and compositional information about the specimen. Hummer VII Sputter Coating Device (ANATECH, USA) (Figure 2.16) was used for sample coating. The samples are coated with a very thin layer of a gold-palladium (Au-Pd) alloy.

Figure 2.15 A picture of Scanning Electron Microscope

Figure 2.16 A picture of Sputter Coating Device

2.2.5 Viscosity Measurements

Viscosity measurements were done by using Ubbelohde capillary viscometer. Constant temperature at 25^0C was maintained by using a thermostated water bath. The relative viscosities, $\eta_r = t/t_0$ were measured; where t and t_0 are the flow times for the solution and solvent respectively. The intrinsic viscosity [η] is obtained from the reduced viscosity η_{red} and inherent viscosity η_{inh} versus concentration plots by extrapolation to zero concentration. The viscosity measurements were done as a

measure of polymer degradation.

The reduced viscosity and the inherent viscosity are described by the Huggins and Kraemer equations respectively:

$$\eta_{red} = \eta_{sp}/C = [\eta] + K'[\eta]^2C \quad (2.2)$$

$$\eta_{inh} = \ln\eta_r/C = [\eta] - K''[\eta]^2C \quad (2.3)$$

where;

η_{sp} is the specific viscosity and $\eta_{sp} = \eta_r - 1$

η_r is the relative viscosity

C is the concentration (g/dl)

$[\eta]$ is the intrinsic viscosity (dl/g)

K' is the Huggins constant

K'' is the Kraemer constant

The Huggins and Kraemer constants are related as shown below;

$$K'-K'' = 0.5 \quad (2.4)$$

The Huggins and Kraemer equations provide the most common procedure for evaluation of $[\eta]$ from experimental data. This involves a dual extrapolation according to equations 2.2 and 2.3 and gives $[\eta]$ as the mean intercept of the lines of both equations. The intrinsic viscosities were obtained from the mean intercepts.

2.2.6 Kirby-Bauer Disc Diffusion Antibiotic Sensitivity Testing

Kirby-Bauer disc diffusion antibiotic sensitivity testing uses antibiotic-impregnated wafers to test whether particular bacteria are susceptible to specific antibiotics. The bacterium is swabbed on the agar in petri dishes. After obtaining a bacteria film over the plate surface antibiotic loaded discs are placed into the agar.

The antibiotic diffuses from the disc into the agar. After a period of incubation, sensitivity or resistance to the antibiotic can be determined by measuring the zone that forms around the disc. Large zones mean the bacteria are sensitive to the drug, small or nonexistent zones are signs of resistance. If the bacteria are susceptible to a particular antibiotic, an area of clearing surrounds the wafer where bacteria are not capable of growing (called a zone of inhibition). The size of the zone and the rate of antibiotic diffusion are used to estimate the bacteria's sensitivity to that particular antibiotic. This test is easy to apply and essential for the selection of antibiotics for deciding better treatment ways.

After the test, radius of the zone of inhibition areas is measured by using a milimetric ruler. The results are compared with the control disc's results and the concentration and effectiveness of the other applied antibiotic discs can be determined by using these results. An example of the tests after incubation time can be demonstrated as in Figure 2.17.

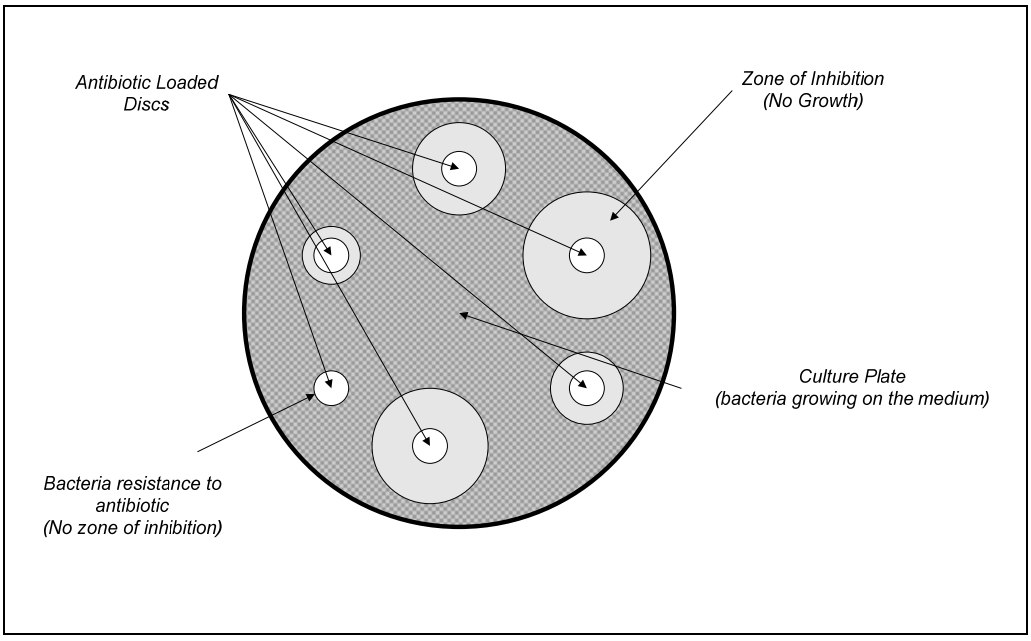

Figure 2.17 Kirby-Bauer disc diffusion antibiotic sensitivity testing

2.2.7 Energy Dispersive X-Ray Spectroscopy (EDX)

Energy Dispersive X-Ray Spectroscopy (EDX) is an analytical technique used to identify and quantify the elemental composition of the sample. EDX spectroscopy is usually used in conjunction with SEM. EDX can provide elemental analysis on specimen areas as small as nanometers in diameter. In principle, the specimen is bombarded by SEM's electron beam and then electrons are ejected from the atoms that are available at sample's surface. Resulting electron vacancies are filled by the electrons at higher state. Emitted X-ray's energy that is characteristic for the element responsible for emission is determined by detector. The number of X-rays is counted for each particular energy and results are given as counts vs. energy graph. EDX is mainly composed of four components: beam source, X-ray detector, processor and analyzer [179].

For this study, EDX analyses were done to understand the changes in elemental composition of the surface of implant materials after surface modification studies.

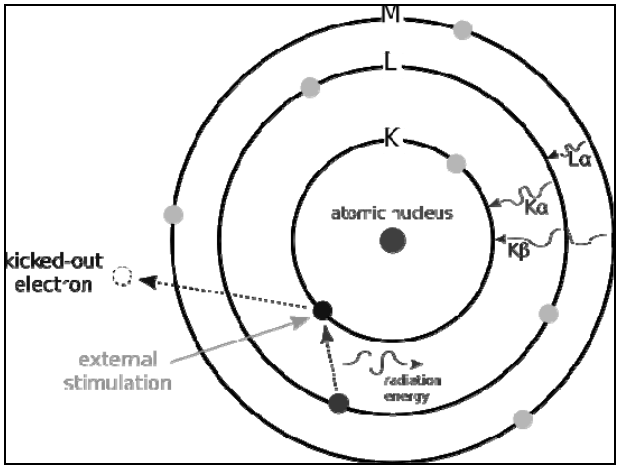

Figure 2.18 Working principle of EDX [179]

2.3 Experimental Methods

2.3.1 Studies on Metal Surface Geometry

Metal implants were chosen as the substrates for controlled releasing agents and the hip joint was chosen as a main implant to be processed, however, the success of the methods will result in use of other metal based implant materials.

A porous surface morphology was formed at the acetabular component and at the ½ upper part of femoral handle of the hip joint. In these parts, it is possible to load the antibiotic including polymer coatings more effectively than the other surfaces in question.

For the lower part of the body, a surface treatment was done by processing with 5 M NaOH for 48 hours at 60^0C and placing in an oven for 1 hour at 600^0C. This process was performed in order to produce a surface with high adhesion and can be preferred for plaque and tooth implants where porous morphology can not be applied.

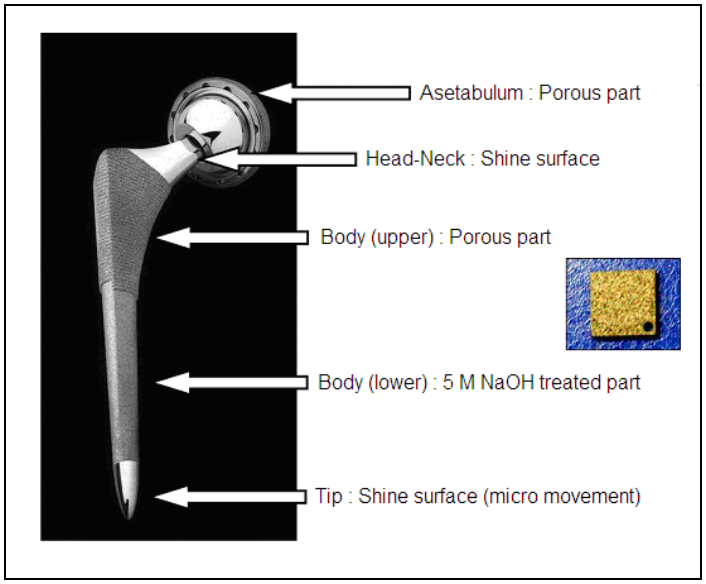

Figure 2.19 An approach to the hip joint design, Grade 2 titanium sample used for the experiments can be seen at right

2.3.2 Indent Prototype Studies

To increase the loading efficiency on the smooth implant surfaces, indentation studies were performed. Five different indentations were applied for this purpose (Figure 2.20).

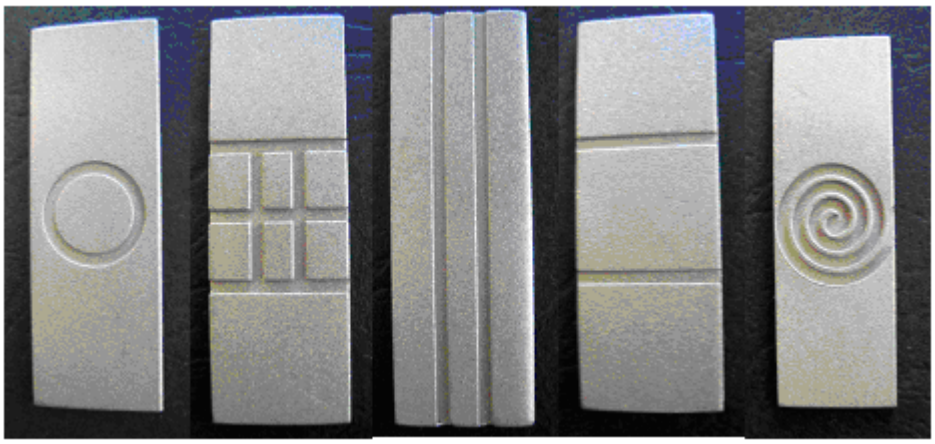

Figure 2.20 Different indentations applied to implants

2.3.3 Determination of Biomechanical Changes Related to the Indentation

The different indentations were applied (as described in Section 2.3.2) on 316L stainless steel and medical grade Ti-Al-V alloy samples and biomechanical tests were done on these samples. The S-N figures of the fatigue tests on these samples were drawn.

2.3.4 Computer Simulation and Fatigue Tests in Virtual Media

Computer simulations and fatigue tests were applied to all of the indentations

(n=5) and materials (n=2) in virtual media. Ansys Workbench 10.0 (ANSYS, Inc., USA) program was used for virtual media analysis. The models of titanium and stainless steel samples were made in virtual media and 100 N load was applied by using again with a computer modeled punch. Simulated mash vision of indentation and punch and the applied force graph are given in Figure 2.21.

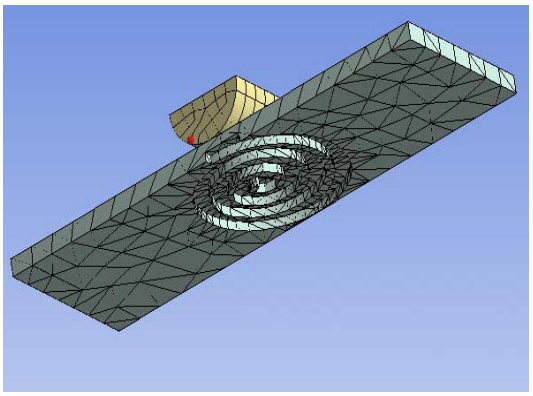

Mash vision of Model 4

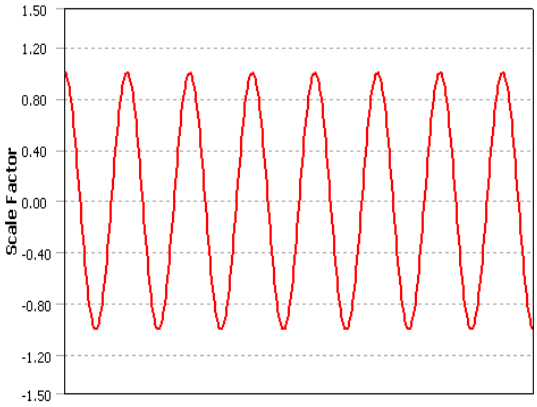

Applied Force Graph

Figure 2.21 Mash vision for Model 4 and applied force graph

2.3.5 Hardness, Gloss and Measuring Adhesion by Tape Tests

Solutions of 10% (w/v) PVOHs in water, 10% (w/v) RG 504 and LC 703 in chloroform and 5% (w/v) PCL and L 209S in chloroform were prepared and precleaned glass plates were coated with these polymers to obtain a film thickness of 50 µm. Mechanically controlled coating stage was used to obtain uniform coating. These glass plates were used for hardness, gloss and adhesion by tape tests measurements. For adhesion tests 3M Company Scotch® Magic™ Tape (USA) was employed.

2.3.6 Coating Thickness and Coating Density Measurements

15% (w/v) solutions were prepared in water with two different PVOHs. Cleaned titanium plates were coated by dipping two times into this solution and plates were dried for 1 day and 7 hours in an oven at 40 ^{0}C. By calculating the coating area, coating densities were found. Thickness measurements were done by using a micrometer (Mitutoyo, USA).

2.3.7 Calibration Curves for Different Drugs

Calibration curves for Vancomycin, Amoxicillin, Ceftazidime, Cefazolin and Ceftriaxone based drugs were obtained by using UV spectrophotometer. For this purpose, varying concentrations of antibiotics were prepared and their absorbances were measured at definite wavelengths. Then, absorbance vs. concentration graph was obtained by using the data. The equations of calibration curves were found and these equations were used to calculate the amount of released drugs in the drug release studies. Two parallel sets of solutions were studied to minimize the errors.

2.3.8 Preparation of Coating Solutions

Polymers in question were dissolved in an appropriate solvent (water or chloroform) with continuous stirring by using a magnetic stirrer. Then drugs were dispersed in the medium. By continuous stirring, homogeneous suspensions are obtained for coating. For inert multiple coatings, polymer solution, without antibiotic, was used. The different procedures and amount of materials used will be given where needed.

2.3.9 Coating Procedure

Metal plates were coated by applying a dip coating procedure. Drying process

for coatings was achieved in 37^0C constant temperature vacuum oven.

2.3.10 Surface Modification of Titanium Plates

Different surface modifications and surface cleaning procedures were applied to titanium plates prior to the coating applications and information about these procedures are given in relevant sections.

2.3.11 Drug Release Studies

Drug release amounts at definite time intervals from coatings were measured in an aqueous medium. Simulated body fluid or triple distilled water was used as drug release medium. Drug loaded metal plates were immersed in the liquid medium. Release studies were done in a 37^0C constant temperature vacuum oven. At predetermined time intervals, plates were taken to a fresh solvent. On the remaining solutions, absorbance measurements were done by using UV spectrophotometer. Then, by using the calibration curves, the concentrations and the amounts of drug released were calculated.

2.3.12 Polymer Degradation Studies

Degradation of polymers used for coating was analyzed by solution viscosity measurements. Polymer coated plates were put into the triple distilled water and at definite time intervals, polymers were dissolved in chloroform and their solution viscosities were measured. By using flow times of these solutions in capillary viscometer, comments were done on degradation profiles of polymers.

2.3.13 Kirby-Bauer Disc Diffusion Antibiotic Sensitivity Tests

To check the antibiotic release results obtained by UV analysis, Kirby-Bauer disc diffusion antibiotic sensitivity tests were also performed. For these studies, bacteria seeded petri dishes and solutions obtained from release experiments were used. The existence and the amount of antibiotics in the aqueous solutions were estimated from the zone diameters.

2.3.14 SEM Analysis

Pure plates, coated plates and plates after drug release studies were analyzed and surfaces of the implants were investigated by using SEM analysis.

2.3.15 In Vivo Tests

At this stage of the study, drug loaded implants were placed at the dorsal muscle of six six-month old native rabbits. Test subjects were not infected initially. These implants were followed for six months and implant surfaces and surrounding tissues were investigated histologically.

CHAPTER 3

RESULTS AND DISCUSSION

3.1 Investigation of Solubility of Polymers and Drugs

It was observed that polyvinyl alcohols (PVOHs) were soluble in water; PLGA RG 504 was soluble in ethyl acetate, chloroform, acetone and tetrahydrofuran; Poly (L-lactide) L 209S, Poly (L-lactide-co-ε-caprolactone) LC 703 and polycaprolactone were soluble in chloroform. Therefore, it was decided to use water and chloroform as solvents. All of the antibiotics used were soluble in water.

3.2 Film Formation and Coating Thickness Studies

For coating thickness and coating density measurements, 15 % (w/v) PVOH (high molecular weight) solutions were prepared in water. Titanium plates with different surface treatments were used for coatings (Table 3.1). They were; as received, polished, 4 No sandpapered, wire emery applied and sandblasted titanium plates. Plates were cleaned with detergent-triple distilled water-acetone-triple distilled water cycle prior to coating. Film coatings were done by dip coating method for two times and coated plates were dried in an oven at 37^0C for 30 hours.

Coating thicknesses were measured by using a micrometer. For coating density calculations, the surface areas of titanium plates were measured and initial and final weights of plates were recorded from which the coating density can be calculated. These measurements were done twice and average values given in Table 3.1.

Table 3.1 Coating thickness and coating density measurements

Titanium plate	Coating thickness (mm)	Coating density (g/m^2)
As received	0.16	30.85
Polished	NA	NA
4 No sandpapered	0.17	32.10
Wire Emery	0.12	29.75
Sandblasted	0.17	33.60

Coating thicknesses were nearly the same for four samples. Coating densities were around 30 g/m^2. The highest value measured for sandblasted one as expected. It was concluded that the antibiotic including polymer coatings were loaded more effectively on sandblasted porous surfaces than the other surfaces in question. For polished samples, homogeneous coatings were not achievable.

3.3 Indent Prototype Studies

In these studies, to increase the loading efficiency, five different indentation patterns were applied to the Grade 2 titanium alloy and 316L stainless steel plates.

Grade 2 Titanium plates 316L Stainless Steel plates

Figure 3.1 Indent Prototypes (indent 1 is the upper, indent 5 is the bottom one)

3.3.1 Loading Efficiency on Indentations

For these five different indentations, drug containing polymer loading values were measured and given in Table 3.2.

Table 3.2 Polymer loading on different indentations

	Indent 1	**Indent 2**	**Indent 3**	**Indent 4**	**Indent 5**
Loading amount (g)	0.13	0.22	0.18	0.14	0.27
% Increase	29	107	82	44	156

It was observed in indent prototypes No.2 and No.5, % increase in polymer loading was greater than 100 %. Therefore, it was concluded that such indentations are applicable to implant surfaces such as smooth implants and screw necks.

3.3.2 Biomechanical Changes Related to the Indentation

Fatigue tests were applied on the plates with five different indentations. S-N curves of both used materials are given in Figure 3.2.

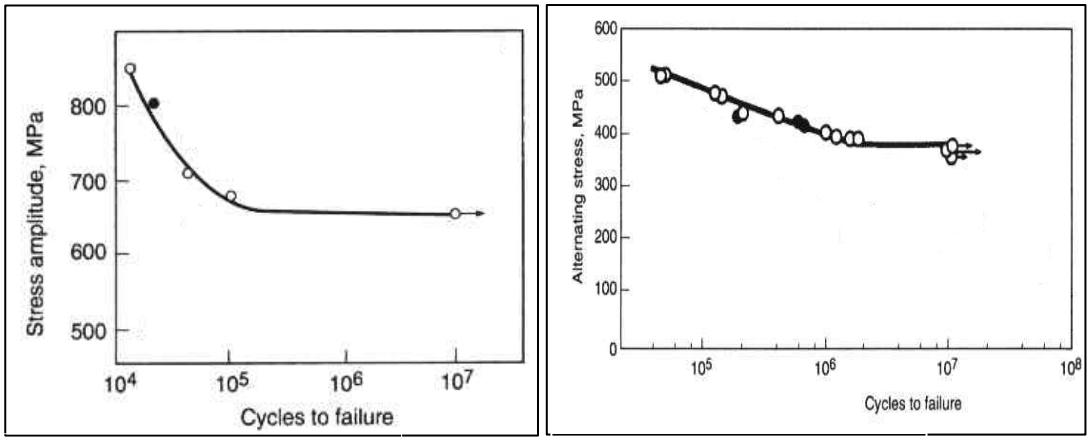

a) Titanium Alloy (Grade 2) b) Stainless Steel 316L

Figure 3.2 S-N figures for (a) grade 2 titanium alloy and (b) stainless steel 316L

It was found that 10^7 times loading on the samples of both materials with and without indentation did not cause the fatigue failure. For this reason, it was concluded that the indentations can be used safely for the plaque and screw applications.

Computer simulations and fatigue tests in virtual media analysis applied to all indentations (n=5) and materials (n=2). Ansys Workbench 10.0 (ANSYS, Inc., USA) program was used for virtual media analysis. The models of titanium and stainless steel samples were done in computer programs and 100 N load was applied by using again with a virtual punch.

Indentation Model 1

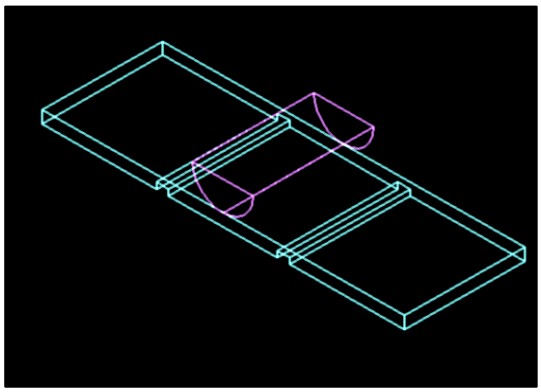

Virtual media model

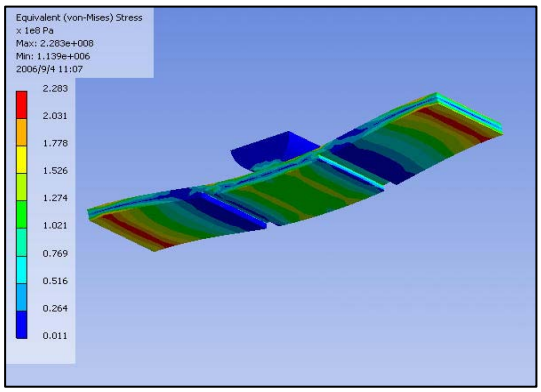

FEA stress distribution

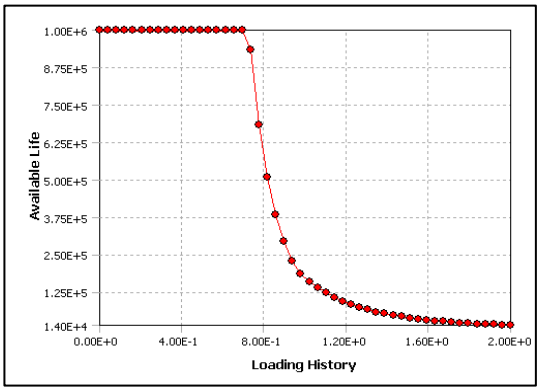

Titanium (Grade 2) S-N diagram

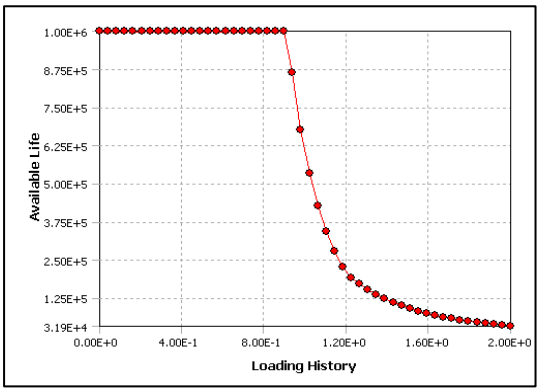

Stainless Steel 316L S-N diagram

Figure 3.3 Virtual media model, FEA stress distribution and S-N diagrams for Indentation Model 1

Indentation Model 2

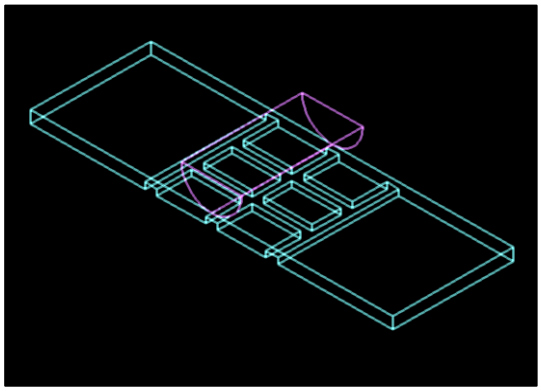

Virtual media model

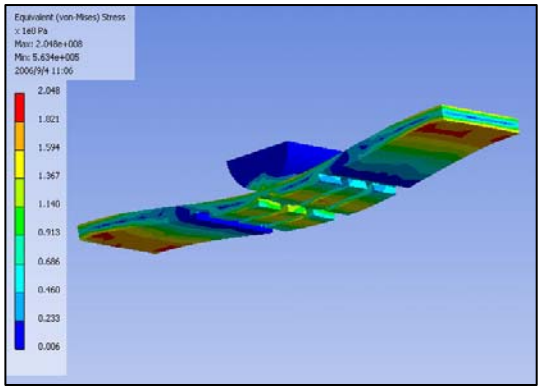

FEA stress distribution

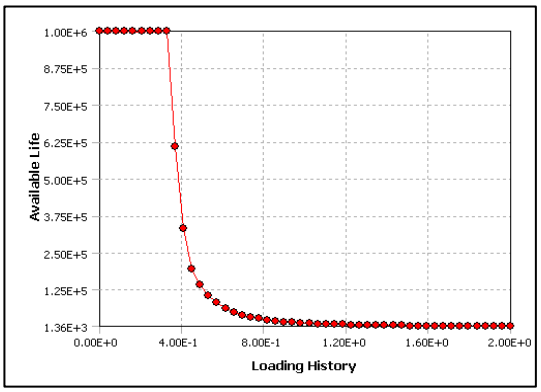

Titanium (Grade 2) S-N diagram

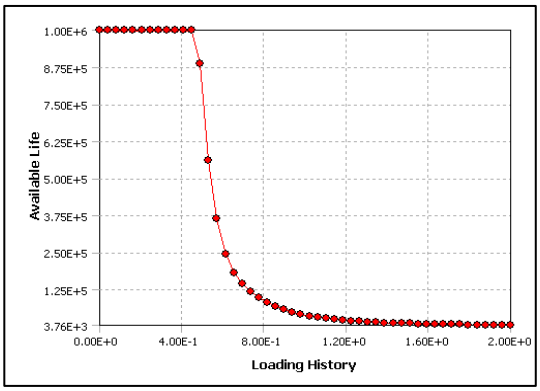

Stainless Steel 316L S-N diagram

Figure 3.4 Virtual media model, FEA stress distribution and S-N diagrams for Indentation Model 2

Indentation Model 3

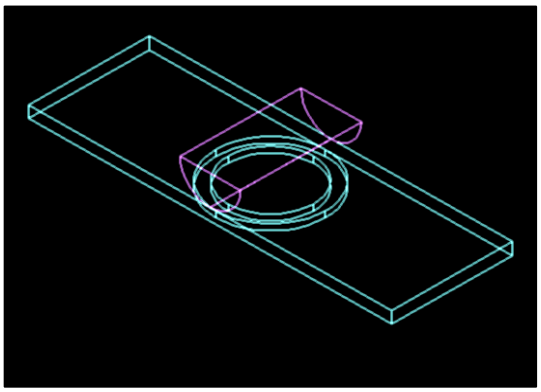

Virtual media model

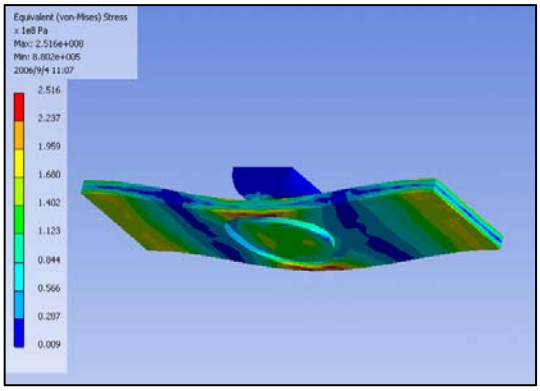

FEA stress distribution

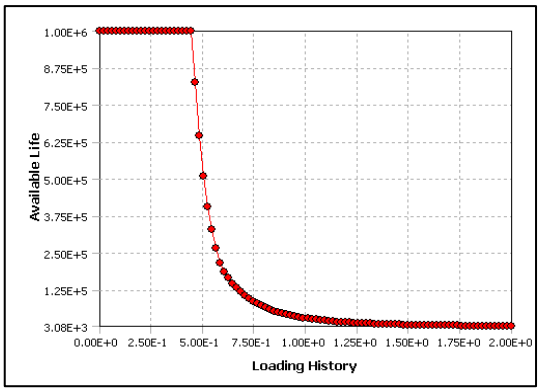

Titanium (Grade 2) S-N diagram

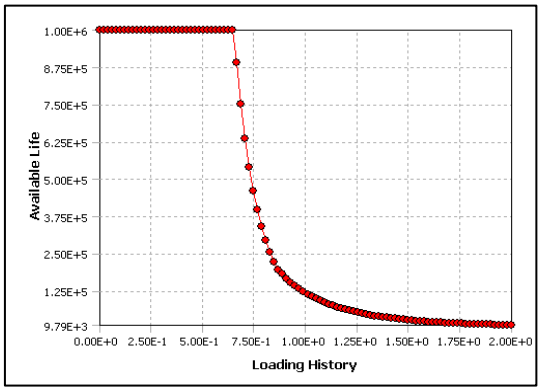

Stainless Steel 316L S-N diagram

Figure 3.5 Virtual media model, FEA stress distribution and S-N diagrams for Indentation Model 3

Indentation Model 4

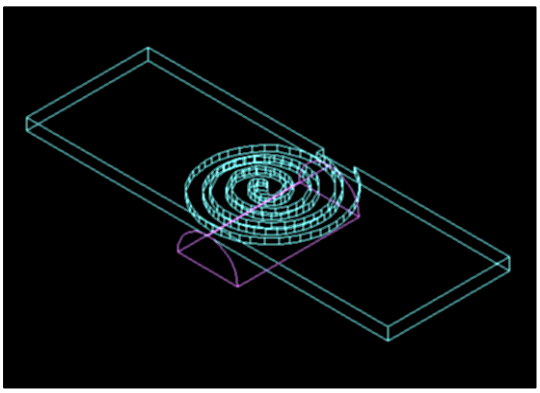

Virtual media model

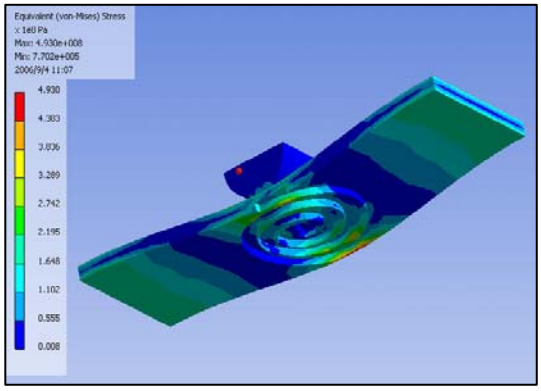

FEA stress distribution

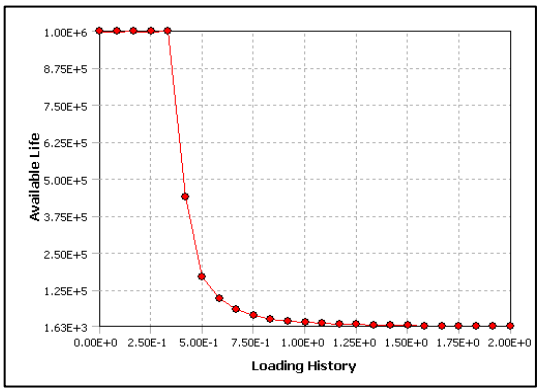

Titanium (Grade 2) S-N diagram

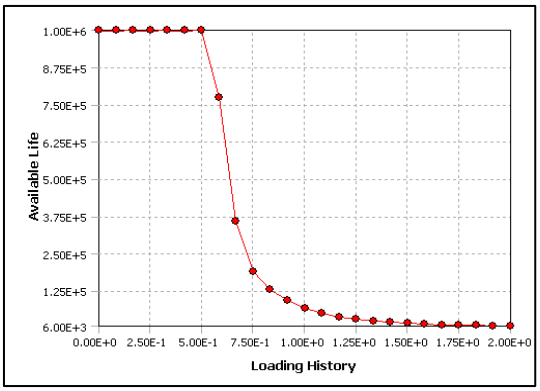

Stainless Steel 316L S-N diagram

Figure 3.6 Virtual media model, FEA stress distribution and S-N diagrams for Indentation Model 4

Indentation Model 5

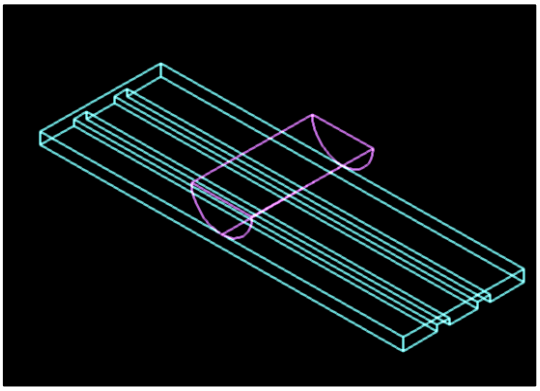

Virtual media model

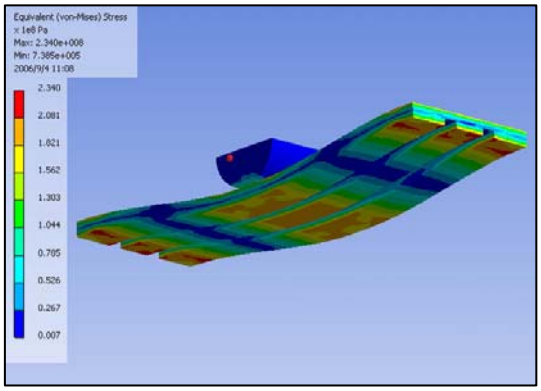

FEA stress distribution

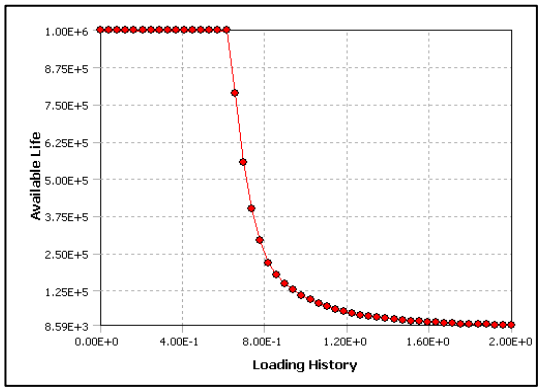

Titanium (Grade 2) S-N diagram

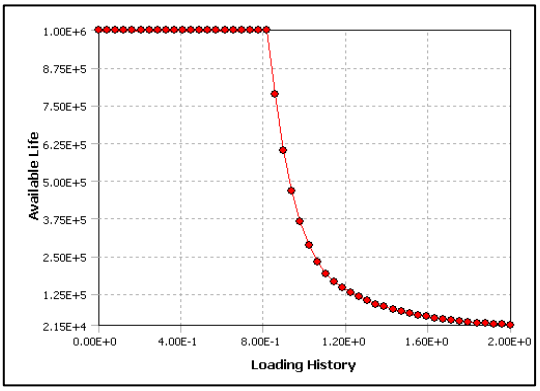

Stainless Steel 316L S-N diagram

Figure 3.7 Virtual media model, FEA stress distribution and S-N diagrams for Indentation Model 5

According to the results obtained from the computer simulations and virtual fatigue tests, it was determined that indentations applied on the grade 2 titanium and stainless steel 316L samples did not cause any damage to the integrity of the implant materials. Such indentations can be applied to implant material to obtain homogeneous high amount of drug containing polymer coatings.

3.4 Surface Treatment Studies on Titanium Plates

3.4.1 Surface Treatment

In this part, different surface pretreatments on titanium plates were applied. The following steps were followed:

- Titanium plates were sandpapered by using 400 number SiC sandpaper and then cleaned with alcohol for 15 minutes in an ultrasonic bath.
- The samples were kept in 5 M NaOH solution at varying time intervals. Solution temperature was set at 48^0C for sample 4 and was set 60^0C for the other samples.
- The plates were cleaned by dipping 3-5 times into distilled water. Plates were dried at 40^0C. Each plate was kept in an oven for 1 hour at 600^0C.
- SEM and EDX analysis were done on the samples.

The treatment duration and alkaline solutions used for surface treatments on titanium plates are given in Table 3.3.

Table 3.3 Solutions used, treatment duration and temperatures for surface treatments

Sample No	Solution	Treatment Duration
1	5M NaOH, 60 ^{0}C	1 day
2	5M NaOH, 60 ^{0}C	2 days
3	5M NaOH, 60 ^{0}C	3 days
4	5M NaOH, 48 ^{0}C	7 days

3.4.2 SEM Analysis

For SEM analysis, micrographs were obtained at magnification 2000X and 5000X for each sample.

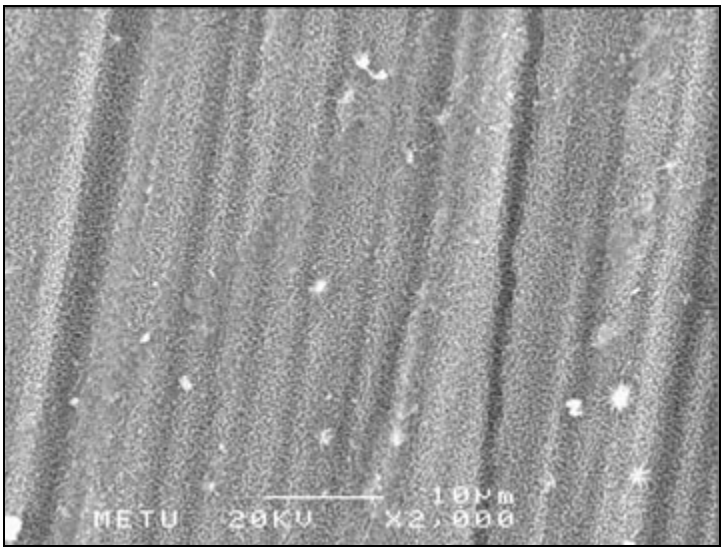

Figure 3.8 SEM image for sample 1 (1 day, 60 ^{0}C, 2000X)

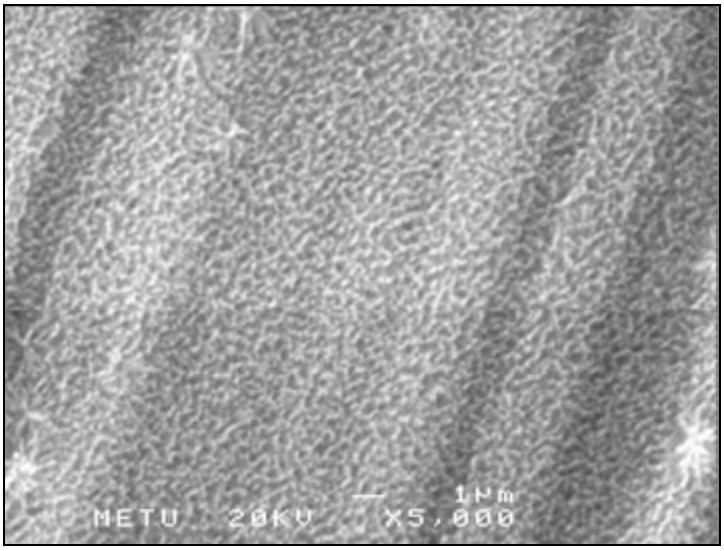

Figure 3.9 SEM image for sample 1 (1 day, 60 ^{0}C, 5000X)

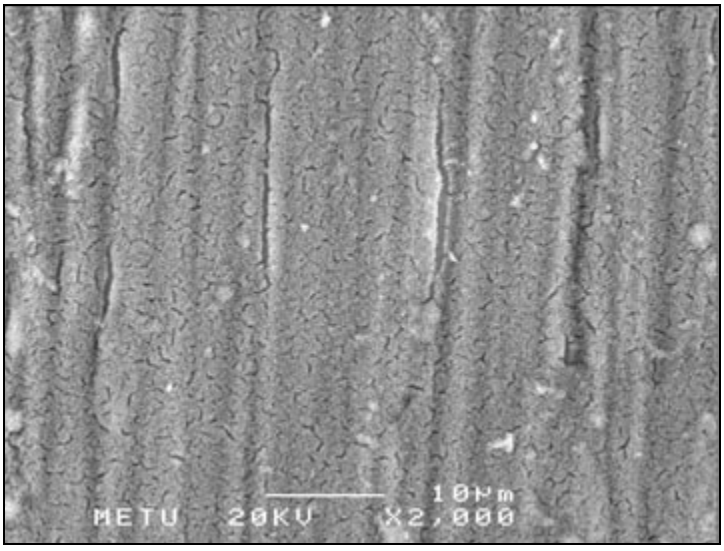

Figure 3.10 SEM image for sample 2 (2 days, 60 ^{0}C, 2000X)

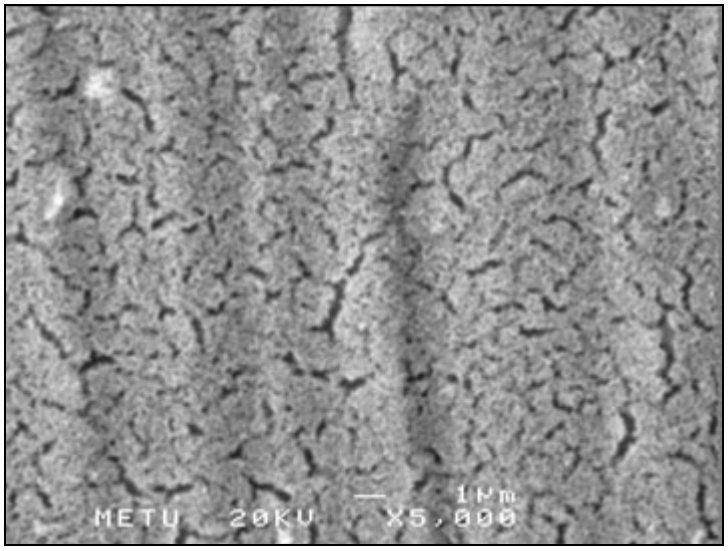

Figure 3.11 SEM image for sample 2 (2 days, 60 ^{0}C, 5000X)

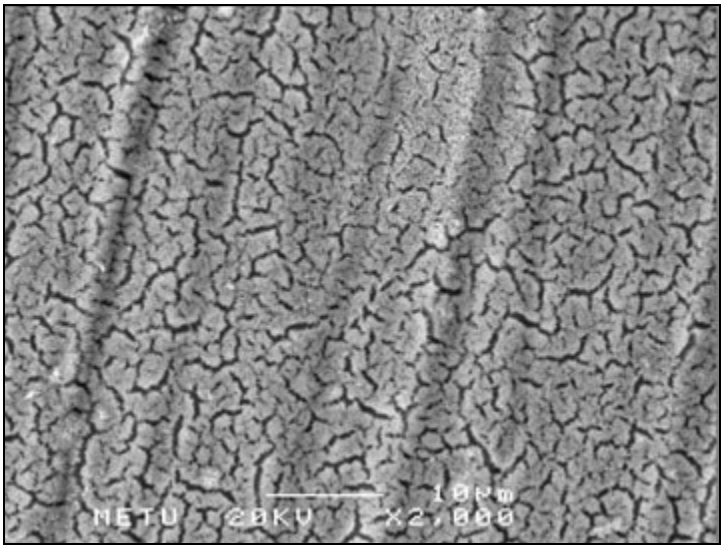

Figure 3.12 SEM image for sample 3 (3 days, 60 ^{0}C, 2000X)

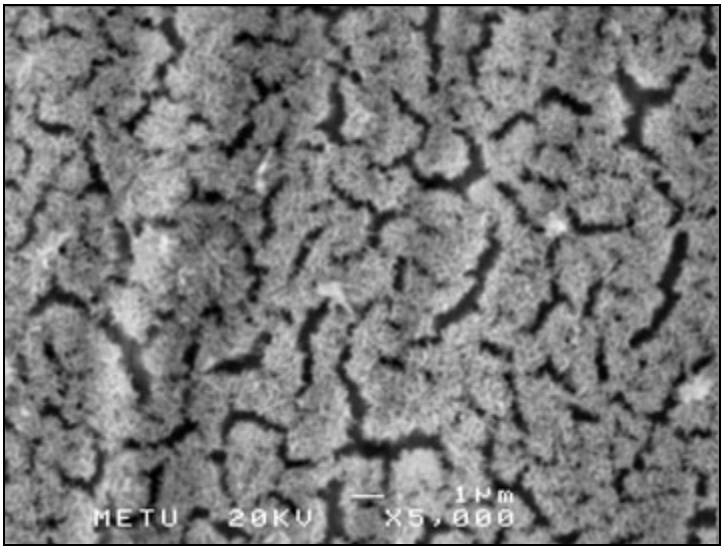

Figure 3.13 SEM image for sample 3 (3 days, 60 ^{0}C, 5000X)

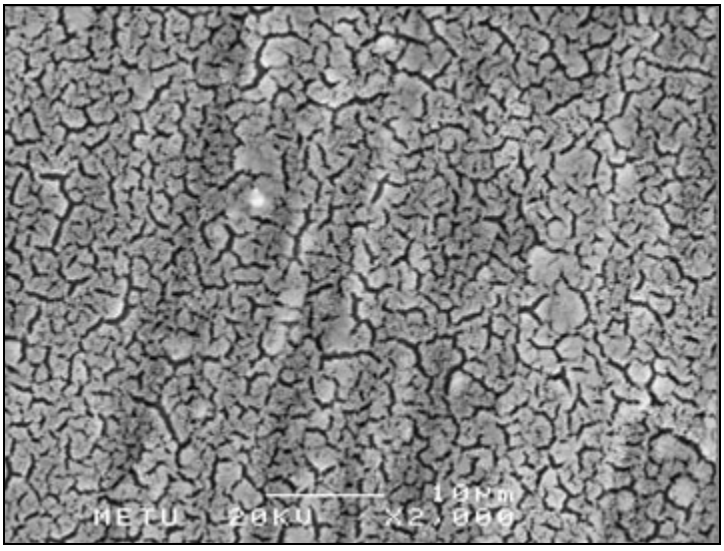

Figure 3.14 SEM image for sample 4 (7 days, 48 ^{0}C, 2000X)

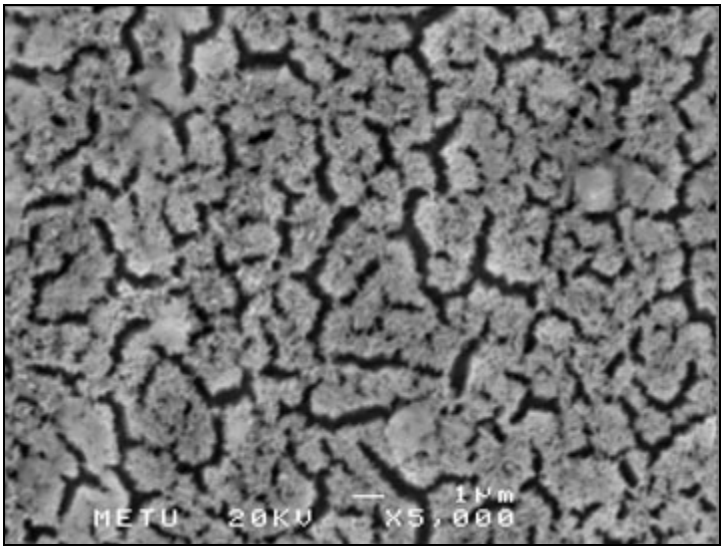

Figure 3.15 SEM image for sample 4 (7 days, 48 ^{0}C, 5000X)

Figures 3.8 to 3.15 show SEM photographs of the surfaces of titanium alloys subjected to 5 M NaOH treatments. From these images, it can be concluded that smooth surfaces of titanium alloys become more porous when they are treated with 5 M NaOH alkaline solution at 60^{0}C and 48^{0}C. Increasing the treatment time, a more

porous structure was observed for the samples. Obtaining macroporous layer on titanium alloy surfaces has a major importance since these materials are not bioactive. In many publications, it is given that NaOH treatments followed by heat treatments increases bioactivity of titanium based implant materials and bonelike apatite layer forms over the surfaces when they are inserted into the body. It is also reported that when surface treated implants immersed in simulated body fluids (SBFs), a bonelike apatite layer forms on the surface of the implant material. This gives the implant a bone bonding property and integration with the living bone is succeeded by this way [74, 78, 80, 180-184].

3.4.3 EDX Analysis

To gain information about the surface chemical element surface composition after surface treatments, EDX scanning analysis were done at 2000X. EDX graphs of titanium plates are as follows:

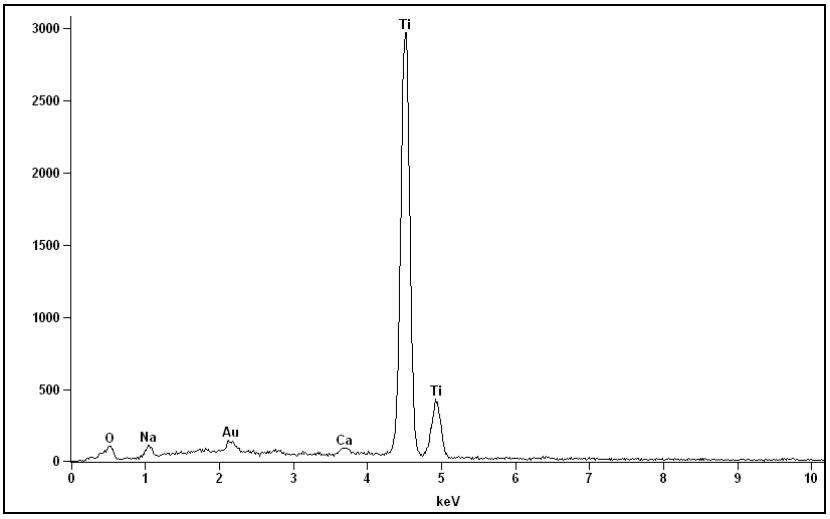

Figure 3.16 EDX graph for sample 1 (1 day, 60 ^{0}C)

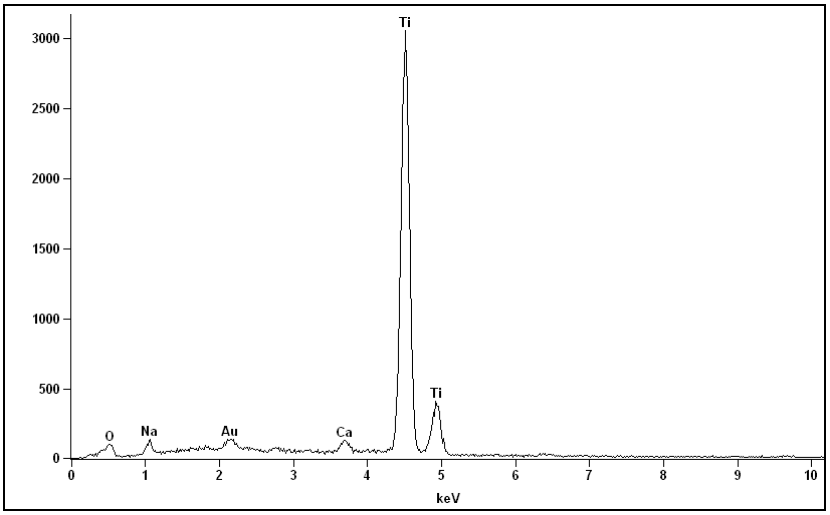

Figure 3.17 EDX graph for sample 2 (2 days, 60 ^{0}C)

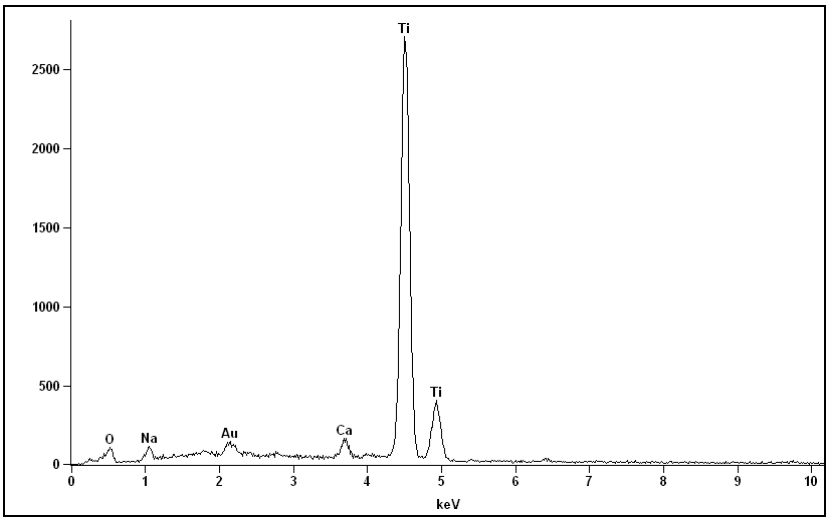

Figure 3.18 EDX graph for sample 3 (3 days, 60 ^{0}C)

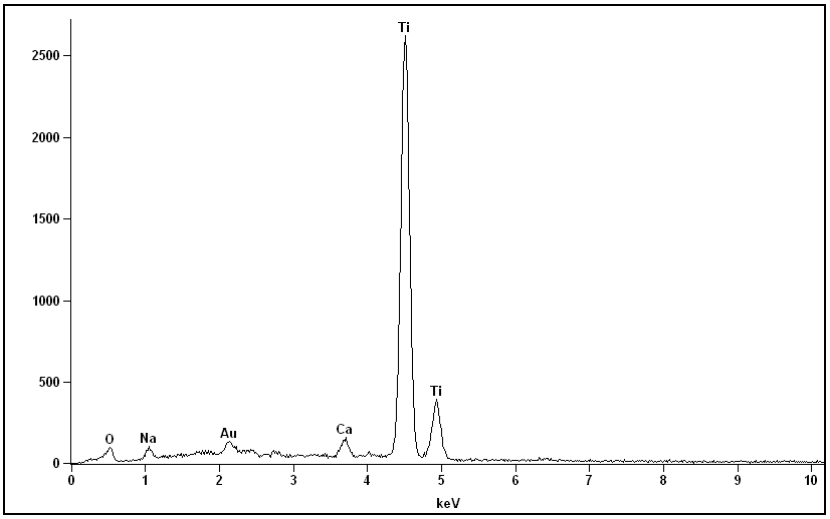

Figure 3.19 EDX graph for sample 4 (7 days, 48 ^{0}C)

At the end of these analyses, stable and defined amorphous sodium titanate layer was defined over all of the samples' surfaces. In addition to the sodium peak, calcium peak was also detected in all EDX graphs. Figure 3.20 outlines the steps in the formation of bonelike layer on the titanium surfaces.

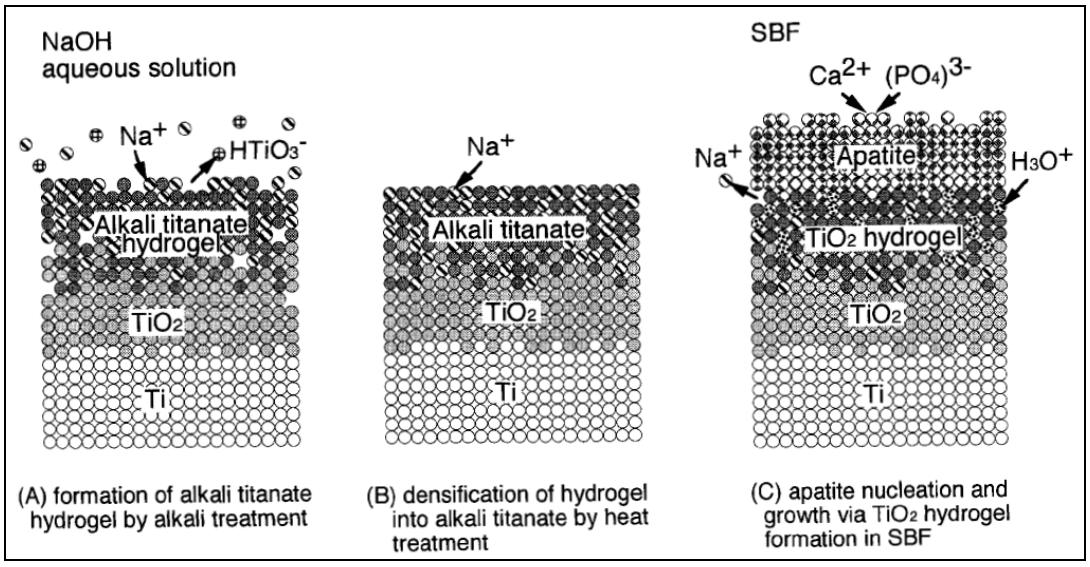

Figure 3.20 Schematic representation of structural change of Ti metal with alkali treatment (A), heat treatment (B) and apatite formation mechanism in SBF(C) [182]

3.4.4 Surface Cleaning of Titanium Alloys Prior to Coating

Another surface treatment prior to surface coating steps was done according to ASTM D2651-90 "Standard Guide for Preparation Metal Surfaces for Adhesive Bonding" [178]. According to this procedure (10.2.1 Acid Etch) following steps were applied on titanium alloy surfaces:

- Immerse for 2 min at room temperature in the following solution: 841 ml orthophosphoric acid (reagent grade, 85 to 87%), to 63 ml hydrofluoric acid (reagent grade, 60%).
- Rinse.
- Oven dry for 15 min at 88 to 93 ^{0}C.

This surface treatment technique was used to increase the bonding ability of titanium alloy implant surfaces. Then, these titanium alloy samples were used for coating applications.

3.5 Persoz Hardness Tests

Solutions of 10% (w/v) PVOHs in water, 10% (w/v) RG 504 and LC 703 in chloroform and 5% (w/v) PCL and L 209S in chloroform were prepared and precleaned glass plates (9,5 cm x 10 cm) were coated with these polymers to obtain a film thickness of 50 μm. Pendule Persoz & Konig Model 3034 from Braive Instruments was used for hardness tests. Measurements were done on three different points of coated glass plates and average values are given in Table 3.4.

Table 3.4 Persoz hardness results of polymer coatings

Sample	Persoz Hardness (ASTM)
PVOH (Mwt:31000-50000)	389
PVOH (Mwt:13000-23000)	386
L 209S	424
RG 504	351
LC 703	225
PCL	253

According to the hardness results, Poly(L-lactide) L 209S has the highest hardness value as expected. The hardness values are in the following order:

L 209S > PVOH (high Mwt.) > PVOH (low Mwt.) > RG 504 >PCL > LC 703

The hardness order gives some information about the degradation profiles of the polymers that is responsible for controlled drug release. Since drug release is mainly affected by diffusion and by degradation, the hardness values have importance for drug release studies. In this regard, the information obtained from this study is helpful in designing a polymeric system for coating applications. Also, the hardness values are a measure of deformation of polymeric coatings. Coatings applied on the implant material should maintain its uniformity during the application to the body, therefore the hardness value of polymeric film should be comparatively high.

3.6 Gloss Tests

The samples used for hardness tests are also used for gloss tests. Since the final appearance of coated implant material is important, gloss measurements were done. The results are given in Table 3.5.

Table 3.5 Gloss measurements of polymer coatings

Sample	Gloss		
	20^0	60^0	85^0
PVOH (Mwt:31000-50000)	163.9	141.9	111.0
PVOH (Mwt:13000-23000)	163.5	144.9	110.6
L 209S	140.0	133.2	108.6
RG 504	62.2	84.7	74.6
LC 703	148.4	137.5	111.5
PCL	47.1	63.8	93.8

Gloss results give information about the surface shininess and coating roughness. Higher the gloss value means smoother the surface. It can be concluded from the gloss results, PCL and RG 504 coatings have much less smooth surface appearance than the other coatings.

3.7 Measuring Adhesion by Tape Test

Adhesion measurement by tape test according to ASTM standards was applied to the polymer coated glass specimens. For these tests, coatings were cut in small squares and pressure sensitive tape from 3M Company was applied. Then the tape was pulled back and adhesion was determined and evaluated from 5B to 0B.

Table 3.6 Adhesion measurements of polymer coatings by Tape Tests

Sample	Adhesion (Tape Test)
PVOH (Mwt:31000-50000)	0B
PVOH (Mwt:13000-23000)	0B
L 209S	1B
RG 504	1B
LC 703	0B
PCL	0B

According to the results, the adhesions of the polymers are weak and coating integrity can be easily broken. These tests were applied to measure the difference in adhesional properties of different polymers we plan to use in drug release experiments. Poly(L-lactide) L 209S and PLGA RG 504 coatings have better adhesional properties over the other polymer coatings.

3.8 Lap Shear Tests

Surface modified titanium alloy plates (Table 3.7) were used for lap shear tests. As film forming material, PLGA RG 504 and poly(L-lactide) L 209S polymers were used. Titanium plates were cleaned in sequence with detergent-triple distilled water-0.1 M NaOH-triple distilled water cycle and dried at 37^0C prior to application of coating materials. Tests were applied for three times to each kind of titanium alloy. The samples were dried again at 37^0C for one day before applying the tests. Maximum force values at failure were measured and comments on the type of failure were given. The application of these tests is described in Section 2.2.1.3. Forms and dimensions of specimens used are explained in Figure 2.9. Tensile testing machine used for lap shear tests is shown in Figure 2.10. In Figure 3.21, typical load-propagation extension graph for lap shear tests is given.

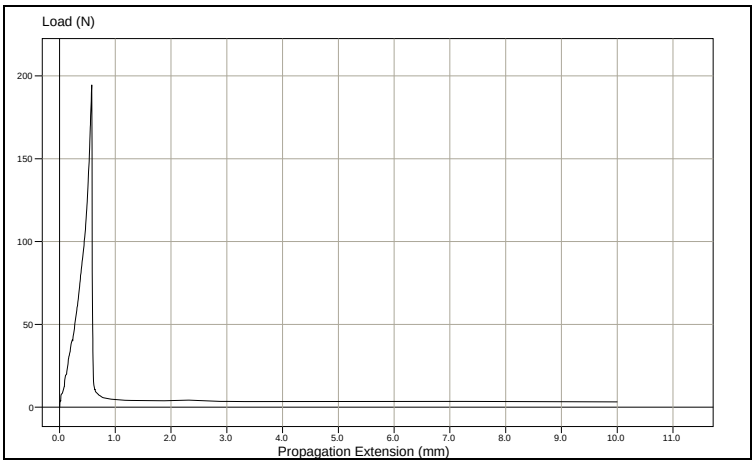

Figure 3.21 Typical load-propagation extension graph for lap shear tests

3.8.1 Lap Shear Tests for PLGA RG 504

10% (w/v) RG 504 solution was prepared in chloroform and this solution was used as an adhesive material. Bonded plates were dried in an oven at 37^0C for one day. Samples prepared were tested by using a tensile testing machine, Lloyd Instruments, AMETEK (UK), LR5K. 5 kN capacity load cell and TG15 model self tightening sliding wedge grip were used for analyses. Preload force was 2 N and crosshead speed was 10 mm/min during the tests. NEXYGEN material test and data analysis software was used for processing the data. The results of these tests are as following:

Table 3.7 Lap shear test results for RG 504

Titanium Plate	**Force at Break (N)**	**Average Force (N)**	**Shear Stress (N/cm^2)**
Not-treated	1)313.79 2)703.46 3)340.70	452.65±177.69	70.18±27.55
4 No Sandpapered	1)378.70 2)716.72 3)984.04	693.16±247.69	107.47±38.40
Wire Emery	1)302.86 2)449.43 3)384.08	378.79±59.95	58.73±9.29
Sandblasted	1)777.40 2)112.93 3)277.40	389.24±282.56	60.35±43.81

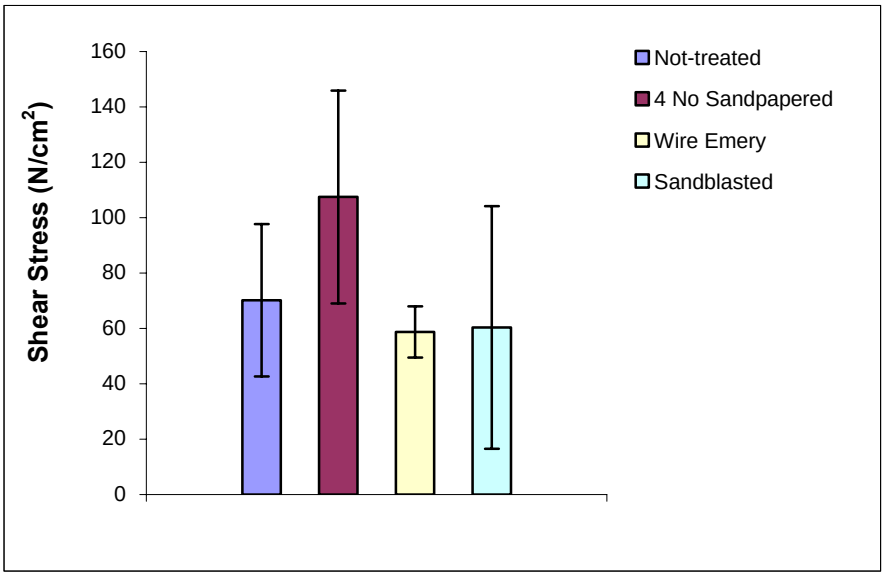

Figure 3.22 Comparisons of RG 504 Lap Shear tests

3.8.2 Lap Shear Tests for Poly(L-lactide) L 209S

5% (w/v) L 209S solution was prepared in chloroform and this solution was used as an adhesive material. Bonded plates were dried in an oven at 37^0C for one day. Prepared samples were tested by using a tensile testing machine, Lloyd Instruments, AMETEK (UK), LR5K. 5 kN capacity load cell and TG15 model self tightening sliding wedge grip were used for analyses. Preload force was 2 N and crosshead speed was 10 mm/min during the tests. NEXYGEN material test and data analysis software was used for processing the data. The results of these tests are as following:

Table 3.8 Lap shear test results for L 209S

Titanium Plate	Force at Break (N)	Average Force (N)	Shear Stress (N/cm^2)
Not-treated	1)51.29 2)114.75 3)40.46	68.84±32.77	10.67±5.08
4 No Sandpapered	1)129.46 2)260.54 3)NA	195.00±65.54	30.23±10.16
Wire Emery	1)194.60 2)268.92 3)310.08	257.87±47.79	39.98±7.41
Sandblasted	1)170.14 2)402.41 3)220.54	264.37±99.76	40.99±15.47

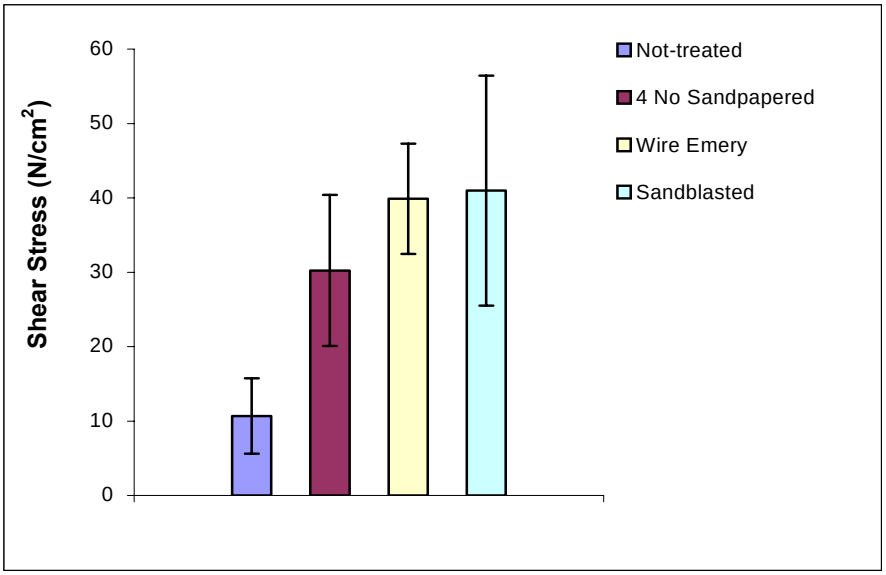

Figure 3.23 Comparisons of L 209S Lap Shear tests

Drug dispersed L 209S solutions in chloroform was prepared and lap shear tests were applied by using this suspension as an adhesive.

Table 3.9 Lap shear test results for L 209S + drugs

a) 5% (w/v) L 209S in chloroform (2.5g/50ml)+0.1268 g Cefamezin

Titanium plate	Force at Break (N)	Shear Stress (N/cm^2)
Not-treated	NA	NA
4 No Sandpapered	31.49	4.88
Wire Emery	86.62	13.43
Sandblasted	119.39	18.51

b) 5% (w/v) L 209S in chloroform (2.5g/50ml)+0.1261 g Rocephin

Titanium plate	Force at Break (N)	Shear Stress (N/cm^2)
Not-treated	85.84	13.31
4 No Sandpapered	222.79	34.54
Wire Emery	249.37	38.66
Sandblasted	228.87	35.48

As a result, the best adhesional property was observed in 4 No sandpapered titanium samples with PLGA RG 504 adhesive. Sandblasted samples had the highest adhesional force values with poly(L-lactide) L 209S. All samples' failures occurred from polymer adhesives (adhesive failure). Strength at failure values for both polymers was high enough to resist surface detachments during application of implants to the body. Poly(L-lactide) L 209S has a more viscous and higher crystalline structure; therefore its high adhesional ability is observed on porous surfaces. However, PLGA RG 504 has higher adhesional properties on smooth or nearly smooth surfaces.

When antibiotics are added (Cefamezin and Rocephin) to the adhesives, it was observed that on not-treated and unmodified titanium surfaces, failures occurred at very low shear stress values. Better adhesional results were observed for the other samples. For adhesive L 209S, the same trend observed that is, high stress at failure value for porous surfaces is valid. When compared to the lap shear tests with pure L 209S, big decrease in shear stress values were observed for the samples containing Cefamezin. On the other hand, slight decrease in shear stress values occurred in the Rocephin containing samples.

3.9 T-Peel Tests

Surface modified titanium alloy plates (Table 3.10) were used for T-peel tests. As adhesive material, PLGA RG 504 and poly(L-lactide) L 209S polymers were used. Since the adhesional ability is much more affected from the cleanliness of the surfaces, titanium plates were cleaned in sequence with detergent-triple distilled water-0.1 M NaOH-triple distilled water cycle and dried at 37^0C prior to application of coating materials. Tests were applied for three times to each kind of titanium alloy. The samples were dried again at 37^0C for one day before applying the tests. Maximum force values at failure were recorded and comments on the type of failure were given. The application of these tests is described in Section 2.2.1.4. Forms and dimensions of specimens used are explained in Figure 2.11. Tensile testing machine used for T-peel tests is shown in Figure 2.10. In figure 3.24, typical load-propagation extension graph for T-peel tests is given.

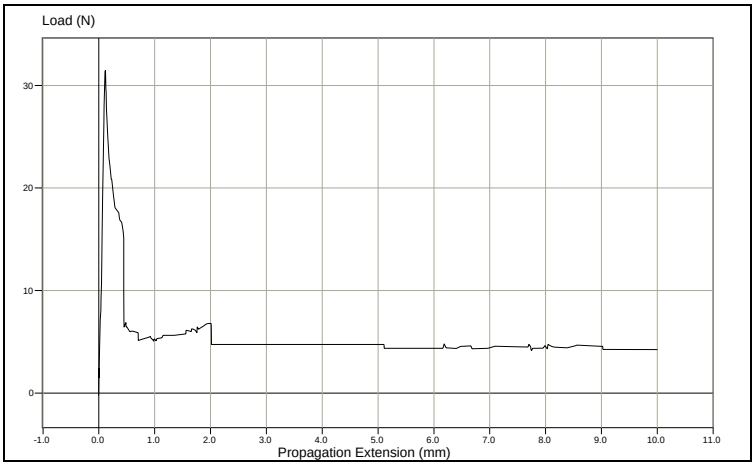

Figure 3.24 Typical load-propagation extension graph for T-peel tests

3.9.1 T-Peel Tests for PLGA RG 504

10% (w/v) RG 504 solution was prepared in chloroform and this solution was used as adhesive material. Bonded plates were dried in an oven at 37^0C for one day. Samples prepared were tested by using a tensile testing machine, Lloyd Instruments, AMETEK (UK), LR5K. 5 kN capacity load cell and TG15 model self tightening sliding wedge grip were used for analyses. Preload force was 2 N and crosshead speed was 10 mm/min during the tests. NEXYGEN material test and data analysis software was used for processing the data. The results of these tests are as following:

Table 3.10 T-peel test results for RG 504

Titanium Plate	Force at Break (N)	Average Force (N)	Shear Stress (N/cm^2)
Not-treated	1)32.18 2)62.66 3)63.85	52.90±14.66	2.98±0.82
4 No Sandpapered	1)25.61 2)80.78 3)38.99	48.46±23.50	2.73±1.32
Wire Emery	1)34.13 2)44.27 3)44.80	41.07±4.91	2.31±0.28
Sandblasted	1)29.43 2)59.14 3)66.84	51.80±16.13	2.91±0.91

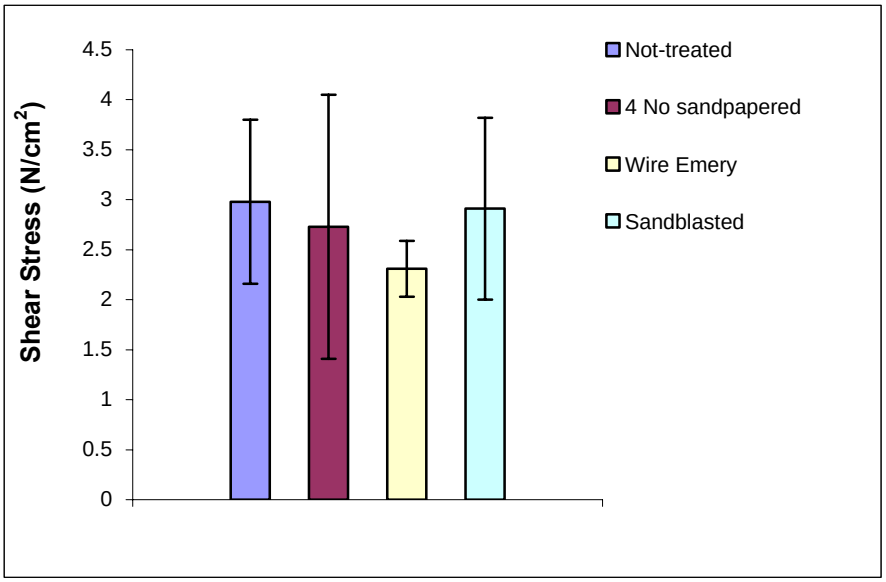

Figure 3.25 Comparisons of RG 504 T-peel tests

3.9.2 T-Peel Tests for Poly(L-lactide) L 209S

5% (w/v) L 209S solution was prepared in chloroform and this solution was used as adhesive material. Bonded plates were dried in an oven at 37^0C for one day. Samples prepared were tested by using a tensile testing machine, Lloyd Instruments, AMETEK (UK), LR5K. 5 kN capacity load cell and TG15 model self tightening sliding wedge grip were used for analyses. Preload force was 2 N and crosshead speed was 10 mm/min during the tests. NEXYGEN material test and data analysis software was used for processing the data. The results of these tests are as following:

Table 3.11 T-peel test results for L 209S

Titanium Plate	Force at Break (N)	Average Force (N)	Shear Stress (N/cm^2)
Not-treated	1)22.75 2)37.98 3)38.30	33.01±7.26	1.86±0.41
4 No Sandpapered	1)31.46 2)36.92 3)36.56	34.98±2.49	1.97±0.14
Wire Emery	1)37.14 2)41.98 3)51.87	43.66±6.13	2.46±0.34
Sandblasted	1)26.01 2)73.03 3)43.52	47.52±19.40	2.67±1.09

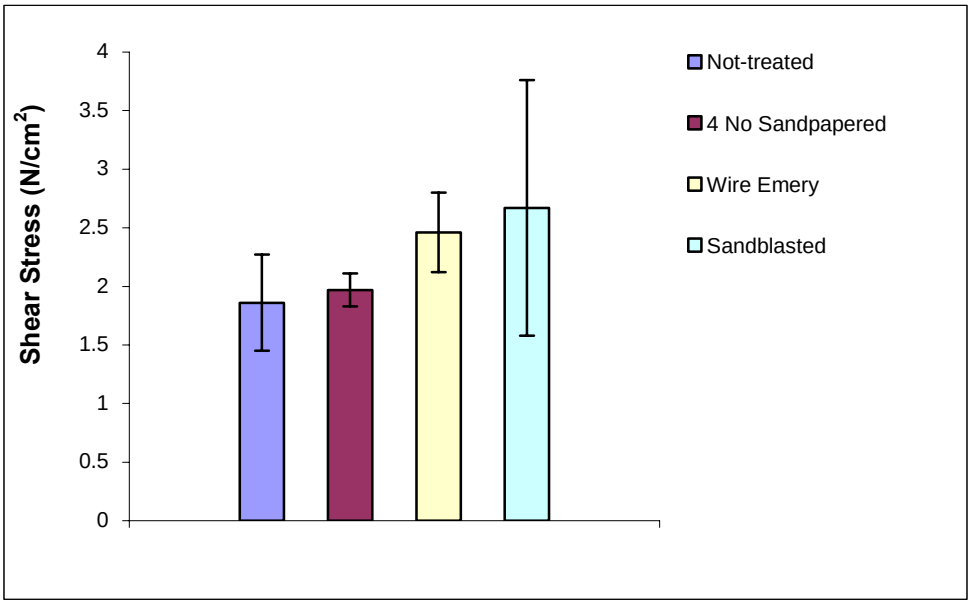

Figure 3.26 Comparisons of L 209S T-peel tests

The same tendency with lap shear tests can be seen in T-peel tests. RG 504

samples have higher failure force values on smooth surfaces. L 209S, on the other hand, have shown higher force values with more porous surfaces. All samples' failures occurred from polymer adhesives (adhesive failure). Strength at failure values for both polymers was high enough to resist surface detachments during application of implants to the body.

3.10 Polymer Degradation Studies

In this part, degradation profiles of PLGA RG 504 and poly(L-lactide) L 209S polymers were investigated. Viscosity measurements were done by using a capillary viscometer. The metabolic degradation schema for polylactide and polyglycolide is shown in Figure 3.27.

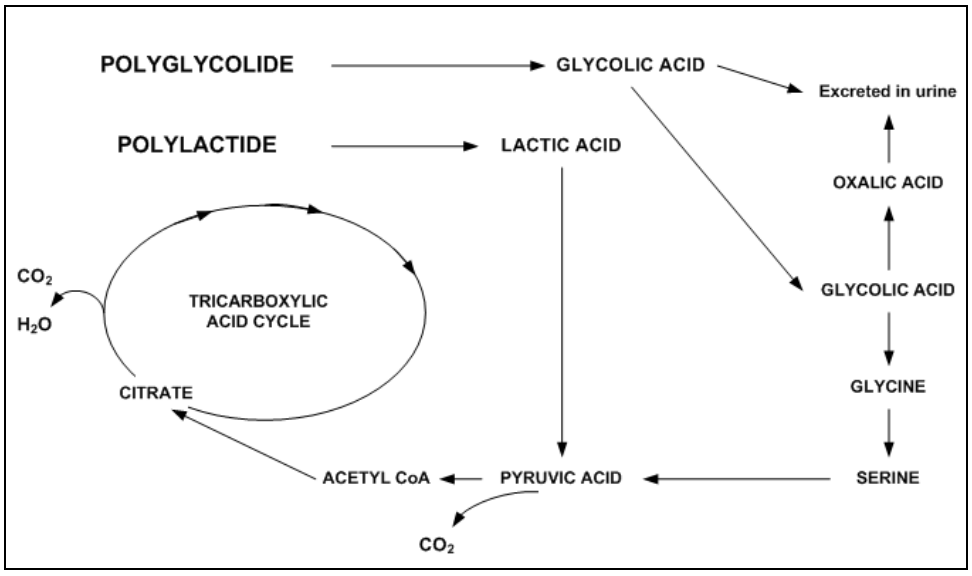

Figure 3.27 Metabolic degradation pathways for polyglycolide and polylactide polymers (Böstman OM) [98]

3.10.1 Degradation Profile for PLGA RG 504

0.5 g polymer was dissolved in 100 ml chloroform under constant stirring. Polymer films were obtained by evaporating the solvent. Then, these films were placed into the 20 ml DI water in an oven at 37 ^{0}C. At predetermined time intervals, the films were taken, dried and dissolved again with initial amount of chloroform. Then the flow times were measured by using Ubbelohde viscometer. For this purpose, constant temperature water bath held at 25 ^{0}C was used. Set of solutions was prepared by dilution with chloroform and flow time of each solution was measured at least three times to ensure the reliability.

a) Stock Solution (RG 504)

10 ml polymer solution (0.5 g/dl) was taken and dilutions were done by adding 5 ml portions of chloroform. At each step, thermal equilibrium was established by holding the solution in constant temperature water bath for 15 min. before the measurements.

Table 3.12 Intrinsic viscosity values for RG 504 (stock solution)

C (g/dl)	*solvent*	*0.500*	*0.333*	*0.250*	*0.200*
Flowtime (s)	103.31	166.22	144.39	134.95	127.71
η_{rel}		1.609	1.398	1.306	1.236
η_{inh}		0.951	1.006	1.068	1.059
η_{red}		1.218	1.195	1.224	1.180

Regression	
	[η] (dl/g)
From η_{inh} vs C line	1.1487
From η_{red} vs C line	1.1802
Average	1.1645

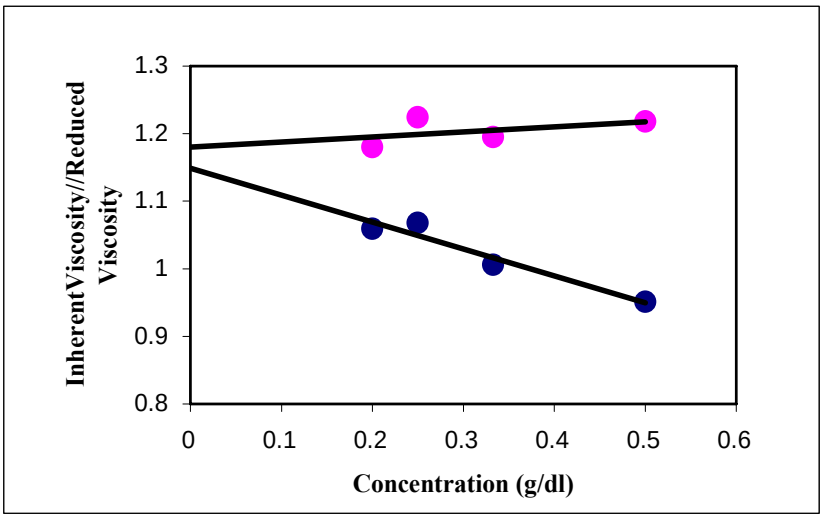

(• dots stand for η_{red} vs. C data, • dots stand for η_{inh} vs. C data)

Figure 3.28 η_{inh} // η_{red} vs. Concentration graph for stock solution (RG 504)

b) Degradation of RG 504

20 ml polymer solutions (0.5 g/dl) were taken and chloroform was evaporated to obtain clear polymer films. Then, these films were put into 20 ml DI water at 37^0C for 2 days, 1 week, 4 weeks and 6 weeks. These films were taken out of water, dried in an oven at 37^0C and dissolved again in 20 ml chloroform. From each solution, 10 ml was taken and used for viscosity measurements. At each step, thermal equilibrium was established by holding the solution in constant temperature water bath for 15 min. before the measurements.

Table 3.13 Intrinsic viscosity values of RG 504 at various degradation times

Degradation Time	[η]		
	From η_{inh} vs. C line	From η_{red} vs. C line	Average
0	1.1487	1.1802	1.1645
2 days	1.0077	1.0329	1.0203
1 week	1.0002	1.0415	1.0209
4 weeks	0.1424	0.1265	0.1345
6 weeks	0.1092	0.1073	0.1083

From the interpretation of the data, intrinsic viscosity values for RG 504 polymer films degraded in water at different time intervals were calculated (see Appendix F). It can be easily seen that degradation of these polymer films are continuous and very fast. Intrinsic viscosity values of RG 504 in chloroform decreased to nearly 9 % of its initial value after 6 weeks degradation in water. Major degradation occurs in 30 days mostly. Intrinsic viscosity vs. degradation time graph can be seen in Figure 3.29.

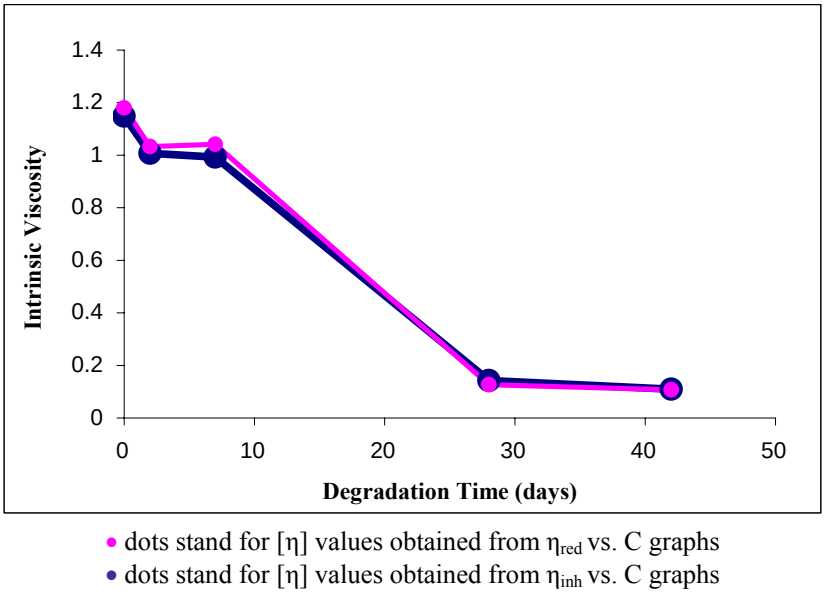

Figure 3.29 Intrinsic viscosity vs. degradation time graph for RG 504

For linear and unbranched polymers such as Resomer® RG 504, the viscosity of a diluted polymer solution is directly correlated to the $\overline{Mv}$ (viscosity average molecular weight) by the Mark-Houwink equation that is given below [185]:

$$[\eta] = K\ \overline{Mv}^{a} \qquad (3.1)$$

By using the solution viscometry results, the change in $\overline{Mv}$ with degradation time can be calculated. Mark-Houwink constants for 50:50 poly(D,L-lactide-co-glycolide) in chloroform are given as $K = 1.333 \times 10^{-3}$ dl/g, and a = 0.544 [185, 186]. The change in $\overline{Mv}$ values with degradation time can be seen in Figure 3.30.

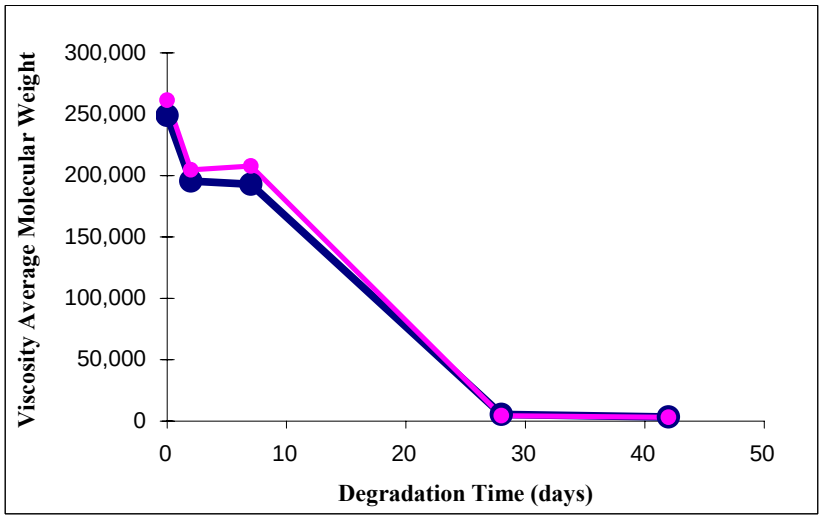

Figure 3.30 Change in $\overline{Mv}$ of RG 504 with degradation time

As it can be seen from the Figure 3.30, $\overline{Mv}$ for RG 504 decreased to nearly 1.3% of its initial value after 6 weeks degradation in water. Most of the degradation occurred in 4 weeks.

3.10.2 Degradation Profile for Poly(L-lactide) L 209S

0.25 g polymer was dissolved in 100 ml chloroform under constant stirring. Polymer films were obtained by evaporating the solvent. Then, these films were placed into the 20 ml DI water in an oven at 37 ^{0}C. At predetermined time intervals, the films were taken, dried and dissolved again with initial amount of chloroform. Then the flow times were measured by using Ubbelohde viscometer. For this purpose, constant temperature water bath held at 25 ^{0}C was used. Set of solutions was prepared by dilution with chloroform and flow time of each solution was measured at least three times to ensure the reliability.

a) Stock Solution (L 209S)

10 ml polymer solution (0.25 g/dl) was taken and diluted with 10 ml chloroform. From this solution, 10 ml was taken and 5 ml chloroform was added. For measurements, dilutions were done by adding 5 ml portions of chloroform. At each step, thermal equilibrium was established by holding the solution in constant temperature water bath for 15 min. before the measurements.

Table 3.14 Intrinsic viscosity values for L 209S (stock solution)

C (g/dl)	***solvent***	***0.0833***	***0.0625***	***0.0500***	***0.0417***
Flowtime (s)	103.31	283.82	231.47	201.34	180.65
η_{rel}		2.747	2.241	1.949	1.749
η_{inh}		12.131	12.911	13.346	13.406
η_{red}		20.972	19.856	18.980	17.962

Regression	
	[η] (dl/g)
From η_{inh} vs C line	14.852
From η_{red} vs C line	15.309
Average	15.081

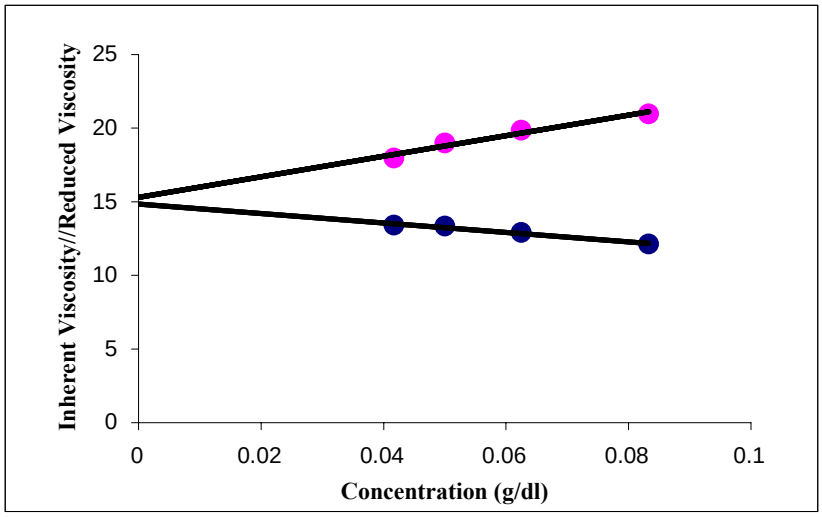

(● dots stand for η_{red} vs. C data, • dots stand for η_{inh} vs. C data)

Figure 3.31 η_{inh} // η_{red} vs. Concentration graph for stock solution (L 209S)

b) Degradation of L 209S

20 ml polymer solutions (0.25 g/dl) were taken and chloroform was evaporated to obtain clear polymer films. Then, these films were put into 20 ml DI water at 37^0C for 2 days, 1 week, 4 weeks and 6 weeks. These films were taken out of water, dried in an oven at 37^0C and dissolved again in 20 ml chloroform. From each solution, 10 ml was taken and diluted with 10 ml chloroform. Then, 10 ml was taken and 5 ml chloroform was added. For measurements, dilutions were done by adding 5 ml portions of chloroform. At each step, thermal equilibrium was established by holding the solution in constant temperature water bath for 15 min. before the measurements.

Table 3.15 Intrinsic viscosity values of L 209S at various degradation times

Degradation Time	[η]		
	From η_{inh} vs. C line	From η_{red} vs. C line	Average
0	14.852	15.309	15.081
2 days	13.972	14.465	14.219
1 week	11.714	10.761	11.238
4 weeks	11.152	11.295	11.224
6 weeks	12.083	12.026	12.055

From the interpretation of the data, intrinsic viscosity values for L 209S polymer films degraded in water at different time intervals were calculated (see Appendix G). It can be easily seen that degradation of these polymer films are relatively slow. Intrinsic viscosity values of L 209S in chloroform decreased to nearly 75-80 % of its initial value after 6 week degradation in water. Intrinsic viscosity vs. degradation time graph can be seen in Figure 3.32.

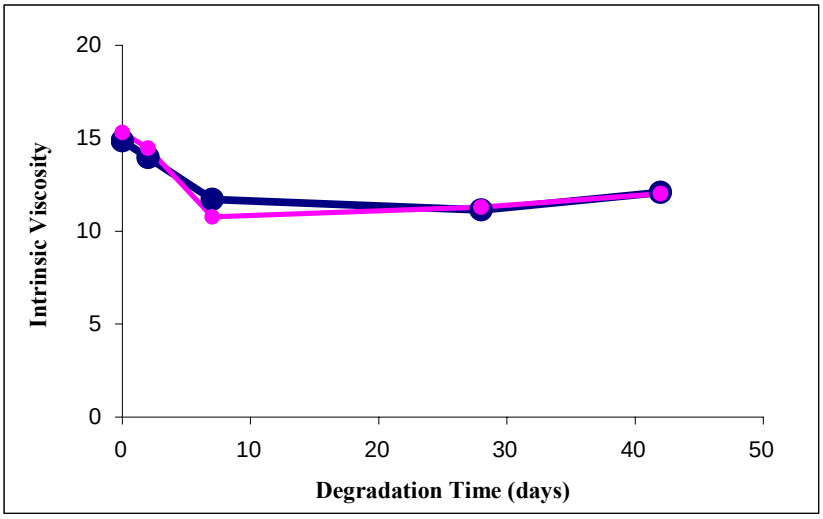

Figure 3.32 Intrinsic viscosity vs. degradation time graph for L 209S

As a result, it can be concluded that the degradation profile of L 209S sample is very slow. Therefore, L 209S inert coatings were thought to be helpful to control the drug release from the interior RG 504 coatings.

By using the solution viscometry results, the change in $\overline{Mv}$ with degradation time can be calculated. Mark-Houwink constants for poly(L-lactide) in chloroform are given as K = 6.774x10^{-4} dl/g, and a = 0.700 [185, 186]. The change in $\overline{Mv}$ values with degradation time can be seen in Figure 3.33.

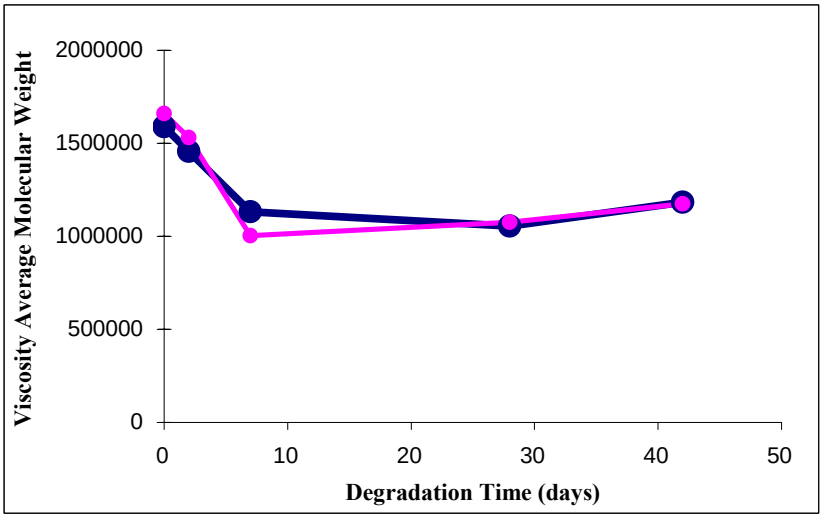

• dots stand for $\overline{Mv}$ values obtained by using η_{red} vs. C graphs
• dots stand for $\overline{Mv}$ values obtained by using η_{inh} vs. C graphs

Figure 3.33 Change in $\overline{Mv}$ of L 209S with degradation time

As it can be seen from the Figure 3.33, $\overline{Mv}$ for L 209S decreased to approximately 60-70 % of its initial value after 1 week of degradation in water. During the rest of the time until 6 weeks, no major change in $\overline{Mv}$ was detected.

According to degradation profiles of PLGA RG 504 and poly(L-lactide) L209S polymers in aqueous media, it can be concluded that degradation rate of RG 504 is higher than L 209S. That means, L 209S is more stable in terms of hydrolysis.

Depending on the degradation kinetics obtained for both polymers, different uses of them can exist. Preferably, RG 504 was decided mostly to be used as drug carrier and L 209S as inert coating agent.

3.11 Calibration Curves for Antibiotics Used in Release Studies

In this part, calibration curves of different drugs used were obtained. For this purpose, antibiotics were dissolved in water at different concentrations. In some trials, PBS (for preparation, see Appendix E) was used as solvent to compare if there were any difference. Two concentration sets of drugs were prepared to ensure the reliability. The maximum absorbance values were measured at predetermined wavelengths by using a UV-Visible spectrophotometer. Data obtained were used to prepare a calibration curve (absorbance vs. concentration curve). The line equations obtained from these curves were used to calculate the released amounts of antibiotics in drug release experiments.

3.11.1 Calibration Curve for Vancomycin

To obtain a calibration curve for Vancomycin, various concentrations of Vancomycin were prepared in triple distilled water. UV-Vis spectrophotometer was used for absorbance measurements. It was found that Vancomycin has a maximum absorbance at 281 nm. Detection limits were found between 5 μg/ml and 500 μg/ml concentration. Two parallel sets were prepared and used for absorbance measurements to maintain accuracy.

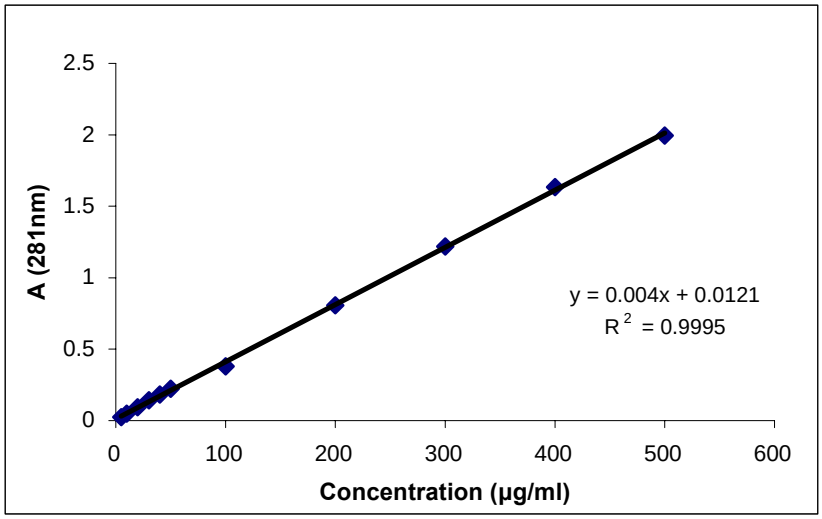

Figure 3.34 Calibration curve for Vancomycin (at 281 nm)

3.11.2 Calibration Curve for Alfoxil (Amoxicillin)

In the study for obtaining calibration curve for Alfoxil (amoxicillin), various concentrations of Alfoxil were prepared in PBS. UV-Vis spectrophotometer was used for absorbance measurements. It was found that Alfoxil has a maximum absorbance at 206 nm. Detection limits were found between 1 µg/ml and 25 µg/ml concentration. Two parallel sets were prepared and used for absorbance measurements to maintain accuracy.

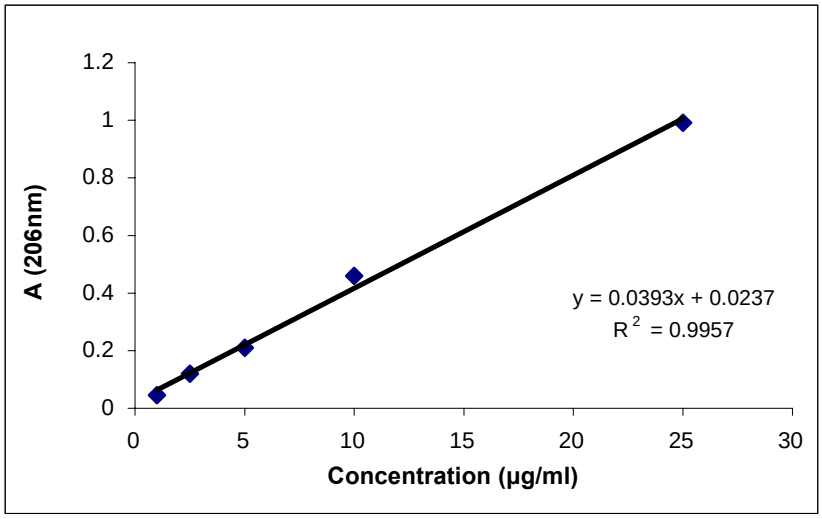

Figure 3.35 Calibration curve for Alfoxil (at 206 nm)

3.11.3 Calibration Curve for Augmentin (Amoxicillin)

In the study for obtaining calibration curve for Augmentin (amoxicillin), various concentrations of Augmentin were prepared in PBS. UV-Vis spectrophotometer was used for absorbance measurements. It was found that Augmentin has a maximum absorbance at 289 nm. Concentration range used was between 50 µg/ml and 1000 µg/ml. Two parallel sets were prepared and used for absorbance measurements to maintain accuracy.

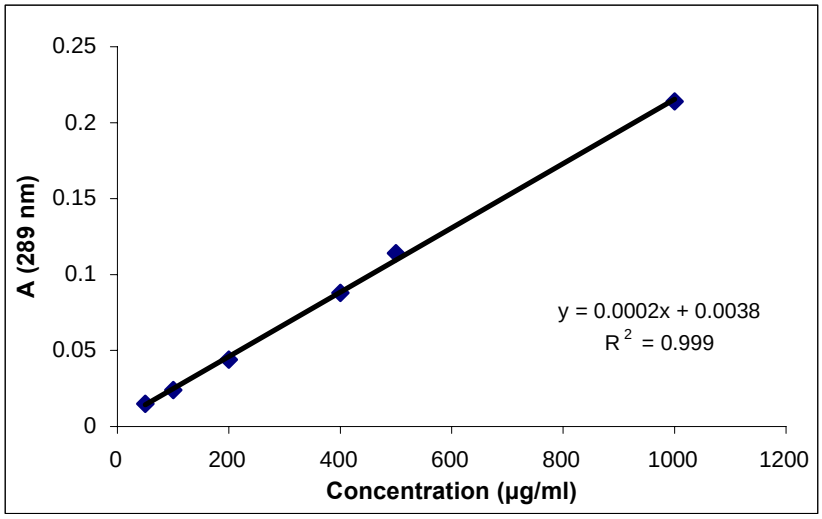

Figure 3.36 Calibration curve for Augmentin (at 289 nm)

3.11.4 Calibration Curve for Fortum (Ceftazidime)

In the study for obtaining calibration curve for Fortum (ceftazidime), various concentrations of Fortum were prepared in PBS. UV-Vis spectrophotometer was used for absorbance measurements. It was found that Fortum has a maximum absorbance at 208 nm and 256 nm. Concentration range used was between 2.5 µg/ml and 25 µg/ml. Two parallel sets were prepared and used for absorbance measurements to maintain accuracy.

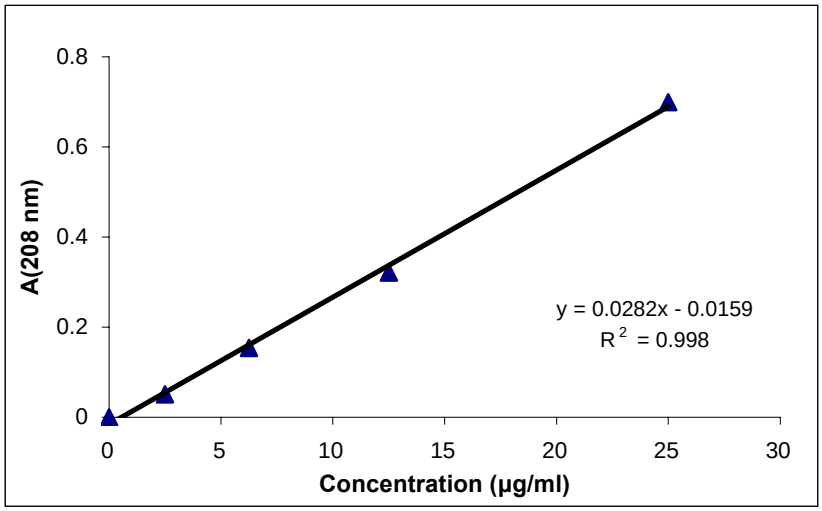

(a)

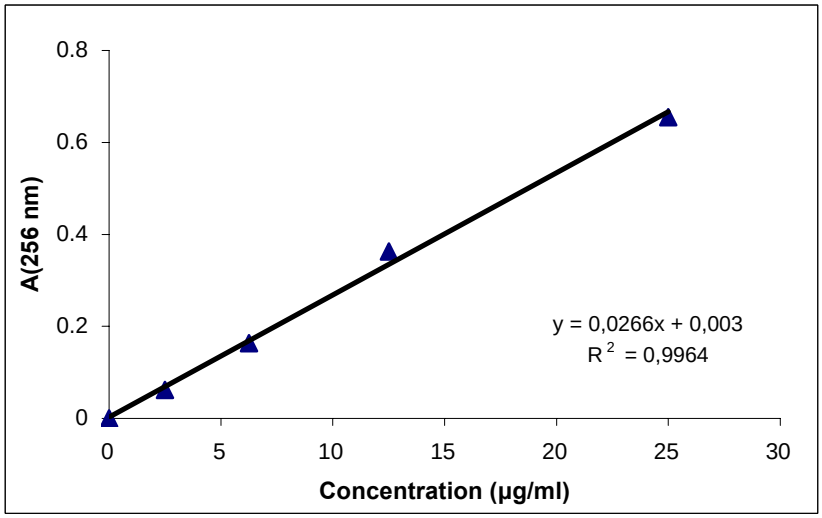

(b)

Figure 3.37 Calibration curves for Fortum a) at 208 nm, b) at 256 nm

3.11.5 Calibration Curve for Cefamezin (Cefazolin)

In the study for obtaining calibration curve for Cefamezin (cefazolin), various concentrations of Cefamezin were prepared in PBS. UV-Vis spectrophotometer was used for absorbance measurements. It was found that Cefamezin has a maximum absorbance at 289.5 nm. Concentration range used was between 10 µg/ml and 50 µg/ml. Two parallel sets were prepared and used for absorbance measurements to maintain accuracy.

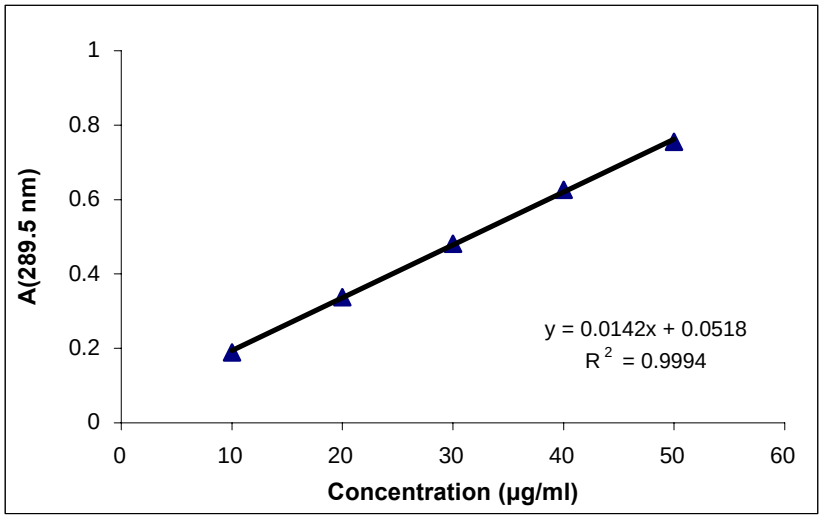

Figure 3.38 Calibration curve for Cefamezin (289.5 nm)

3.11.6 Calibration Curve for Rocephin (Ceftriaxone)

In the study for obtaining calibration curve for Rocephin (ceftriaxone), various concentrations of Rocephin were prepared in PBS. UV-Vis spectrophotometer was used for absorbance measurements. It was found that Cefamezin has a maximum absorbance at 290 nm. Concentration range used was between 10 µg/ml and 50 µg/ml. Two parallel sets were prepared and used for absorbance measurements to maintain accuracy.

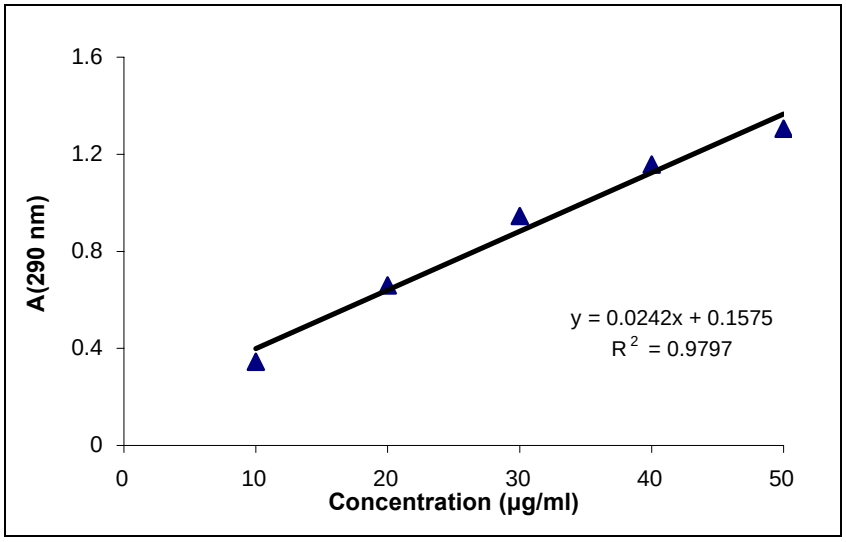

Figure 3.39 Calibration curve for Rocephin (at 290 nm)

3.12 Drug Release Studies

In these studies, drug containing polymers were used to coat different implant surfaces. In general, coated implants were immersed in the aqueous medium and at definite time intervals, some amount of solvent was taken out and its absorbance was measured or medium is completely refreshened and obtained solution was used for absorbance measurements. UV analyses were done on the aqueous samples and by using the calibration curves and equations, released drug concentrations and amounts could be calculated. Special features about metal surfaces and coating formulations will be given where needed in the following separate sections.

3.12.1 Drug Release Studies from Augmentin (Amoxicillin Derivative) Loaded Implants

15 ml solutions of 5% (w/v) poly(L-lactide) L 209S and 10% (w/v) poly(L-lactide-co-caprolactone) LC 703 were taken and 0.3 g of Augmentin was dispersed in each of the solutions. Cleaned (in a detergent-triple distilled water-0.1 M NaOH-

triple distilled water cycle) titanium plates (dimensions with 1 cm x 1 cm x 0.15 cm) were coated with these solutions and dried for 1 day in an oven held at 37^0C. Then, these plates were put into the UV cells with PBS and placed in an oven at 37^0C. Absorbance values at 289 nm were measured at predetermined time intervals. After 20 and 48 hours, solvent was freshened. For all the samples, no reliable absorbance values can be measured after 72 and 96 hours in refreshened solutions.

Table 3.16 Absorbance and drug releases for Augmentin loaded plates

Coating formulation	Coating Weight (g)	A (1h)	A (6h)	A* (20h)	A (24h)	A* (48h)	A (72h)	A (96h)
L209S +	0.0073	0.506	0.759	0.825	0.128	0.432	NA	NA
Augmentin	0.0085	0.496	0.758	0.856	0.208	0.737	0.043	NA
LC703 +	0.0070	0.335	0.507	0.657	0.225	0.688	NA	NA
Augmentin	0.0080	0.378	0.623	0.788	0.205	0.619	NA	NA

*After 20 and 48 hours, PBS was refreshened.

	Total Amount of Released Drug (g)						
Coating formulation	1 hour	6 hours	20 hours	24 hours	48 hours	72 hours	96 hours
L209S +	$2,5x10^{-3}$	$3,8x10^{-3}$	$4,1x10^{-3}$	$4,7x10^{-3}$	$6,2x10^{-3}$	NA	NA
Augmentin	$2,5x10^{-3}$	$3,8x10^{-3}$	$4,3x10^{-3}$	$5,3x10^{-3}$	$7,9x10^{-3}$	$8,1x10^{-3}$	NA
LC703 +	$1,7x10^{-3}$	$2,5x10^{-3}$	$3,3x10^{-3}$	$4,4x10^{-3}$	$6,7x10^{-3}$	NA	NA
Augmentin	$1,9x10^{-3}$	$3,1x10^{-3}$	$3,9x10^{-3}$	$4,9x10^{-3}$	$7,0x10^{-3}$	NA	NA

Fast releases of the drug were observed for all of the samples studied. Therefore, new approaches (such as multiple inert coatings) were applied in the following sections. Antibiotic releases are mostly completed in 2 day time period for all the samples.

3.12.2 Drug Release Studies from Alfoxil (Amoxicillin) Loaded Implants

3.12.2.1 Effect of Polymer Type on Drug Release

Polymer solutions were prepared in triple distilled water (for two kinds of PVOHs) and chloroform (for the other polymers) with magnetic stirrer. Then, 10 ml from these solutions were taken and Alfoxil was added to these solutions to be 10 % of the total weight (polymer+drug). Obtained suspensions were placed in ultrasonic stirrer for 4.5 hours to attain homogeneity. By using these suspensions, two kinds of titanium plates were coated. Plates with codes 1-6 were in the dimensions of 2x1x0.28 cm and surface modification was done according to ASTM D 2651-90 with orthophosphoric acid (aq) plus hydrofluoric acid (aq) (described in Section 3.4.4). Plates with codes 1A-6A were in the dimensions of 1x1x0.15 cm and no further surface modifications were done on these samples. These two different titanium plates can be seen in Figure 3.40. Coated samples were dried in an oven at 37 ^{0}C for 1 day and used in release experiments. All of the samples were placed in a 40 ml PBS solution and put in an oven held at 37 ^{0}C. At definite time intervals, 4 ml sample was taken and used for UV analysis. Samples were frozen until absorbance measurements. By using the calibration curve for Alfoxil, released drug concentrations can be calculated. Coating formulations, absorbance measurements, released drug concentrations and total release concentrations are given in Table 3.17, and 3.18. In the Figures 3.41 to 3.46, total released Alfoxil concentration with time graphs can be seen.

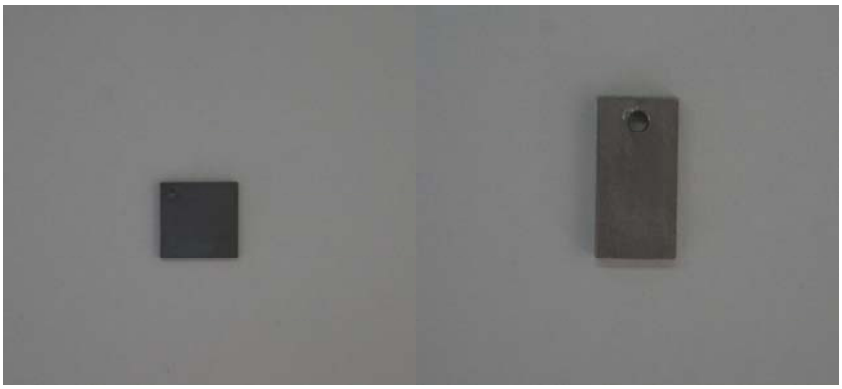

Figure 3.40 Titanium plates used for the experiments ("A-coded" sample on the left, "number-coded" sample on the right)

Table 3.17 Coating formulations and absorbance measurements on Alfoxil loaded titanium plates

Sample Code	Coating formulation	Coating weight (g)	A (1 day)	A (2 days)	A (1 week)	A (2 weeks)	A (4 weeks)	A (6 weeks)
1	10% (w/v) PVOH	0.0033	0.302	0.268	0.272	0.308	0.336	0.347
1A	(low Mwt) +Alfoxil	0.0016	0.312	0.227	0.235	0.261	0.229	0.236
2	10% (w/v) PVOH	0.0031	0.356	0.315	0.302	0.346	0.361	0.403
2A	(high Mwt) +Alfoxil	0.0028	0.245	0.238	0.253	0.293	0.302	0.288
3	10% (w/v) PCL +	0.0074	0.806	0.779	0.749	0.785	0.796	0.818
3A	Alfoxil	0.0029	0.298	0.282	0.306	0.343	0.612	0.385
4	10% (w/v) RG 504 +	0.0053	0.395	0.396	0.410	0.434	0.444	0.554
4A	Alfoxil	0.0026	0.168	0.146	0.163	0.220	0.194	0.242
5	10% (w/v) LC 703 +	0.0079	0.602	0.589	0.590	0.657	0.608	0.820
5A	Alfoxil	0.0041	0.335	0.332	0.342	0.397	0.366	0.428
6	5% (w/v) L 209S +	0.0047	0.354	0.335	0.343	0.407	0.381	0.441
6A	Alfoxil	0.0030	0.200	0.205	0.244	0.315	0.302	0.361

*Coating solutions were 10 ml and drugs were added to be 10% of the polymer matrix.

Table 3.18 Total released drug concentrations from Alfoxil loaded titanium plates

Sample Code	Polymer Type	Theoretical Drug Weight (mg)	Total Drug Concentration in PBS (µg/ml)					
			1 day	2 days	1 week	2 weeks	4 weeks	6 weeks
1	PVOH	0.33	7.09	6.31	6.39	7.02	7.46	7.60
1A	(low Mwt.)	0.16	7.34	5.40	5.56	6.02	5.53	5.62
2	PVOH	0.31	8.46	7.52	7.26	8.04	8.27	8.81
2A	(high Mwt.)	0.28	5.64	5.48	5.78	6.50	6.63	6.45
3	PCL	0.74	19.92	19.30	18.69	19.27	19.50	19.78
3A		0.29	6.98	7.30	7.11	7.77	11.88	8.99
4	RG 504	0.53	9.45	9.48	9.77	10.19	10.34	11.74
4A		0.26	3.67	3.17	3.52	4.53	4.14	4.75
5	LC 703	0.79	14.73	14.42	14.45	15.65	14.90	17.60
5A		0.41	7.93	7.86	8.07	9.05	8.57	9.36
6	L 209S	0.47	8.41	7.98	8.14	9.28	8.88	9.65
6A		0.30	4.49	4.61	5.40	6.67	6.47	7.22

* Total released drug concentrations are calculated for 40 ml solution medium.

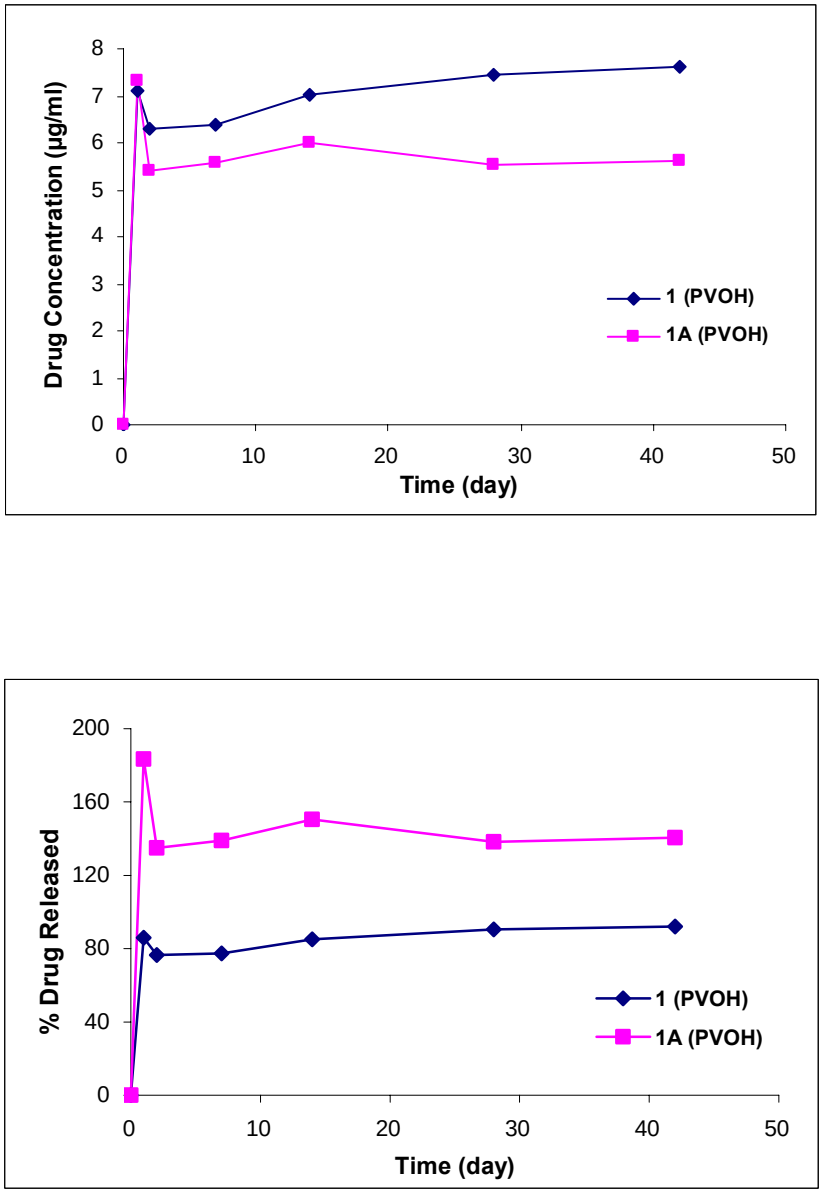

Figure 3.41 Alfoxil release and % release from PVOH (low molecular weight)

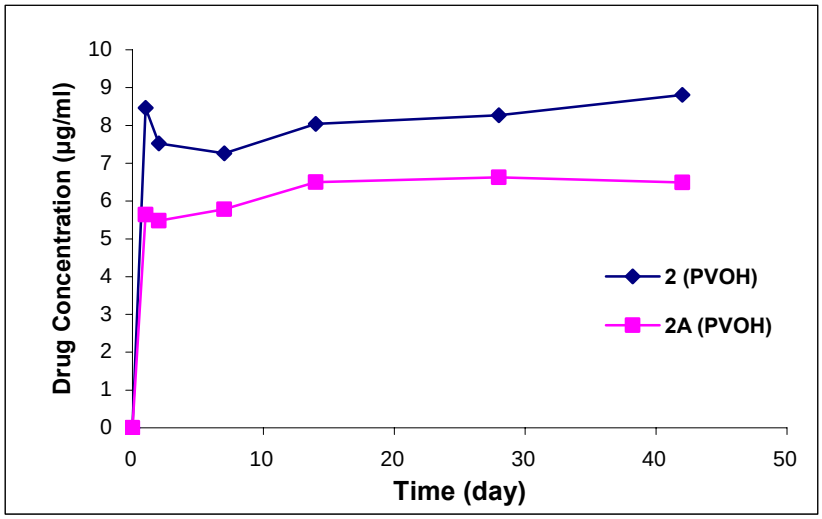

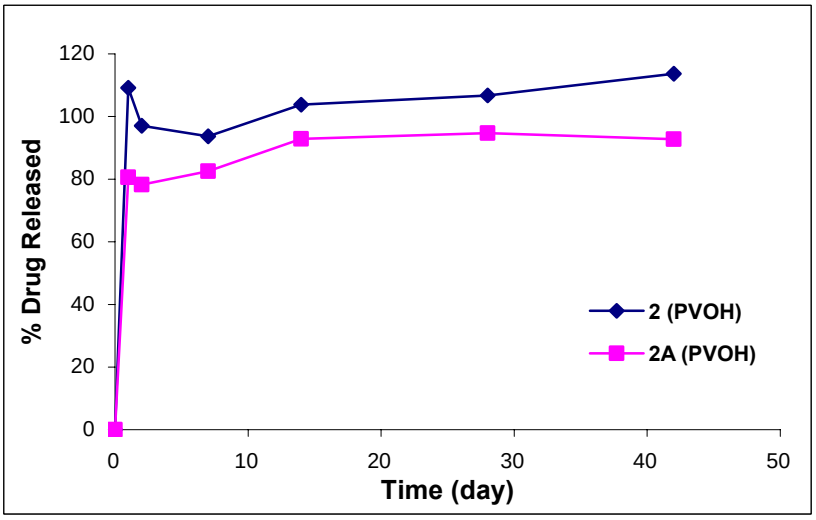

Figure 3.42 Alfoxil release and % release from PVOH (high molecular weight)

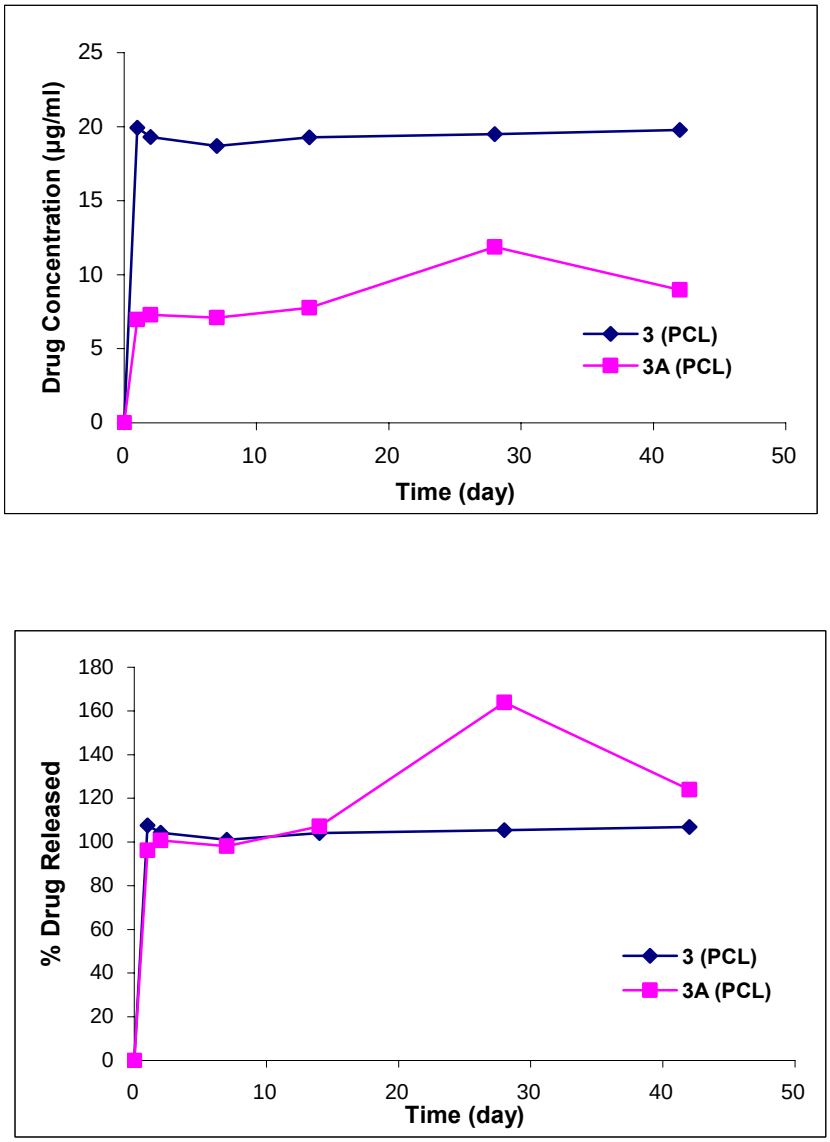

Figure 3.43 Alfoxil release and % release from Polycaprolactone

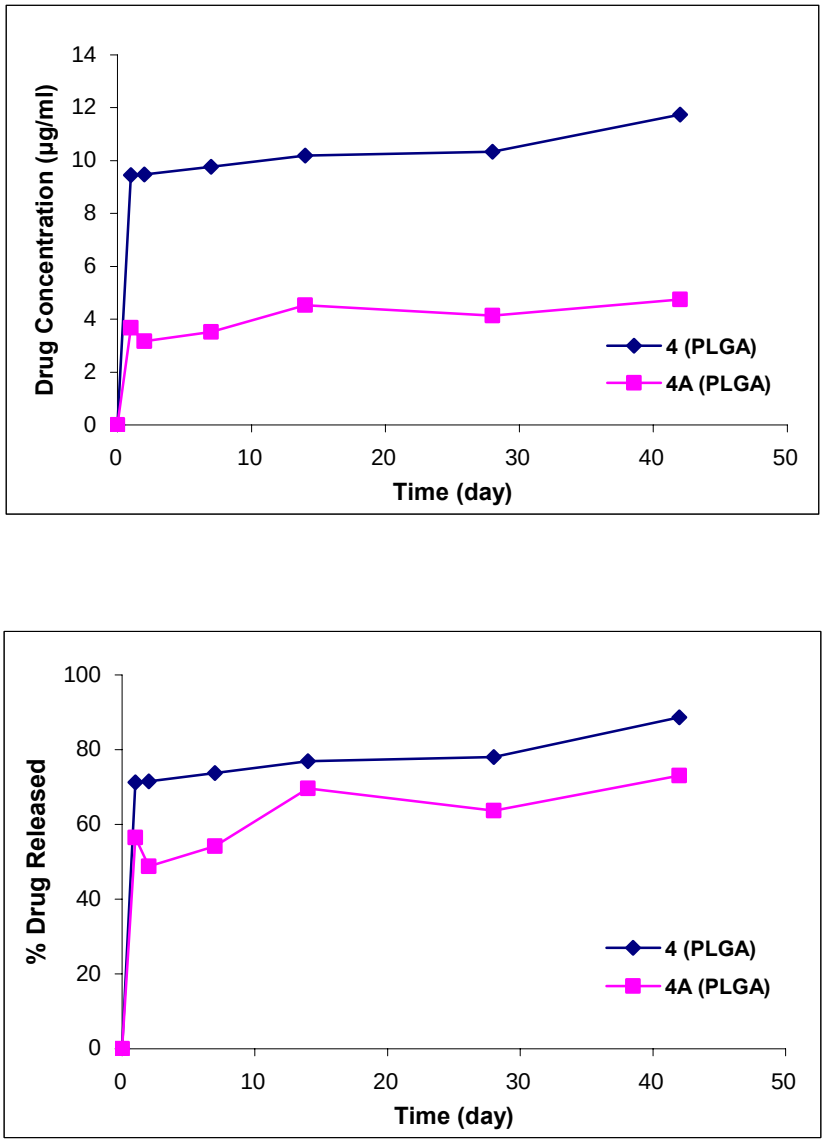

Figure 3.44 Alfoxil release and % release from PLGA RG 504

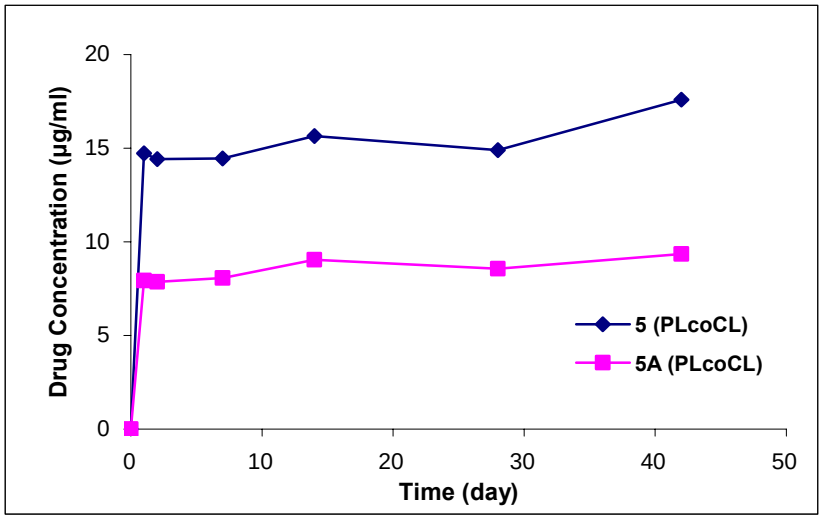

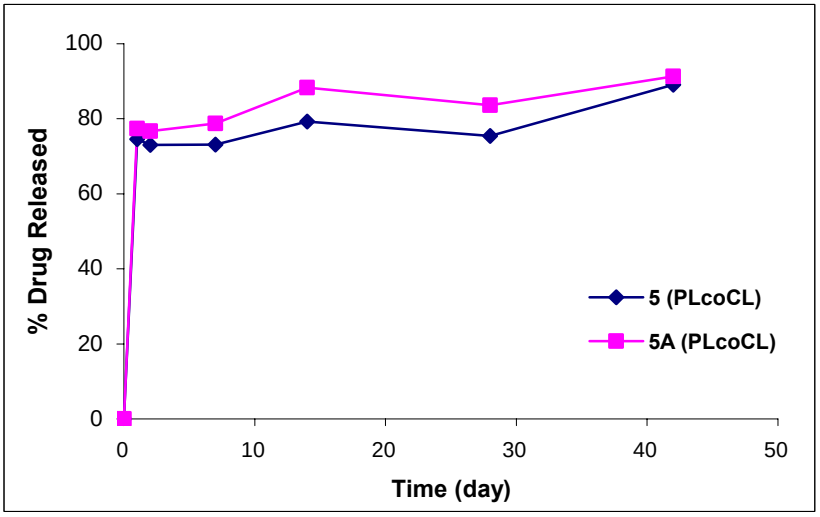

Figure 3.45 Alfoxil release and % release from poly(D,L-lactide-co-ε-caprolactone) LC 703

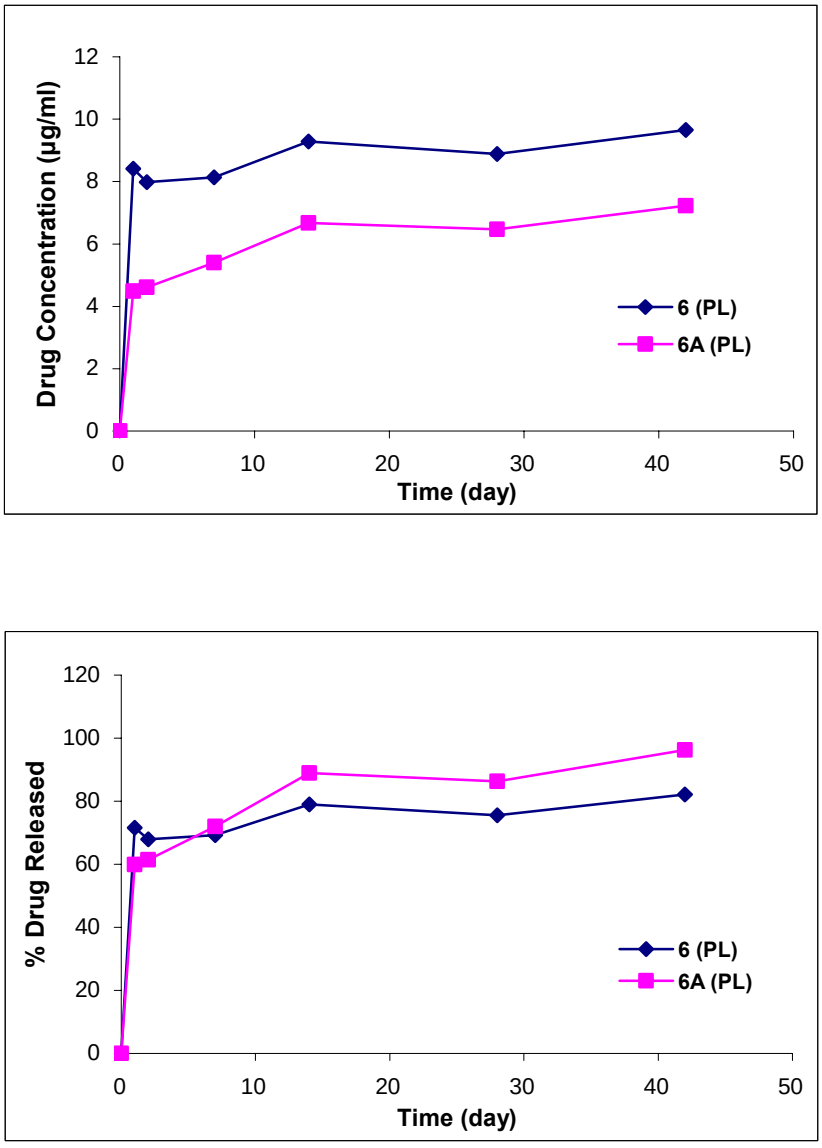

Figure 3.46 Alfoxil release and % release from Poly(L-lactide) L 209S

From the graphs and calculated released drug amounts, released drug percentages in one day release time were 85.9% for sample 1, 80.6% for sample 2A and 96.3% for sample 3A. For samples 1A, 2 and 3, released drug percentages exceeded the total theoretical amount of loaded drug. This may be due to inhomogeneous distribution of the antibiotic in the polymer phase. During drying of the polymer-film solution, homogeneity of the drugs can be lost due to unexpected

physical changes. On the remaining samples, the released drug percentages in one day release time decreased to 71.3% for sample 4, 56.5% for sample 4A, 74.6% for sample 5, 77.4% for sample 5A, 71.6% for sample 6 and 59.9% for sample 6A. Therefore, in general, it can be concluded that almost the entire drug was released in one day for homopolymers. On the other hand, for copolymers, drug releases continued in a very slow manner. At the end of 6 week drug release time, the released drug percentages increased to 88.6% for sample 4, 73.1% for sample 4A, 89.1% for sample 5, 91.3% for sample 5A, 82.1% for sample 6 and 96.3% for sample 6A. At the end of this section, it is found that preventing burst release of drugs could not be achieved by this method. Almost all of the loaded drugs were released in one day. The remainder of the drugs was not enough to maintain a feasible amount of release for antibiotic activity. Changes in the sample preparation were made to prevent burst release and achieve better controlled drug release implant models. These changes are the introduction of inert coating on the polymer+drug composite and use of tricalcium phosphate (TCP) as drug carrier is explained in the forthcoming sections.

3.12.2.2 Drug Release Studies from Inert Coating Applied Implants

To solve the burst release problem faced in the previous section, inert coatings applied over the drug containing polymer layer. 10% (w/v) PLGA RG 504 solution was prepared in chloroform and Alfoxil drug was added to this solution that the final weight of it was 10% of the total weight (polymer+drug). Obtained suspension was placed in ultrasonic stirrer for 4.5 hours to achieve homogeneity. By using this drug dispersed suspension, titanium plates were coated once. Then 1, 2 and 4 layers of 10% (w/v) RG 504 coatings (without drug) were applied to the titanium plates to prevent the burst release of drug from implant samples. Before each coating layer applied, samples were dried in an oven held at 37^0C. Then, these samples were put into the 20 ml PBS containing closed glass vessels. The drug release experiments were carried out in an oven held at 37^0C. At predetermined time intervals, samples were taken out from the vessels and placed in fresh PBS containing ones. The UV

measurements were done on the PBS solutions to find out the released drug amounts.

Table 3.19 Absorbance measurements and released drug concentrations for Alfoxil loaded titanium implant samples (inert coating applied)

Sample Code	A (6 h)	A (1 day)	A (2 days)	A (1 week)	A (2 weeks)	A (4 weeks)
1 layer	0.677	0.538	0.151	1.167	0.329	1.874
2 layers	0.262	0.492	0.382	1.097	0.347	0.569
4 layers	0.227	0.317	0.346	0.329	0.235	1.744

Sample Code	Total Drug Concentration in PBS (µg/ml)					
	6 h	**1 day**	**2 days**	**1 week**	**2 weeks**	**4 weeks**
1 layer	16.64	29.74	32.98	62.09	69.86	116.97
2 layers	6.07	17.99	27.11	54.44	62.67	76.56
4 layers	5.18	12.65	20.86	28.63	34.01	77.81

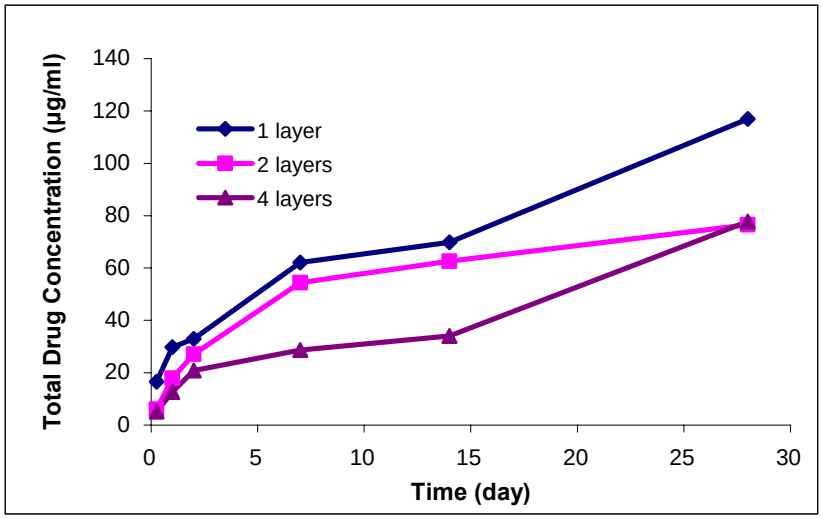

Figure 3.47 Effect of inert coatings on Alfoxil release

As a result of these studies, promising improvements were achieved. The slower rate of drug release and therefore managing the burst release at initial times was achieved. Also, with increasing the number of inert coatings, drug release

profiles seemed to be much more controllable and long-lasting. With these promising results, further and much more detailed studies on inert coating applications were performed.

In the following studies on inert coating applications, firstly, the sandblasted titanium plates were rinsed with detergent-DI water-acetone-DI water cycle and dried in an oven. Polymer PLGA RG 504 was dissolved in chloroform to be 10% (w/v). Alfoxil, as a drug, was dispersed in the polymer solution to obtain 10% (w/w) drug content with respect to the dissolved polymer. The suspension was placed in ultrasonic stirrer for 4.5 hours to achieve homogeneity. Titanium plate used in this study (dimensions 1.5 cm x 1.5 cm x 0.25 cm) can be seen in Figure 3.48.

Figure 3.48 Titanium plate used for inert coating applications ("Y-coded" sample)

The first coating layers for all samples studied were done with drug containing solutions. The samples were dried in an oven at 37^0C and inert coatings were applied by using the RG 504 solution which contains no drug in it. The samples were coated with 0, 1, 2, and 4 inert coatings. Before each coating layer applied, samples were dried in an oven held at 37^0C. Two samples were studied for each kind of application. Samples 1Y-2Y have single inert PLGA layer, 3Y-4Y have 2 inert PLGA layers, 5Y-6Y have 4 inert layers and 7Y-8Y have no inert layers. Total weight, coating weight and theoretical loaded drug weight measurements are given in

the Table 3.20 and 3.21.

Table 3.20 Sample weights for inert coating applications (RG 504+Alfoxil)

Sample Code	W_0(g)	W_1(g)	W_2(g)	W_3(g)	W_4(g)
1Y	1.8598	1.8640	1.8710	-	-
2Y	1.8938	1.8984	1.9049	-	-
3Y	1.8786	1.8833	1.8900	1.8974	-
4Y	1.8589	1.8632	1.8700	1.8791	-
5Y	1.8534	1.8584	1.8654	1.8746	1.8842
6Y	1.8538	1.8588	1.8670	1.8759	1.8873
7Y (control)	1.8960	1.9001	-	-	-
8Y	1.8696	1.8741	-	-	-

* W_0 stands for weight of titanium plate
W_1 stands for weight of a plate+drug containing coating layer
W_2 stands for weight of W_1+1 inert coating layer
W_3 stands for weight of W_1+2 inert coating layers
W_4 stands for weight of W_1+4 inert coating layers

Table 3.21 Coating weights and theoretical drug weight for inert coating applications (RG 504+Alfoxil)

Sample Code	Coating Weight (mg)				Theoretical Drug Weight (mg)
	1st	2nd	3rd	4th	
1Y	4.2	7.0	-	-	0.42
2Y	4.6	6.5	-	-	0.46
3Y	4.7	6.7	7.4	-	0.47
4Y	4.3	6.8	9.1	-	0.43
5Y	5.0	7.0	9.2	9.6	0.50
6Y	5.0	8.2	8.9	11.4	0.50
7Y (control)	4.1	-	-	-	0.41
8Y	4.5	-	-	-	0.45

All the samples were put into the 20 ml PBS containing closed glass vessels. The drug release experiments were carried out in an oven held at 37^0C. At predetermined time intervals (5 hours, 1, 2, 7, 14, 28, and 42 days), samples were taken out from the vessels and placed in a fresh PBS containing ones (pH 7.4). Absorbance values were measured at 206 nm to determine the amount of drug released at each time interval. The absorbance values and corresponding amount of drugs released are given in Table 3.22 and 3.23.

Table 3.22 Absorbance measurements (RG 504+Alfoxil)

Sample Code	**Absorbance (206 nm)**						
	5 h	**1 day**	**2 days**	**7 days**	**14 days**	**28 days**	**42 days**
1Y	0.207	0.385	0.321	0.509	0.183	0.609	1.201
2Y	0.427	0.382	0.293	0.408	0.283	0.419	1.180
3Y	0.293	0.540	0.366	0.375	0.200	0.468	0.821
4Y	0.395	0.207	0.961	0.768	0.238	0.438	1.327
5Y	0.296	0.737	0.179	0.386	0.157	0.928	1.894
6Y	0.355	0.423	0.435	0.259	0.257	0.893	1.528
7Y (control)	-	-	-	-	-	-	1.436
8Y	0.791	0.354	0.256	0.148	0.177	0.281	0.225

Table 3.23 Released drug concentrations (RG 504+Alfoxil)

Sample Code	**Drug Concentration in PBS (µg/ml)**						
	5 h	**1 day**	**2 days**	**7 days**	**14 days**	**28 days**	**42 days**
1Y	4.67	9.20	7.57	12.36	4.06	14.90	29.98
2Y	10.27	9.12	6.86	9.79	6.60	10.07	29.44
3Y	6.86	13.15	8.72	8.95	4.49	11.31	20.30
4Y	9.46	4.67	23.87	18.95	5.46	10.55	33.19
5Y	6.93	18.16	3.95	9.23	3.39	23.03	47.62
6Y	8.44	10.17	10.47	5.99	5.94	22.14	38.31
7Y (control)	-	-	-	-	-	-	35.96
8Y	19.54	8.41	5.92	3.17	3.90	6.55	5.13

Total drug release profiles of all kinds of samples can be seen in Figure 3.49, 3.50, 3.51 and 3.52.

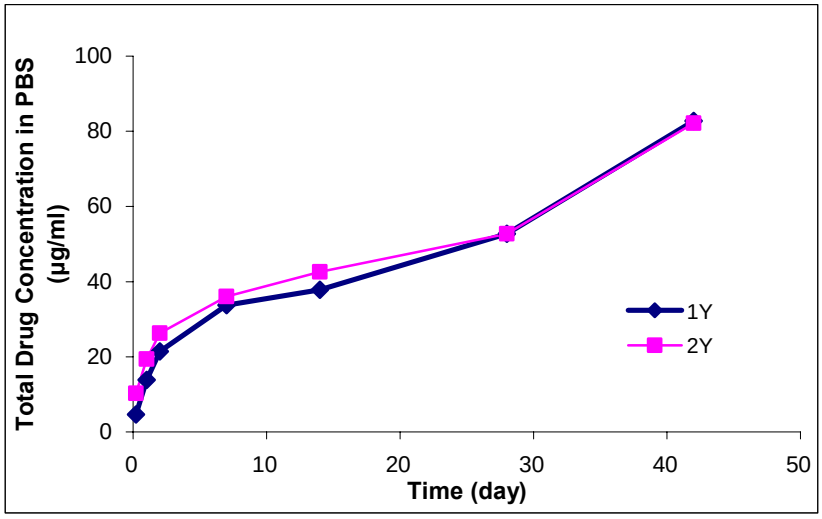

Figure 3.49 Alfoxil release profiles for samples 1Y and 2Y

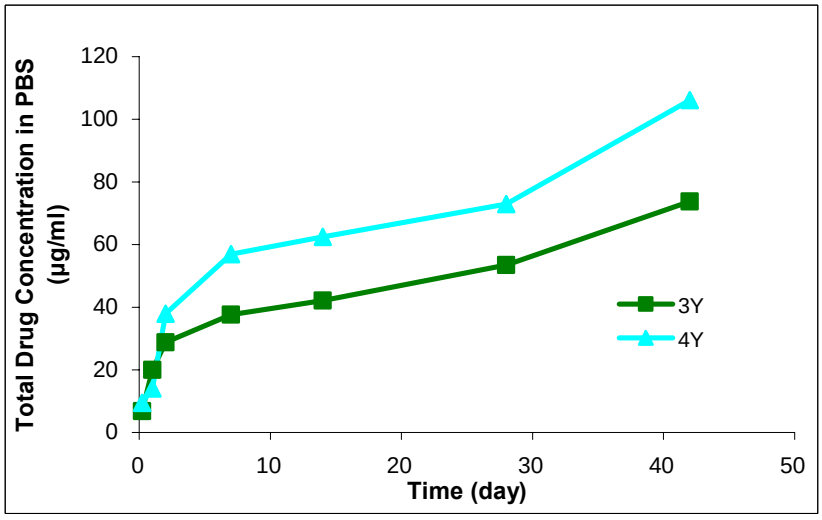

Figure 3.50 Alfoxil release profiles for samples 3Y and 4Y

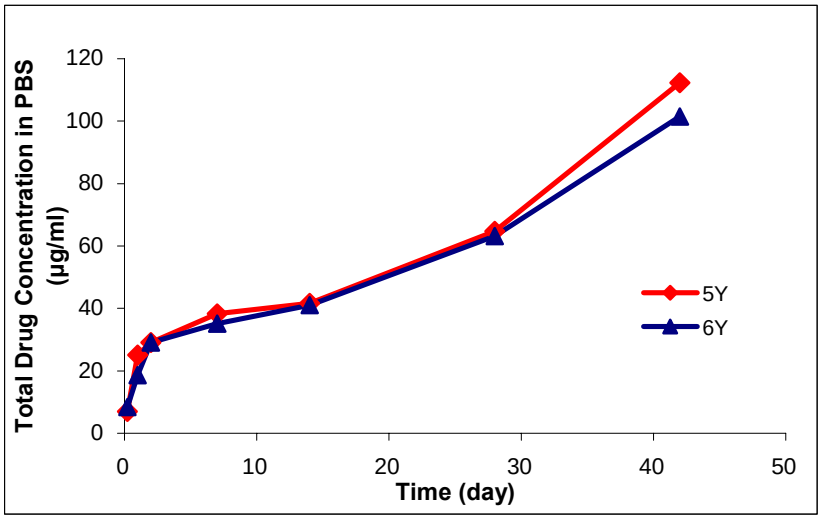

Figure 3.51 Alfoxil release profiles for samples 5Y and 6Y

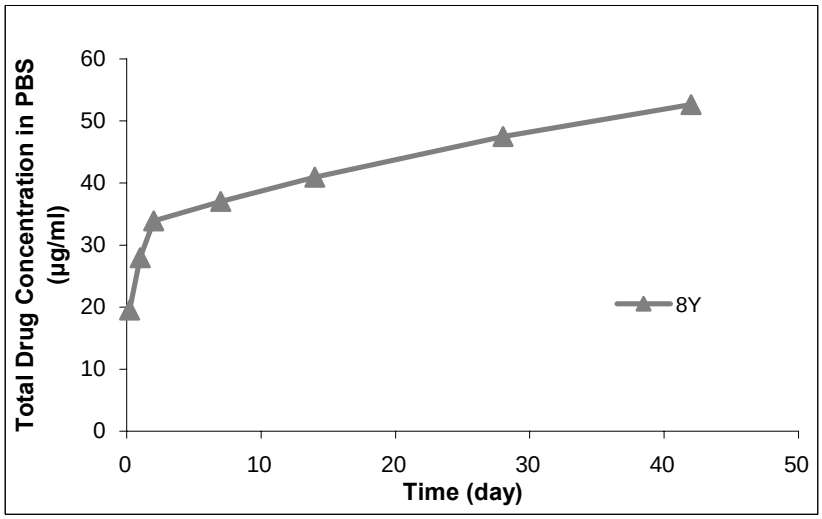

Figure 3.52 Alfoxil release profile for sample 8Y

According to the results obtained, improved controlled releases could be achieved by the application of inert coatings on the implant samples. Sample 8Y with no inert coating show burst release initially. With the application of inert coatings, burst release was reduced and a remarkable amount of drug releases in the following weeks were observed. The control sample (7Y) released lesser amount of drug than

the other samples in 42 day release period which may be a result for not changing the PBS with fresh ones. Diffusion of the drug from the polymer matrix was possibly reduced. There are some points that need careful consideration. Firstly, multiple coatings should be applied in a fast manner to prevent the dissolution of the previous coating layers. Secondly, total released amount of the drugs was higher than the theoretical loadings. Since drug is suspended in the polymer solution, actual loaded amounts may differ from the theoretical values. Drug particles possibly prefer to attach to the surface of titanium implant samples during the coating applications. Also, polymer degradation products had a contribution to the absorbance measurements at that wavelength. Therefore, for Alfoxil loaded samples much more precise experimental detection techniques, such as High Performance Liquid Chromatography (HPLC) with suitable columns should be applied.

3.12.3 Drug Release Studies from Fortum (Ceftazidime) Loaded Implants

3.12.3.1 Drug Release Studies from Inert Coating Applied Implants

10% (w/v) PLGA RG 504 solution was prepared in chloroform and Fortum drug was added to this solution to have 10% of the total polymer comprising Fortum weight. The suspension was placed in ultrasonic stirrer for 4.5 hours to achieve homogeneity. Two kinds of sandblasted titanium plates (dimensions 1.5 cm x 1.5 cm x 0.25 cm) were used for this part that can be seen in Figure 3.53. These implant samples were cleaned with the same cleaning cycle as described before prior to the coating applications. By using the drug dispersed suspension, titanium plates were coated once. Then 1, 2 and 4 layers of 10% (w/v) RG 504 coatings (without drug) were applied to the titanium plates to prevent the burst release of drug from implant samples. Before each coating layer application, samples were dried in an oven held at 37^0C. Then, these samples were put into the 20 ml PBS containing closed glass vessels. The drug release experiments were carried out in an oven held at 37^0C. At predetermined time intervals, samples were taken out from the vessels and placed in

fresh PBS containing ones. The UV measurements were done on the PBS solutions to find out the released drug amounts. For each kind of specimen, 4 different samples were prepared. Two of the samples were used for drug release studies and the other two were used for microbial tests. Total sample weights for both kinds of specimens at each coating application are given in Table 3.24 and 3.26. Coating weights and theoretical loaded drug weights are given in Table 3.25 and 3.27.

Figure 3.53 Titanium plates used for the experiments ("A-coded" sample on the left, "S-coded" sample on the right)

Table 3.24 Sample weights with coatings for specimen A

Sample Code	W_0(g)	W_1(g)	W_2(g)	W_3(g)	W_4(g)
1A	2.0086	2.0120	2.0165	2.0240	2.0418
2A	2.0066	2.0102	2.0139	2.0209	2.0380
3A	1.9699	1.9740	1.9786	1.9873	2.0039
4A	1.9593	1.9635	1.9678	1.9747	1.9925
5A	2.0228	2.0272	2.0322	2.0408	-
6A	1.9825	1.9868	1.9923	2.0018	-
7A	1.9708	1.9765	1.9816	1.9896	-
8A	2.0209	2.0249	2.0291	2.0366	-
9A	2.0090	2.0129	2.0181	-	-
10A	2.0062	2.0104	2.0150	-	-
11A	1.9447	1.9490	1.9535	-	-
12A	1.9784	1.9823	1.9870	-	-
13A	2.0229	2.0275	-	-	-
14A	1.9726	1.9770	-	-	-
15A	2.0162	2.0210	-	-	-
16A	2.0081	2.0138	-	-	-

* W_0 stands for weight of titanium plate
W_1 stands for weight of a plate+drug containing coating layer
W_2 stands for weight of W_1+1 inert coating layer
W_3 stands for weight of W_1+2 inert coating layers
W_4 stands for weight of W_1+4 inert coating layers

Table 3.25 Coating weights and theoretical drug weights for specimen A

Sample Code	Coating Weight (mg)				Theoretical Drug Weight (mg)
	1st	2nd	3rd	4th	
1A	3.4	4.5	7.5	17.8	0.34
2A	3.6	3.7	7.0	17.1	0.36
3A	4.1	4.6	8.7	16.6	0.41
4A	4.2	4.3	6.9	17.8	0.42
5A	4.4	5.0	8.6	-	0.44
6A	4.3	5.5	9.5	-	0.43
7A	5.7	5.1	8.0	-	0.57
8A	4.0	4.2	7.5	-	0.40
9A	3.9	5.2	-	-	0.39
10A	4.2	4.6	-	-	0.42
11A	4.3	4.5	-	-	0.43
12A	3.9	4.7	-	-	0.39
13A	4.6	-	-	-	0.46
14A	4.4	-	-	-	0.44
15A	4.8	-	-	-	0.48
16A	5.7	-	-	-	0.57

Table 3.26 Sample weights with coatings for specimen S

Sample Code	W_0(g)	W_1(g)	W_2(g)	W_3(g)	W_4(g)
1S	2.0949	2.1007	-	-	-
2S	2.1329	2.1386	-	-	-
3S	2.0038	2.0094	2.0172	-	-
4S	2.0262	2.0315	2.0387	-	-
5S	2.0379	2.0441	2.0525	2.0599	-
6S	2.0959	2.1017	2.1093	2.1169	-
7S	2.0802	2.0862	2.0944	2.1021	2.1246
8S	2.1293	2.1358	2.1432	2.1508	2.1757
9S	2.0446	2.0512	2.0583	2.0652	2.0862
10S	2.0891	2.0958	2.1034	2.1111	2.1328
11S	1.9750	1.9801	1.9864	1.9929	-
12S	2.0740	2.0806	2.0882	2.0969	-
13S	2.0648	2.0710	2.0777	-	-
14S	2.0809	2.0868	2.0930	-	-
15S	2.0641	2.0708	-	-	-
16S	2.1706	2.1764	-	-	-

* W_0 stands for weight of titanium plate
W_1 stands for weight of a plate+drug containing coating layer
W_2 stands for weight of W_1+1 inert coating layer
W_3 stands for weight of W_1+2 inert coating layers
W_4 stands for weight of W_1+4 inert coating layers

Table 3.27 Coating weights and theoretical drug weights for specimen S

Sample Code	Coating Weight (mg)				Theoretical Drug Weight (mg)
	1st	2nd	3rd	4th	
1S	5.8	-	-	-	0.58
2S	5.7	-	-	-	0.57
3S	5.6	7.8	-	-	0.56
4S	5.3	7.2	-	-	0.53
5S	6.2	8.4	7.4	-	0.62
6S	5.8	7.6	7.6	-	0.58
7S	6.0	8.2	7.7	22.5	0.60
8S	6.5	7.4	7.6	24.9	0.65
9S	6.6	7.1	6.9	21.0	0.66
10S	6.7	7.6	7.7	21.7	0.67
11S	5.1	6.3	6.5	-	0.51
12S	6.6	7.6	8.7	-	0.66
13S	6.2	6.7	-	-	0.62
14S	5.9	6.2	-	-	0.59
15S	6.7	-	-	-	0.67
16S	5.8	-	-	-	0.58

All the samples were put into the 20 ml PBS containing closed glass vessels. The drug release experiments were carried out in an oven held at 37^0C. At predetermined time intervals (5 hours, 1, 2, 7, 14, 28, and 42 days), samples were taken out from the vessels and placed in a fresh PBS containing ones (pH 7.4). Absorbance values were measured at 208 nm and 256 nm to determine the amount of drug released at each time interval. The absorbance values are given in Table 3.28 and 3.29.

Table 3.28 Absorbance measurements for specimen A (RG 504+Fortum)

Sample Code	Absorbance (208 nm)					
	5 h	**1 day**	**2 days**	**14 days**	**28 days**	**42 days**
3A	0.215	0.505	0.583	0.459	1.817	2.080
4A	0.333	0.292	0.525	0.900	1.418	1.891
7A	0.523	0.404	0.378	0.722	1.447	2.378
8A	0.362	0.383	0.253	0.643	1.655	1.806
11A	0.677	0.631	0.726	1.372	1.169	1.375
12A	0.536	0.518	0.171	1.519	1.392	0.550
15A	1.265	0.468	0.729	1.170	0.870	1.589
16A(control)	-	-	-	-	-	NA

Sample Code	Absorbance (256 nm)					
	5 h	**1 day**	**2 days**	**14 days**	**28 days**	**42 days**
3A	0.073	0.176	0.150	0.195	0.273	0.303
4A	0.118	0.118	0.133	0.285	0.177	0.265
7A	0.288	0.178	0.135	0.337	0.279	0.446
8A	0.183	0.139	0.074	0.205	0.347	0.318
11A	0.376	0.207	0.230	0.358	0.272	0.289
12A	0.313	0.191	0.048	0.355	0.305	0.083
15A	0.956	0.186	0.182	0.243	0.191	0.319
16A(control)	-	-	-	-	-	1.438

Table 3.29 Absorbance measurements for specimen S (RG 504+Fortum)

Sample Code	Absorbance (208 nm)					
	5 h	**1 day**	**2 days**	**14 days**	**28 days**	**42 days**
9S	0.381	0.869	1.227	0.667	1.321	1.218
10S	0.417	0.918	0.686	0.984	2.241	1.738
11S	0.590	0.327	0.252	0.957	1.134	2.195
12S	0.401	0.739	0.442	2.057	0.917	2.041
13S	0.678	0.437	0.173	0.449	0.651	1.458
14S	0.683	0.450	0.433	0.471	0.371	1.732
15S	1.108	0.391	0.247	1.273	0.907	1.443
16S(control)	-	-	-	-	-	1.734

Table 3.29 Cont'd.

Sample Code	Absorbance (256 nm)					
	5 h	**1 day**	**2 days**	**14 days**	**28 days**	**42 days**
9S	0.130	0.349	0.382	0.310	0.157	0.079
10S	0.147	0.371	0.266	0.406	0.432	0.131
11S	0.232	0.182	0.134	0.322	0.195	0.411
12S	0.210	0.280	0.184	0.635	0.141	0.361
13S	0.470	0.223	0.088	0.139	0.119	0.322
14S	0.429	0.234	0.145	0.143	0.087	0.346
15S	0.859	0.164	0.057	0.256	0.209	0.301
16S(control)	-	-	-	-	-	0.761

Drug concentrations related to this absorbance values are given in Table 3.30 and 3.31.

Table 3.30 Released drug concentrations for specimen A (RG 504+Fortum)

Sample Code	Drug Concentration in PBS (µg/ml) (208 nm)					
	5 h	**1 day**	**2 days**	**14 days**	**28 days**	**42 days**
3A	8.19	18.47	21.24	16.84	65.00	74.32
4A	12.37	10.92	19.18	32.48	50.85	67.62
7A	19.11	14.89	13.97	26.17	51.88	84.89
8A	13.40	14.15	9.54	23.37	59.25	64.61
11A	24.57	22.94	26.31	49.22	42.02	49.32
12A	19.57	18.93	6.63	54.43	49.93	20.07
15A	45.42	17.16	26.41	42.05	31.41	56.91
16A(control)	-	-	-	-	-	NA

Table 3.30 Cont'd.

Sample Code	Drug Concentration in PBS (µg/ml) (256 nm)					
	5 h	**1 day**	**2 days**	**14 days**	**28 days**	**42 days**
3A	2.63	6.50	5.53	7.22	10.15	11.27
4A	4.32	4.32	4.89	10.60	6.54	9.85
7A	10.71	6.58	4.96	12.56	10.38	16.65
8A	6.77	5.11	2.67	7.59	12.93	11.84
11A	14.02	7.67	8.53	13.35	10.11	10.75
12A	11.65	7.07	1.69	13.23	11.35	3.01
15A	35.83	6.88	6.73	9.02	7.07	11.88
16A(control)	-	-	-	-	-	53.95

Table 3.31 Released drug concentrations for specimen S (RG 504+Fortum)

Sample Code	Drug Concentration in PBS (µg/ml) (208 nm)					
	5 h	**1 day**	**2 days**	**14 days**	**28 days**	**42 days**
9S	14.07	31.38	44.07	24.22	47.41	43.76
10S	15.35	33.12	24.89	35.46	80.03	62.20
11S	21.49	12.16	9.50	34.50	40.78	78.40
12S	14.78	26.77	16.24	73.51	33.08	72.94
13S	24.61	16.06	6.70	16.49	23.65	52.27
14S	24.78	16.52	15.92	17.27	13.72	61.98
15S	39.85	14.43	9.32	45.71	32.73	51.73
16S(control)	-	-	-	-	-	62.05

Sample Code	Drug Concentration in PBS (µg/ml) (256 nm)					
	5 h	**1 day**	**2 days**	**14 days**	**28 days**	**42 days**
9S	4.77	13.01	14.25	11.54	5.79	2.86
10S	5.41	13.83	9.89	15.15	16.13	4.81
11S	8.61	6.73	4.92	11.99	4.96	15.34
12S	7.78	10.41	6.80	23.76	5.19	13.46
13S	17.56	8.27	3.20	5.11	4.36	11.99
14S	16.02	8.68	5.34	5.26	3.16	12.89
15S	32.18	6.05	2.03	9.51	7.74	11.20
16S(control)	-	-	-	-	-	28.50

Drug release profiles for all of the samples studied in this section can be seen in the Figure 3.54 to 3.77.

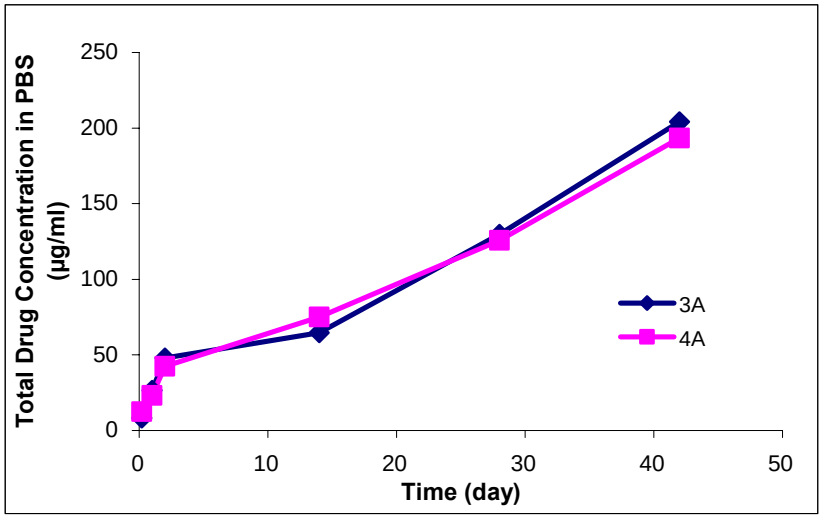

Figure 3.54 Fortum release profiles for samples 3A and 4A (208 nm)

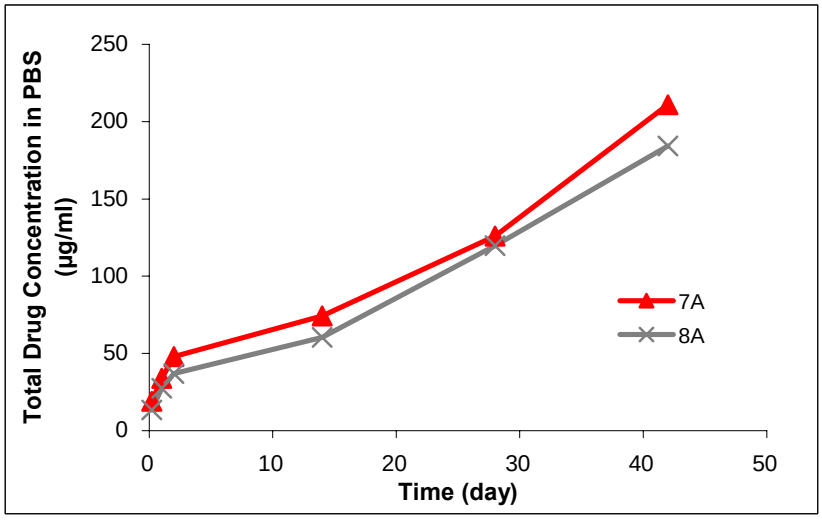

Figure 3.55 Fortum release profiles for samples 7A and 8A (208 nm)

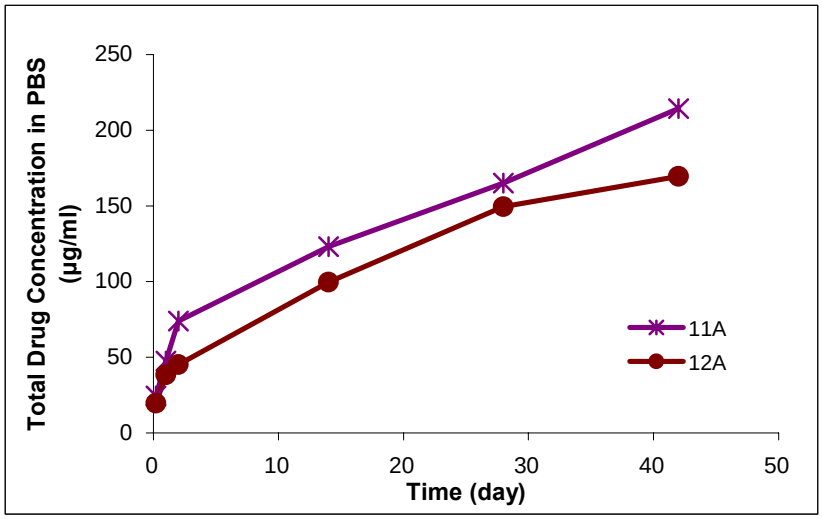

Figure 3.56 Fortum release profiles for samples 11A and 12A (208 nm)

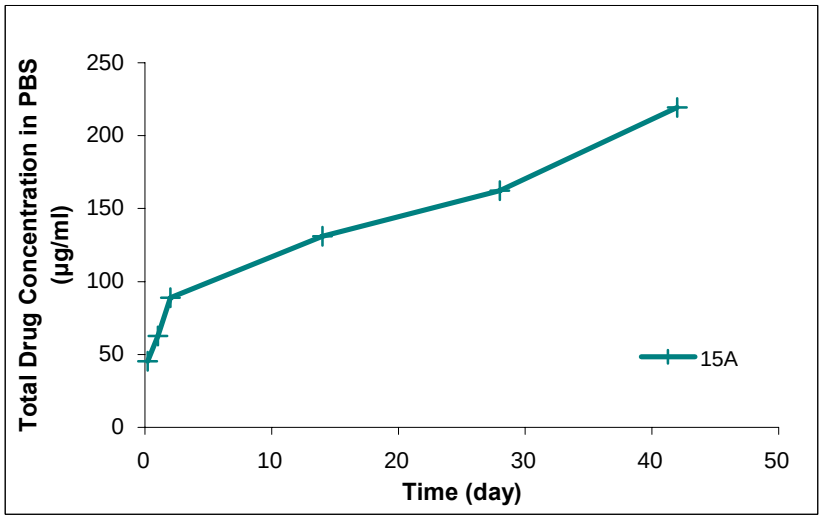

Figure 3.57 Fortum release profile for sample 15A (208 nm)

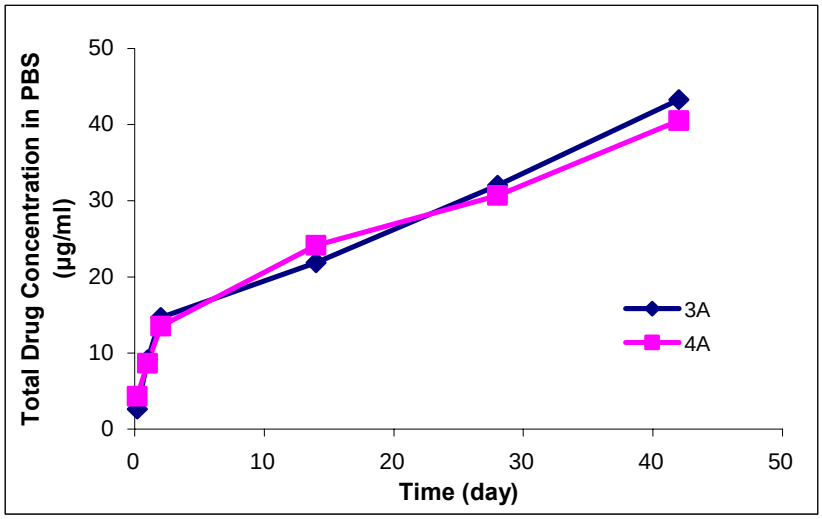

Figure 3.58 Fortum release profiles for samples 3A and 4A (256 nm)

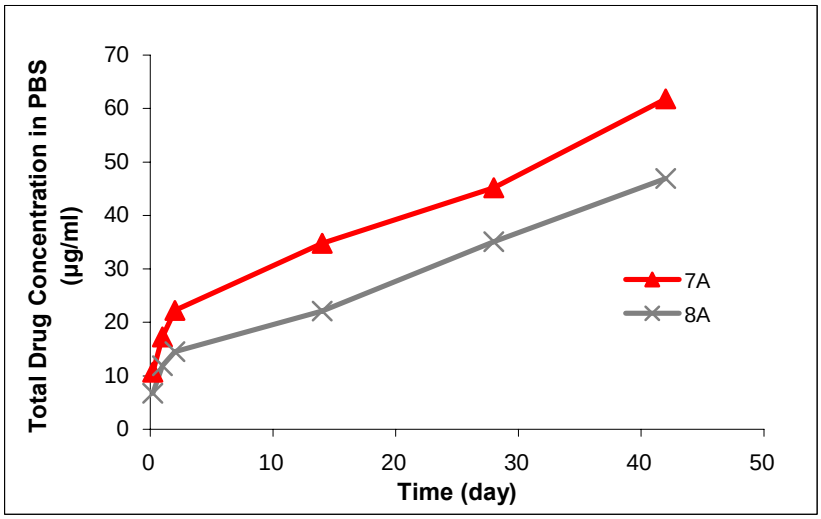

Figure 3.59 Fortum release profiles for samples 7A and 8A (256 nm)

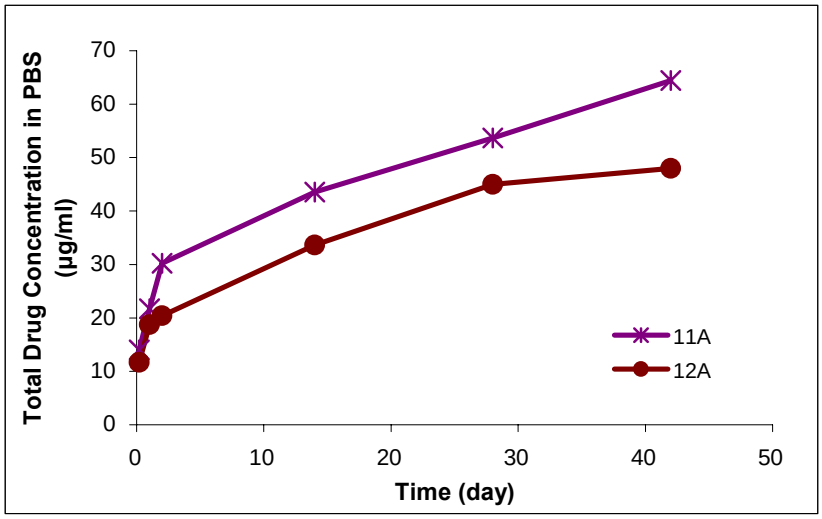

Figure 3.60 Fortum release profiles for samples 11A and 12A (256 nm)

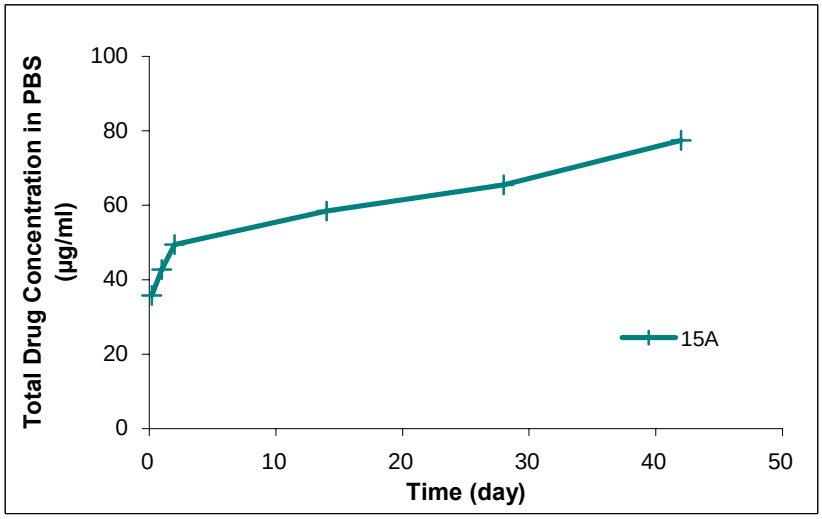

Figure 3.61 Fortum release profile for sample 15A (256 nm)

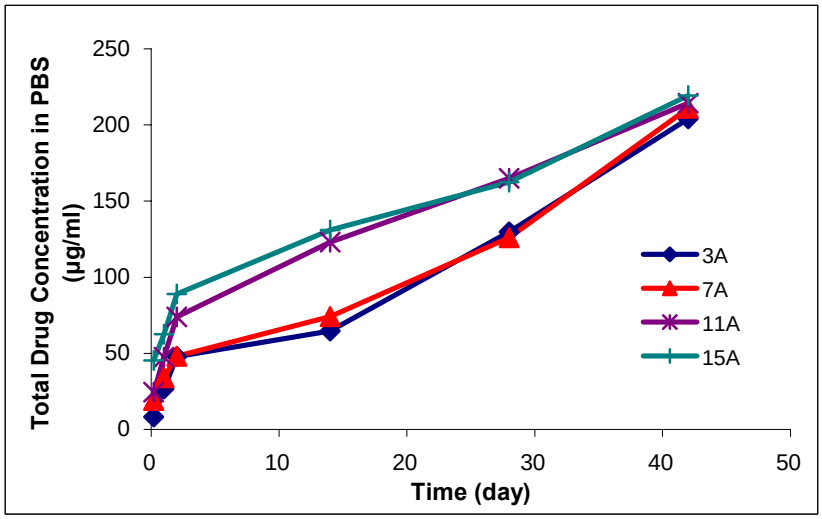

Figure 3.62 Fortum release profiles for samples 3A, 7A, 11A and 15A (208 nm)

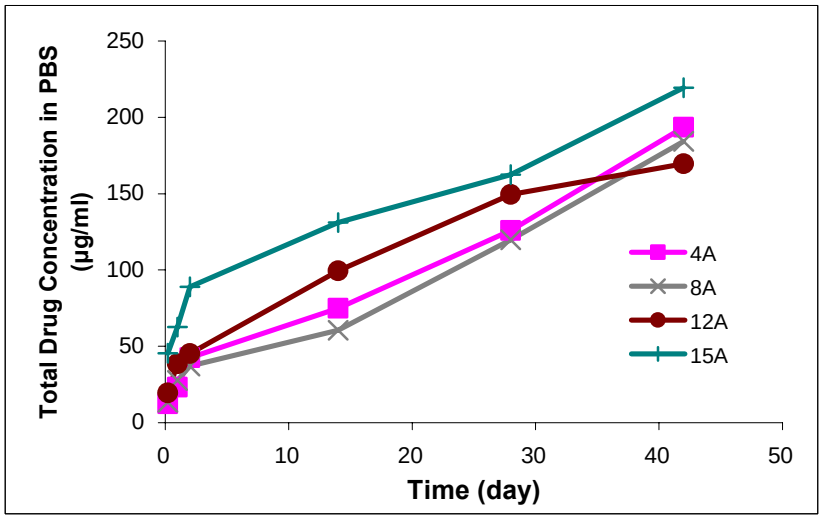

Figure 3.63 Fortum release profiles for samples 4A, 8A, 12A and 15A (208 nm)

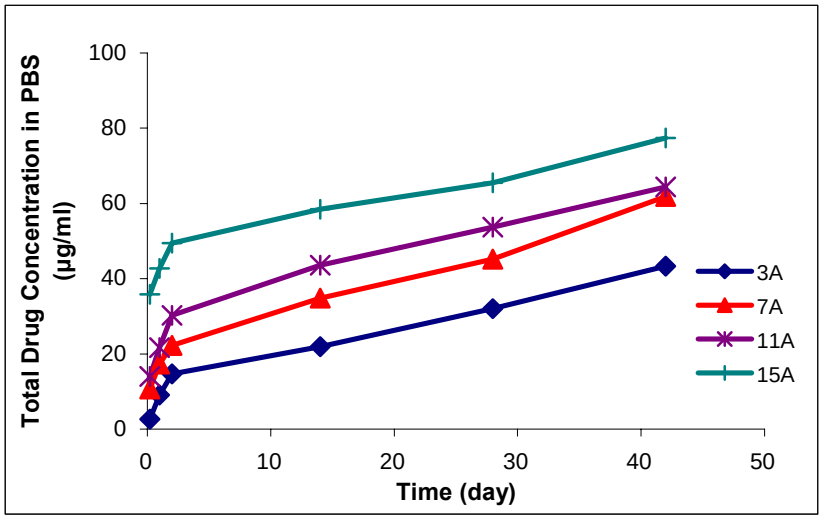

Figure 3.64 Fortum release profiles for samples 3A, 7A, 11A and 15A (256 nm)

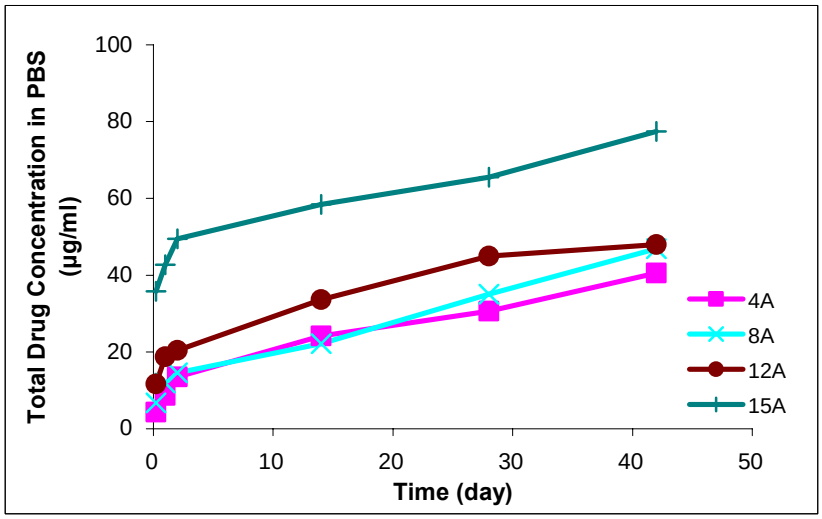

Figure 3.65 Fortum release profiles for samples 4A, 8A, 12A and 15A (256 nm)

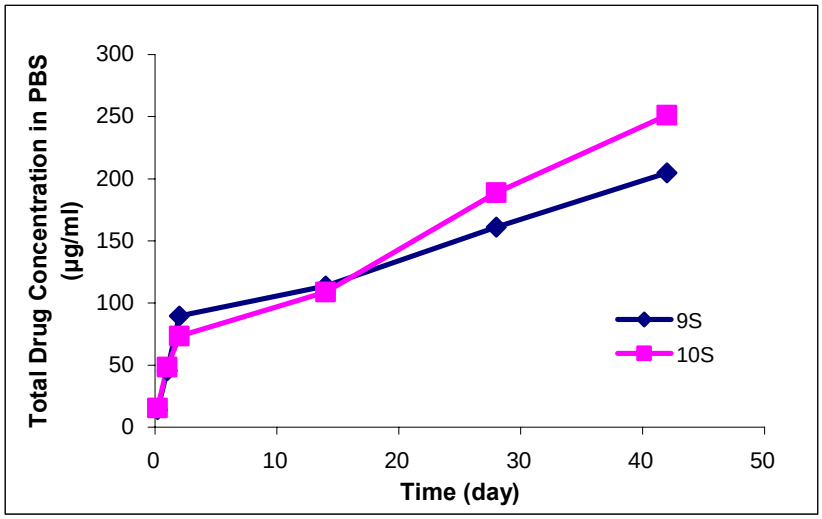

Figure 3.66 Fortum release profiles for samples 9S and 10S (208 nm)

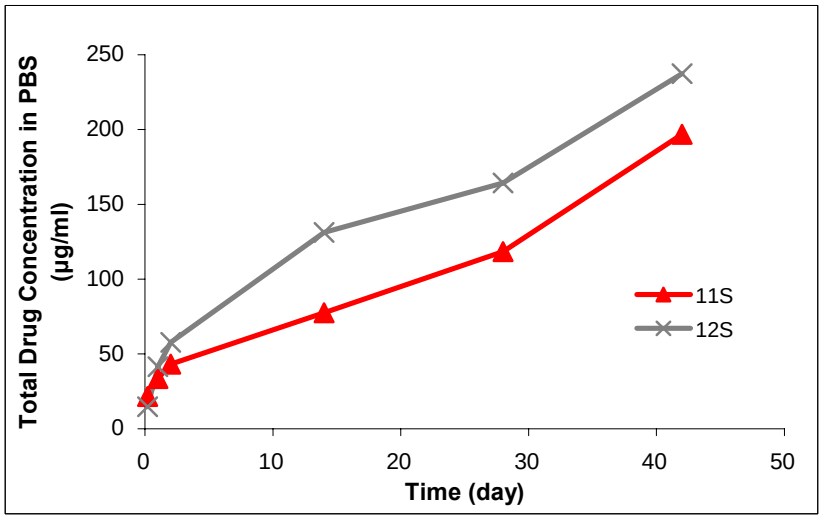

Figure 3.67 Fortum release profiles for samples 11S and 12S (208 nm)

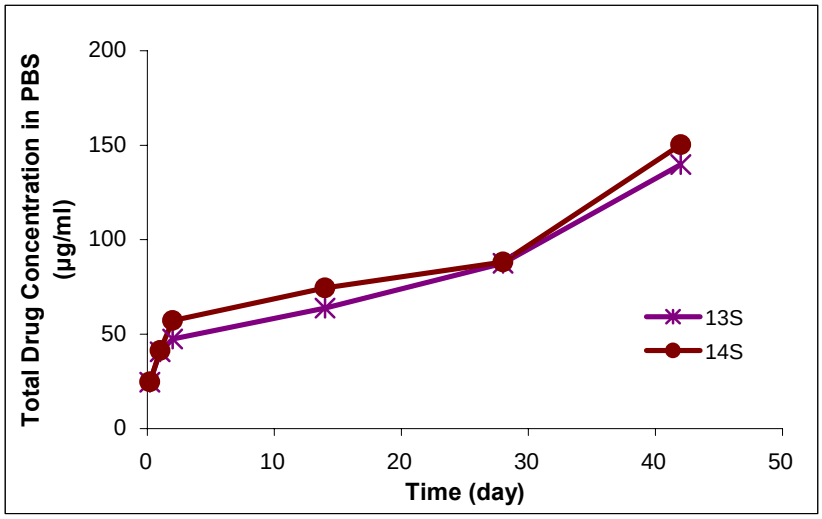

Figure 3.68 Fortum release profiles for samples 13S and 14S (208 nm)

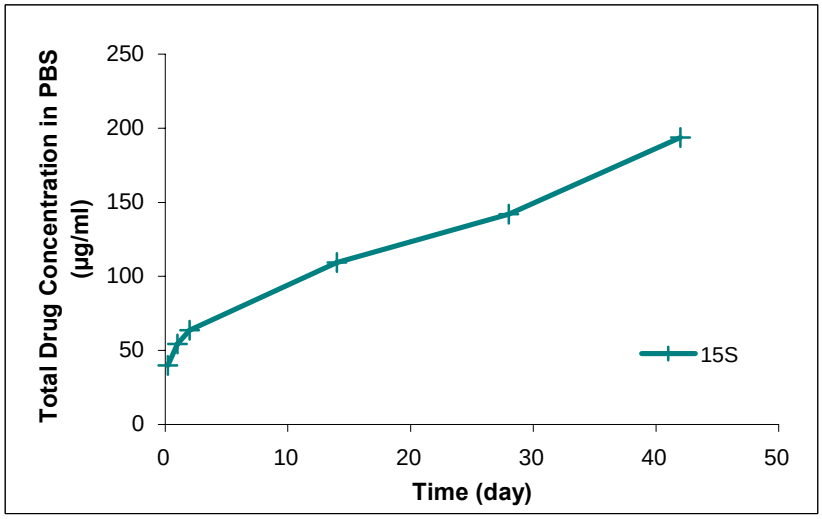

Figure 3.69 Fortum release profile for sample 15S (208 nm)

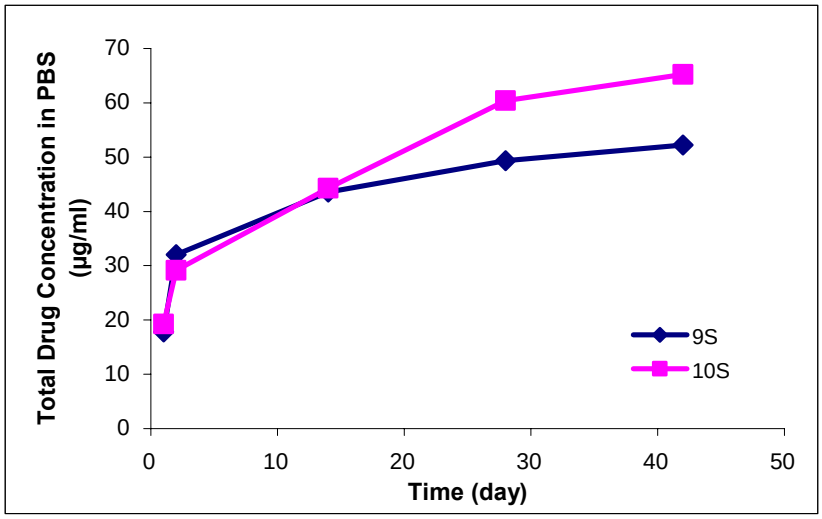

Figure 3.70 Fortum release profiles for samples 9S and 10S (256 nm)

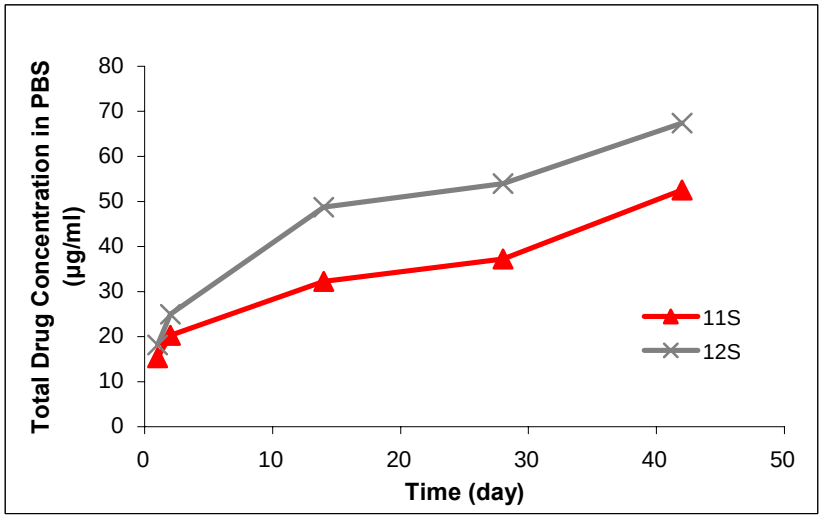

Figure 3.71 Fortum release profiles for samples 11S and 12S (256 nm)

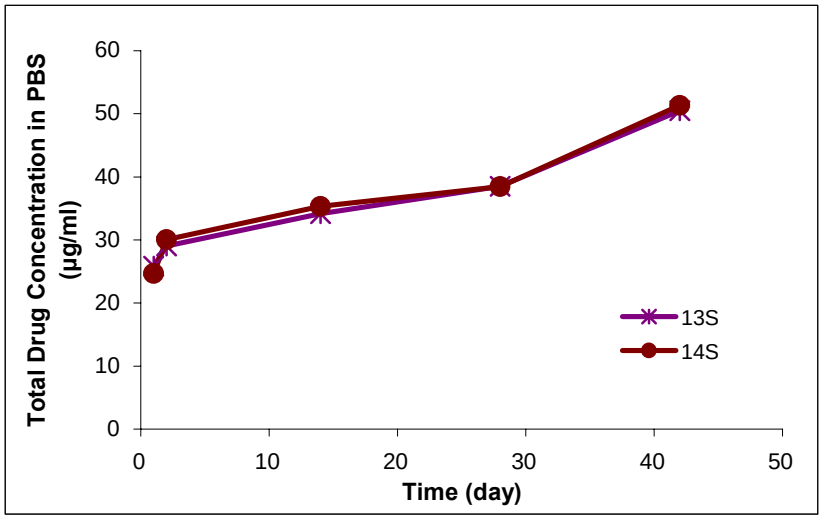

Figure 3.72 Fortum release profiles for samples 13S and 14S (256 nm)

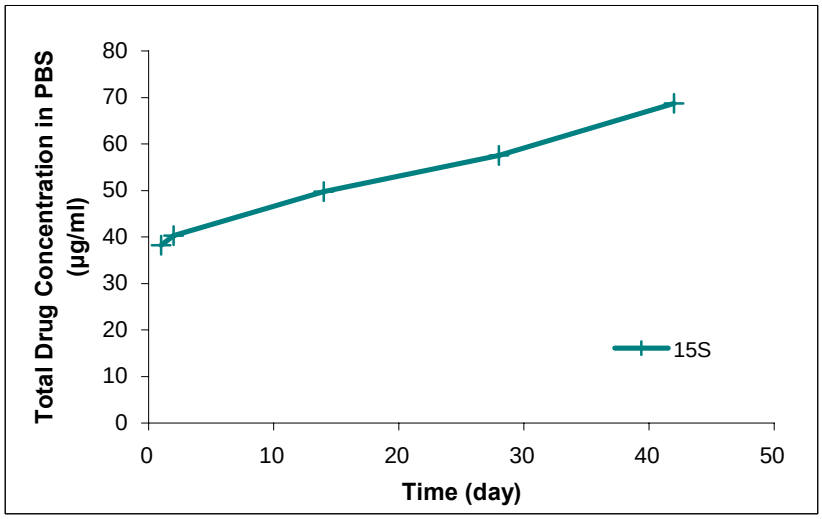

Figure 3.73 Fortum release profile for sample 15S (256 nm)

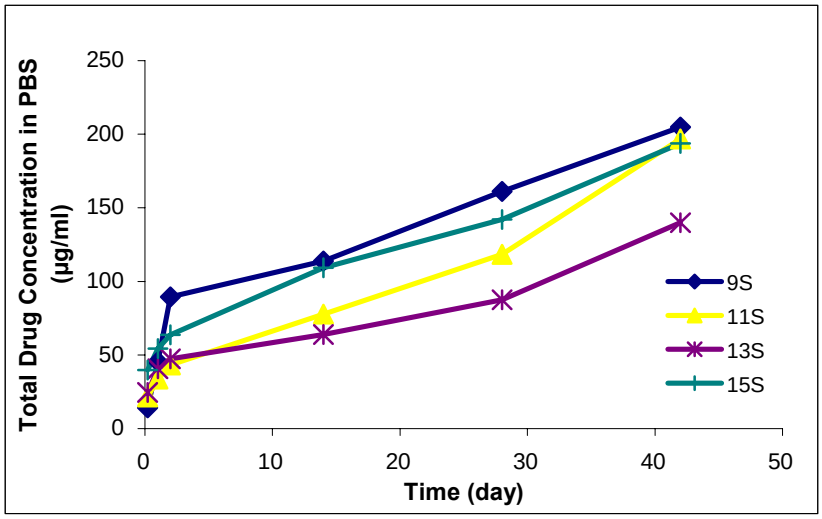

Figure 3.74 Fortum release profiles for samples 9S, 11S, 13S and 15S (208 nm)

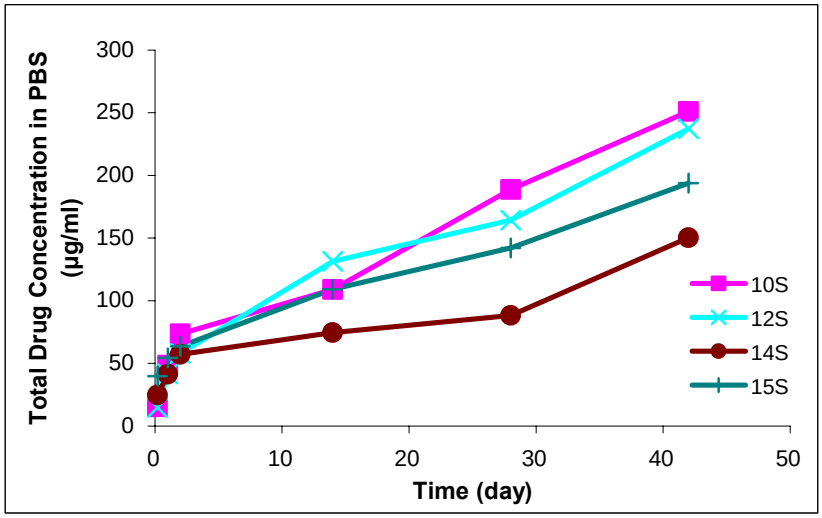

Figure 3.75 Fortum release profiles for samples 10S, 12S, 14S and 15S (208 nm)

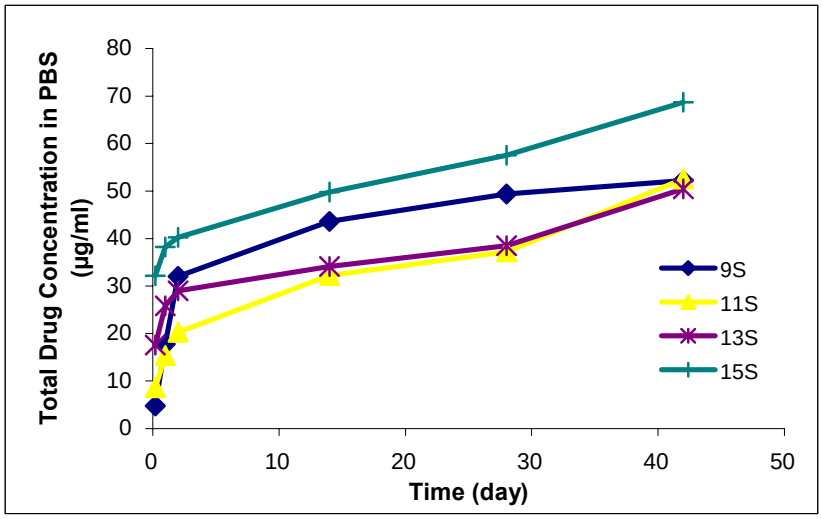

Figure 3.76 Fortum release profiles for samples 9S, 11S, 13S and 15S (256 nm)

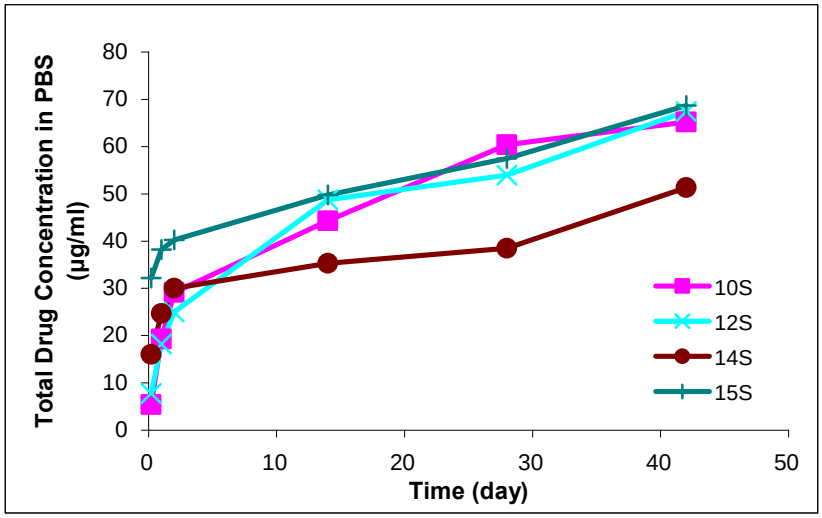

Figure 3.77 Fortum release profiles for samples 10S, 12S, 14S and 15S (256 nm)

Following results can be concluded with the information obtained from the absorbance measurements, drug concentrations related to this absorbance values and drug release profiles.

At 208 nm absorbance measurements, 3A and 4A samples have nearly same

drug release profiles (Figure 3.54) verifying their almost equal drug containing coating weights. Samples 7A-8A (Figure 3.55) and 11A-12A (Figure 3.56) pairs also have release profiles verifying their drug containing coating weights. From the overall drug release profiles given in Figure 3.62 and 3.63, it can be seen that multiple inert coatings are helpful in reducing the burst release occuring in the initial times for drug release. In sample 15A (no inert coating), after 5 hours, the released concentration of drug was equal to 45.42 μg/ml, for samples 11A and 12A (1 inert coating) this concentration was reduced to 24.57 and 19.57 μg/ml, for samples 7A and 8A (2 inert coatings) it was further reduced to 19.11 and 13.40 μg/ml and finally for samples 3A and 4A (4 inert coatings) released drug concentration was 8.19 and 12.37 μg/ml respectively.

For samples 9S to 14S at 208 nm absorbance measurements, relevancy of drug release profiles with drug containing layer weights can be seen between the samples 9S and 10S in Figure 3.66, 11S and 12S in Figure 3.67, and 13S and 14S in Figure 3.68. Also, it can be seen that multiple inert coatings are helpful in reducing the burst release occuring in the initial times for drug release. In sample 15S (no inert coating), after 5 hours, the released concentration of drug was equal to 39.85 μg/ml, for samples 13S and 14S (1 inert coating) this concentration was reduced to 24.61 and 24.78 μg/ml, for samples 11S and 12S (2 inert coatings) it was further reduced to 21.49 and 14.78 μg/ml and finally for samples 9S and 10S (4 inert coatings) released drug concentration was 14.07 and 15.35 μg/ml respectively. Another conclusion can be done on these samples that much more higher loadings for the first layer can be achieved in S type of specimens with respect to A type ones (almost 40% increase in loading weight). Therefore, in need of loading high weight coatings, S type samples can be used.

At 256 nm absorbance measurements, 3A and 4A samples have nearly same drug release profiles again (Figure 3.58) verifying their almost equal drug containing coating weights. Samples 7A-8A (Figure 3.59) and 11A-12A (Figure 3.60) pairs also have release profiles verifying their drug containing coating weights. From the overall drug release profiles given in Figure 3.64 and 3.65, it can be seen that

multiple inert coatings are helpful in reducing the burst release occuring in the initial times for drug release. In sample 15A (no inert coating), after 5 hours, the released concentration of drug was equal to 35.83 μg/ml, for samples 11A and 12A (1 inert coating) this concentration was reduced to 14.02 and 11.65 μg/ml, for samples 7A and 8A (2 inert coatings) it was further reduced to 10.71 and 6.77 μg/ml and finally for samples 3A and 4A (4 inert coatings) released drug concentration was 2.63 and 4.32 μg/ml respectively. In Figure 3.64 and 3.65, overall comparison of these different specimens' drug releases can be seen. The effect of application of multiple inert coatings on drug release rates and burst releases can easily be seen in these figures. The improvements on these parameters are much clearer in the UV measurements done at 256 nm.

For samples 9S to 14S at 256 nm absorbance measurements, relevancy of drug release profiles with drug containing layer weights can be seen between the samples 9S and 10S in Figure 3.70, 11S and 12S in Figure 3.71, and 13S and 14S in Figure 3.72. Also, it can be seen that multiple inert coatings are helpful in reducing the burst release occuring in the initial times for drug release. In sample 15S (no inert coating), after 5 hours, the released concentration of drug was equal to 32.18 μg/ml, for samples 13S and 14S (1 inert coating) this concentration was reduced to 17.56 and 16.02 μg/ml, for samples 11S and 12S (2 inert coatings) it was further reduced to 8.61 and 7.78 μg/ml and finally for samples 9S and 10S (4 inert coatings) released drug concentration was 4.77 and 5.41 μg/ml respectively. Overall drug release profiles are given in Figure 3.76 and 3.77 respectively.

In these studies, burst releases reduced and drug release times were extended as aimed. However, total drug release amounts on all the samples were found higher than the theoretical loading values. Therefore, drug loading control studies were done and explained in details in the following part.

3.12.3.2 Drug Loading Control Studies

10% PLGA RG 504 (w/v) in chloroform was prepared. Then, suitable amount of Fortum was taken and dispersed in 20 ml of this solution to obtain 10% (w/w) of the coatings. Sandblasted titanium plates were cleaned in the clean cycle described before and coated with this solution.

Table 3.32 Samples used for drug loading control studies

Sample No	w_0 (g)	w_1 (g)	w_f (g)
1	1.9773	1.9810	1.9770
2	1.9797	1.9828	1.9799
3	1.9869	1.9910	-
4	1.9844	1.9884	-

The samples 1 and 2 were coated with drug containing PLGA solution and samples 3 and 4 were coated with only PLGA solution. w_0 values stands for the weight of titanium plates, w_1 values stands for the weight of coated samples and w_f values stands for the weight of the samples after removing the coatings.

For samples 1 and 2, after coating procedure, the films were removed by dissolving in 25 ml chloroform. Separatory funnel was used to collect the polymer and the antibiotic in chloroform and PBS phases respectively. The aim was take the water soluble drug into the PBS phase. Then, PBS phase used in UV analysis. The absorbance values measured at 256 nm were 0.155 for sample 1 and 0.127 for sample 2 respectively. From the coating weights, theoretical drug loadings are 0.37 mg for the former and 0.31 mg for the latter. From the absorbance measurements, loaded drug values are 0.29 mg for sample 1 and 0.23 mg for sample 2. This means, in average, 76 % of the theoretical drug loading could be achieved.

Sample 3 and 4 were coated with pure PLGA and put into 20 ml PBS solution to understand that whether polymer coatings degradation had a contribution to the

absorbance values. After 2 weeks, the measurements at 256 nm gave absorbance values of 0.151 for sample 3 and 0.128 for sample 4. After these results, it can be concluded that, the absorption values were much higher than the actual ones because of PLGA degradation products. It introduced an error in the long term analysis. Also ceftazidime activity was time dependant. In water or PBS, the activity of drug changed with time and absorbance peaks became broader. That is why, the measurements for the amount of total drug released in 6 weeks release period exceeded the theoretical drug loadings.

3.12.3.3 Disk Diffusion Antibiotic Sensitivity Tests

Calibration curve was drawn for Fortum by using disk diffusion antibiotic sensitivity tests. For this purpose, different concentrated drug samples were placed into bacteria seeded petri dishes for 1 day and zone diameters cleaned from bacteria were measured.

Table 3.33 Zone diameter data for Fortum

Concentration (µg/ml)	Zone Diameter (mm)
250	35
125	30
62.5	24
31.7	20
15.7	18
7.8	14
3.9	12

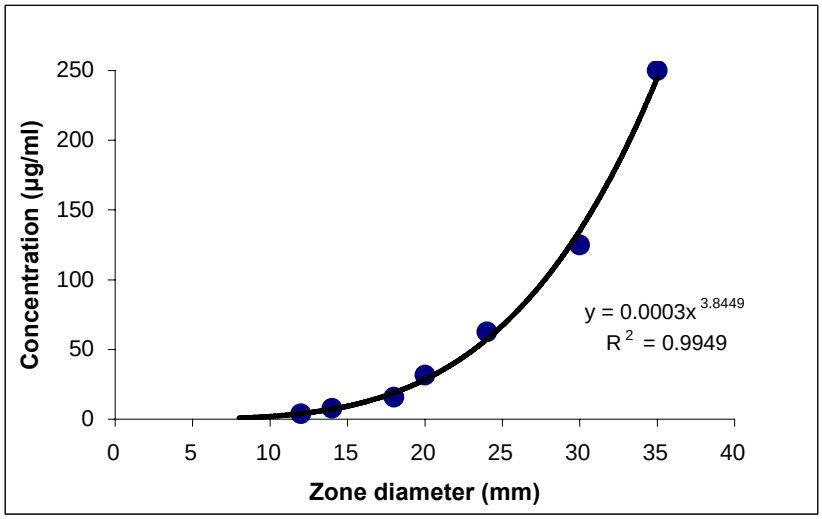

Figure 3.78 Calibration curve for Fortum in terms of zone diameters

The remaining samples prepared previously were used in the disk diffusion antibiotic tests to control their drug releasing properties. Zone diameters occuring for each sample and corresponding drug concentrations are given in the following table.

Table 3.34 Disk diffusion antibiotic sensitivity test results

Sample Code	Zone diameter (mm)	Concentration (µg/ml)
1A	12	4.2
2A	12	4.2
5A	14	7.7
6A	15	10.0
9A	17	16.1
10A	15	10.0
13A	20	30.2
14A	15	10.0
1S	15	10.0
2S	17	16.1
3S	16	12.8
4S	14	7.7
5S	13	5.8
6S	15	10.0
7S	11	3.0
8S	7	0.5

From Table 3.34, sample 1A, 2A, 7S and 8S (4 inert layers) has the lowest drug release amounts in comparison with the other samples. The general tendency was observed as expected; drug release amounts increased as the number of inert layers decreased.

3.12.3.4 Ceftazidime (Fortum) Activity Control Studies

For the activity tests of Fortum, known concentration in triple distilled water and PBS solutions of this drug was prepared. Absorbance measurements were done initially, after 1, 3, 9, 15, 21, 35 and 42 days in water and initially, 1, 2, 7, 14, 21, 28, 35, 42 and 49 days in PBS samples. Samples were put in an oven held at 37^0C during these time intervals. Change in solutions' absorbance values with time can be seen in Figure 3.79 and 3.80.

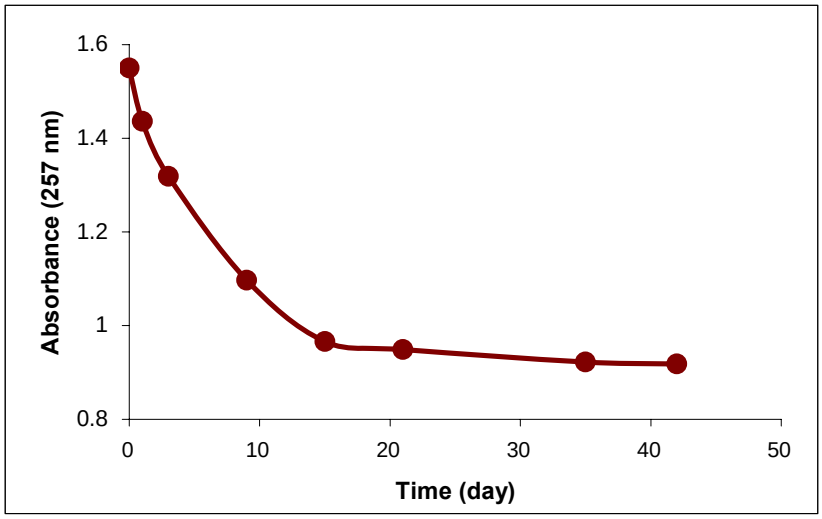

Figure 3.79 Change in Fortum activity with time (in water)

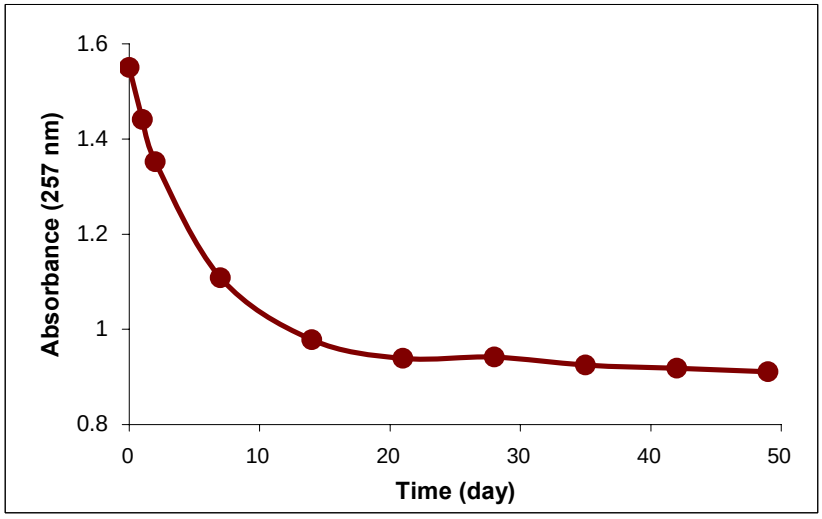

Figure 3.80 Change in Fortum activity with time (in PBS)

As it can be seen from these figures, Fortum's activity decreases with time and it can be concluded that activity of this drug is time-dependant. Also, maximum absorbance value shifted to lower wavelengths as time proceeds. When comparing the colors of the solutions, it was observed that they changed into a yellowish color in time.

3.12.4 Drug Release Studies from Vancomycin Loaded Implants

3.12.4.1 Vancomycin Activity Control Studies

Vancomycin solutions prepared in triple distilled water at varying concentrations (for concentrations, refer to Figure 3.34) were used for these studies. The solutions' absorbances were measured at 281 nm wavelength by using UV-Vis spectrophotometer. Then these solutions were placed in an oven held at 37^0C. After 2 weeks, solutions' absorbances were measured again. The initial and after-two-week absorbance measurements can be seen in Figure 3.81.

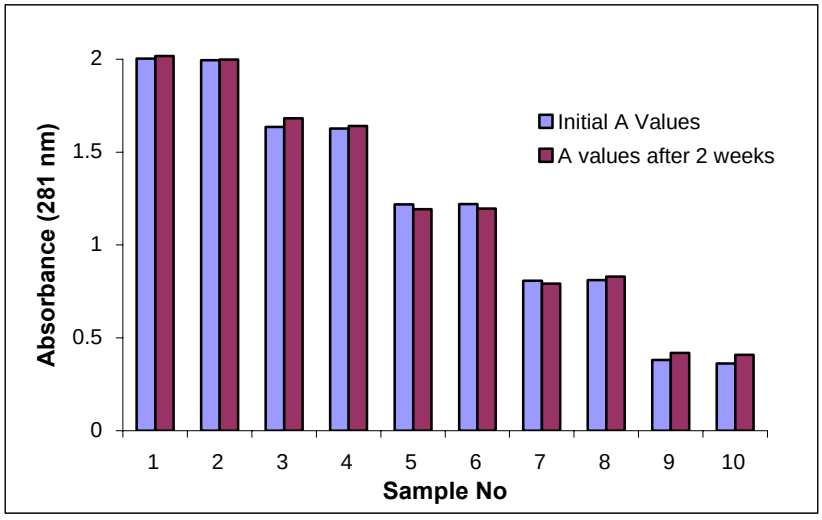

Figure 3.81 Change in Vancomycin activity with time

According to Figure 3.81, it can be concluded that Vancomycin did not lose its activity in aqueous solution and Vancomycin activity can be accepted as time independent within this interval.

3.12.4.2 Drug Release Studies on Vancomycin Impregnated TCP

In this section, Vancomycin release properties of implants were studied. TCP was used as an assisting agent to the polymer matrix (a polymer composite). The aim was to regulate the drug release kinetics and to help to eliminate the burst release of drugs. The expectation was that TCP has a porous structure and it can provide a controlled release with a favorable kinetics. Another aspect of choosing TCP was its biodegradable and biocompatible properties.

3.12.4.2.1 Packing Density Measurement of TCP

In the packing density studies of TCP, previously weighed TCP was tapped in a graduated cylinder for half an hour and the volume of it was estimated. This study was repeated for three times and the average apparent density of TCP was found as 0.843 g/ml compared to the intrinsic density which is 3.140 g/ml. The overall, macro and micro, porosity can be calculated as 1 minus the ratio of apparent density to that of intrinsic density as 0.73.

3.12.4.2.2 Drug Release Studies

In the drug release studies, after dissolving 0.5 g Vancomycin in triple distilled water, 2.594 g TCP was added and content was mixed continuously by using magnetic stirrer for 6 hours. For the mixture to set, it was placed at room temperature for 1 day. Then, water was evaporated in a vacuum oven held at 45-50 ^{0}C. The solid obtained was powdered and used for drug release studies.

1.5 g of this powder (TCP+Vancomycin) was dispersed in a 5 ml 10% (w/v) PLGA RG 504 solution in chloroform. Modified titanium plates (same with S-coded samples) were cleaned with a cleaning cycle described previously and coated by dipping into the suspension. After drying the plates in an oven held at 37^{0}C for 1 day,

they were inert coated by dipping into the 5% (w/v) poly(L-lactide) L 209S solution for a short time. Finally, they were dried in an oven again for 1 day prior to the drug release analysis. Two parallel samples L-1 and L-2 were prepared as explained above and their weights after each drying stage are given in Table 3.35.

Table 3.35 Sample weights for inert coating applications for samples L-1 and L-2

Sample	w_0 (g)	w_1 (g)	w_2 (g)
L-1	2.1011	2.1952	2.2016
L-2	2.0803	2.1507	2.1574

In this table w_0 stands for the plate's weight, w_1 stands for the weight of plate with drug loaded and w_2 stands for the weight of plate with inert coating applied.

The coating weights at each coating application and corresponding theoretical drug weight is given in Table 3.36.

Table 3.36 Coating weights and theoretical drug weights for samples L-1 and L-2

Sample Code	Coating Weight (mg)		Theoretical Drug Weight (mg)
	1st layer	2nd layer	
L-1	94.1	6.4	11.4
L-2	70.4	6.7	8.6

After coating procedure, these plates were placed into the 2 ml triple distilled water containing closed glass vessels and placed in an oven at 37^0C. At predetermined time intervals, plates were put into the fresh solvents and solutions used for UV analysis. Solutions were frozen until the absorbance measurements. Absorbance measurements were done at 281 nm and results are given in Table 3.37.

Table 3.37 Absorbance measurements for specimens L-1 and L-2

Sample Code	Absorbance (281 nm)							
	1 day	**2 days**	**5 days**	**8 days**	**12 days**	**16 days**	**21 days**	**26 days**
L-1	2.500	2.493	2.495	1.600	1.158	0.792	0.909	1.224
L-2	2.496	2.492	2.432	1.090	0.639	0.482	0.475	0.601

Corresponding released drug concentrations with these absorbance measurements were calculated by using the Vancomycin calibration curve equation and results are given in Table 3.38. Note that these values are not cumulative. After each measurement, the aqueous phase was refreshened. Therefore, 2 days means the amount of antibiotic released between end of day 1 and end of day 2.

Table 3.38 Released Vancomycin concentrations for specimens L-1 and L-2

Sample Code	Drug Concentration (µg/ml)							
	1 day	**2 days**	**5 days**	**8 days**	**12 days**	**16 days**	**21 days**	**26 days**
L-1	622	620	621	397	287	195	224	303
L-2	621	620	605	269	157	117	116	147

Total drug release profiles of specimens L-1 and L-2 with time can be seen in Figure 3.82. The slow release profile is evident in Figure 3.82.

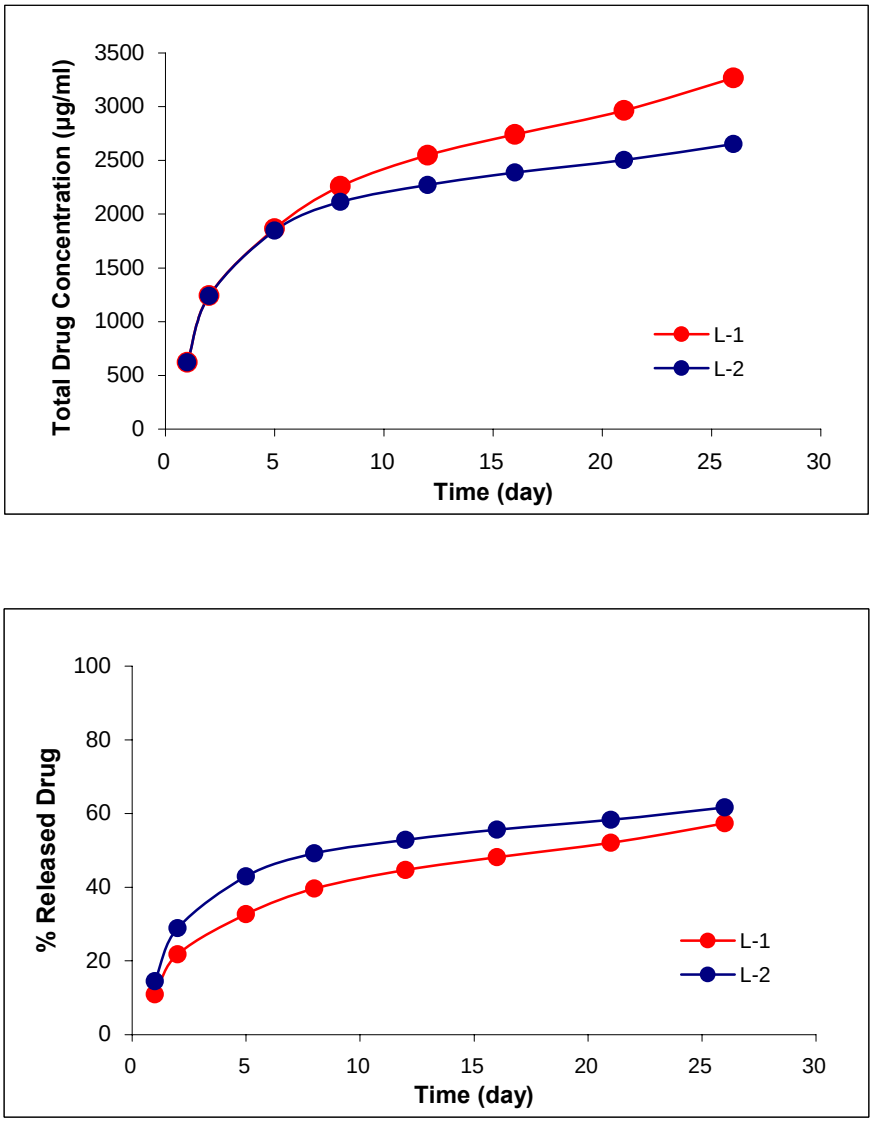

Figure 3.82 Vancomycin release and % release profiles for samples L-1 and L-2

According to Figure 3.82, 57.4 % of the Vancomycin loaded from L-1 sample and 61.7 % of the Vancomycin loaded from sample L-2 was released in 26 days. Relatively faster drug release profiles for both samples were observed in the first five days. However, drug release rate decreased to a smaller value after 8 days. But an increase in the drug release is observed after 3 weeks as before which is due to polymer degradation. Eventually, the drug release curves for these samples can be divided into five separate parts which are curve between 1 to 2 days, 2 to 5 days, 5 to

8 days, 8 to 21 days and 21 to 26 days. For L-1 sample, slope of the curve is 620 between 1 to 2 days and it decreases to 207 between 2 to 5 days, 132 between 5 to 8 days and finally slope becomes 53.5 from 8 to 21 days of drug release. However slight increase in slope (60.6) was detected after 3 weeks. In the same way, for L-2 sample, slope of the curve is 620 between 1 to 2 days and it decreases to 201.7 between 2 to 5 days, 89.7 between 5 to 8 days and finally slope becomes 29.7 up to 26 days of drug releases. No major increase in the slope was detected between 21 to 26 days for this sample. If this trend continues after 8 days, drug release period can last approximately 70-80 days for all loaded drug to be released.

3.12.4.2.3 Disk Diffusion Antibiotic Sensitivity Tests

Disk diffusion antibiotic sensitivity tests of the samples obtained from L-1 and L-2's drug release studies were applied on the bacteria seeded petri dishes and drug activities and releases were determined by using the zone diameters (Figure 3.83).

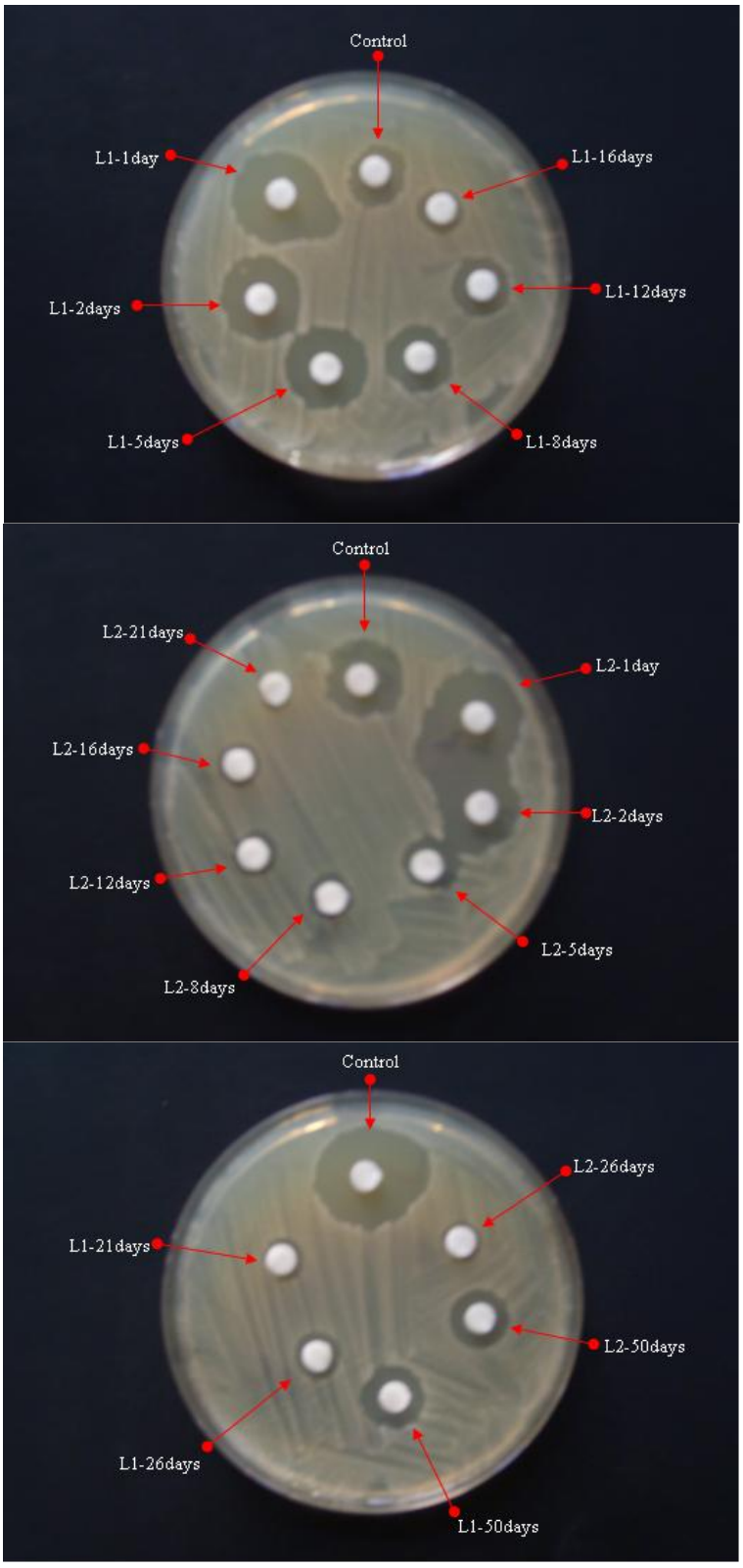

Figure 3.83 Disk diffusion antibiotic sensitivity tests for L-1 and L-2

From the measurements of zone diameters which occurred in disk diffusion antibiotic sensitivity tests, done by using a computer program, drug release profiles of the samples could be followed. In every case, control spot refers to 100 µg/ml drug concentration. Zone diameters are given in Table 3.39 and total drug release profiles can be seen in Figure 3.84.

Table 3.39 Disk diffusion antibiotic sensitivity test results for L-1 and L-2

Sample Code	Zone diameter (unit)*	Concentration (µg/ml)
L1-1 day	17.5 (control: 11)	159.1
L1-2 days	15.5 (control: 11)	140.9
L1-5 days	15.5 (control: 11)	140.9
L1-8 days	12 (control: 11)	109.1
L1-12 days	11 (control: 11)	100.0
L1-16 days	8.5 (control: 11)	77.3
L1-21 days	7.8 (control: 19.2)	40.6
L1-26 days	8.4 (control: 19.2)	43.8
L1-50 days	11.5 (control: 19.2)	104.5
L2-1 day	16.5 (control: 15)	110.0
L2-2 days	14.2 (control: 15)	94.7
L2-5 days	9.3 (control: 15)	62.0
L2-8 days	8 (control: 15)	53.3
L2-12 days	9 (control: 15)	60.0
L2-16 days	8.5 (control: 15)	56.7
L2-21 days	8 (control: 15)	53.3
L2-26 days	8.3 (control: 19.2)	43.2
L2-50 days	11 (control: 19.2)	57.3

* The unit is a virtual mm obtained from images of the antibiotic sensitivity tests by using a computer program.

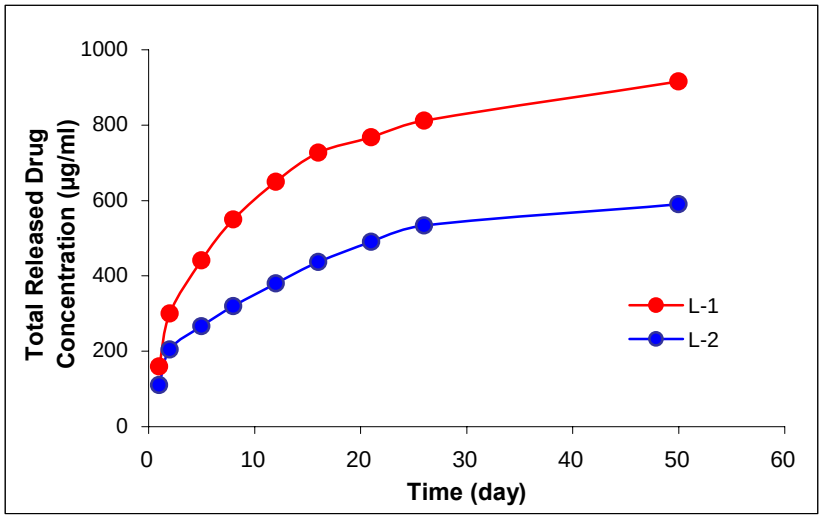

Figure 3.84 Vancomycin release profiles for samples L-1 and L-2 according to disk diffusion antibiotic sensitivity tests

As it can be seen in Figure 3.84, drug release profiles for samples in question are almost the same. These two types of experiments, disk diffusion and drug release, support each other and give similar results. Vancomycin impregnated in TCP suspension in PLGA RG 504 solution had promising results for controlled drug release metal implant production. After obtaining these promising results, it was decided to make deeper investigations on these formulations to compare the effect of making inert coating and using a TCP (a polymer composite approach).

3.12.4.3 Further Drug Release Studies on Vancomycin Loaded Implants

3.12.4.3.1 Drug Release Studies from Antibiotic-Polymer Coated and Antibiotic-TCP-Polymer Coated Metal Substrates

In Vancomycin release studies from drug loaded implants, mainly four different samples were prepared. Three samples for each kind were used to compare results with each other. For samples 1V to 3V and 7V to 9V, no inert coating was

applied. For the rest of the specimens, inert coating application was done. Samples 1V to 6V did not contain any TCP, whereas samples 7V to 12V, TCP were used as a drug carrying material.

Titanium based implant samples were cleaned with the cleaning cycle described previously. Mainly, two sets of samples were prepared.

As a first set (samples 1V to 6V), drug containing layer had the formulation of 0.25 g Vancomycin dispersed in 10 ml 10% (w/v) RG 504 solution in chloroform. After coating with this suspension, inert coating was applied on the samples 4V to 6V by using 5% (w/v) L 209S solution in chloroform. All of the coating mixtures prepared under constant stirring for 6 hours. Each coating layer was dried for one day in 37^0C oven and second coating layer was applied after drying period.

For the second set of samples (7V to 12 V), 1g TCP+Vancomycin mixture (preparation described in section 3.12.3.2.2) was dispersed in 10 ml 10% (w/v) RG 504 solution in chloroform. First layer of coating was done with this suspension. For samples 10V to 12V, inert coating was applied by using 5% (w/v) L 209S solution in chloroform. All of the coating mixtures prepared under constant stirring for 6 hours. Each coating layer was dried for one day in 37^0C oven and second coating layer was applied after drying period.

Coating weights of prepared samples and theoretical loaded drug weights are given in Table 3.40. For samples 1Vto 6V, drug weight is equal to the 20% of the coating weight; for samples 7V to 12V, drug weight is equal to the 8.1% of the coating weight.

Table 3.40 Coating weights and theoretical drug weights for specimen V

Sample Code	w_1 (mg)	w_2 (mg)	Theoretical drug weight (mg)
1V	4.8	-	0.96
2V	5.8	-	1.16
3V	6.0	-	1.20
4V	5.4	3.5	1.08
5V	6.7	3.6	1.34
6V	6.8	3.4	1.36
7V	7.0	-	0.57
8V	7.1	-	0.58
9V	7.0	-	0.57
10V	9.6	2.8	0.78
11V	8.1	3.2	0.66
12V	7.9	4.1	0.64

After coating procedure, these samples were placed into the 2 ml triple distilled water containing closed glass vessels and placed in an oven at 37^0C. At predetermined time intervals, plates were placed in the fresh solvents and solutions used for UV analysis. Solutions were frozen until the absorbance measurements were done. Absorbance measurements were done at 281 nm and results are given in Table 3.41.

Table 3.41 Absorbance measurements (1V to 12V)

Sample Code	Absorbance (281 nm)								
	1 day	**2 days**	**5 days**	**10 days**	**14 days**	**21 days**	**28 days**	**37 days**	**55 days**
1V	1.728	0.078	0.041	0.056	0.015	0.030	0.049	0.016	-
2V	2.147	0.107	0.047	0.060	0.037	-	0.029	-	0.058
3V	2.277	0.153	0.065	0.041	0.030	0.069	0.043	0.023	0.061
4V	1.407	0.293	0.189	0.123	0.059	0.081	0.076	0.102	0.169
5V	1.620	0.465	0.280	0.195	0.084	0.095	0.051	0.050	0.113
6V	1.654	0.307	0.300	0.198	0.086	0.115	0.084	0.067	0.147
7V	0.335	0.065	0.037	0.033	0.025	0.038	0.060	0.022	0.075
8V	0.353	0.042	0.042	0.051	0.037	0.050	0.112	0.021	0.076
9V	0.311	0.055	0.033	0.053	0.031	0.050	0.060	0.018	0.144
10V	0.130	0.048	0.066	0.068	0.044	0.072	0.082	0.058	0.157
11V	0.112	0.060	0.087	0.084	0.051	0.079	0.113	0.059	0.128
12V	0.114	0.062	0.082	0.071	0.053	0.083	0.063	0.061	0.124

Drug concentrations related to this absorbance values are given in Table 3.42.

Table 3.42 Released drug concentrations for specimen V

Sample Code	Released Drug Concentration (µg/ml) (281 nm)								
	1 day	**2 days**	**5 days**	**10 days**	**14 days**	**21 days**	**28 days**	**37 days**	**55 days**
1V	428.98	16.48	7.23	10.98	0.73	4.48	9.23	0.98	-
2V	533.73	23.73	8.73	11.98	6.23	-	4.23	-	11.48
3V	566.23	35.23	13.23	7.23	4.48	14.23	7.73	2.73	12.23
4V	348.73	70.23	44.23	27.73	11.73	17.23	15.98	22.48	39.23
5V	401.98	113.23	66.98	45.73	17.98	20.73	9.73	9.48	25.23
6V	410.48	73.73	71.98	46.48	18.48	25.73	17.98	13.73	33.73
7V	80.73	13.23	6.23	5.23	3.23	6.48	11.98	2.48	15.73
8V	85.23	7.48	7.48	9.73	6.23	9.48	24.98	2.23	15.98
9V	74.73	10.73	5.23	10.23	4.73	9.48	11.98	1.48	32.98
10V	29.48	8.98	13.48	13.98	7.98	14.98	17.48	11.48	36.23
11V	24.98	11.98	18.73	17.98	9.73	16.73	25.23	11.73	28.98
12V	25.48	12.48	17.48	14.73	10.23	17.73	12.73	12.23	27.98

Drug release profiles for all of the samples studied in this section can be seen in the Figure 3.85 to 3.88. Note that these values are not cumulative. After each measurement, the aqueous phase was refreshened. Therefore, 2 days means the amount of antibiotic released between end of day 1 and end of day 2.

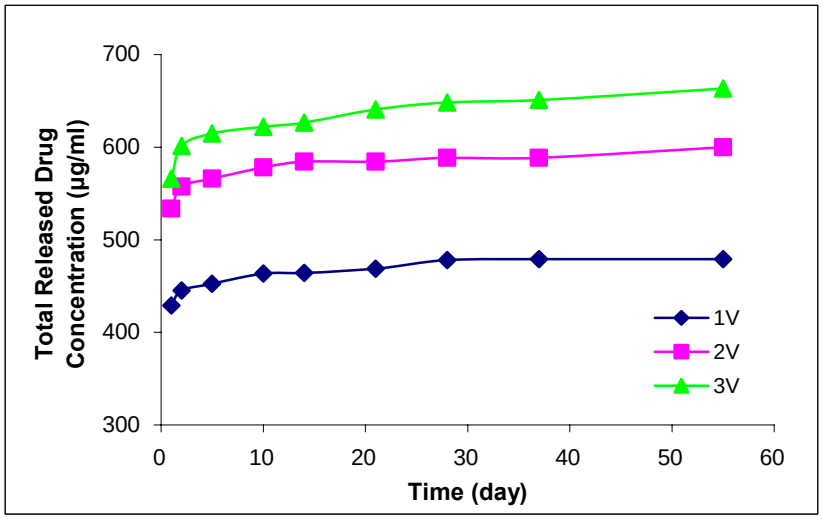

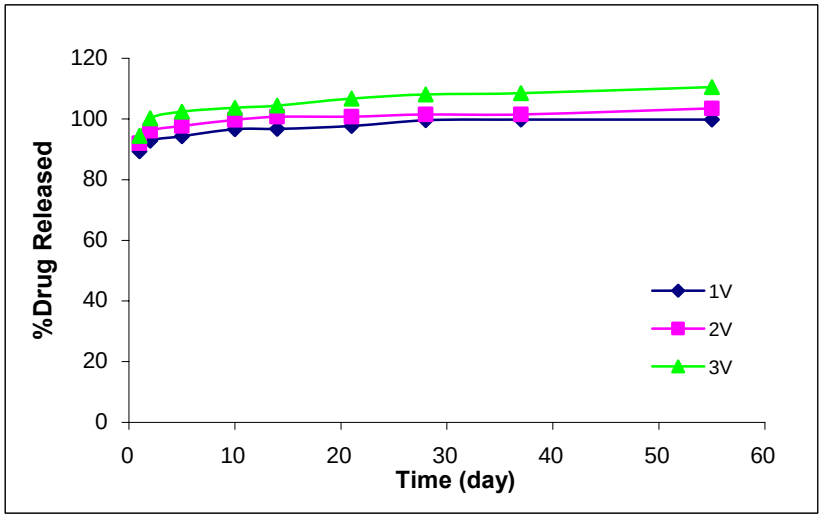

Figure 3.85 Vancomycin release and % release profiles for samples 1V to 3V

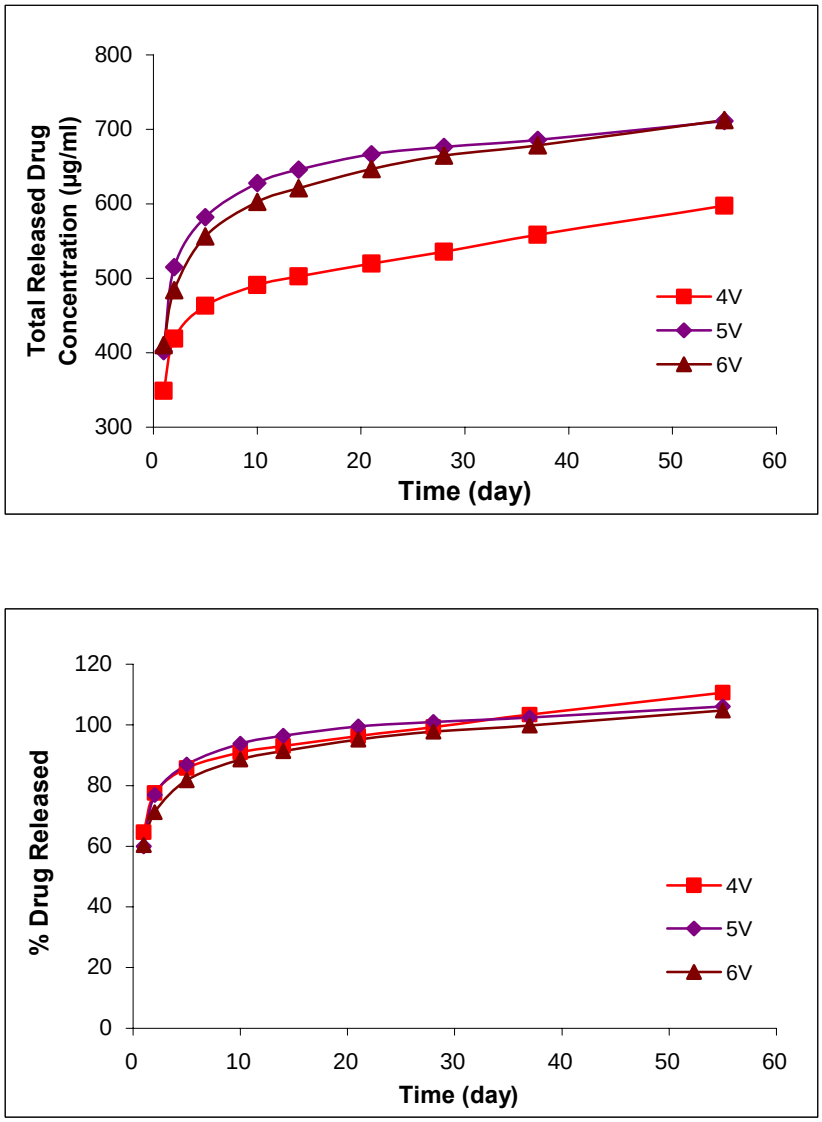

Figure 3.86 Vancomycin release and % release profiles for samples 4V to 6V

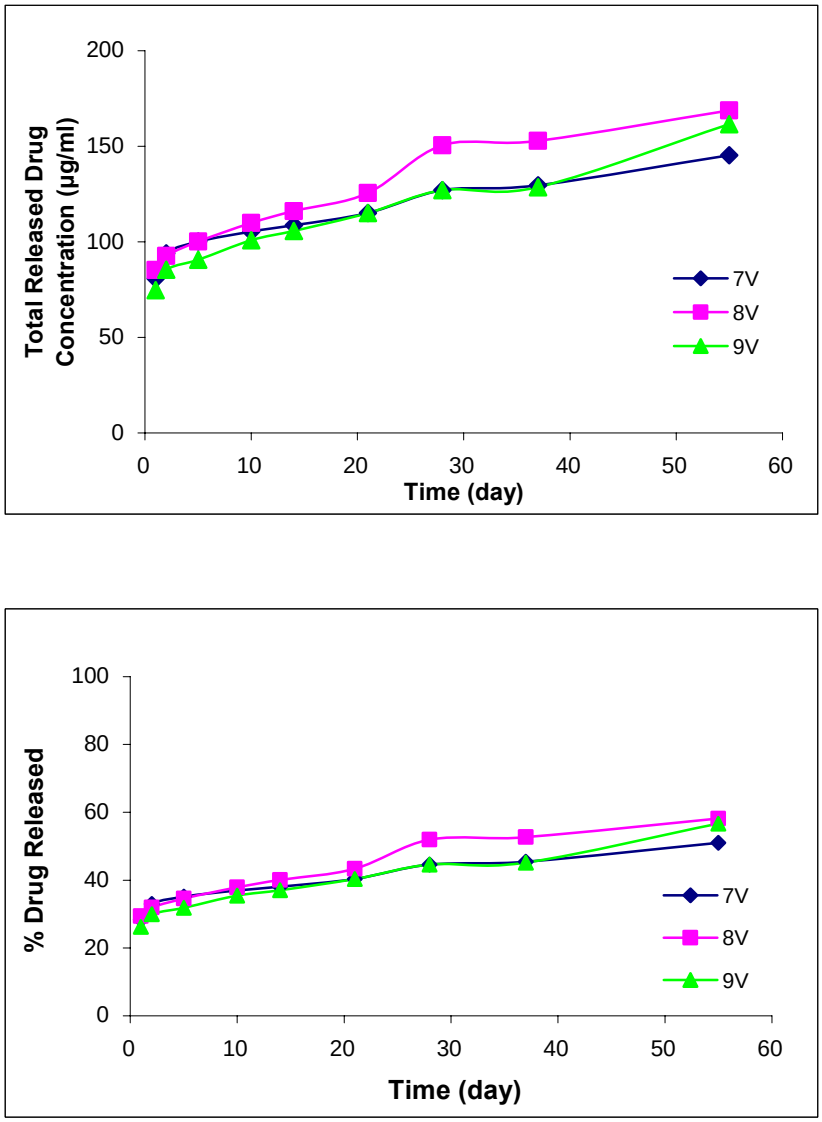

Figure 3.87 Vancomycin release profiles for samples 7V to 9V

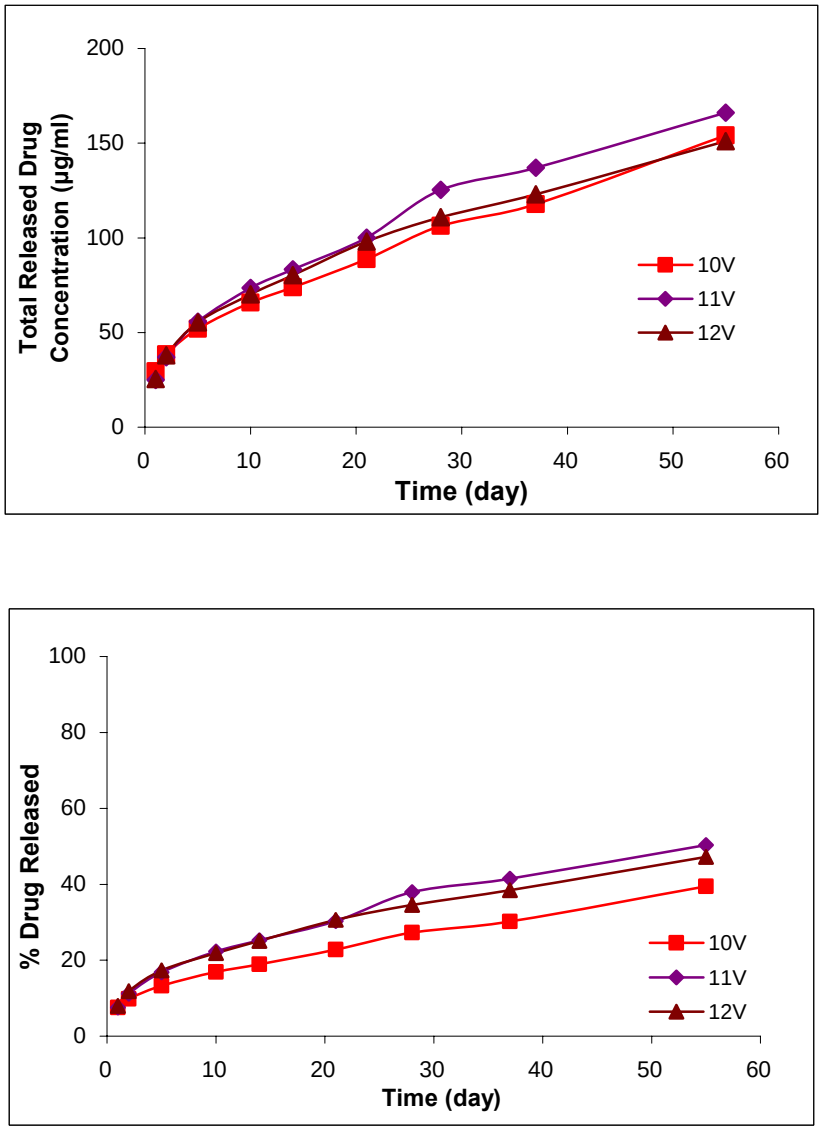

Figure 3.88 Vancomycin release profiles for samples 10V to 12V

For samples 1V to 3V, initial burst releases were obvious. As the time proceeds, very little drug was released from these samples. In 55 days release period, the entire theoretical total drug released from these samples. 89.5% of total drug loaded was released from sample 1V in 1st day and in 10 day 96.8% of drug release was completed. Likely, 88.9% of total drug loaded from sample 2V was released in 1 day and 96.3% of total drug was released in 10 days. Finally, for sample 3V, released drug percentage was 85.4% in 1 day and 93.8% of the total drug loaded was released

in 10 days. From these results, it can be concluded that Vancomycin dispersed in RG504 solution coated implants do not have long lasting controlled drug release profiles. High percentage of the loaded drugs is released within a few days.

For samples 4V to 6V, inert coating with L 209S solution was applied on to the drug containing first layer. The improved drug release profiles can be seen in Figure 3.86. In 55 days release period, the entire theoretical total drug was released from these samples. Higher release rates occurred in 10 days of release period with respect to the rest of the 55 days. Drug releases continued from these samples with smaller and at almost same rates as the time proceeds. Also initial burst releases were reduced with the application of inert coating. For sample 4V, 58.4%; for sample 5V, 56.5% and for sample 6V, 57.6% of the total drug loaded was released in 1 day. These amounts are much smaller in comparison with samples 1V to 3V. In 10 days release period, 82.2% of the total drug loaded was released for sample 4V, 88.3% of the total drug loaded was released for sample 5V and 84.6% of the total drug loaded was released for sample 6V. For these samples, burst release was reduced to a smaller extent and drug releases continued up to the 55 days of release period. It can be concluded that inert coating application reduces initial burst release and long lasting release profiles can be achieved.

For samples 7V to 9V, Vancomycin impregnated in TCP and this powder is homogeneously distributed in RG504 solution. These samples release profiles can be seen in Figure 3.87. As it is clear from this figure, nearly linear drug release profiles were obtained in these samples. For 55 days of drug releases, 51.0% of the loaded drug was released from sample 7V, 58.2% of the loaded drug was released from sample 8V and 56.7% of the loaded drug was released from sample 9V. That means drug releases can continue up to extended time periods. For sample 7V, 55.6%; for sample 8V, 50.5% and for sample 9V, 46.3% of the total drug loaded was released in 1 day. By this method, initial burst releases can be reduced and almost linear drug release profiles can be obtained. Also, drug release times can be further extended.

Finally, for samples 10V to 12V, inert coating of L 209S solution was applied. The linear drug release profiles with higher slopes can be seen in Figure 3.88. Also initial burst releases were further reduced. In 55 days drug release period, 39.5% of loaded drug from sample 10V, 50.3% of loaded drug from sample 11V and 47.2% of loaded drug from sample 12V were released. For sample 10V, 19.1%; for sample 11V, 15.0% and for sample 12V, 16.9% of the total drug loaded was released in 1 day. From these samples, it can be concluded that burst release can be further reduced and linear drug release profiles can be obtained with the application of inert coating to this coating system. Also, drug release times can be further extended by this method.

3.12.4.3.2 Disk Diffusion Antibiotic Sensitivity Tests

The samples obtained from 1V to 12V specimens were used for disk diffusion antibiotic sensitivity tests. Solutions taken at predetermined time intervals from the glass vessels were applied on the bacteria seeded petri dishes and drug activities and releases were determined by using the zone diameters. Solutions were frozen until the analysis. The results of these tests are shown in Figure 3.89.

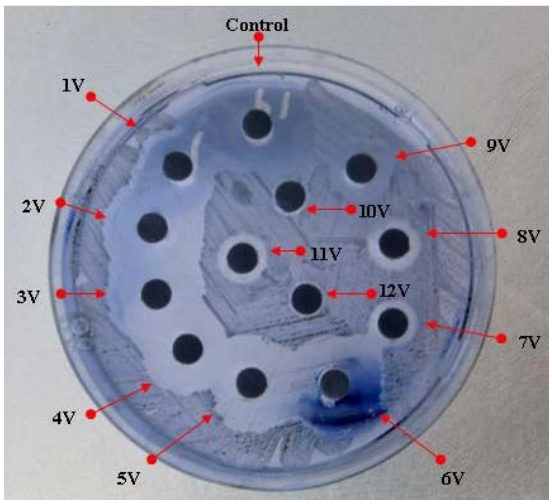

(a) 1 day

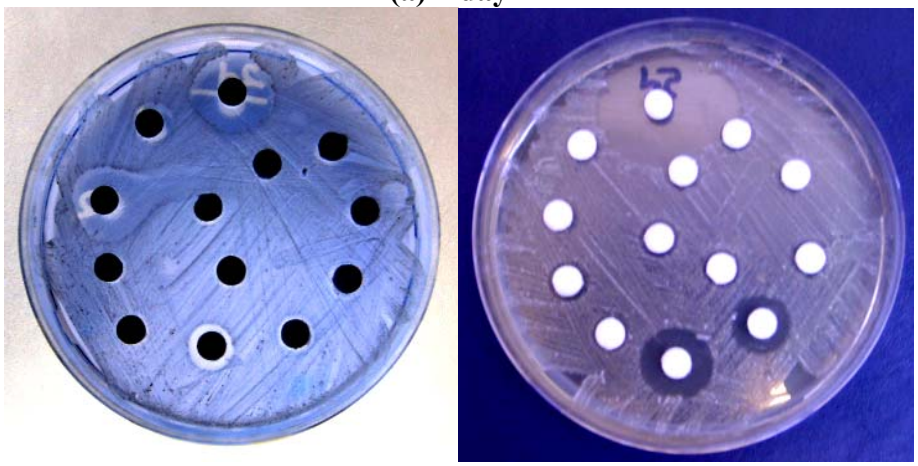

(b) 2 days **(c) 5 days**

Figure 3.89 Disk diffusion antibiotic sensitivity tests for V samples

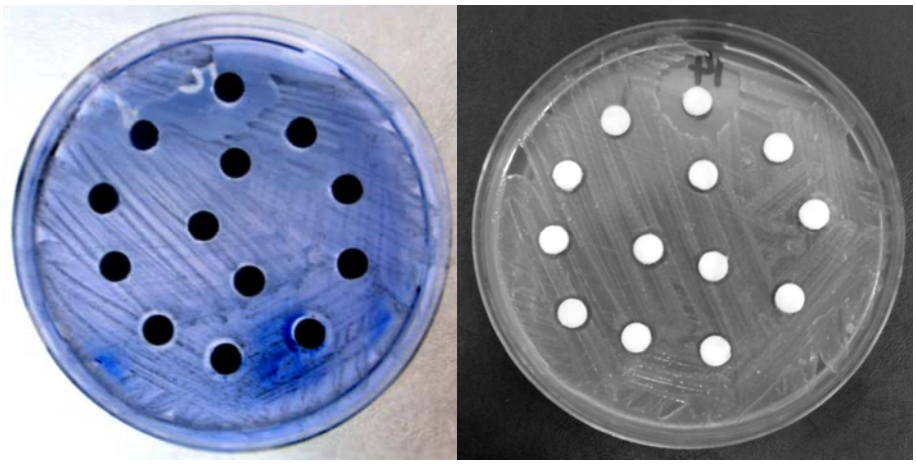

(d) 10 days **(e) 14 days**

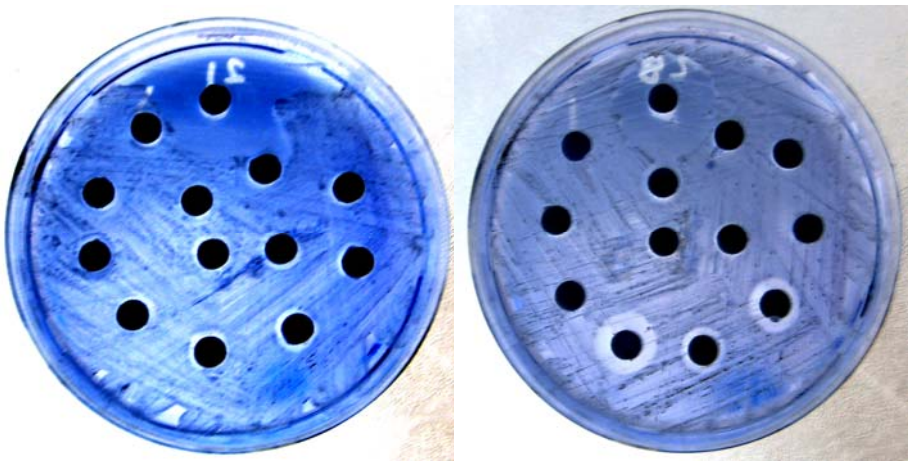

(f) 21 days **(g) 28 days**

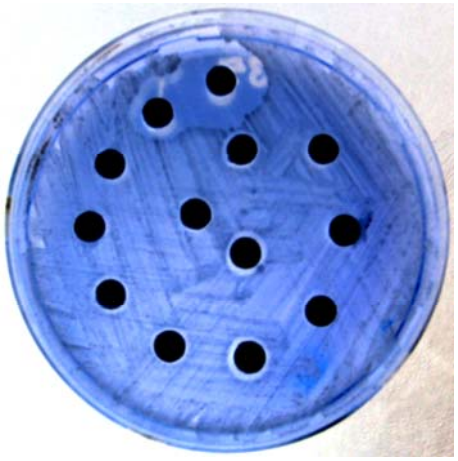

(h) 35 days

Figure 3.89 Continued; refer to Figure 3.89 (a) for sample numbers

From the measurements of zone diameters done by using a computer program, drug release profiles of the samples could be followed. In every case, control spot refers to 100 μg/ml drug concentration. Zone diameters and corresponding released drug concentrations are given in Table 3.43 and Table 3.44. Total drug release profiles according to disk diffusion antibiotic sensitivity tests can be seen in Figure 3.90 to Figure 3.93.

Table 3.43 Disk diffusion antibiotic sensitivity test results for V samples

Sample Code	**Zone Diameter (unit)***							
	1 day	**2 days**	**5 days**	**10 days**	**14 days**	**21 days**	**28 days**	**35 days**
1V	71	36	-	-	32	32	-	47
2V	87	60	-	-	32	32	-	-
3V	85	-	32	-	32	32	-	-
4V	76	-	31	32	34	32	42	34
5V	78	38	54	36	32	32	34	34
6V	83	32	40	40	32	34	38	40
7V	40	32	32	-	32	34	-	32
8V	46	-	-	-	32	32	-	32
9V	52	-	32	-	32	32	-	32
10V	34	-	32	32	32	32	32	34
11V	44	-	32	32	32	34	31	32
12V	34	-	32	32	32	34	31	38
Control	86	70	82	76	64	80	74	80

* The unit is a virtual mm obtained from images of the antibiotic sensitivity tests by using a computer program.

Table 3.44 Drug releases from disk diffusion antibiotic sensitivity tests for V samples

Sample Code	Released Drug Concentration (µg/ml)							
	1 day	**2 days**	**5 days**	**10 days**	**14 days**	**21 days**	**28 days**	**35 days**
1V	82.6	51.4	-	-	50.0	40.0	-	58.8
2V	101.2	85.7	-	-	50.0	40.0	-	-
3V	98.8	-	39.0	-	50.0	40.0	-	-
4V	88.4	-	37.8	42.1	53.1	40.0	56.8	42.5
5V	90.7	54.3	65.9	47.4	50.0	40.0	45.9	42.5
6V	96.5	45.7	48.8	52.6	50.0	42.5	51.4	50.0
7V	46.5	45.7	39.0	-	50.0	42.5	-	40.0
8V	53.5	-	-	-	50.0	40.0	-	40.0
9V	60.5	-	39.0	-	50.0	40.0	-	40.0
10V	39.5	-	39.0	42.1	50.0	40.0	43.2	42.5
11V	51.2	-	39.0	42.1	50.0	42.5	41.9	40.0
12V	39.5	-	39.0	42.1	50.0	42.5	41.9	47.5

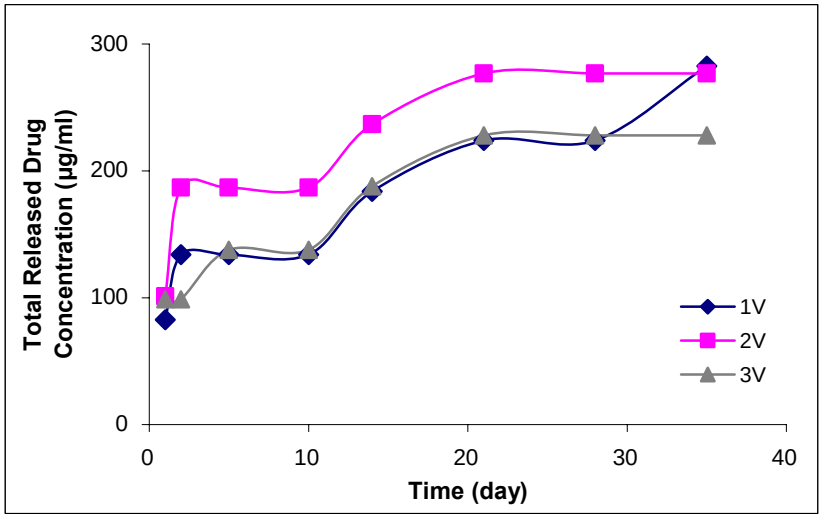

Figure 3.90 Vancomycin release profiles for samples 1V to 3V according to disk diffusion antibiotic sensitivity tests

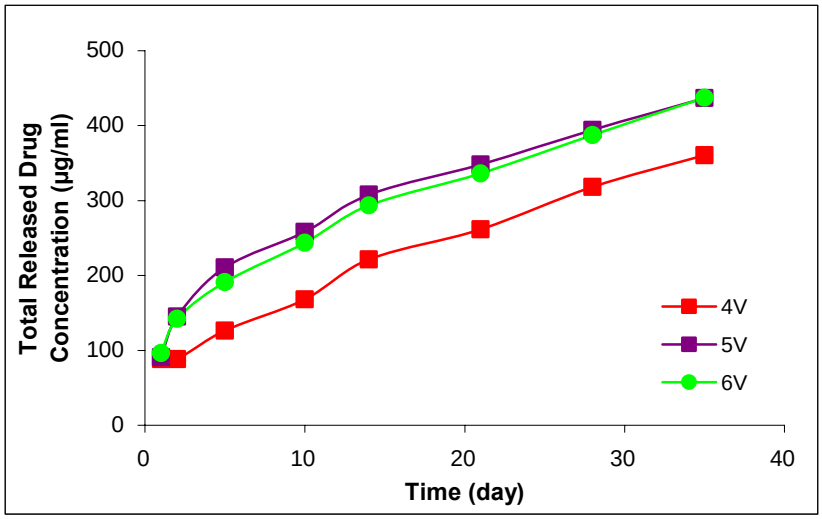

Figure 3.91 Vancomycin release profiles for samples 4V to 6V according to disk diffusion antibiotic sensitivity tests

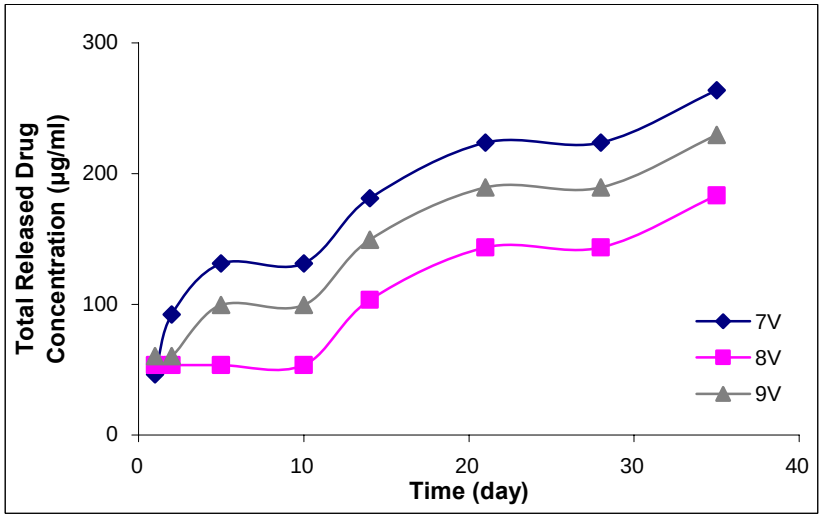

Figure 3.92 Vancomycin release profiles for samples 7V to 9V according to disk diffusion antibiotic sensitivity tests

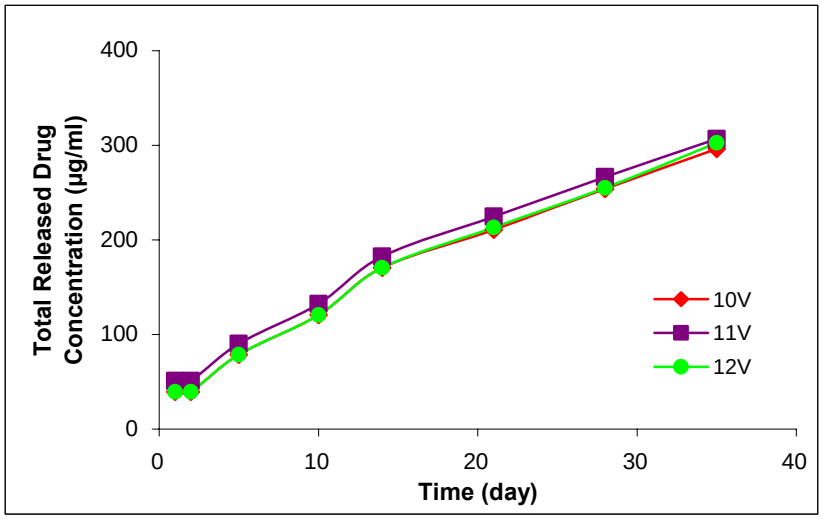

Figure 3.93 Vancomycin release profiles for samples 10V to 12V according to disk diffusion antibiotic sensitivity tests

Same comments can be done with the drug release profiles obtained from absorbance measurements. Disk diffusion antibiotic sensitivity tests have shown that inert coatings with L 209S solution were helpful in reducing the initial burst release. Linear release profiles were obtained with the samples 10V to 12V. These microbial tests were also evidence to the continuity of drug releases for studied time periods. Concentration measurements were different than the ones obtained from absorbance measurements. Absorbance measurements possibly gave more accurate results. However, the trends in the drug release profiles were found mostly same for both techniques.

3.12.4.3.3 SEM Analysis

Scanning electron micrographs were taken for the samples at different time intervals. These micrographs can be seen in Figure 3.94.

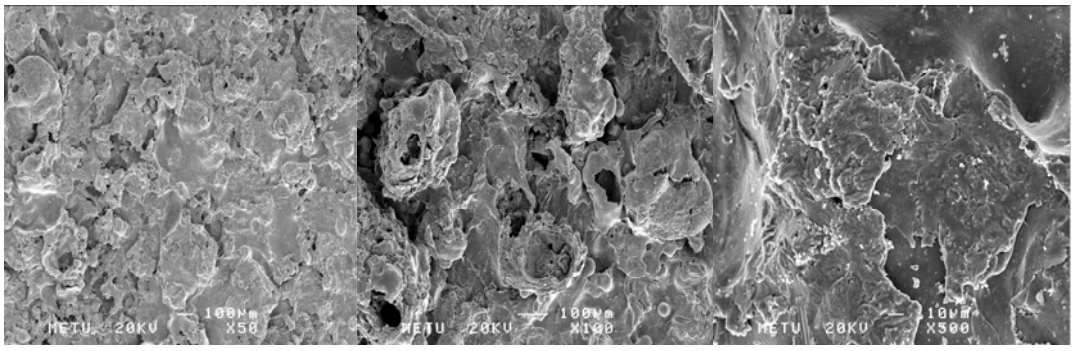

(A) Titanium alloy implant surfaces

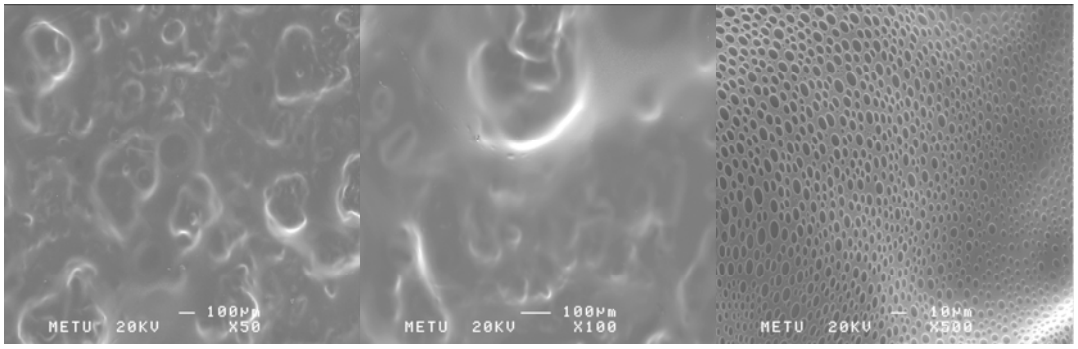

(B) Coated implants

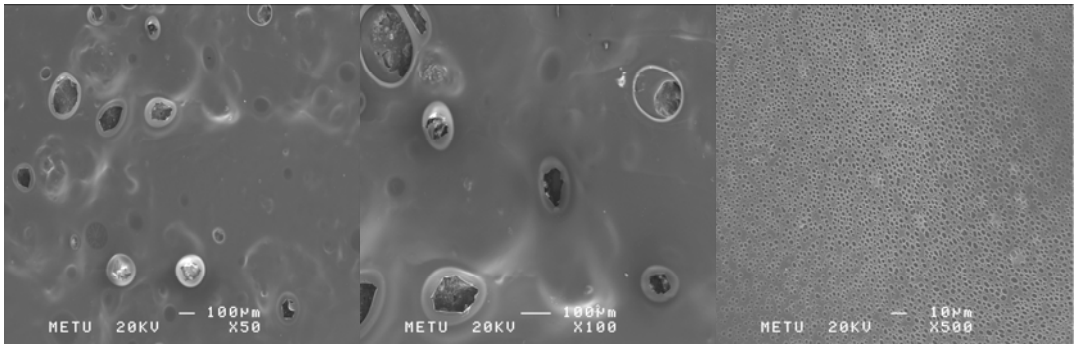

(C) After 1 week of drug release study

Figure 3.94 Scanning Electron Micrographs: (A) Uncoated macroporous surfaces of titanium implants. (B) Coated titanium implants; first layer with Vancomycin impregnated β-TCP (16.2% (w/w) Vancomycin, 1g) dispersed PLGA RG 504 solution in chloroform (10% w/v) and second layer inert coating with PL L209S solution in chloroform (5% w/v). (C) After 1 week immersion in water at 37^0C. (D) After 2 weeks immersion in water at 37^0C. (E) After 3 weeks immersion in water at 37^0C. (F) After 4 weeks immersion in water at 37^0C. (G) After 6 weeks immersion in water at 37^0C.

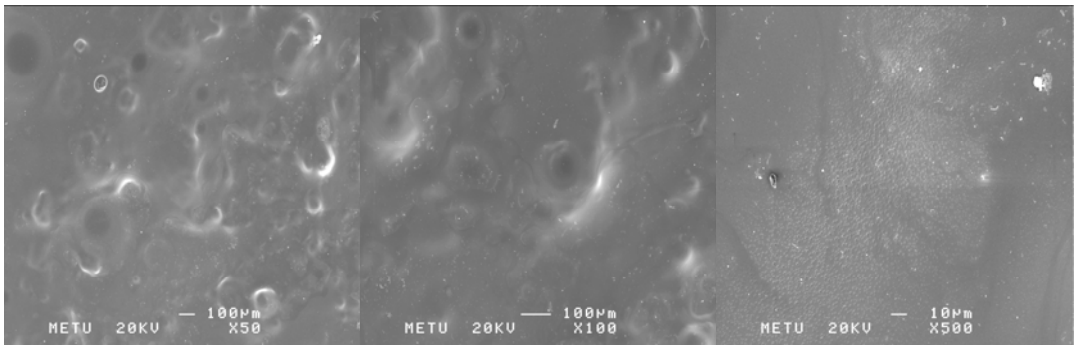

(D) After 2 weeks of drug release study

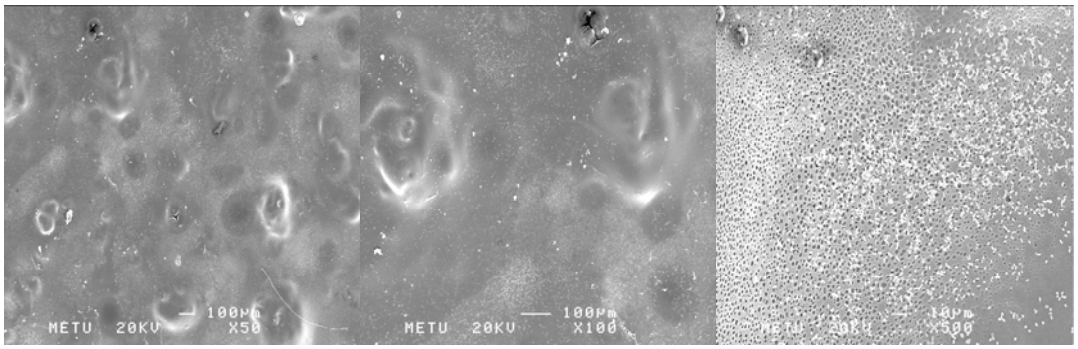

(E) After 3 weeks of drug release study

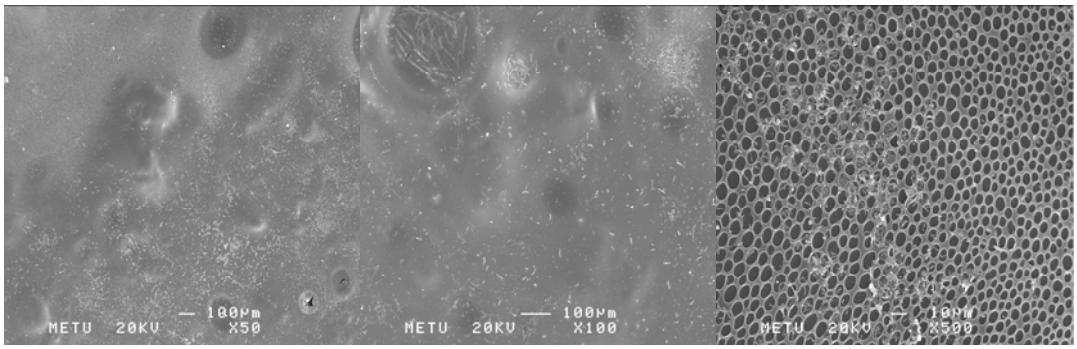

(F) After 4 weeks of drug release study

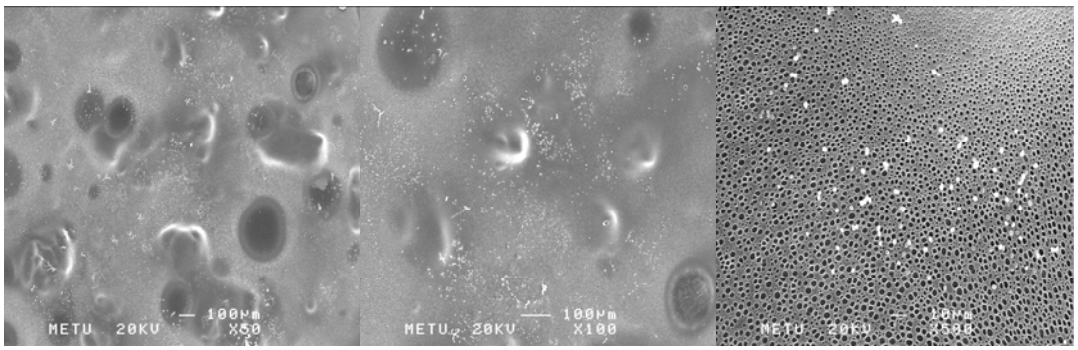

(G) After 6 weeks of drug release study

Figure 3.94 Scanning Electron Micrographs: (Cont'd…)

The surface topography of the implants seen in Figure 3.94-A was resulted in the higher loading capacity implants in comparison to the smoother implant surfaces. Also, the attachment of the films on such surfaces was stronger. For the coated implants (Figure 3.94-B), coating with polymer films was achieved and in 500x magnification, porous structure of the inert layer was obvious. This layer was controlling drug release kinetics without stopping the release. The thought was that drug release is primarily controlled by diffusion from the matrix and secondly by polymer erosion. The porous structure of the inert layer is due to chloroform evaporation. After 2 weeks of immersion in water, degradation of the polymer matrix can be seen. Surface whitening and TCP particles were obvious. Also from this time on, bacteria colonization on the samples was observed.

3.12.4.3.4 In Vivo Analysis

For in vivo analysis, drug loaded titanium implants (first coating layer with Vancomycin impregnated β-TCP (16.2% (w/w) Vancomycin, 1g) dispersed PLGA RG 504 solution in chloroform (10% w/v) and second coating layer with Polylactide L 209S solution in chloroform (5% w/v)) were placed at the dorsal muscle of six six-month native rabbits. These implants were followed for six weeks and implant surfaces and surrounding tissues investigated histologically.

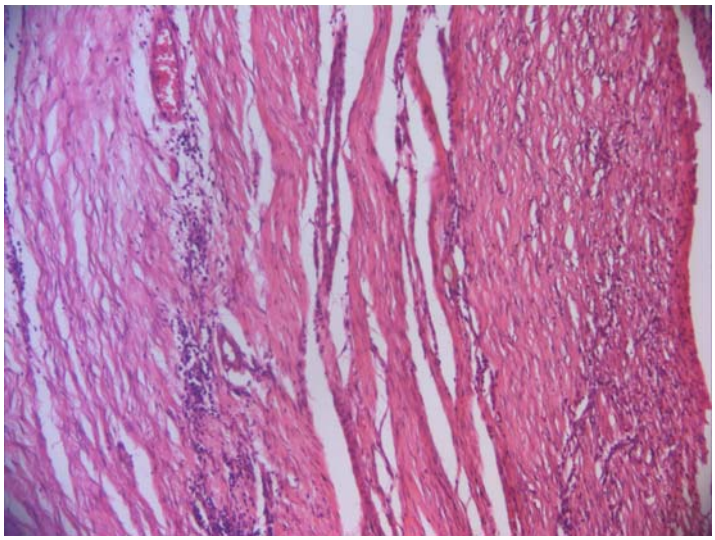

Figure 3.95 6 weeks after implantation (hematoxylin and eosin stain, x 200). No evidence for necrosis and tissue damage was observed. Implant material does not damage muscle structure

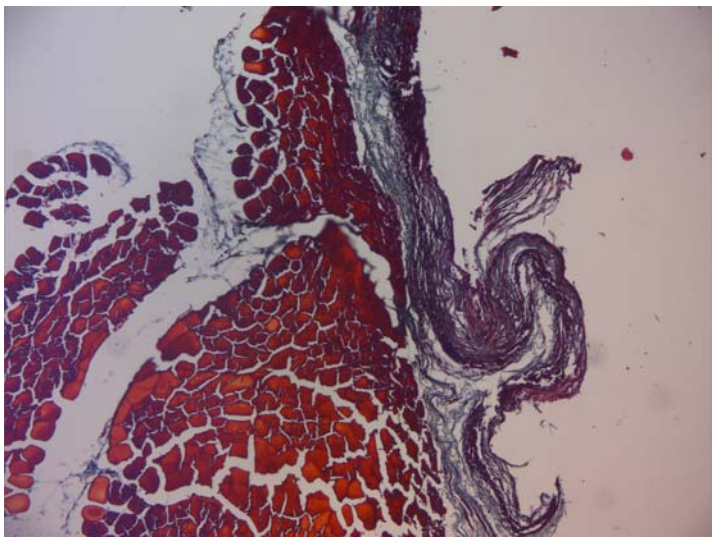

Figure 3.96 6 weeks after implantation (Masson's Trichrome stain, x 100). Ligament formation was observed in the area between implant and muscle. No macrophage formation was observed in formed ligament

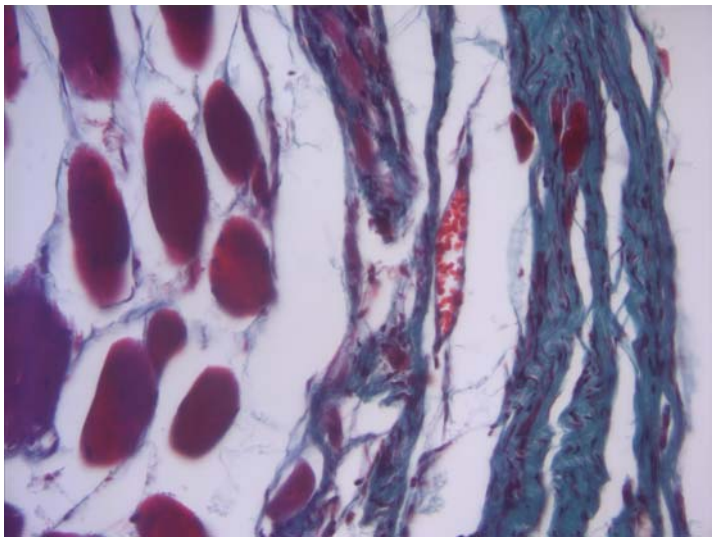

Figure 3.97 6 weeks after implantation (Masson's Trichrome stain, x 400). It was observed that implant material allowed new blood vessel formation

As a result of the in vivo applications, consistency of the implants with surrounding tissue was observed. Implants did not cause any tissue damage and no macrophage formation was detected. In addition, ligament formation in some areas was observed.

3.12.4.4 Drug Release Kinetics

In this section, controlled drug release kinetics of the in vitro analysis was investigated. For this purpose, a curve fitting analysis was performed. In order to study the mechanism of drug releases from polymer matrices, in vitro drug release data were fitted to kinetic models such as zero order, first order, Higuchi equation [187] and Korsmeyer-Peppas equation [188].

The rate equations of zero order and first order kinetics are given in the following equations (Equations 3.2 and 3.3) respectively;

$$M_t/M_\infty = kt \quad (3.2)$$

$$M_t = M_\infty e^{-kt} \quad (3.3)$$

where M_t is the amount of drug released at time t, M_∞ is the amount of drug released at infinite time and k is a release rate constant.

Higuchi equation describes the Fickian diffusion of drug and simply expressed as in the following equation (Equation. 3.4);

$$M_t/M_\infty = k_H t^{1/2} \quad (3.4)$$

where M_t/M_∞ is the drug release fraction, k_H is the Higuchi's kinetic constant and t is the release time.

Finally, Korsmeyer-Peppas equation which is widely used for describing drug release kinetics from polymeric systems is given below (Equation 3.5);

$$\log (M_t/M_\infty) = \log k + n \log t \quad (3.5)$$

where M_t/M_∞ is the drug release fraction, k is the release rate constant, t is the release time and n is the diffusional exponent describes the mechanism of drug release.

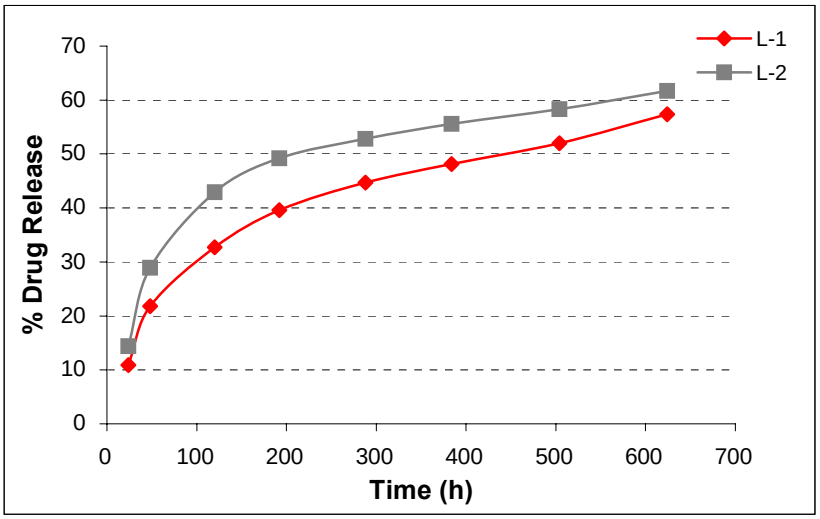

Figure 3.98 Plot of kinetic data in accordance with zero-order release model for samples L-1 and L-2

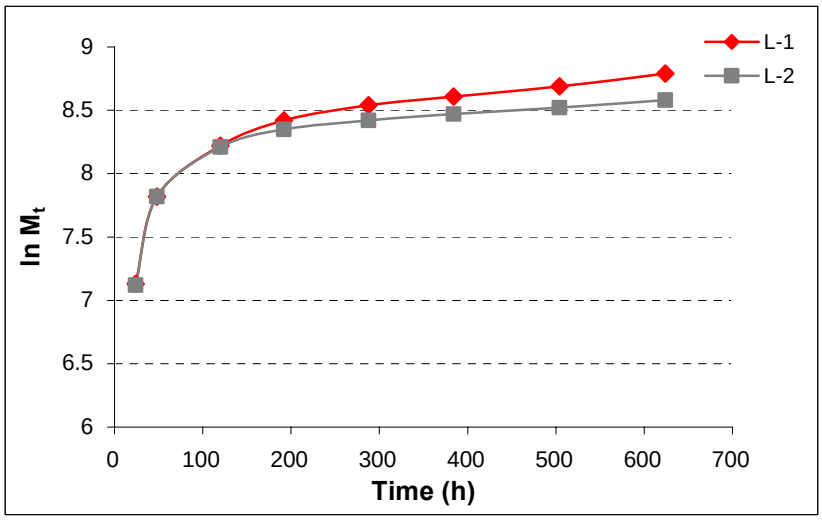

Figure 3.99 Plot of kinetic data in accordance with first-order release model for samples L-1 and L-2

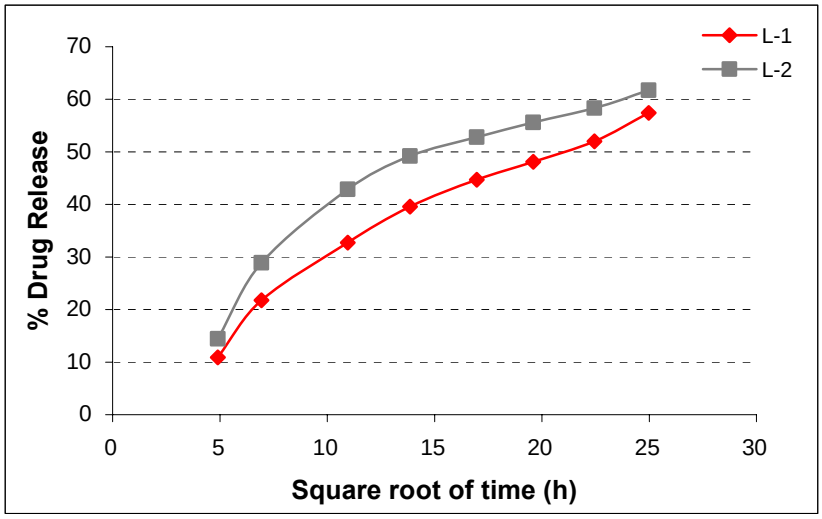

Figure 3.100 Plot of kinetic data in accordance with Higuchi release model for samples L-1 and L-2

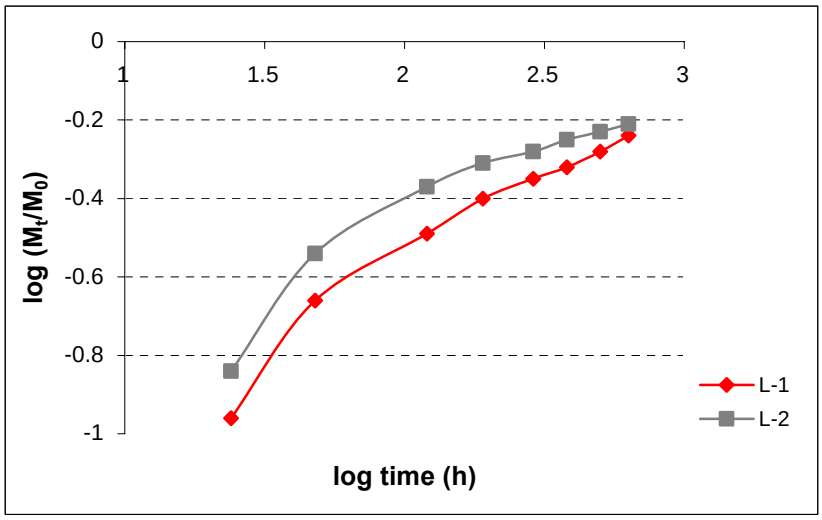

Figure 3.101 Plot of kinetic data in accordance with Korsmeyer-Peppas release model for samples L-1 and L-2

Table 3.45 Kinetic parameters for samples L-1 and L-2

Sample	Zero order		First order		Higuchi		Korsmeyer-Peppas		
Code	R^2	K_0	R^2	K_1	R^2	K_H	R^2	n	K_{KP}
L-1	0.8619	0.0673	0.6871	0.0021	0.9586	2.1412	0.9501	0.47	0.0308
L-2	0.7519	0.0674	0.5993	0.0018	0.8859	2.1162	0.9059	0.41	0.0515

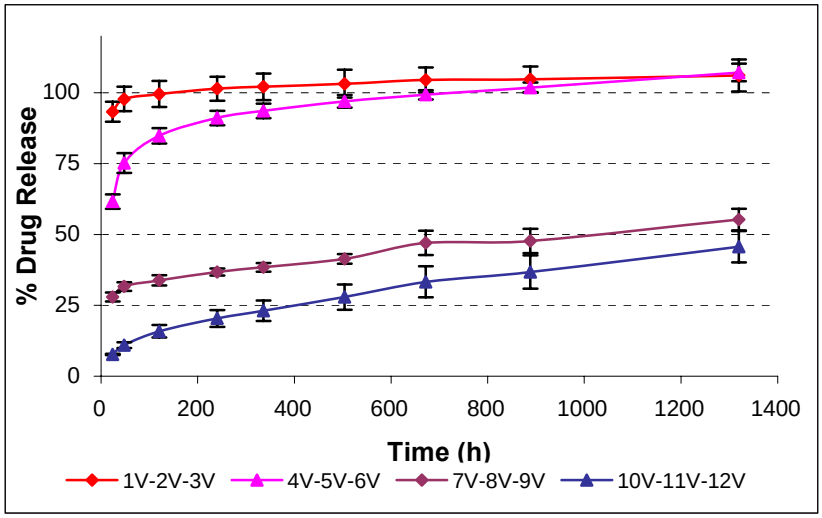

Figure 3.102 Plot of kinetic data in accordance with zero-order release model for V samples. Each result shows the mean ± SD, (n=3)

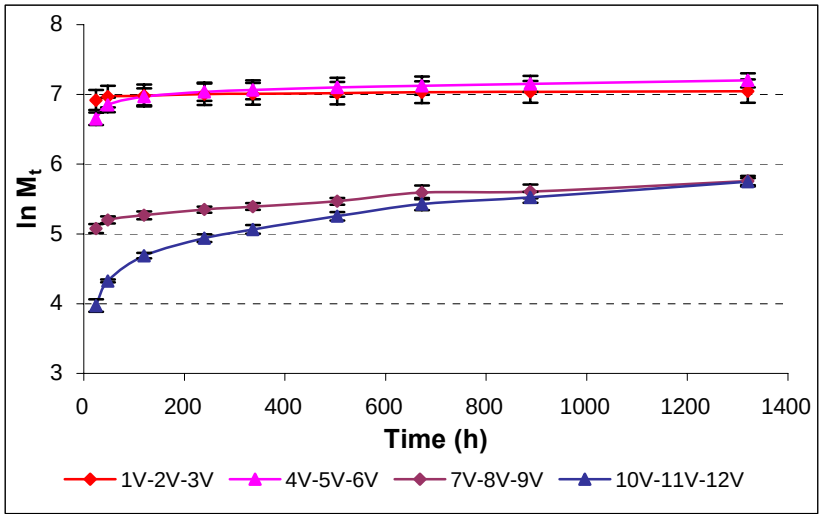

Figure 3.103 Plot of kinetic data in accordance with first-order release model for V samples. Each result shows the mean ± SD, (n=3)

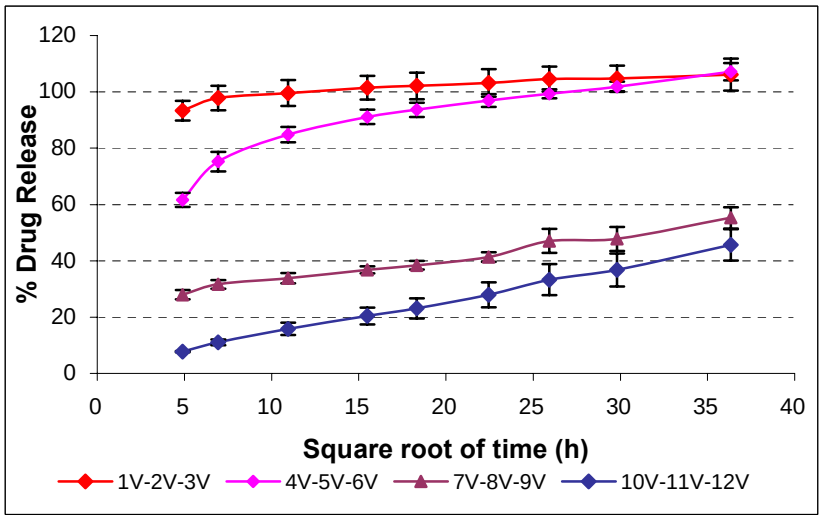

Figure 3.104 Plot of kinetic data in accordance with Higuchi release model for V samples. Each result shows the mean ± SD, (n=3)

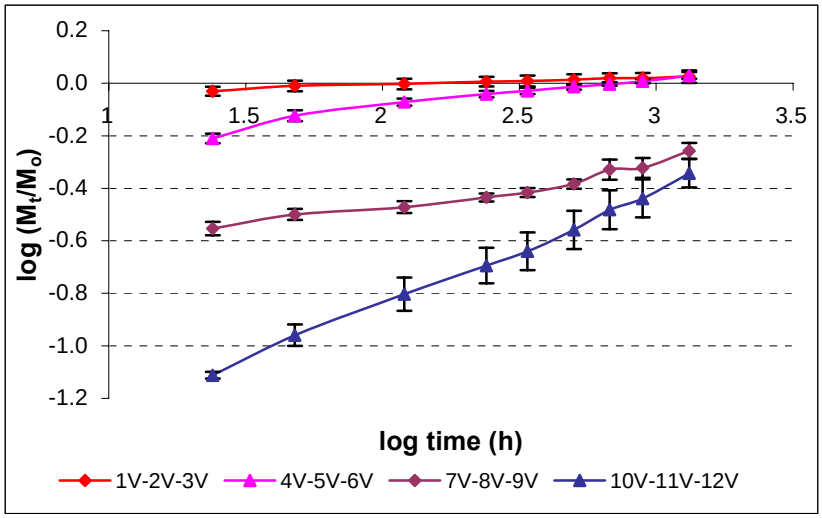

Figure 3.105 Plot of kinetic data in accordance with Korsmeyer-Peppas release model for V samples. Each result shows the mean ± SD, (n=3)

Table 3.46 Kinetic parameters for V coded samples

Kinetic model		Sample Code			
		1V-2V-3V	4V-5V-6V	7V-8V-9V	10V-11V-12V
Zero-order	R^2	0.7119	0.7036	0.9579	0.9553
	K_0	0.0078	0.0276	0.0197	0.0281
First-order	R^2	0.6938	0.6328	0.9137	0.8029
	K_1	$8x10^{-5}$	0.0003	0.0005	0.0012
Higuchi	R^2	0.8698	0.8661	0.9831	0.9975
	K_H	0.3543	1.2545	0.8171	1.1759
Korsmeyer-Peppas	R^2	0.9692	0.9541	0.9411	0.9962
	n	0.0292	0.1250	0.1555	0.4268
	K_{KP}	0.8616	0.4457	0.1653	0.0201

For biodegradable polymer matrix devices, the drug is dispersed in the matrix and drug releases from this matrix is usually diffusion and degradation controlled. With the application of inert coatings, drug diffusion rates were lowered and drug releases maintained for a longer time periods. Burst releases were reduced and both

drug release pathways became important for drug release rates.

According the results obtained, zero-order and first-order kinetics failed to explain the drug releases from samples L-1 and L-2. Korsmeyer-Peppas plot gave the highest correlation coefficient (R^2) values for these samples with n values 0.47 and 0.41. That means, drug release mechanism is Fickian diffusion and drug release is dependent to the square root of time. Higuchi plot also gave higher correlation coefficient results.

In the same manner, zero and first-order kinetics were failed to explain drug releases from samples 1V to 6V (without β-TCP). Korsmeyer-Peppas plot gave the highest R^2 values for these samples. For the rest of the samples, Higuchi and Korsmeyer-Peppas plots' gave higher R^2 values. For samples 10V-12V, Korsmeyer-Peppas plot gave R^2 value of 0.9962 with n value 0.43. In general, for β-TCP used samples, Higuchi model explained the drug release kinetics best with R^2 values of 0.9831 and 0.9975. As a result, drug release mechanism is mostly Fickian diffusion and drug release is dependent on the square root of time of release.

CHAPTER 4

CONCLUSIONS

A lot of infectious cases have been reported as a result of metal implant application to the human body. Some of them can be overcome by using medical drugs. On the other hand, most of the infections remain active without taking the infected implant, medication of the infected area and reapplication of the clean implant again. This painful process has economical and uncomfortable consequences to the patient. This study mainly includes the pathways to solve these problems.

The main purpose of this study is the production of metal implants; especially titanium based ones, coated with polymer films in which relevant drug were dispersed. The ultimate goal is to remove the necessity of painful process in infectious conditions explained above occurring in metal implant applications. Implants can be turned out to be controlled and long-lasting drug release agents with such coating applications.

Polymers investigated were soluble in water (PVAls) and chloroform (PCL, RG 504, L 209S and LC 703) and all the drugs were soluble in water. Coating weights for PVAls for different surface prepared metal implants were almost the same. The result of coating density is 30 g/m^2 in average. For the chosen loading applications, no homogeneous coatings were achieved with polished surfaced implants. Among the polymers investigated, PVAls did not give promising long release profiles in aqueous medium therefore they were not used for further investigations. The PCL also was not found to be suitable biodegradable coating

material.

In the indent prototyping applications to the implant surfaces, it was observed that loading amounts of drug plus polymer can be increased. Since the polymer coatings included drugs, large amounts of drugs can be loaded to the same implants with indentations. It was found that 10^7 cycling loading on the samples of stainless steel and titanium based implant materials with and without indentation did not cause fatigue failure. For this reason, it was concluded that the indentations can be used for the plaque and screw applications. According to the results obtained from the computer simulations and virtual fatigue tests, indentations applied on the implant samples did not harm the integrity of the implant materials; therefore, such indentations can be applied to the suitable implant material in need of loading higher amounts of drug carrying polymer coatings.

In the SEM photographs of the surfaces of titanium alloys, it is found that smooth surfaces of titanium alloys become more porous when they are treated with 5 M NaOH alkaline solution at 60^0C and 48^0C followed by post heat treatments. Increasing the duration of treatments, porosity of the samples' surfaces increased. Obtaining macroporous layer on titanium alloy surfaces has major importance since the metal is not bioactive. The bioactivity of such implant materials increases by the formation of apatite layer along the surfaces when they are inserted into the body. In EDX analysis, stable amorphous sodium titanate layer was found over all of the samples' surfaces.

Hardness tests indicated that polymeric coatings had enough strength to maintain their uniformity during applications to the human body. Degradation profiles of the different polymers were used to estimate hardness order. The hardness order were found in a decreasing manner as L209S>PVAl(Mwt:31000-50000)>PVAl(Mwt:13000-23000)>RG504>PCL>LC703 for polymer coatings.

From the gloss measurements, it can be concluded that PCL and RG 504 coatings have less smooth final surface appearance than the other coatings.

Adhesion by tape tests revealed that all polymeric coatings tested were not strong enough to resist the test. L 209S and RG 504 coatings had preferable adhesional properties over the other polymer coatings.

According to lap shear tests, the best adhesional property was observed in 4 No sandpapered titanium samples with PLGA RG 504 adhesive. On the other hand, sandblasted samples had the highest adhesional force values with PL L 209S. All samples' failures occurred as adhesive failure. Strength at failure values for both polymers were high enough to resist surface detachments during application of implants to the body. PL L 209S is more viscous and has high crystalline structure; therefore, it shows good adhesional properties. However, PLGA RG 504 has higher adhesional properties on smooth or nearly smooth surfaces compared to other film forming material. With drug added adhesives, it was observed that on pure and unmodified titanium surfaces, failures occurred at very low shear stress values. Better adhesional results were observed for the surface modified samples.

The tendency observed in lap shear tests can also be seen in T-peel tests. RG 504 used samples has higher failure force values with smoother surfaces. L 209S, on the other hand, have shown higher force values with more porous surfaces. All samples' failures occurred as adhesive failure. Strength at failure values for both polymers were high enough to resist surface detachments during application of implants to the body.

In the study of degradation of polymer films, it can easily be seen that degradation of RG 504 polymer films are continuous and very fast. Intrinsic viscosity values of RG 504 in chloroform decreased to nearly 9 % of its initial value after 6 week degradation in water. Major degradation occurs in 30 days. $\overline{Mv}$ for RG 504 decreased to nearly 1.3% of its initial value after 6 weeks of degradation in water. On the other hand, degradation of L 209S polymer films is relatively slow. Intrinsic viscosity values of L 209S in chloroform decreased to nearly 75-80 % of its initial value after 6 week degradation in water. $\overline{Mv}$ for L 209S decreased to

approximately 60-70% of its initial value after 1 week of degradation in water. During the rest of the time until 6 weeks, no major change in $\overline{Mv}$ was detected.

By using the calibration curves, released drug concentrations at predetermined time intervals is calculated. In Augmentin containing L 209S and LC 703 coating implants, initial burst release was very high and no meaningful absorbance value was measured after 48 hours of drug release. In the same manner, for the Alfoxil containing polymer coatings on implant materials, most of the loaded drugs were released in one day. The remaining drugs were not enough to maintain the controlled and prolonged drug release from titanium based implants.

To solve the burst release problem faced, inert coatings were applied over the drug containing polymer layer. 1, 2 and 4 layers of RG 504 coatings over Alfoxil containing RG 504 layer were applied. These coatings are called inert since they did not contain antibiotics. A slower rate of drug release was obtained and burst release was eliminated. With increasing the number of inert coatings, drug release profiles seemed to be much slower and long-lasting. The multiple inert coatings should be applied in a fast manner to prevent the dissolution of the previously coated layers. For the Fortum loaded samples, initial release rates were reduced more with increasing the number of inert coatings. Much higher loading amounts were achieved by using macroporous surfaces (at least 40% increase in comparison to the smooth surfaces). In these studies, burst releases were also reduced and drug release durations were extended as aimed. Disk diffusion antibiotic sensitivity tests proved that drug release amounts decreased as the number of inert layers increased.

In the drug loading control experiments, in average 76 % of drug loading by weight could be achieved in comparison to the theoretical values for some of the antibiotics. Pure RG 504 coated samples give absorbance values during release times employed and it was concluded that higher drug amounts found in release experiments were as a result of contribution of degradation products of polymers to the absorbance values.

In the drug activity measurements, it was found that the activity of Fortum is time-dependent and decreases with time. With Fortum, therefore, the absorbance measurements may not reflect the actual released amount. They will underestimate the amount of drug released. On the other hand, Vancomycin activity did not change with time that is activity of Vancomycin is time-independent.

Coating of implants with Vancomycin impregnated β-TCP, dispersed in RG 504 solutions, gave promising results. Inert coating of L 209S were applied on the samples. Almost 60% of the loaded Vancomycin was released from L-coded samples in 26 days. According to the release profiles, it was estimated that Vancomycin release can last approximately 70 days. Drug releases and release profiles were also investigated by disk diffusion antibiotic tests. After these promising results, it was decided to make a thorough investigation of the effect of inert coating of L 209S and use of TCP as a drug carrying material.

Due to the long-term stability of Vancomycin in aqueous solutions The studies are concentrated on this antibiotic and, V-coded samples were prepared. For samples 1V to 6V, Vancomycin dispersed RG 504 solution was used as a coating material and drug weight was equal to the 20% of the coating weight. Samples 4V to 6V were inert coated with L 209S solution. For samples 7V to 12V, Vancomycin impregnated β-TCP dispersed RG 504 solution was used as a coating material and drug weight was equal to the 8.1% of the coating weight. Samples 10V to 12V were inert coated with L 209S solution. According to the drug release studies, burst releases for the samples 1V to 3V were obvious and most of the Vancomycin was released in a few days. For the inert coating applied samples (samples 4V to 6V) burst releases were reduced and continuous drug release profiles were obtained. However, 80-90% of the loaded drug was released in 10 days for these samples. For samples 7V to 9V, linear but burst-like release profiles were achieved and 50-60% of loaded Vancomycin was released in 55 days of release period. Burst release was reduced somewhat and release period was extended with these samples. Finally, for the inert coating applied samples (samples 10V to 12V), burst release was further reduced and linear drug release profiles with higher slope could be obtained. Also, drug release times were

further extended. The same trends were found as a result of disk diffusion antibiotic tests.

The surface topography of the samples can be seen from SEM micrographs. This topography resulted in higher loading capacity with respect to smooth surfaces and stronger attachment of polymer films onto the implant surface was achieved. The porous structure of the polymer films could be clearly seen. These pores were as a result of chloroform evaporation and helpful in controlling the drug releases from the inside polymer matrix. Impregnation of Vancomycin in TCP also reduced the initial burst release and extended the drug release time periods. Polymer degradation as a function of release time can also be seen from SEM images.

In in-vivo analysis, implants were placed at the dorsal muscle of six six-month native rabbits. These implants were followed for six weeks and implant surfaces and surrounding tissues investigated histologically. Consistency of the implants with surrounding tissue was observed. Implants did not cause any tissue damage and no macrophage formation was detected. In addition, ligament formation in some areas was observed.

In the study of the drug release kinetics, in vitro drug release data were fitted to kinetic models such as zero order, first order, Higuchi equation and Korsmeyer-Peppas equation. For the L-coded samples, zero and first order models failed to explain the drug releases. Korsmeyer-Peppas and Higuchi models were successful in explaining the drug release kinetics from these samples with high correlation coefficient values. In the same manner, Korsmeyer-Peppas and Higuchi models were successful in explaining the drug release kinetics from V-coded samples with high correlation coefficient values. Drug releases were mainly proportional with the square root of time of release.

To sum up, medical metal implants with the ability of preventing infections were designed. Desired release profiles for at least two months time period were achieved with Vancomycin impregnated β-TCP dispersed in RG 504 coating and

over it L 209S inert coating applied titanium based implants. Initial burst release, which is the major problem in such medical implants, was minimized. The integrity of coatings were tested and found to exhibit resistance to slipping of the coating layer during the application to the body. This proposed technique can be used to impart controlled drug release function to metal implants. Drug releases can be optimized for different shaped implants by changing the amount of dispersed drug or by adjusting the surface morphology of the metal substrates and by application of indentations to the implants.

CHAPTER 5

RECOMMENDATIONS

Various polymer-drug pairs were examined with respect to their controlled and sustained drug release efficiencies on metal based implant samples. From the polymers studied, drug containing poly(D,L-lactide-co-glycolide) interior coating and poly(L-lactide) inert coating over this coating was found to be the best system to achieve this purpose. Further improvement in drug release profiles were obtained by embedding the drug material into the porous structured β-TCP and using this material in the same system with polymers. This improved method was also successful for controlled drug releases from metal implants for over 2 months.

Homogeneous drug loading was achieved by using drug material dispersed in polymer solution. 10 % (w/v) poly(D,L-lactide-co-glycolide) solution in chloroform and 5 % (w/v) poly(L-lactide) solution in chloroform were viscous enough to obtain uniform polymer coatings over implant surfaces.

Polymer coatings over implant surfaces were strong enough to maintain their integrity for the process of application into the body. Their strengths were measured by using tape tests, lap shear tests and T-peel tests.

During the application of coating process, the dipping times should be held at minimum since the new applied layer can dissolve the interior layer and deform its integrity. End points of implant surfaces can be nonhomogeneous with dip coating applications. This problem can be resolved by using spray coating technique or by

using removable end points.

The experimental technique developed in this study is used for the powdered solid drugs after making suitable optimizations. Drug loadings can be adjusted by changing the drug percentages or by using more porous implant surfaces. Also, loading amounts can be increased by using different indentations on implant surfaces in question. Finally, it is concluded that metal implants for various purposes can be rendered with controlled drug release property as shown in this thesis.

For detailed clinical studies, application of coating materials over implant surfaces should be performed in a clean room. In an industrial application, spray coating systems with continuous mixing ability will be helpful in achieving homogeneous coatings. Implant surface cleaning is another important aspect for obtaining uniform coatings. γ-rays can be used for the sterilization of implants since no measurable effects of these rays on the polymer systems and drug releases were detected in our systems.

Developed drug release systems can also be used without a metal base (e.g. cold molding). The area of usage of these systems can be extended by such applications.

Finally, HPLC analysis can be done for more precise antibiotic release measurements for obtaining a final product. In vitro biocompatibility tests and in vivo infection models should be studied prior to the production of an implant material.

REFERENCES

[1] Dickers, K.J., Milroy, G.E., Huatan, H., Cameron, R.E., "The use of biodegradable polymers in drug delivery systems to provide pre-programmed release", The Drug Delivery Companies Report, Autumn/Winter 2002.

[2] Ramchandani, M., Robinson, D., "In vitro and in vivo release of ciprofloxacin from PLGA 50:50 implants", Journal of Controlled Release, 54, 167-175, 1998.

[3] Darouiche, R.O., "Treatment of infections associated with surgical implants", New England Journal of Medicine, 350; 14, 1422-1428, 2004.

[4] Lucke, M., Schmidmaier, G., Sadoni, S., Wildemann, B., Schiller, R., Haas, N.P., Raschke, M., "Gentamicin coating of metallic implants reduces implant-related osteomyelitis in rats", Bone, 32, 521-531, 2003.

[5] Price, J.S., Tencer, A.F., Arm, D.M., Bohach, G.A., "Controlled release of antibiotics from coated orthopedic implants", Journal of Biomedical Materials Research, Vol.30, 281-286, 1996.

[6] Griffith, L.G., "Polymeric Biomaterials", Acta Materialia, 48, 263-267, 2000.

[7] Bhat, S.V., "Biomaterials", Alpha Science International Ltd., 2002.

[8] Ramakrishna, S., Mayer, J., Wintermantel, E., Leong, K.W., "Biomedical applications of polymer-composite materials: a review", Composites Science and Technology, 61, 1189-1224, 2001.

[9] Hildebrand, H.F., Blanchemain, N., Mayer, G., Chai, F., Lefebvre, M., Boschin, F., "Surface coatings for biological activation and functionalization of medical devices", Surface & Coatings Technology, 200, 6318–6324, 2006.

[10] Park, J.B., Bronzino, J.D., "Biomaterials Principles and Applications", CRC Press LLC, 2003.

[11] Ratner, B.D., Hoffman, A.S., Schoen, F.J., Lemons, J.E., "Biomaterials Science, An Introduction to Materials in Medicine", Academic Press, 1996.

[12] Ebewele, R.O., "Polymer Science and Technology", CRC Press LLC, 2000.

[13] Stuart, B.H., "Polymer Analysis", John Wiley & Sons, 2002.

[14] Billmeyer Jr., F.W., "Textbook of Polymer Science", John Wiley & Sons, 1984.

[15] Fried, J.R., "Polymer Science and Technology", Prentice Hall PTR, 1995.

[16] Young, R.J., Lovell, P.A., "Introduction to Polymers", Chapman & Hall, 2nd Ed., 1991.

[17] Seymour, R.B., "Introduction to Polymer Chemistry", McGraw-Hill, 1971.

[18] Munk, P., Aminabhavi, T.M., "Introduction to Macromolecular Science", John Wiley & Sons, 2nd Ed., 2002.

[19] Sun, S.F., "Physical Chemistry of Macromolecules", John Wiley & Sons, 2nd Ed., 2004.

[20] Carraher Jr., C.E., "Polymer Chemistry, An Introduction", Marcel Dekker Inc., 4th Ed., 1996.

[21] Tağıt, O., "Development and analysis of controlled release polymeric rods containing vancomycin", Master Thesis, METU, January 2005.

[22] Lloyd, A.W., "Interfacial bioengineering to enhance surface biocompatibility", Medical Device Technology, 13: 18-21, 2002.

[23] Nair, L.S., Laurencin, C.T., "Biodegradable polymers as biomaterials", Progress in Polymer Science, 32, 762-798, 2007.

[24] Lewis, D.H., in: Chasin, M., Lagner, R., (Eds.), "Biodegradable Polymers as Drug Delivery Systems", Vol. 45, Marcel Dekker, New York, 1-8, 1990.

[25] Lu, Y., Chen, S.C., "Micro and nano-fabrication of biodegradable polymers for drug delivery", Advanced Drug Delivery Reviews, 56, 1621-1633, 2004.

[26] Vert, M., "Aliphatic polyesters: Great degradable polymers that cannot do everything", Biomacromolecules, 6, 538-546, 2005.

[27] Lactide/Glycolide copolymers: Review on toxicity, biocompatibility and clinical application (data up to 1999), Ghimas S.p.A, 1-17.

[28] Bohlmann, G.M., "Handbook of Biodegradable Polymers, Chapter 6: General characteristics, processability, industrial applications and market evolution of biodegradable polymers", Bastioli, C. (Ed), Rapra Technology Limited, United Kingdom, 191-192, 2005.

[29] Huh, K.M., Cho, Y.W., Park, K., "PLGA-PEG block copolymers for drug formulations", Drug Delivery Technology, Vol.3, No.5, July/August 2003.

[30] Kovalchuk, A., Fischer, W., Epple, M., "Controlled release of goserelin from microporous polyglycolide and polylactide", Macromolecular Bioscience, 5, 289-298, 2005.

[31] Kranz, H., Ubrich, N., Maincent, P., Bodmeier, R., "Physicomechanical properties of biodegradable poly(D,L-lactide) and poly(D,L-lactide-co-glycolide) films in the dry and wet states", Journal of Pharmaceutical Sciences, Vol.89, 1558-1566, 2000.

[32] Drumright, R.E., Gruber, P.R., Henton, D.E., "Polylactic acid technology", Advanced Materials, 12, No.23, 1841-1846, 2000.

[33] Vert, M., Christel, P., Chabot, F., Leray, J., Hastings, G.W., Ducheyne, P., (Eds.), Macromolecular Biomaterials, CRC Press, Boca Raton., 119-142, 1984.

[34] Gunatillake, P.A., Adhikari, R., "Biodegradable synthetic polymers for tissue engineering", European Cells and Materials, Vol.5, 1-16, 2003.

[35] Williams, D.F., Mort, E., "Enzyme-accelerated hydrolysis of polyglycolic acid", Journal of Bioengineering, 1, 231-238, 1977.

[36] In't Veld, P.J.A., Velner, E.M., Van De Witte, P., Hamhuis, J., Dijkstra, P.J., Feijen, J., "Melt block copolymerization of ε-caprolactone and L-lactide", Journal of Polymer Science Part A: Polymer Chemistry, Vol.35, 219-226, 1997.

[37] Storey, R.F., Taylor, A.E., "Effect of stannous octoate on the composition, molecular weight, and molecular weight distribution of ethylene glycol-initiated poly(ε-caprolactone)", Journal of Macromolecular Science, Part A: Pure and Applied Chemistry, A35(5), 723-750, 1998.

[38] Kronenthal, R.L., "Biodegradable polymers in medicine and surgery", Polymer Science and Technology, Vol.8: 119-137, 1975.

[39] Holland, S.J., Tighe, B.J., "Biodegradable polymers. In: Advances in pharmaceutical science", Academic Press, London, Vol.6, 101-164, 1992.

[40] Middleton, J.C., Tipton A.J., "Synthetic biodegradable polymers as orthopedic devices", Biomaterials, 21, 2335-2346, 2000.

[41] Gabelnick, H.L., "Long acting steroid contraception. In: Advances in human fertility and reproductive endocrinology", Mishell Jr., D.R., Ed. Raven Press, New York, Vol.3, 149-173, 1983.

[42] Baimark, Y., Molloy, R., "Synthesis and characterization of poly(L-lactide-co-ε-caprolactone) copolymers: Effects of stannous octoate initiator and diethylene glycol coinitiator concentrations", ScienceAsia, 30, 327-334, 2004.

[43] Schindler, A., Jeffcoat, R., Kimmel, G.L., Pitt, C.G., Wall, M.E., Zweidinger, R., "Biodegradable polymers for sustained drug delivery, In: Contemporary topics in polymer science", Vol.2 (Eds.) Pearce, J.R., Schaefger, E.M., Plenum, New York, USA, 251-289, 1977.

[44] Ge, H., Hu, Y., Yang, S., Jiang, X., Yang, C., "Preparation, characterization and drug release behaviors of drug-loaded ε-caprolactone/L-lactide nanoparticles", Journal of Applied Polymer Science, Vol.75, 874-882, 2000.

[45] Nakamura, T., Shimizu, Y., Matsui, T., Okumura, N., Hyon, S.H., Nishiya, K., "A novel bioabsorbable monofilament surgical suture made from (ε-caprolactone, L-lactide) copolymer, In: Degradation Phenomena in Polymeric Materials" (Eds.) Planck, H., Dauner, M., Renardy M., Springer-Verlag, Berlin, Germany, 153-162, 1992.

[46] Tomihata, K., Suzuki, M., Oka, T. and Ikada, Y., "A new resorbable monofilament suture", Polymer Degradation and Stability, 59, 13-18, 1998.

[47] Den Dunnen, W.F.A., Van der Lei, B., Robinson, P.H., Holwerda, A., Pennings, A.J., Schakenraad, J.M., "Biological performance of a degradable poly(lactic acid-ε-caprolactone) nerve guide: Influence of tube dimensions", Journal of Biomedical Materials Research, 29, 757-766, 1995.

[48] Jeong, S.I., Kim, B-S., Kang, S.W., Kwon, J.H., Lee, Y.M., Kim, S.H., Kim, Y.H., "In vivo biocompatibilty and degradation behavior of elastic poly(L-lactide-co-ε-caprolactone) scaffolds", Biomaterials, 25, 5939–5946, 2004.

[49] Chiellini, E., Corti, A., D'Antone, S., Solaro, R., "Biodegradation of poly (vinyl alcohol) based materials", Progress in Polymer Science, 28, 963–1014, 2003.

[50] Hay, J.M., Lyon, D., "Vinyl alcohol: a stable gas phase species", Nature, 216, 790-1, 1967.

[51] Mayer, J.M., Kaplan, D.L., "Biodegradable materials: Balancing degradability and performance", Trends in Polymer Science, 2, 7, 227, 1994.

[52] Matsumura, S., Maeda, S., Takahashi, J., Yoshikawa, S., Japanese Journal of Polymer Science and Technology, Kobunshi Robunshu, 45, 4, 317, 1988.

[53] Park, J.B., Lakes, R.S., "Biomaterials - An Introduction, 2nd Ed., Plenum Pres, New York, 1992.

[54] Lemons, J.E., "Ceramics: Past, Present, and Future", Bone, Vol.19, No.1, Supplement, 121S-128S, 1996.

[55] Loher, S., Reboul, V., Brunner, T.J., Simone, M., Dora, C., Neuenschwander, P., Stark, W.J., "Improved degradation and bioactivity of amorphous aerosol derived tricalcium phosphate nanoparticles in poly(lactide-co-glycolide)", Nanotechnology, 17, 2054-2061, 2006.

[56] Legeros, R.Z., Lin, S., Rohanizadeh, R., Mijares, D., Legeros, J.P., "Biphasic calcium phosphate bioceramics: preparation, properties and applications", Journal of Materials Science: Materials in Medicine, 14, 201-209, 2003.

[57] Ogose, A., Hotta, T., Kawashima, H., Kondo, N., Gu, W., Kamura, T., Endo, N., "Comparison of hydroxyapatite and beta tricalcium phosphate as bone substitutes after excision of bone tumors", Journal of Biomedical Materials Research Part B: Applied Biomaterials, Vol.72B, 94–101, 2005.

[58] Yamada, S., Heymann, D., Bouler, J.-M., Daculsi, G., "Osteoclastic resorption of calcium phosphate ceramics with different hydroxyapatite/β-tricalcium phosphate ratios", Biomaterials, 18, 1037-1041, 1997.

[59] Shimazaki, K., Mooney, V., "Comparative study of porous hydroxyapatite and tricalcium phosphate as bone substitute", Journal of Orthopaedic Research, 3:301-310, 1985.

[60] Gbureck, U., Hölzel, T., Biermann, I., Barralet, J.E., Grover, L.M., "Preparation of tricalcium phosphate/calcium pyrophosphate structures via rapid prototyping", Journal of Materials Science: Materials in Medicine, 19:1559-1563, 2008.

[61] Yin, Y., Ye, F., Cui, J., Zhang, F., Li, X., Yao, K., "Preparation and characterization of macroporous chitosan-gelatin/β-tricalcium phosphate composite scaffolds for bone tissue engineering", Journal of Biomedical Materials Research, 67A: 844-855, 2003.

[62] Tanimoto, Y., Nishiyama, N., "Preparation and physical properties of tricalcium phosphate laminates for bone-tissue engineering", Journal of Biomedical Materials Research, 85A: 427-433, 2008.

[63] Furuzono, T., Walsh, D., Yasuda, S., Sato, K., Tanaka, J., Kishida, A., "Preparation of plated β-tricalcium phosphate containing hydroxyapatite for use in bonded inorganic-organic composites", Journal of Materials Science, 40, 2595-2597, 2005.

[64] Park, Y.M., Ryu, S.C., Yoon, S.Y., Stevens, R., Park, H.C., "Preparation of whisker-shaped hydroxyapatite/β-tricalcium phosphate composite", Materials Chemistry and Physics, 109, 440-447, 2008.

[65] Metsger, S., Driskell, T.D., Paulsrud, J.R., "Tricalcium phosphate ceramic-a resorbable bone implant: Review and current status", Journal of the American Dental Association, 105:1035-1038, 1982.

[66] Lemons, J.E., Niemann, K.M.W., "Porous tricalcium phosphate ceramic for bone replacement", 25th Annual ORS Meetings, San Francisco, CA, February 20-22, 162, 1979.

[67] Biehl, V., Breme, J., "Metallic Biomaterials", Mat.-wiss. u. Werkstofftech., 32, 137-141, 2001.

[68] Hanawa, T., "Evaluation techniques of metallic biomaterials in vitro", Science and Technology of Advanced Materials, 3, 289–295, 2002.

[69] Niinomi, M., "Fatigue characteristics of metallic biomaterials", International Journal of Fatigue, 29, 992–1000, 2007.

[70] Lemons, J., Freese, H., "Metallic biomaterials for surgical implant devices", BONEZone, 7-10, 2002.

[71] Staiger, M.P., Pietak, A.M., Huadmai, J., Dias, G., "Magnesium and its alloys as orthopedic biomaterials: A review", Biomaterials, 27, 1728–1734, 2006.

[72] Niinomi, M., “Recent metallic materials for biomedical applications”, Metallurgical and Materials Transactions A, Vol.33A, 477-486, March 2002.

[73] Okazaki, Y., Gotoh, E., “Comparison of metal release from various metallic biomaterials in vitro”, Biomaterials, 26, 11–21, 2005.

[74] Fatehi, K., Moztarzadeh, F., Solati-Hashjin, M., Tahriri, M., Rezvannia, M., Ravarian, R., “In vitro biomimetic deposition of apatite on alkaline and heat treated Ti6Al4V alloy surface”, Bulletin of Materials Science, Vol.31, No.2, 101-108, April 2008.

[75] Koike, M., Cai, Z., Fujii, H., Brezner, M., Okabe, T., “Corrosion behavior of cast titanium with reduced surface reaction layer made by a face-coating method”, Biomaterials, 24, 4541-4549, 2003.

[76] Reclaru, L., Lerf, R., Eschler, P.-Y., Blatter, A., Meyer, J.-M., “Evaluation of corrosion on plasma sprayed and anodized titanium implants, both with and without bone cement”, Biomaterials, 24, 3027-3038, 2003.

[77] Moreno, L.C., Garcia-Pineros, J., Delgado-Mejia, E., “Triple alkaline treatment of titanium surfaces for calcium phosphates growth”, Brazilian Journal of Physics, Vol.36, No.3b, Sept. 2006.

[78] Kim, H.-M., Kokubo, T., Fujibayashi, S., Nishiguchi, S., Nakamura, T., “Bioactive macroporous titanium surface layer on titanium substrate”, Journal of Biomedical Materials Research, 52, 553-557, 2000.

[79] Takeuchi, M., Abe, Y., Yoshida, Y., Nakayama, Y., Okazaki, M., Akagawa, Y., “Acid pretreatment of titanium implants”, Biomaterials, 24, 1821-1827, 2003.

[80] Bocardo, J.C.E., Heredia, M.A.L, Hernandes, D.A.C., Ramirez, A.M., Robles, J.M.A., "Apatite formation on cobalt and titanium alloys by a biomimetic process", Advances in Technology of Materials and Materials Processing, 7[2], 141-148, 2005.

[81] Fini, M., Cigada, A., Rondelli, G., Chiesa, R., Giardino, R., Giavaresi, G., Aldini, N.N., Torricelli, P., Vicentini, B., "In vitro and in vivo behavior of Ca- and P-enriched anodized titanium", Biomaterials, 20, 1587-1594, 1999.

[82] Cheng, X., Filiaggi, M., Roscoe, S.G., "Electrochemically assisted co-precipitation, of protein with calcium phosphate coatings on titanium alloy", Biomaterials, 25, 5395-5403, 2004.

[83] Radin, S., Duchayne, P., "Controlled release of Vancomycin from thin sol-gel films on titanium alloy fracture plate material", Biomaterials, 28, 1721-1729, 2007.

[84] Stigter, M., Bezemer, J., de Groot, K., Layrolle, P., "Incorporation of different antibiotics into carbonated hydroxyapatite coatings on titanium implants, release and antibiotic efficacy", Journal of Controlled Release, 99, 127-137, 2004.

[85] Zilberman, M., Elsner, J.J., "Antibiotic-eluting medical devices for various applications", Journal of Controlled Release, 130, 202–215, 2008.

[86] Rutledge, B., Huyette, D., Day, D., Anglen, J., "Treatment of osteomyelitis with local antibiotics delivered via bioabsorbable polymer", Clinical Orthopaedics and Related Research, Number 411, 280-287, 2003.

[87] Ueng, S.W.N., Yuan, L.-J., Lee, N., Lin, S.-S., Liu, S.-J., Chan, E.-C., Weng, J.-H., "In vivo study of hot compressing molded 50:50 poly(DL-lactide-co-glycolide) antibiotic beads in rabbits", Journal of Orthopaedic Research, 20, 654-661, 2002.

[88] Fuchs, T., Schmidmaier, G., Raschke, M. J., Stange, R., "Bioactive-coated implants in trauma surgery", European Journal of Trauma and Emergency Surgery, 34, 60-68, 2008.

[89] Hetrick, E.M., Schoenfisch, M.H., "Reducing implant-related infections: Active release strategies", Chemical Society Reviews, 35, 780-789, 2006.

[90] Schmidmaier, G., Lucke, M., Wildemann, B., Haas, N.P., Raschke, M., "Prophylaxis and treatment of implant-related infections by antibiotic-coated implants: a review", Injury, International Journal of the Care of the Injured, 37, S105-S112, 2006.

[91] Zimmerli, W., Ochsner, P.E., "Management of infection associated with prosthetic joints", Infection, 30, 99-108, 2002.

[92] Parvizi, J., Wickstrom, E., Zeiger, A.R., Adams, C.S., Shapiro, I.M., Purtill, J.J., Sharkey, P.F., Hozack, W.J., Rothman, R.H., Hickok, N.J., "Titanium surface with biologic activity against infection", Clinical Orthopaedics and Related Research, Vol.429, 33-38, 2004.

[93] Trampuz, A., Zimmerli, W., "Antimicrobial agents in orthopaedic surgery", Drugs, 66(8), 1089-1105, 2006.

[94] Trampuz, A., Widmer, A.F., "Infections associated with orthopedic implants", Current Opinion in Infectious Diseases, Vol.19(4), 349-356, 2006.

[95] Campoccia, D., Montanaro, L., Arciola, C.R., "The significance of infection related to orthopedic devices and issues of antibiotic resistance", Biomaterials, 27, 2331-2339, 2006.

[96] Widmer, A.F., "New developments in diagnosis and treatment of infection in orthopedic implants", Clinical Infection Diseases, 33 (Suppl 2), S94-106, 2001.

[97] Haris, L.G., Mead, L., Müler-Oberlander, E., Richards, R.G., "Bacteria and cell cytocompatibility studies on coated medical grade titanium surfaces", Journal of Biomedical Materials Research, 78A, 50-58, 2006.

[98] Garvin, K., Feschuk, C., "Polylactide-polyglycolide antibiotic implants", Clinical Orthopaedics and Related Research, Number 437, 105-110, 2005.

[99] Stein, A., Bataille, J.F., Drancourt, M., Curvale, G., Argenson, J.N., Groulier, P., Raoult, D., "Ambulatory treatment of multidrug-resistant staphylococcus-infected orthopedic implants with high-dose oral co-trimoxazole (trimethoprim-sulfamethoxazole)", Antimicrobial Agents and Chemotherapy, Vol.42, No.12, 3086-3091, 1998.

[100] Drancourt, M., Stein, A., Argenson, J.N., Zannier, A., Curvale, G., Raoult, D., "Oral rifampin plus ofloxacin for treatment of staphlococcus-infected orthopedic implants", Antimicrobial Agents and Chemotherapy, Vol.37, No.6, 1214-1218, 1993.

[101] Antoci Jr, V., King, S.B., Jose, B., Parvizi, J., Zeiger, A.R., Wickstrom, E., Freeman, T.A., Composto, R.J., Ducheyne, P., Shapiro, I.M., Hickok, N.J., Adams, C.S., "Vancomycin covalently bonded to titanium alloy prevents bacterial colonization", Journal of Orthopaedic Research, 25, 858-866, 2007.

[102] Fujimura, S., Sato, T., Mikami, T., Kikuchi, T., Gomi, K., Watanabe, A., "Combined efficacy of clarithromycin plus cefazolin or vancomycin against staphylococcus aureus biofilms formed on titanium medical devices", International Journal of Antimicrobial Agents, 32, 481-484, 2008.

[103] König, D.P., Schierholz, J.M., Münnich, U., Rütt, J., "Treatment of staphylococcal implant infection with rifampicin-ciprofloxacin in stable implants", Archives of Orthopaedic and Trauma Surgery, 121, 297-299, 2001.

[104] Schierholz, J.M., Beuth, J., "Implant infections: a haven for opportunistic bacteria", Journal of Hospital Infection, 49, 87-93, 2001.

[105] Tunney, M.M., Ramage, G., Patrick, S., Nixon, J.R., Murphy, P.G., Gorman, S.P., "Antimicrobial susceptibility of bacteria isolated from orthopedic implants following revision hip surgery", Antimicrobial Agents and Chemotherapy, 3002-3005, 1998.

[106] Van de Belt, H., Neut, D., Schenk, W., Van Horn, J.R., Van der Mei, H.C., Busscher, H.J., "Infection of orthopedic implants and use of antibiotic-loaded bone cements", Acta Orthopaedica Scandinavica, 72(6), 557-571, 2001.

[107] Drancourt, M., Stein, A., Argenson, J.N., Roiron, R., Groulier, P., Raoult, D., "Oral treatment of staphylococcus spp. infected orthopaedic implants with fusidic acid or ofloxacin in combination with rifampicin", Journal of Antimicrobial Chemotherapy, 39, 235-240, 1997.

[108] Dunne Jr., W.M., Mason Jr., E.O., Kaplan, S.L., "Diffusion of rifampin and vancomycin through a staphylococcus epidermis biofilm", Antimicrobial Agents and Chemotherapy, Vol.37, No.12, 2522-2526, 1993.

[109] Antoci Jr., V., Adams, C.S., Parvizi, J., Davidson, H.M., Composto, R.J., Freeman, T.A., Wickstrom, E., Duchayne, P., Jungkind, D., Shapiro, I.M., Hickok, N.J., "The inhibition of staphylococcus epidermis biofilm formation by vancomycin-modified titanium alloy and implications for the treatment of periprosthetic infection", Biomaterials, 29, 4684-4690, 2008.

[110] Zimmerli, W., Widmer, A.F., Blatter, M., Frei, R., Ochsner, P.E., "Role of rifampin for treatment of orthopedic implant-related staphylococcal infections: A randomized controlled trial", Journal of the American Medical Association, 279(19), 1537-1541, 1998.

[111] Hudetz, D., Hudetz, S.U., Haris, L.G., Luginbühl, R., Friederich, N.F., Landmann, R., "Weak effect of metal type and ica genes on staphylococcal infection of titanium and stainless steel implants", Clinical Microbiology and Infection, Vol.14, No.12, 1135-1145, 2008.

[112] Laffer, R.R., Graber, P., Ochsner, P.E., Zimmerli, W., "Outcome of prosthetic knee-associated infection: evaluation of 40 consecutive episodes of a single centre", Clinical Microbiology and Infection, Vol.12, No.5, 433-439, 2006.

[113] Giulieri, S.G., Graber, P., Ochsner, P.E., Zimmerli, W., "Management of infection associated with total hip arthroplasty according to a treatment algorithm", Infection, 32, 222-228, 2004.

[114] Nicolau, D.P., Nie, L., Tessier, P.R., Kourea, H.P., Nightingale, C.H., "Prophylaxis of acute osteomyelitis with absorbable ofloxacin-impregnated beads", Antimicrobial Agents and Chemotherapy, Vol.42, No.4, 840-842, 1998.

[115] Sampath, S.S., Garvin, K., Robinson, D.H, "Preparation and characterization of biodegradable poly(L-lactic acid) gentamicin delivery systems", International Journal of Pharmaceutics, 78, 165-174, 1992.

[116] Naraharisetti, P.K., Lee, H.C.G., Fu, Y.-C., Lee, D.-J., Wang, C,-H., "In vitro and in vivo release of gentamicin from biodegradable discs", Journal of Biomedical Materials Research Part B: Applied Biomaterials, 77B: 329-337, 2006.

[117] Stallmann, H.P., Faber, C., Amerongen, A.V.N., Wuisman, P., "Antimicrobial peptides: review of their application in musculoskeletal infections", Injury, International Journal of the Care of the Injured, 37, S34-S40, 2006.

[118] University of Virginia Health System, www.healthsystem.virginia.edu/uvahealth/adult_bone/osteom.cfm, last visited on 11 January 2009.

[119] Wadvogel, F.A., Medoff, G., Swartz, M.N., "Osteomyelitis: a review of clinical features, therapeutic considerations and unusual aspects", The New England Journal of Medicine, 282, 198-206, 260-266, 316-322, 1970.

[120] Turner, T.M., Urban, R.M., Hall, D.J., Chye, P.C., Segretti, J., Gitelis, S., "Local and systemic levels of tobramycin delivered from calcium sulfate bone graft substitute pellets", Clinical Orthopaedics and Related Research, 437, 97-104, 2005.

[121] Yamashita, Y., Uchida, A., Yamakawa, T., Shinto, Y., Araki, N., Kato, K., "Treatment of chronic osteomyelitis using calcium hydroxyapatite ceramic implants impregnated with antibiotic", International Orthopaedics (SICOT), 22, 247-251, 1998.

[122] Liu, S.J., Tsai, Y.E., Ueng, S.W.N., Chan, E.C., "A novel solvent-free method for the manufacture of biodegradable antibiotic-capsules for a long-term drug release using compression sintering and ultrasonic welding techniques", Biomaterials, 26, 4662-4669, 2005.

[123] Liu, S.J., Chi, P.S., Lin, S.S., Ueng, S.W.N., Chan, E.C., Chen, J.K., "Novel solvent-free fabrication of biodegradable poly-lactic-glycolic acid (PLGA) capsules for antibiotics and rhBMP-2 delivery", International Journal of Pharmaceutics, 330, 45-53, 2007.

[124] Chang, H.-I., Perrie, Y., Coombes, A.G.A., "Delivery of the antibiotic gentamicin sulphate from precipitation cast matrices of polycaprolactone", Journal of Controlled Release, 110, 414-421, 2006.

[125] Liu, S.J., Ueng, S.W.N., Chan, E.C., Lin, S.S., Tsai, C.H., Wei, F.C., Shih, C.H., "In vitro elution of vancomycin from biodegradable beads", Journal of Biomedical Materials Research Part B: Applied Biomaterials, 48, 613-620, 1999.

[126] Cevher, E., Orhan, Z., Mülazımoğlu, L., Şensoy, D., Alper, M., Yıldız, A., Özsoy, Y., "Characterization of biodegradable chitosan microspheres containing vancomycin and treatment of experimental osteomyelitis caused by methicillin-resistant Staphylococcus aureus with prepared microspheres", International Journal of Pharmaceutics, 317, 127-135, 2006.

[127] Gitelis, S., Brebach, G.T., "The treatment of chronic osteomyelitis with a biodegradable antibiotic-impregnated implant", Journal of Orthopaedic Surgery, 10(1), 53-60, 2002.

[128] Wu, P., Grainger, D.W., "Drug/device combinations for local therapies and infection prophylaxis", Biomaterials, 27, 2450-2467, 2006.

[129] Benoit, M.-A., Mousset, B., Delloye, C., Bouillet, R., Gillard, J., "Antibiotic-loaded plaster of Paris implants coated with poly lactide-co-glycolide as a controlled release delivery system for the treatment of bone infections", International Orthopaedics (SICOT), 21, 403-408, 1997.

[130] Garvin, K.L., Miyano, J.A., Robinson, D., Giger, D., Novak, J., Radio, S., "Polylactide/polyglycolide antibiotic implants in the treatment of osteomyelitis. A canine model", The Journal of Bone and Joint Surgery, 76, 1500-1506, 1994.

[131] Korkusuz, F., Uchida, A., Shinto, Y., Araki, N., Inoue, K., Ono, K., "Experimental implant-related osteomyelitis treated by antibiotic-calcium hydroxyapatite ceramic composites", The Journal of Bone and Joint Surgery [Br], 75-B, 111-114, 1993.

[132] Sasaki, S., Ishii, Y., "Apatite cement containing antibiotics: efficacy in treating experimental osteomyelitis", Journal of Orthopaedic Science, 4, 361-369, 1999.

[133] Ruszczak, Z., Friess, W., "Collagen as a carrier for on-site delivery of antibacterial drugs", Advanced Drug Delivery Reviews, 55, 1679-1698, 2003.

[134] Hanssen, A.D., "Session IV: Local Antibiotic Delivery Systems, Local antibiotic delivery vehicles in the treatment of musculoskeletal infection", Clinical Orthopaedics and Related Research, 437, 91-96, 2005.

[135] Gürsel, I., Korkusuz, F., Türesin, F., Alaeddinoğlu, N.G., Hasırcı, V., "In vivo application of biodegradable controlled antibiotic release systems for the treatment of implant-related osteomyelitis", Biomaterials, 22, 73-80, 2001.

[136] Dash, A.K., Cudworth II, G.C., "Therapeutic applications of implantable drug delivery systems", Journal of Pharmacological and Toxicological Methods, 40, 1-12, 1998.

[137] Langer, R., "Drug delivery and targeting, reviews" Nature, Vol.392, Supp., 5-10, 1998.

[138] Park, K., Shalaby, W.S.W., Park, H., "Biodegradable Hydrogels for Drug Delivery", Technomic Publishing Company Inc., Lancaster, 1993.

[139] Orive, G., Hernandez, R.M., Gascon, A.R., Dominguez-Gil, A., Pedraz, J.L., "Drug delivery in biotechnology: present and future", Current Opinion in Biotechnology, 14, 659-664, 2003.

[140] Ranade, V.V., Hollinger, M.A., "Drug Delivery Systems", 2nd Edition, CRC Press LLC, 2004.

[141] Dziubla, T.D., Lowman, A.M., Torjman, M.C., Joseph, J.I., Biomimetic Materials and Design Biointerfacial Strategies, Tissue Engineering and Targeted Drug Delivery, Chapter 16: Implantable drug delivery devices, design of a biomimetic interfacial drug delivery system, (Eds.) Dillow, A.K., Lowman, A.M., Marcel Dekker Inc., 2002.

[142] Schmidmaier, G., Wildemann, B., Bail, H., Lucke, M., Fuchs, T., Stemberger, A., Flyvbjerg, A., Haas, N.P., Raschke, M., "Local application of growth factors (insulin-like growth factor-1 and transforming growth factor-β1) from a biodegradable poly(D,L-lactide) coating of osteosynthetic implants accelerates fracture healing in rats", Bone, Vol.28, No.4, 341–350, 2001.

[143] Schmidmaier, G., Wildemann, B., Stemberger, A., Haas, N.P., Raschke, M., "Biodegradable poly(D,L-Lactide) coating of implants for continuous release of growth factors", Journal of Biomedical Materials Research Part B: Applied Biomaterials, 58, 449-455, 2001.

[144] Wildemann, B., Kandziora, F., Krummrey, G., Palasdies, N., Haas, N.P., Raschke, M., Schmidmaier, G., "Local and controlled release of growth factors (combination of IGF-I and TGF-beta I, and BMP-2 alone) from a polylactide coating of titanium implants does not lead to ectopic bone formation in sheep muscle", Journal of Controlled Release, 95, 249-256, 2004.

[145] Ignatius, A.A., Betz, O., Augat, P., Claes, L.E., "In vivo investigations on composites made of resorbable ceramics and poly(lactide) used as bone graft substitutes", Journal of Biomedical Materials Research Part B: Applied Biomaterials, 58, 701–709, 2001.

[146] Sigma-Aldrich,www.sigmaaldrich.com/catalog/ProductDetail.do?N4=181609|ALDRICH&N5=SEARCH_CONCAT_PNO|BRAND_KEY&F=SPEC, last visited on 23 February 2009.

[147] Boehringer Ingelheim Pharma GmbH&Co. KG. , Certificate of Analysis, Cert. No 70573, Article No 60640915, printed on 10.12.2003.

[148] Boehringer Ingelheim Pharma GmbH&Co. KG. , Certificate of Analysis, Cert. No 59356, Article No 60640662, printed on 03.04.2003.

[149] Boehringer Ingelheim Pharma GmbH&Co. KG. , Certificate of Analysis, Cert. No 00083115, Article No 59827, printed on 08.12.2004.

[150] Boehringer Ingelheim Pharma GmbH&Co. KG. , Product Description of Resomer L 209S, submission date 26.08.2005.

[151] Boehringer Ingelheim Pharma GmbH&Co. KG. , Product Description of Resomer RG 504, submission date 04.08.2008.

[152] Boehringer Ingelheim Pharma GmbH&Co. KG. , Product Description of Resomer LC 703S, submission date 22.02.2006.

[153] Boehringer Ingelheim Pharma GmbH&Co. KG. , Thermal Properties of Selected (co-) polymers, 2008.

[154] Saito, M., Santa, T., Tsunoda, M., Hamamoto, H., Usui, N., "An automated analyzer for vancomycin in plasma samples by column-switching high-performance liquid chromatography with UV detection", Biomedical Chromatography, 18, 735–738, 2004.

[155] Plock, N., Buerger, C., Kloft, C., "Successful management of discovered pH dependence in vancomycin recovery studies: novel HPLC method for microdialysis and plasma samples", Biomedical Chromatography, 19, 237–244, 2005.

[156] Shibata, N., Ishida, M., Prasad, Y.V.R., Gao, W., Yoshikawa, Y., Takada, K., "Highly sensitive quantification of vancomycin in plasma samples using liquid chromatography–tandem mass spectrometry and oral bioavailability in rats", Journal of Chromatography B, 789, 211-218, 2003.

[157] Baranowska, I., Markowski, P., Baranowski, J., "Simultaneous determination of 11 drugs belonging to four different groups in human urine samples by reversed-phase high-performance liquid chromatography method", Analytica Chimica Acta, 570, 46–58, 2006.

[158] Diana, J., Visky, D., Hoogmartens, J., Schepdael, A.V., Adams, E., "Investigation of vancomycin and related substances by liquid chromatography/ion trap mass spectrometry", Rapid Communications in Mass Spectrometry, 20, 685–693, 2006.

[159] McCormick, M.H., Stark, W.M., Pittenger, G.E., Pittenger, R.C., McGuire, J.M., Antibiotics Annual 1955–1956, Medical Encyclopedia, Inc., New York, 606, 1956.

[160] Technical Leaflet, Vancomycin Hydrochloride Powder for Concentrate for Infusion, DBL Mayne Pharma Plc. UK, August 2004.

[161] Technical Prospectus, Alfoxil 1 g. Powder for Injection, Fako İlaçları AŞ. and Afbar İlaç Sanayi ve Ticaret AŞ.

[162] Isla, A., Arzuaga, A., Maynar, J., Gascon, A.R., Solinis, M.A., Corral, E., Pedraz, J.L., "Determination of ceftazidime and cefepime in plasma and dialysate-ultrafiltrate from patients undergoing continuous veno-venous hemodiafiltration by HPLC", Journal of Pharmaceutical and Biomedical Analysis, 39, 996-1005, 2005.

[163] Ferreira, V.S., Zanoni, M.V.B., Furlan, M., Fogg, A.G., "Differential pulse polarographic determination of ceftazidime in urine samples with and without prior extraction", Analytica Chimica Acta, 351, 105-114, 1997.

[164] Technical Prospectus, Fortum™ 1g Enjectable Flacon (i.m, i.v), GlaxoSmithKline UK, 08/21.07.2003/16/C.

[165] Technical Prospectus, Augmentin™ Intravenous 1.2 g, GlaxoSmithKline UK.

[166] Technical Prospectus, Cefamezin® 500 mg IM Injectable Powder Flacon, Eczacıbaşı Turkey, 04.09.2006.

[167] Technical Prospectus, Rocephin® 1 g i.m., i.v., Roche Pharmaceuticals, USA, August 2008.

[168] ENGRASP Worldwide Engineering Solutions, ETBX Module Library Inc., www.engrasp.com/doc/etb/mod/fm1/stresslife/stresslife_help.html,last visited on 16 March 2009.

[169] MATERIALS.CO, Materials Consultancy & Testing, www.materials.co.uk /pendulum.htm, last visited on 21 March 2009

[170] Elcometer 3030 & 3040 Persoz & Konig Pendulum Hardness Testers, Elcometer Instruments GmbH, Data Sheet, V4, 09.11.2005.

[171] ASTM Standards, D 1002-72 "Standard Test Method for Strength Properties of Adhesives in Shear by Tension Loading (Metal to Metal) (Reapproved 1983)", Annual Book of ASTM Standards, Vol.03.01, 47-50, 1983.

[172] ASTM Standards, D 1876-93 "Standard Test Method for Peel Resistance of Adhesives (T-Peel Test)", Annual Book of ASTM Standards, 115-117, 1993.

[173] ASTM Standards, D 3359-92a "Standard Test Methods for Measuring Adhesion by Tape Test", Annual Book of ASTM Standards, 447-450, 1992.

[174] Glossmeters, www.gloss-meters.com/GlossIntro.html, last visited on 3 March 2009.

[175] Pira Testing, www.pira-testing.com/pt/mt/mti_gloss.php, last visited on 14 March 2009.

[176] Silverstein, R.M., Bassler, G.C., Morrill, T.C., "Spectrometric Identification of Organic Compounds", 5th Ed., John Wiley & Sons, Inc., 1991.

[177] Sheffield Hallam University, http://teaching.shu.ac.uk/hwb/chemistry /tutorials/molspec/uvvisab1.htm, last visited on 19 March 2009.

[178] ASTM Standards, D2651-90 “Standard Guide for Preparation Metal Surfaces for Adhesive Bonding”, Annual Book of ASTM Standards, 170-175, 1991.

[179] Wikipedia, http://en.wikipedia.org/wiki/Energy-dispersive_X-ray_ spectroscopy, last access date 23 March 2009.

[180] Kokubo, T., Miyaji, F., Kim, H.-M., Nakamura, T., “Spontaneous formation of bonelike apatite layer on chemically treated titanium metals”, Journal of American Ceramic Society, 79 [4], 1127-1129, 1996.

[181] Takadama, H., Kim, H.-M., Kokubo, T., Nakamura, T., “TEM-EDX study of mechanism of bonelike apatite formation on bioactive titanium metal in simulated body fluid”, Journal of Biomedical Materials Research, 57, 441-448, 2001.

[182] Kim, H.-M., Miyaji, F., Kokubo, T., Nakamura, T., “Preparation of bioactive Ti and its alloys via simple chemical surface treatment”, Journal of Biomedical Materials Research, Vol.32, 409-417, 1996.

[183] Yan, W.-Q., Nakamura, T., Miyaji, F., “Bonding of chemically treated titanium implants to bone”, Journal of Biomedical Materials Research, 37, 267-275, 1997.

[184] Yan, W.-Q., Nakamura, T., Kawanabe, K., Nishigochi, S., Oka, M., Kokubo, T., “Apatite layer-coated titanium for use as bone bonding implants”, Biomaterials, 18, 1185-1190, 1997.

[185] Joerg, W., “N02-06: Molecular Weight of RESOMER®”, N02-06 IV versus SEC.doc., Boehringer-Ingelheim, 7 April 2006.

[186] Gores, F., Kilz, P., Radke, W., Schellhorn, M., “Characterization of the Molecular Weight Distribution of Poly(lactides)”, Polymer Standards Service GmbH and Boehringer Ingelheim Pharma KG, Poster Presentation.

[187] Higuchi, T., “Mechanism of sustained-action medication. Theoretical analysis of rate of release of solid drugs dispersed in solid matrices”, Journal of Pharmaceutical Sciences, Vol.52, Iss.12, 1145-1149, 1963.

[188] Korsmeyer, R.W., Gurny, R., Doelker, E., Buri, P., Peppas, N.A., “Mechanism of solute release from porous hydrophilic polymers”, International Journal of Pharmaceutics, 15(1), 25-35, 1983.

APPENDIX A

DSC THERMOGRAMS OF POLYMERS USED

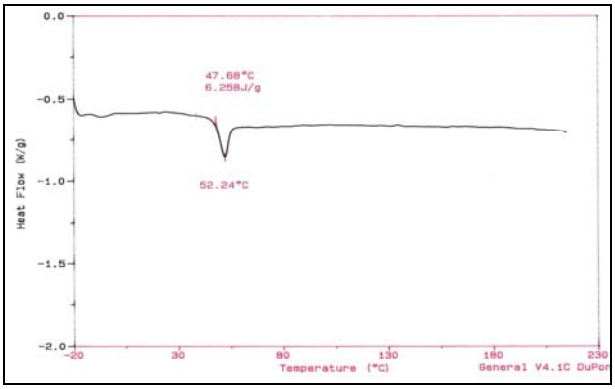

Figure A.1 DSC thermogram of poly(D,L-lactide-co-glycolide) (Resomer RG 504)

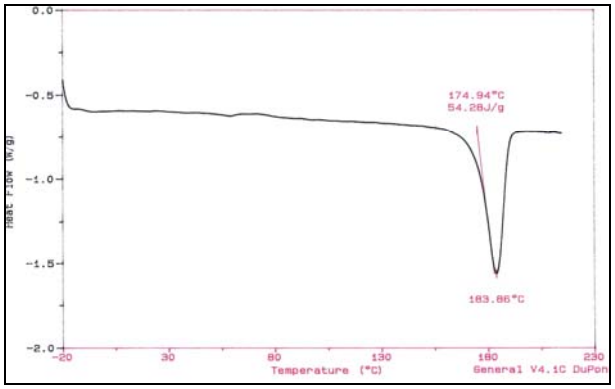

Figure A.2 DSC thermogram of poly(L-lactide) (Resomer L 209S)

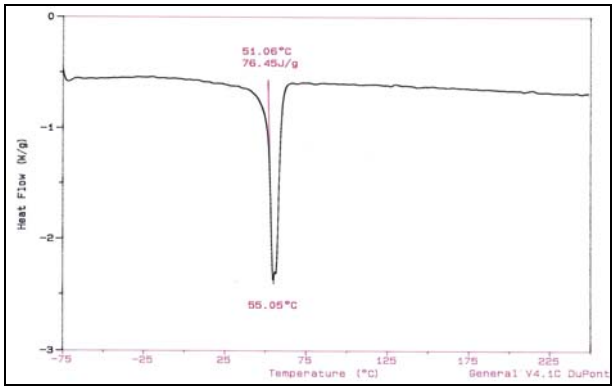

Figure A.3 DSC thermogram of poly(L-lactide-co-caprolactone) (Resomer LC 703)

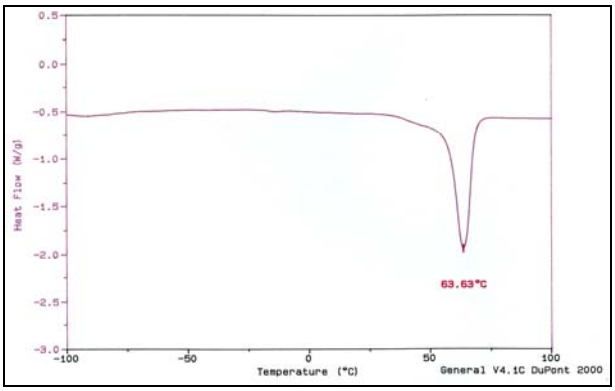

Figure A.4 DSC thermogram of polycaprolactone

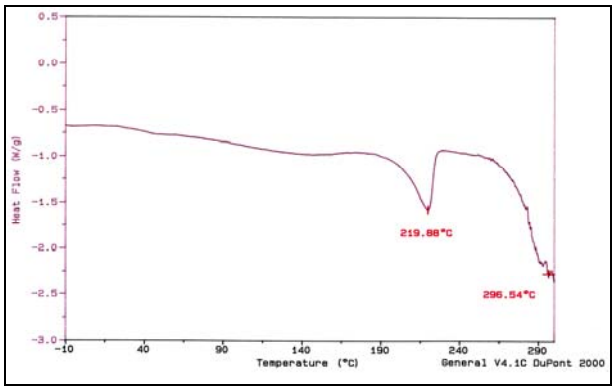

Figure A.5 DSC thermogram of poly(vinyl alcohol) ($\overline{Mw}$:13.000-23.000)

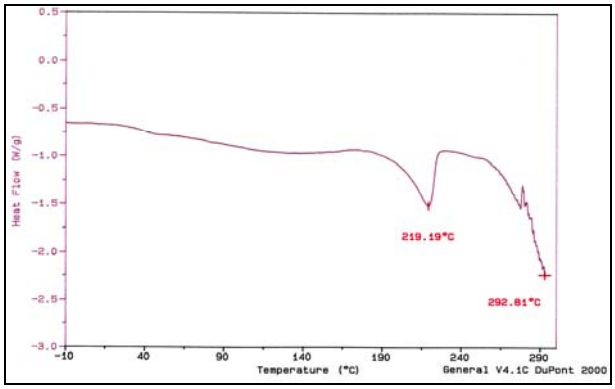

Figure A.6 DSC thermogram of poly(vinyl alcohol) ($\overline{Mw}$:31.000-50.000)

APPENDIX B

REPRESENTATION OF IMAGES OF VANCOMYCIN ITSELF AND AFTER IMPREGNATION INTO β-TCP

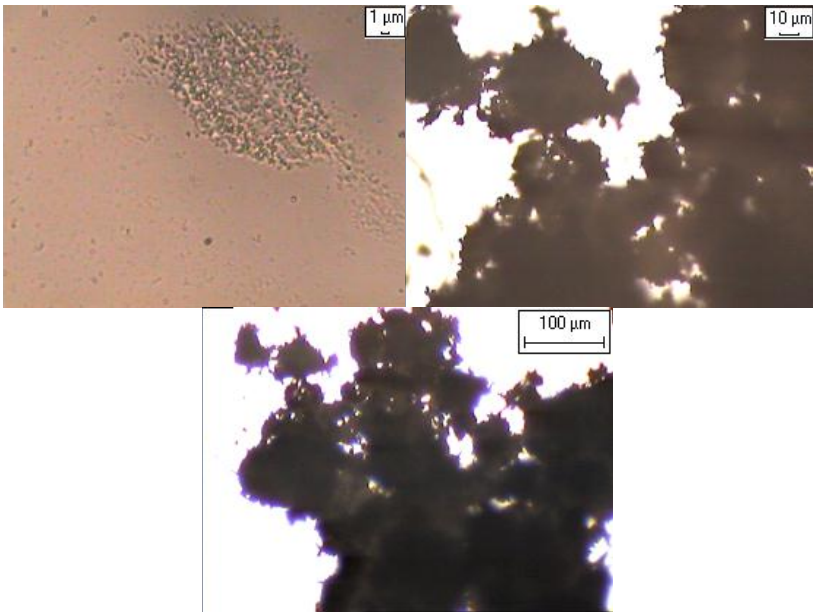

Figure B.1 Images of powder Vancomycin

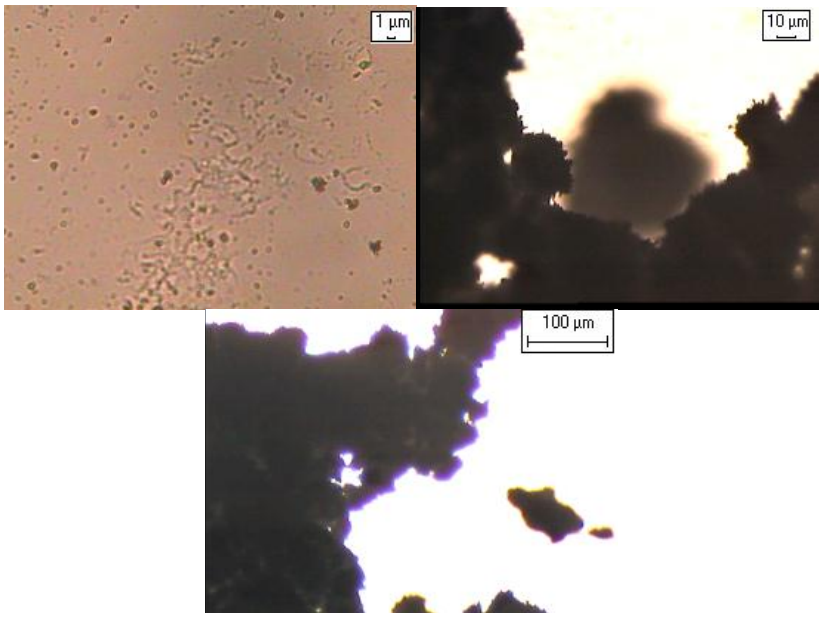

Figure B.2 Images of Vancomycin impregnated β-TCP

APPENDIX C

LAP-SHEAR TESTS

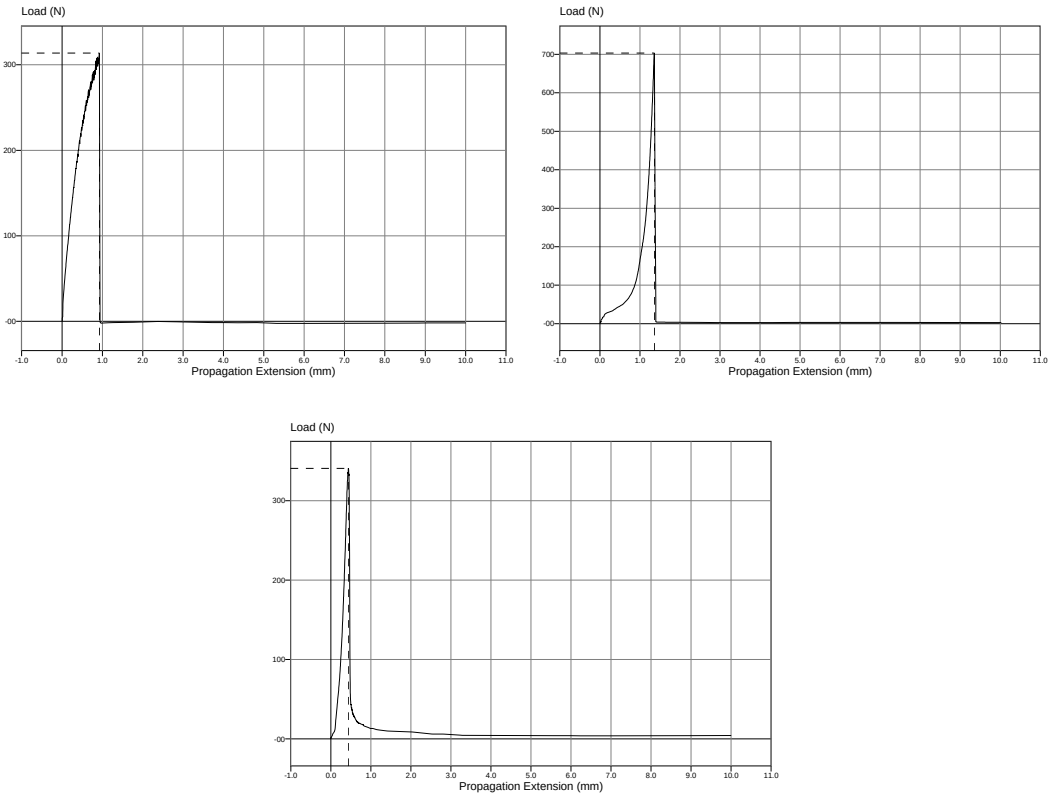

Figure C.1 Lap-shear tests for RG 504 coatings on titanium plates (no surface modification)

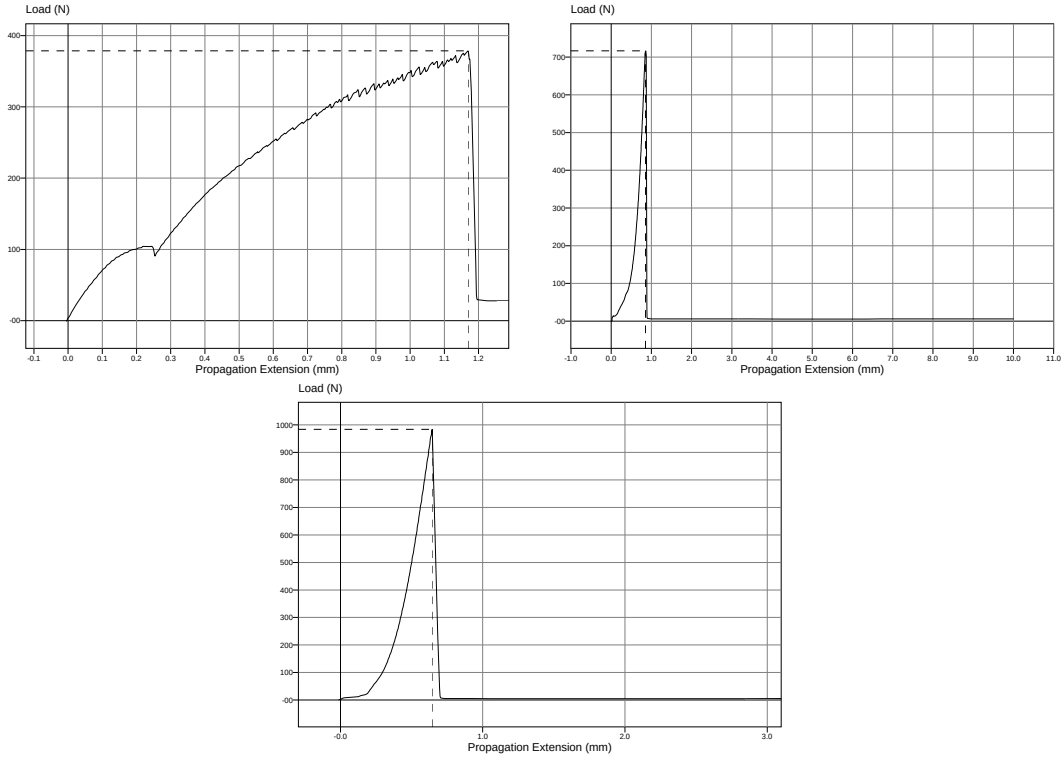

Figure C.2 Lap-shear tests for RG 504 coatings on titanium plates (4 No sandpapered)

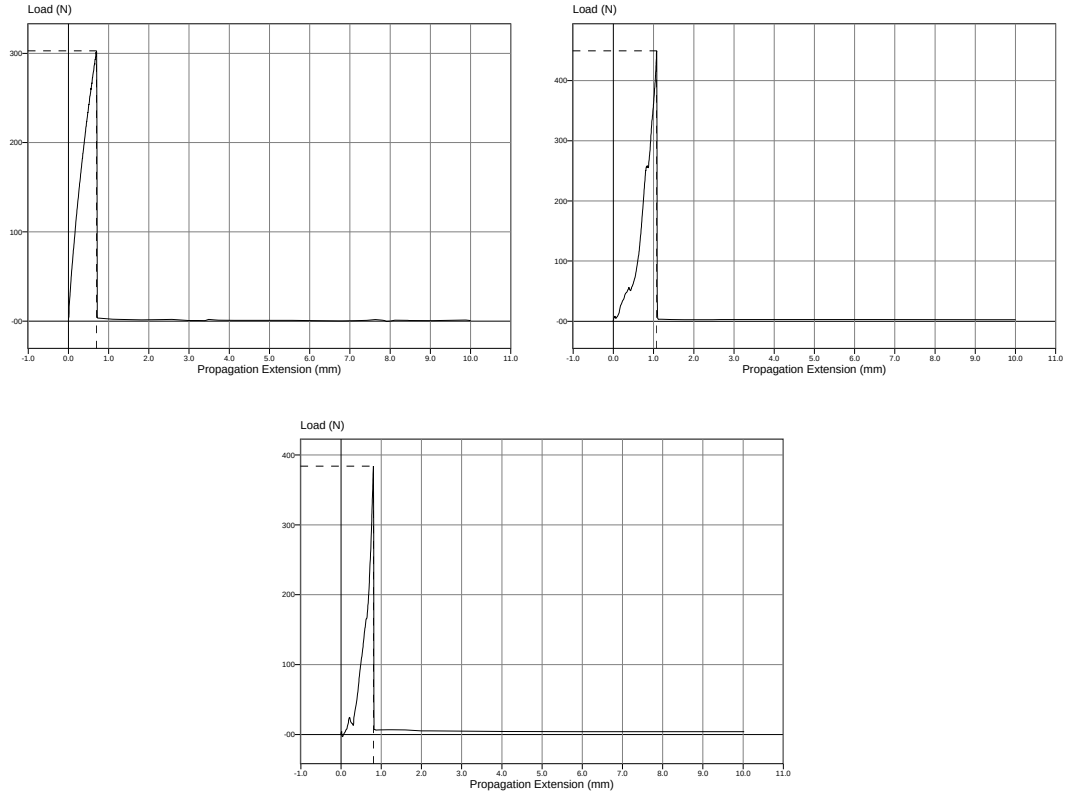

Figure C.3 Lap-shear tests for RG 504 coatings on titanium plates (wire emery)

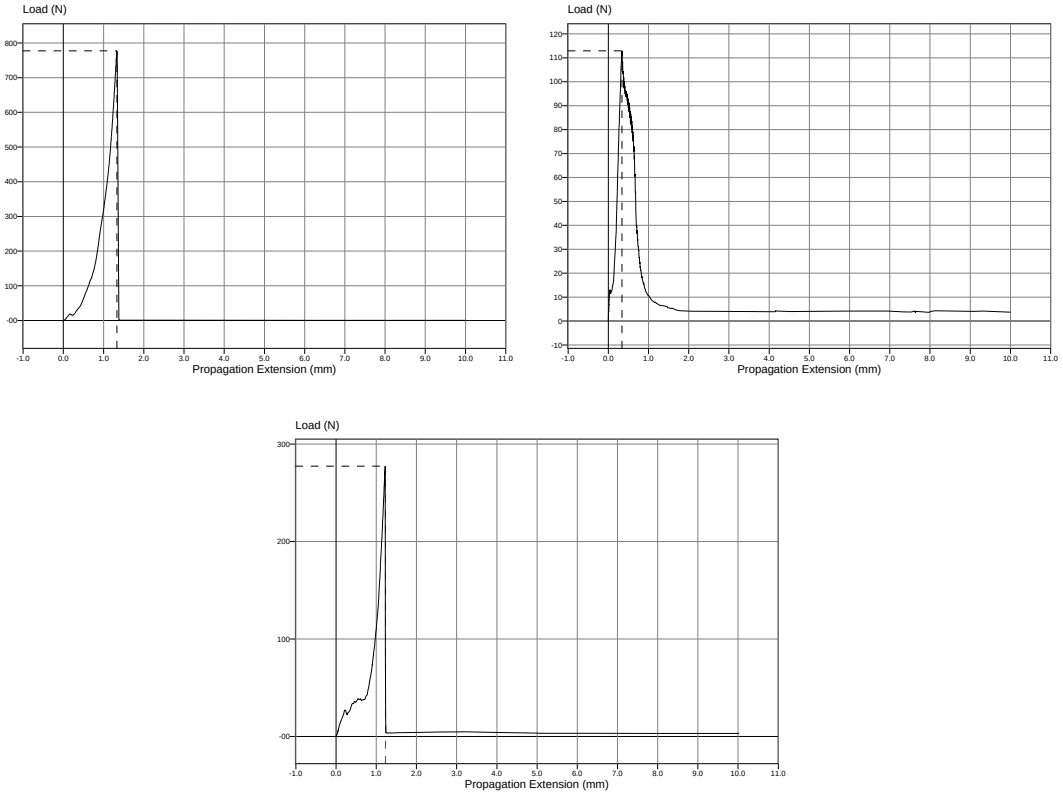

Figure C.4 Lap-shear tests for RG 504 coatings on titanium plates (sandblasted)

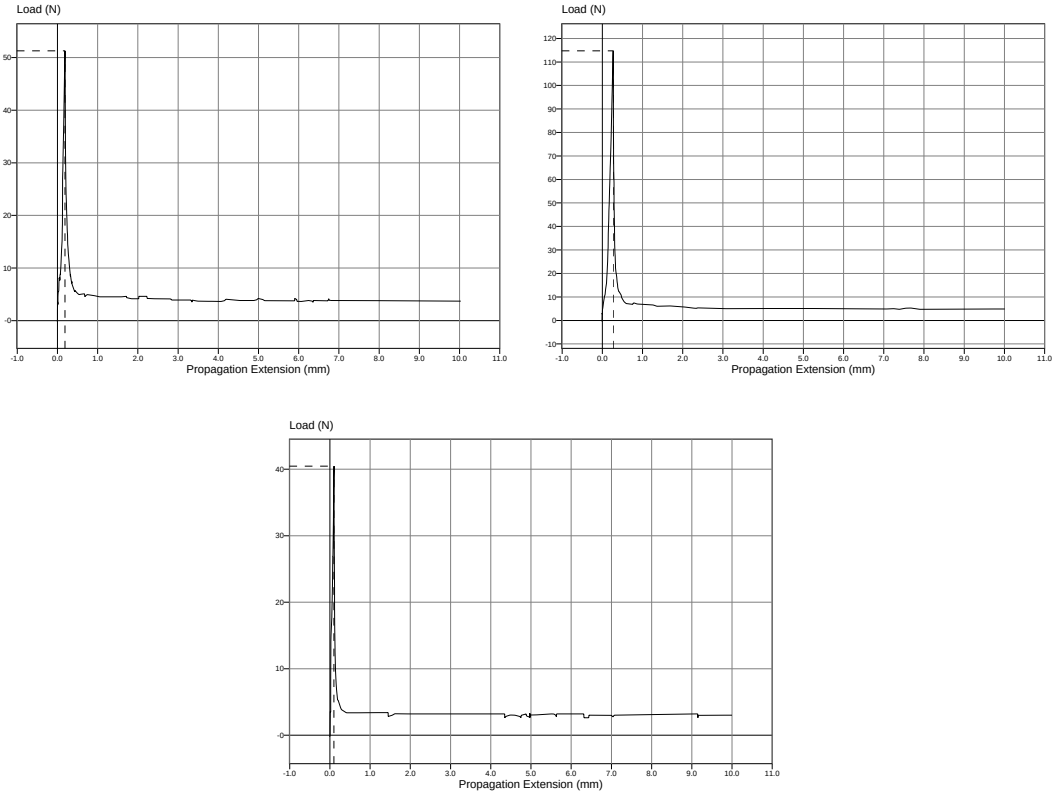

Figure C.5 Lap-shear tests for L 209S coatings on titanium plates (no surface modification)

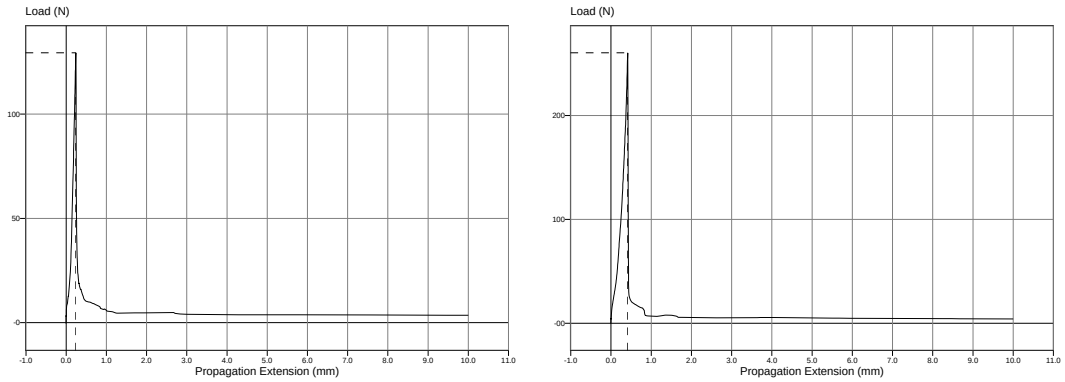

Figure C.6 Lap-shear tests for L 209S coatings on titanium plates (4 No sandpapered)

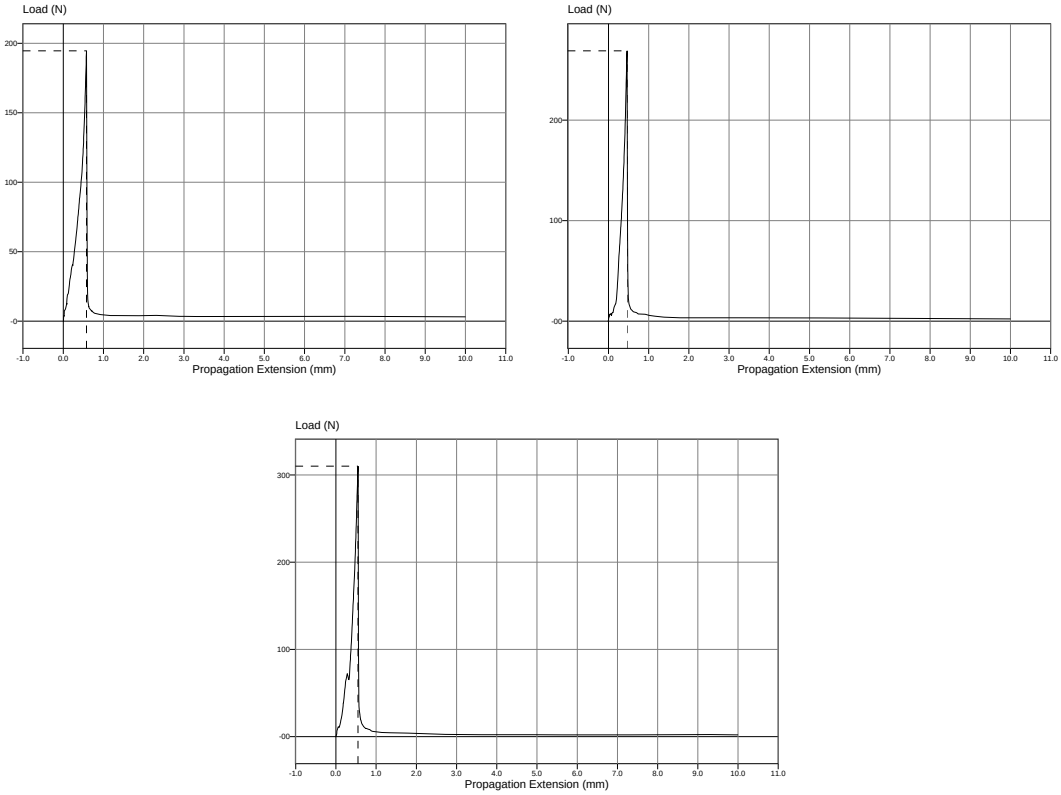

Figure C.7 Lap-shear tests for L 209S coatings on titanium plates (wire emery)

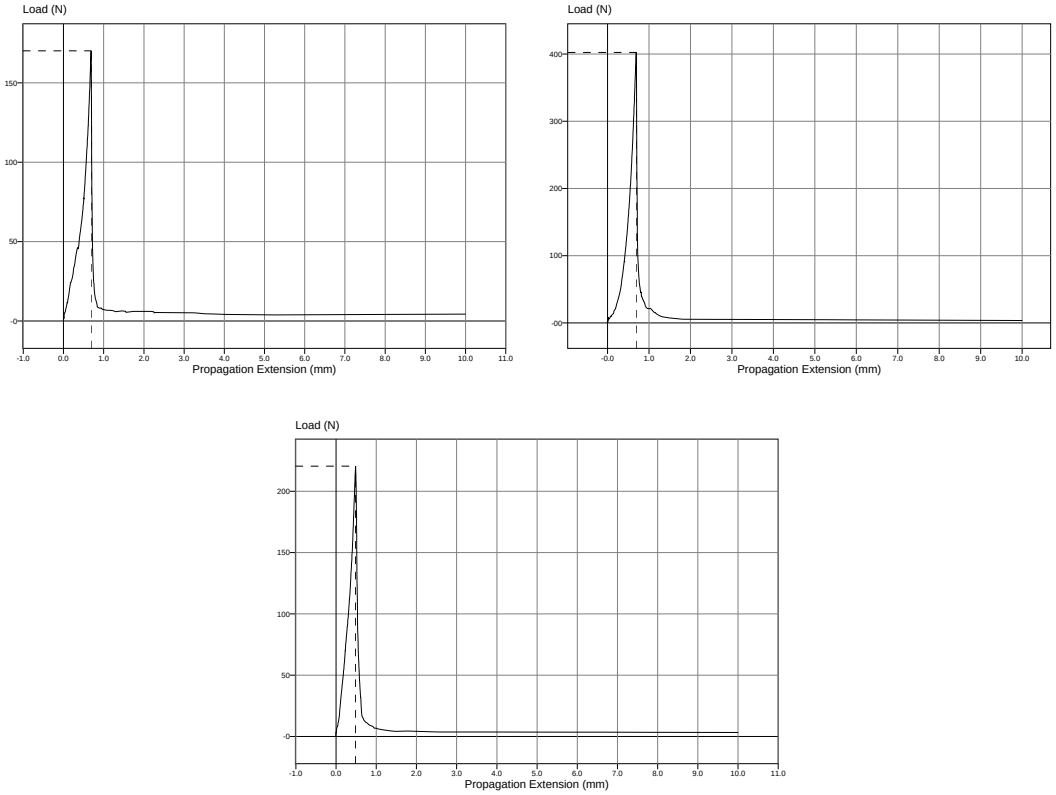

Figure C.8 Lap-shear tests for L 209S coatings on titanium plates (sandblasted)

APPENDIX D

T-PEEL TESTS

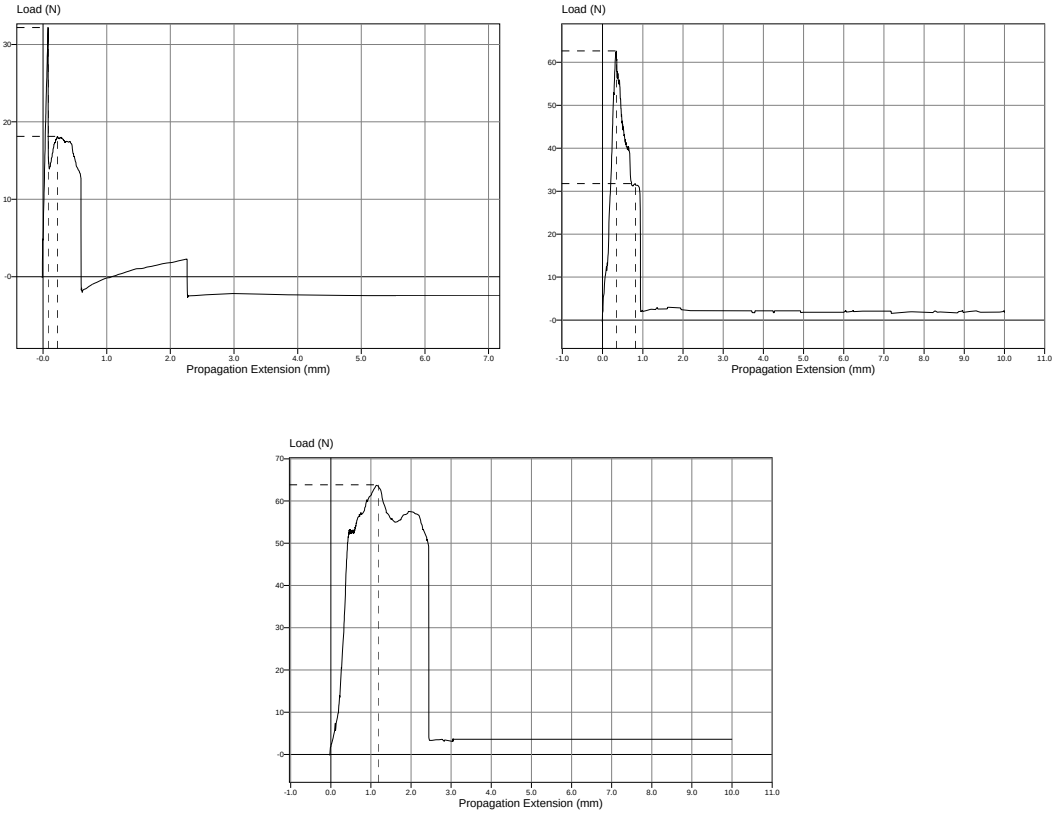

Figure D.1 T-peel tests for RG 504 coatings on titanium plates (no surface modification)

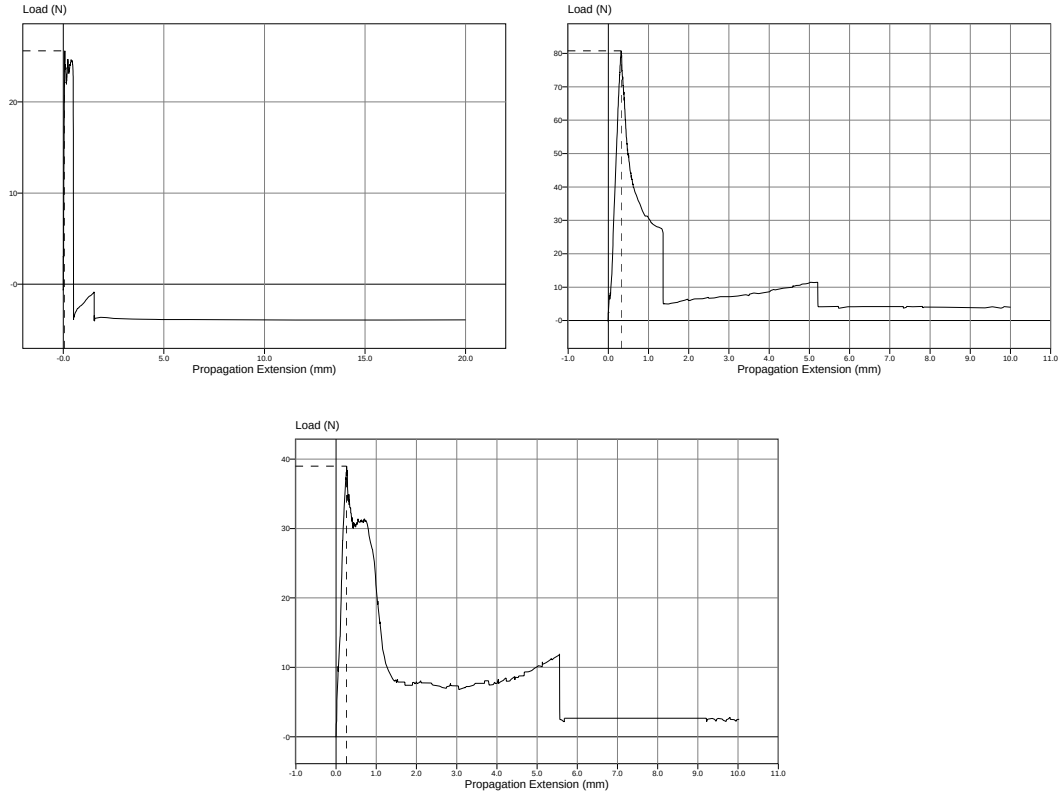

Figure D.2 T-peel tests for RG 504 coatings on titanium plates (4 No sandpapered)

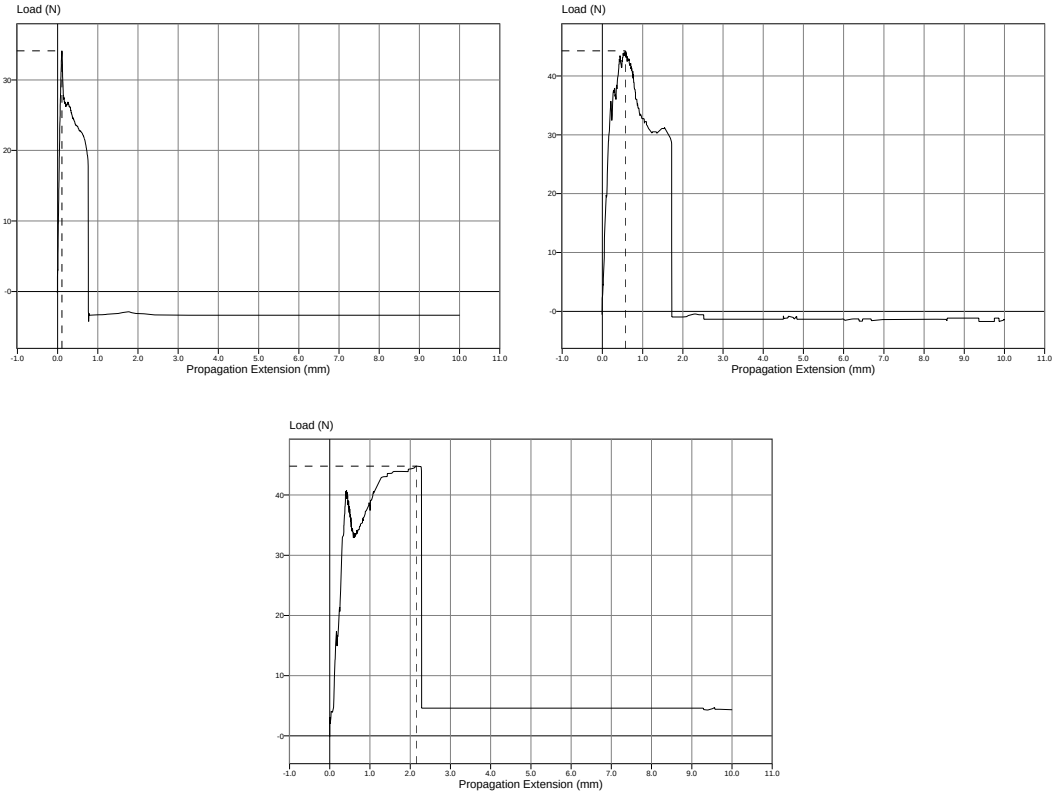

Figure D.3 T-peel tests for RG 504 coatings on titanium plates (wire emery)

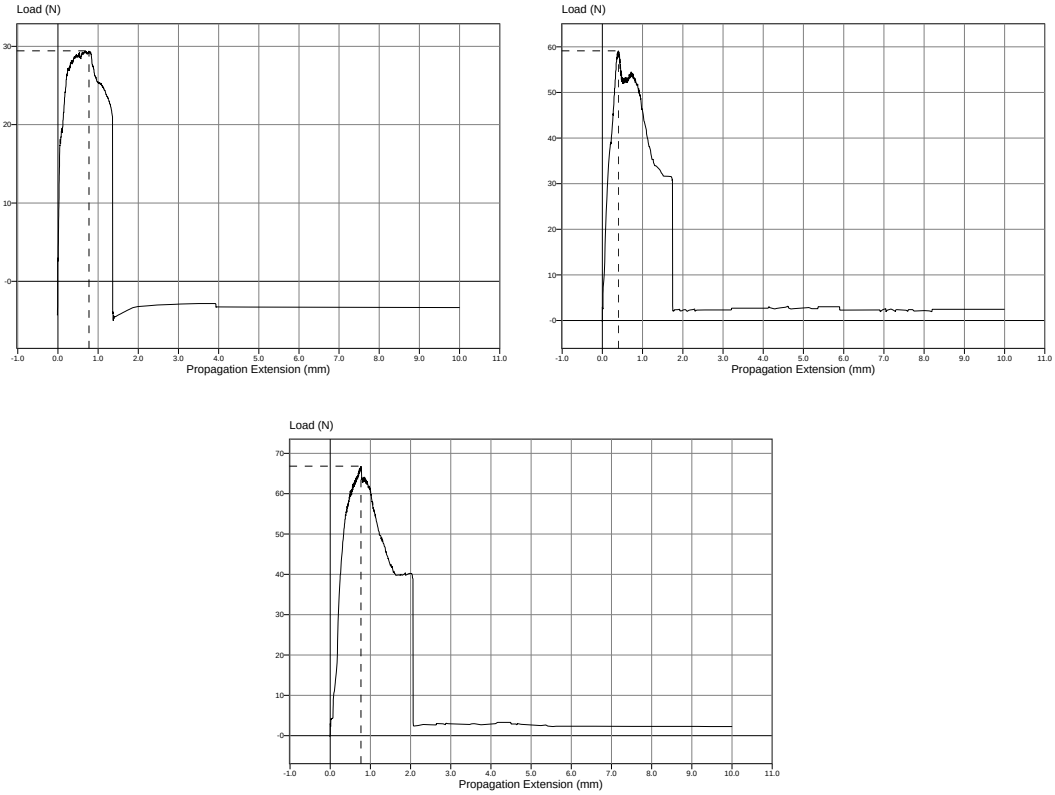

Figure D.4 T-peel tests for RG 504 coatings on titanium plates (sandblasted)

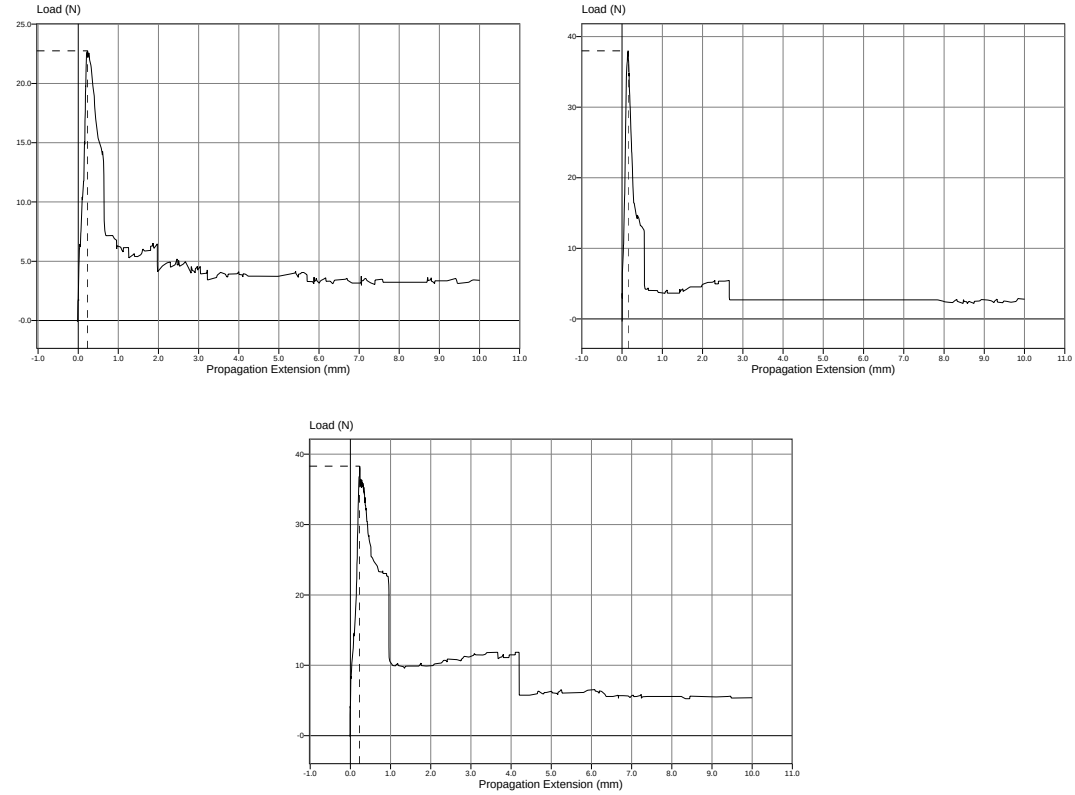

Figure D.5 T-peel tests for L 209S coatings on titanium plates (no surface modification)

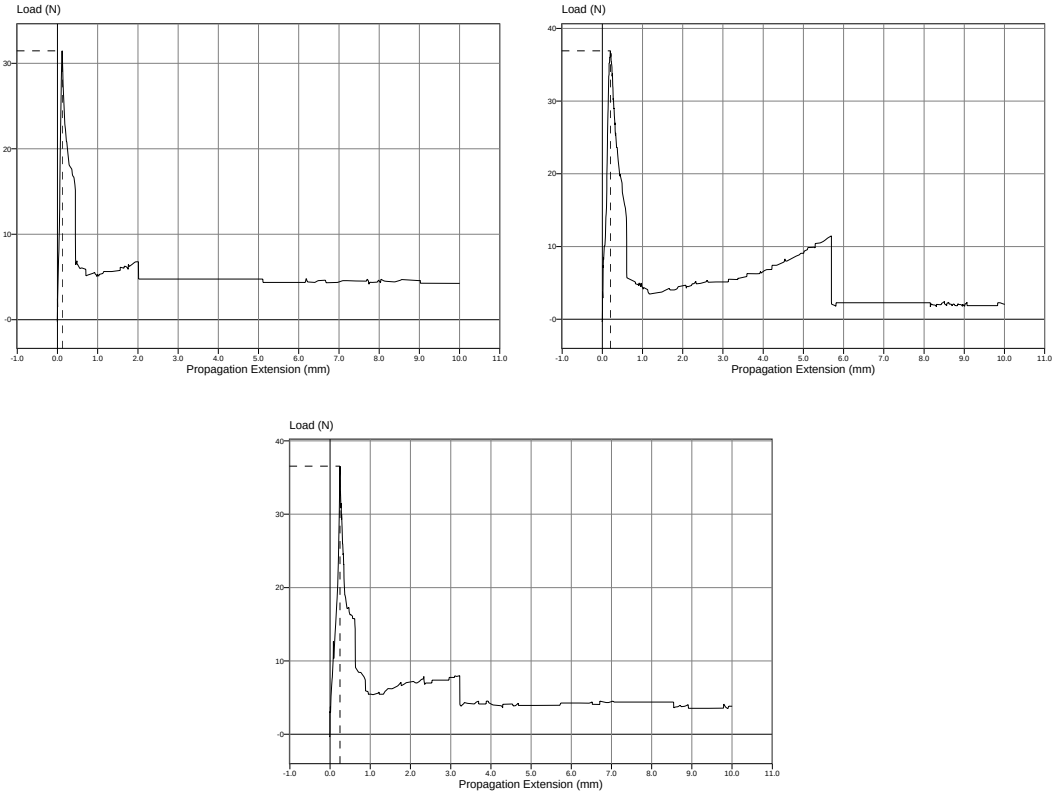

Figure D.6 T-peel tests for L 209S coatings on titanium plates (4 No sandpapered)

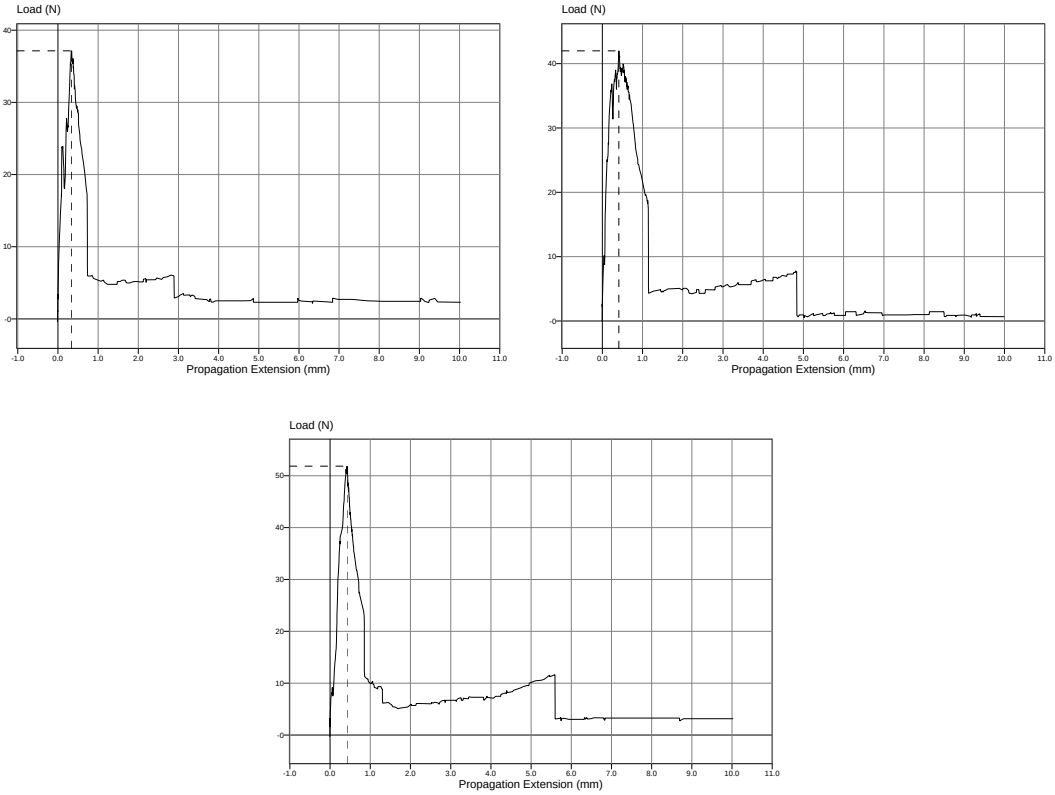

Figure D.7 T-peel tests for L 209S coatings on titanium plates (wire emery)

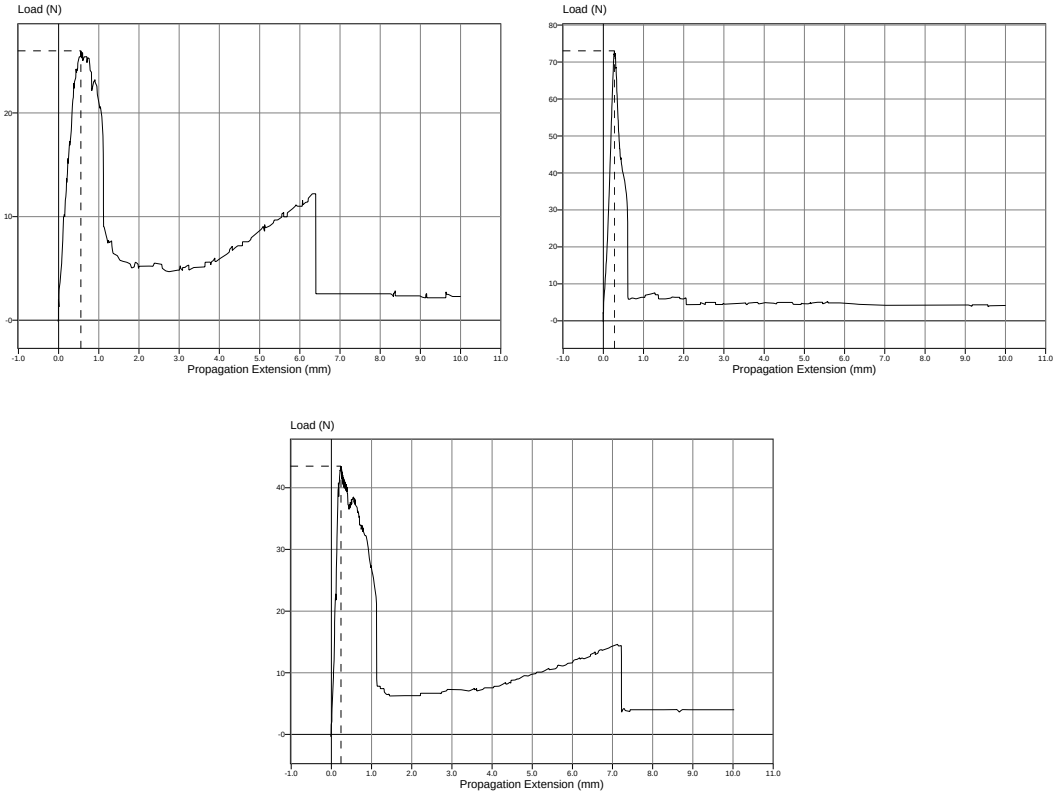

Figure D.8 T-peel tests for L 209S coatings on titanium plates (sandblasted)

APPENDIX E

PREPARATION OF PHOSPHATE BUFFERED SALINE (10 x PBS)

- The following is dissolved in 800 ml distilled water.
  - NaCl (80.0 g)
  - KCl (2.0 g)
  - Na_2HPO_4 (14.4 g)
  - KH_2PO_4 (2.4 g)
- pH is adjusted to 7.4 with HCl or NaOH.
- Distilled water is added for the final volume of 1 L.

APPENDIX F

DEGRADATION STUDIES FOR PLGA RG 504

Table F.1 Intrinsic viscosity calculations for RG 504 (2 days)

C (g/dl)	*solvent*	*0.500*	*0.333*	*0.250*	*0.200*
Flowtime (s)	103.31	156.56	137.97	129.27	125.12
η_{rel}		1.515	1.335	1.251	1.211
η_{inh}		0.831	0.868	0.896	0.957
η_{red}		1.030	1.006	1.004	1.055

Regression	
	[η] (dl/g)
From η_{inh} vs C line	1.0077
From η_{red} vs C line	1.0329
Average	1.0203

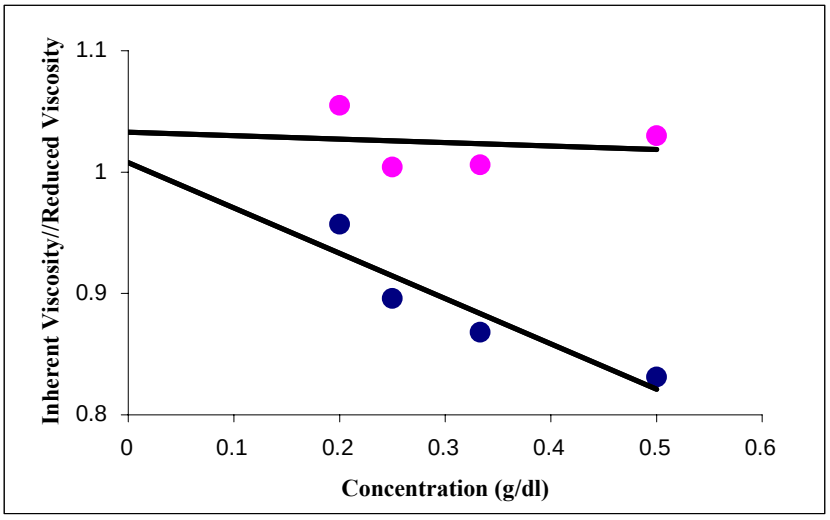

(• dots stand for η_{red} vs. C data, • dots stand for η_{inh} vs. C data)

Figure F.1 η_{inh} // η_{red} vs. Concentration graph for degradation of RG 504 (2 days)

Table F.2 Intrinsic viscosity calculations for RG 504 (1 week)

C (g/dl)	*solvent*	*0.500*	*0.333*	*0.250*	*0.200*
Flowtime (s)	103.31	150.25	134.50	127.60	124.40
η_{rel}		1.454	1.302	1.235	1.204
η_{inh}		0.749	0.792	0.844	0.928
η_{red}		0.908	0.907	0.940	1.020

Regression	
	[η] (dl/g)
From η_{inh} vs C line	1.0002
From η_{red} vs C line	1.0415
Average	1.0209

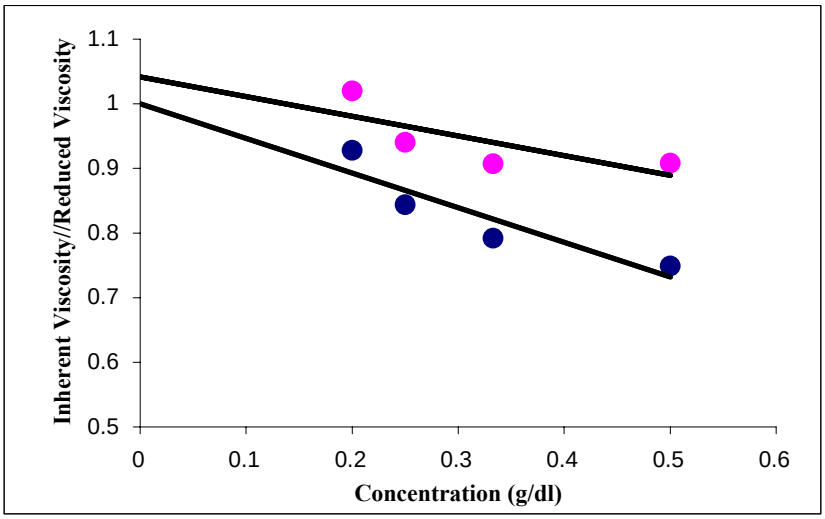

(• dots stand for η_{red} vs. C data, • dots stand for η_{inh} vs. C data)

Figure F.2 η_{inh} // η_{red} vs. Concentration graph for degradation of RG 504 (1 week)

Table F.3 Intrinsic viscosity calculations for RG 504 (4 weeks)

C (g/dl)	*solvent*	*0.500*	*0.333*	*0.250*	*0.200*
Flowtime (s)	103.31	123.76	114.24	111.24	107.49
η_{rel}		1.198	1.106	1.077	1.040
η_{inh}		0.361	0.303	0.297	0.196
η_{red}		0.396	0.318	0.308	0.200

Regression	
	[η] (dl/g)
From η_{inh} vs C line	0.1424
From η_{red} vs C line	0.1265
Average	0.1345

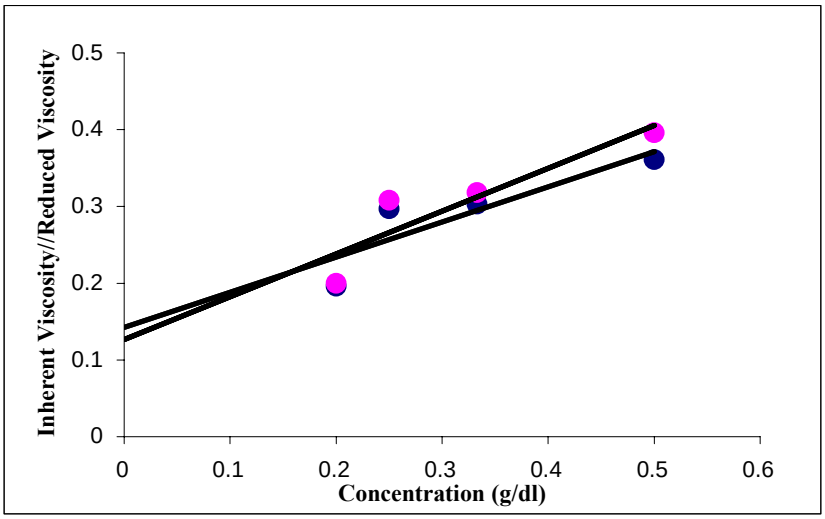

(• dots stand for η_{red} vs. C data, • dots stand for η_{inh} vs. C data)

Figure F.3 η_{inh} // η_{red} vs. Concentration graph for degradation of RG 504 (4 weeks)

Table F.4 Intrinsic viscosity calculations for RG 504 (6 weeks)

C (g/dl)	*solvent*	*0.500*	*0.333*	*0.250*	*0.200*
Flowtime (s)	117.37	127.12	124.82	121.91	120.01
η_{rel}		1.083	1.063	1.039	1.022
η_{inh}		0.159	0.183	0.153	0.109
η_{red}		0.166	0.189	0.156	0.110

Regression	
	[η] (dl/g)
From η_{inh} vs C line	0.1092
From η_{red} vs C line	0.1073
Average	0.1083

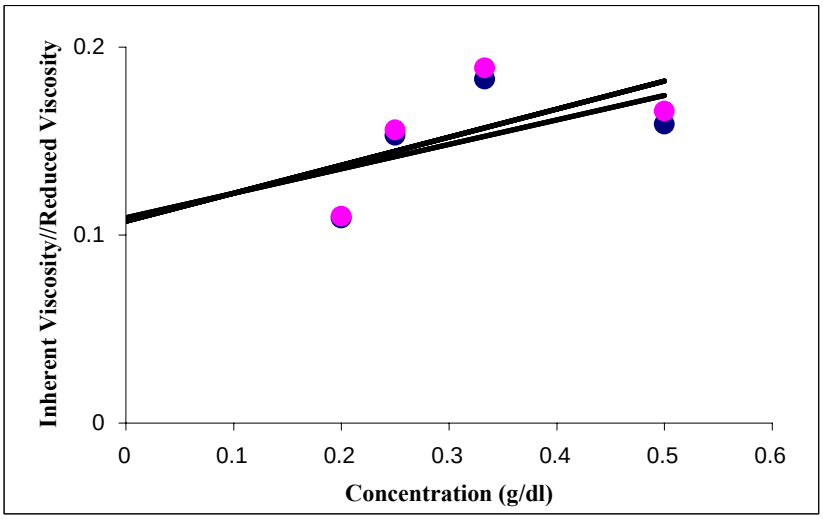

(• dots stand for η_{red} vs. C data, • dots stand for η_{inh} vs. C data)

Figure F.4 η_{inh} // η_{red} vs. Concentration graph for degradation of RG 504 (6 weeks)

APPENDIX G

DEGRADATION STUDIES FOR PL L209 S

Table G.1 Intrinsic viscosity calculations for L 209S (2 days)

C (g/dl)	*solvent*	*0.0833*	*0.0625*	*0.0500*	*0.0417*
Flowtime (s)	103.31	267.25	219.48	193.78	174.69
η_{rel}		2.587	2.124	1.876	1.691
η_{inh}		11.411	12.053	12.583	12.598
η_{red}		19.052	17.984	17.520	16.571

Regression	
	[η] (dl/g)
From η_{inh} vs C line	13.972
From η_{red} vs C line	14.465
Average	14.219

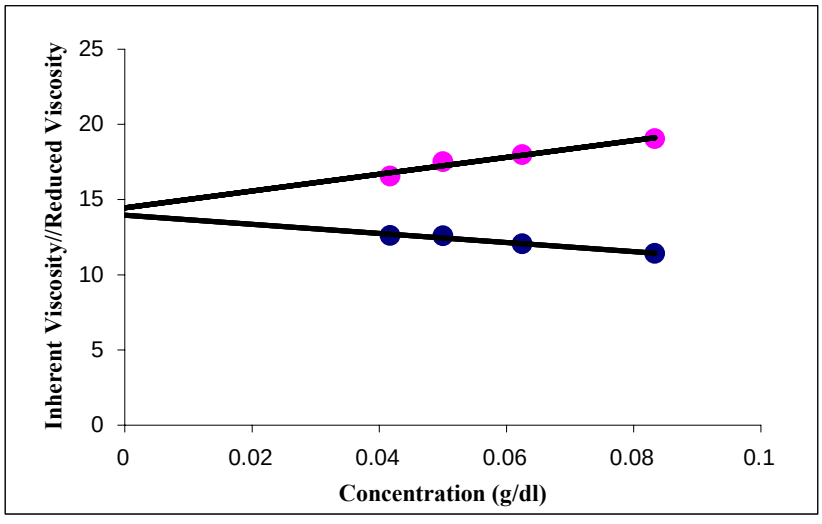

(• dots stand for η_{red} vs. C data, • dots stand for η_{inh} vs. C data)

Figure G.1 η_{inh} // η_{red} vs. Concentration graph for degradation of L 209S (2 days)

Table G.2 Intrinsic viscosity calculations for L 209S (1 week)

C (g/dl)	*solvent*	*0.0833*	*0.0625*	*0.0500*	*0.0417*
Flowtime (s)	103.31	243.59	201.71	176.51	161.22
η_{rel}		2.357	1.952	1.709	1.561
η_{inh}		10.293	10.702	10.718	10.679
η_{red}		16.291	15.232	14.180	13.453

Regression	
	[η] (dl/g)
From η_{inh} vs C line	11.714
From η_{red} vs C line	10.761
Average	11.238

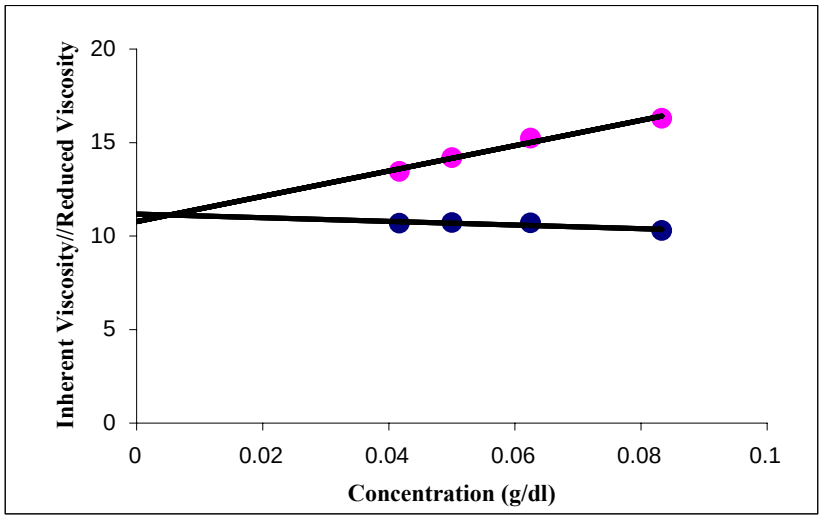

(• dots stand for η_{red} vs. C data, • dots stand for η_{inh} vs. C data)

Figure G.2 η_{inh} // η_{red} vs. Concentration graph for degradation of L 209S (1 week)

Table G.3 Intrinsic viscosity calculations for L 209S (4 weeks)

C (g/dl)	*solvent*	*0.0833*	*0.0625*	*0.0500*	*0.0417*
Flowtime (s)	103.31	229.62	193.15	173.63	158.46
η_{rel}		2.223	1.870	1.681	1.534
η_{inh}		9.590	10.015	10.388	10.261
η_{red}		14.682	13.920	13.620	12.806

Regression	
	[η] (dl/g)
From η_{inh} vs C line	11.152
From η_{red} vs C line	11.295
Average	11.224

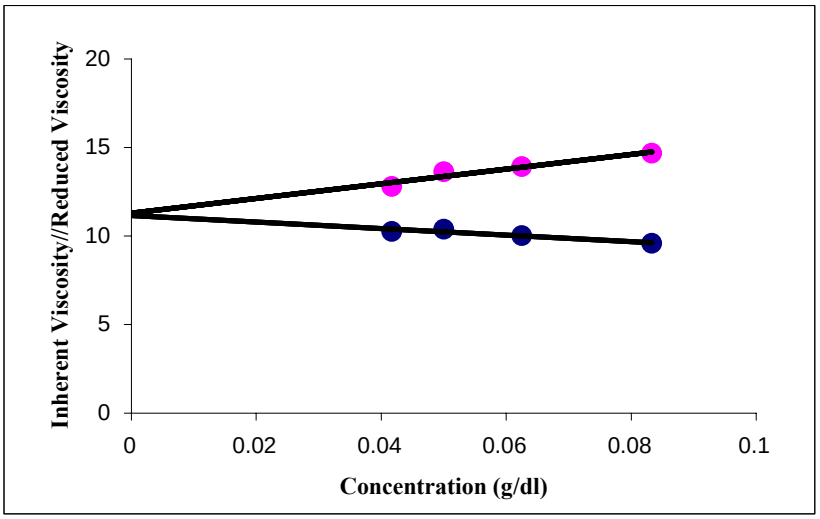

(• dots stand for η_{red} vs. C data, • dots stand for η_{inh} vs. C data)

Figure G.3 η_{inh} // η_{red} vs. Concentration graph for degradation of L 209S (4 weeks)

Table G.4 Intrinsic viscosity calculations for L 209S (6 weeks)

C (g/dl)	*solvent*	*0.0833*	*0.0625*	*0.0500*	*0.0417*
Flowtime (s)	117.37	286.80	232.46	208.43	188.41
η_{rel}		2.444	1.981	1.776	1.605
η_{inh}		10.728	10.938	11.374	11.346
η_{red}		17.335	15.696	15.520	14.508

Regression	
	[η] (dl/g)
From η_{inh} vs C line	12.083
From η_{red} vs C line	12.026
Average	12.055

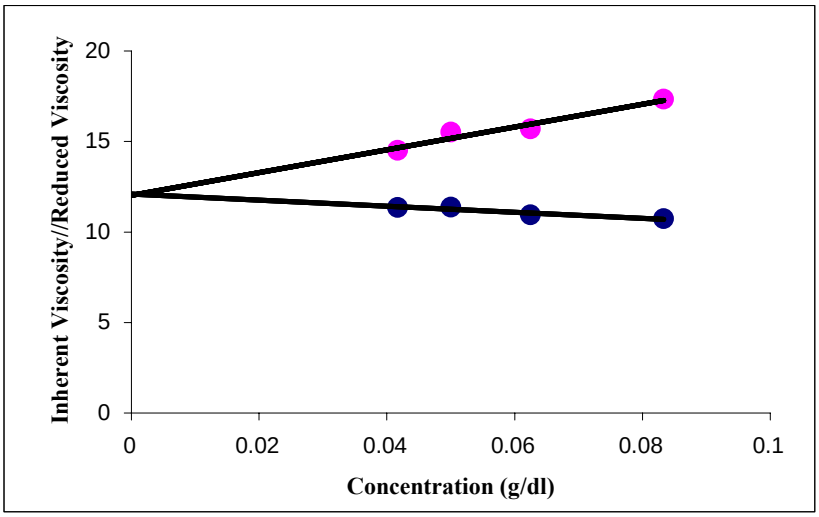

(• dots stand for η_{red} vs. C data, • dots stand for η_{inh} vs. C data)

Figure G.4 η_{inh} // η_{red} vs. Concentration graph for degradation of L 209S (6 weeks)

CURRICULUM VITAE

PERSONAL INFORMATION

Name & Surname : Tuncay Baydemir
Nationality : Turkish (T.C.)
Date and Place of Birth : 16 June 1978, Ankara
Marital Status : Married, one child
e mail : tuncay.baydemir@tubitak.gov.tr

EDUCATION

Degree	Institution	Year
M.Sc.	METU, Polymer Science and Technology	2003
B.Sc.	METU, Chemistry Department	2000
High School	İbn-i Sina High School, Ankara	1995

WORK EXPERIENCE

Year	Place	Enrollment
2007-Now	TÜBİTAK, Science and Society Dept.	Assistant Expert
2004-2007	METU, Chemistry Dept., Physical Chem. Lab.	Teaching Assistant
2000-2004	METU, Chemistry Dept., General Chem. Lab.	Teaching Assistant
Summer-1999	PETKİM, Aliağa Complex	Intern

PROJECTS

TÜBİTAK, Ankara, Turkey
Science Center Project, 2007-Now.

Middle East Technical University, Ankara, Turkey - Orto-Pro and Fame-Med Companies, Turkey
TÜBİTAK TİDEB Project, Project No: 3050095, *"Kontrollü Antibiyotik Salımı Sağlayan Polimer Kaplı Metal İmplantlar"*, Expert Researcher, 2005-2007.

Middle East Technical University, Ankara, Turkey - M&M Mars, New Jersey, USA
"Making Edible Objects by Three Dimensional Printing (3DP)", 2002.

Middle East Technical University, Ankara, Turkey
"Epoxy Coating of Iron Powders by Solution Phase Separation and Wetting Method for The Production Of The Highly Filled Iron Powder Composites", Undergraduate Research, 1999.

PROFESSIONAL ACTIVITIES

Middle East Technical University, Ankara, Turkey
Physical Chemistry Laboratory Coordinator, 2006-2007.

Middle East Technical University, Ankara, Turkey
Organizer and Participant of the METU Representation Days, 2001-2006.

Middle East Technical University, Ankara, Turkey & Darmstadt Technical University, Germany
Polymer Chemistry Assistantship, Polymer Summer School, August 2002.

Middle East Technical University, Ankara, Turkey
Member of Yearbook and Ball Committee, 1999-2000.

RESEARCH INTERESTS

Solid freeform fabrication and Three Dimensional Printing, biodegradable and biocompatible polymers, controlled and sustained drug release, biomedical materials, polymer characterization and processing

FOREIGN LANGUAGES

Advanced English

PRIZES AND ACHIEVEMENTS

Sokullu Mehmet Paşa High School, Ankara, Turkey
First and Third Ranks

İbn-i Sina High School, Ankara, Turkey
First Rank

Middle East Technical University, Ankara, Turkey
Honor and High Honor Degrees

Middle East Technical University, Ankara, Turkey
Polymer Chemistry and Organic Chemistry Options Certificates

PUBLICATIONS

Book:

1. T. Baydemir, S. Kıralp, G. Özkoç, S. Erdoğan, P. Çamurlu and M. Doğan; *"Plastikler"*, Middle East Technical University, Society and Science Center, METU Press (2006).

Periodicals:

1. T. Baydemir, *"Üç Boyutlu Modelleme Teknikleri, Tasarla Modelle Üret!"*, TÜBİTAK Bilim ve Teknik Dergisi, 497, 54-57 (2009).

Oral Presentations:

1. T. Baydemir, E. Bayramlı, II. Ulusal Polimer Bilim ve Teknoloji Kongresi ve Sergisi *"Biobozunur Polimer Kaplamaların İlaç Taşıyıcı Olarak Metal Substratlar Üzerinde Özelliklerinin ve İlaç Salımlarının İncelenmesi"*, Şanlıurfa/Turkey (2008).

Attended Educational Seminars, Conferences, Workshops:

1. NANOBIOMAT Workshop, Nanobiomaterials, Tissue Engineering and Nanobiotechnology, METU, Ankara/Turkey (2007).
2. METU Educational Seminars, METU CC Center, Ankara/Turkey (March-June 2007).
3. I. Ulusal Polimer Bilim ve Teknoloji Kongresi ve Sergisi, METU, Ankara/Turkey (2006).

HOBBIES

Billiards, Football, Basketball, Fishing, Books, Science Magazines, Music, Movies, Computer Technologies